FFI-rapport 2014/01970

Rate table tests of low-cost inertial measurement units

Kjetil Bergh Ånonsen and Atle Skaugen

FFI Forsvarets forskningsinstitutt

Rate table tests of low-cost inertial measurement units

Kjetil Bergh Ånonsen and Atle Skaugen

Norwegian Defence Research Establishment (FFI)

13 November 2014

FFI-rapport 2014/01970

3823

P: ISBN 978-82-464-2458-3
E: ISBN 978-82-464-2459-0

Keywords

Treghetsnavigasjon

Sensorer

Akselerasjon – Måleinstrumenter

Gyro

Approved by

Øyvind Sjøvik	Project Manager
Johnny Bardal	Director

English Summary

This report gives a summary of the results of a series of tests of low cost inertial measurement units conducted at FFI in late 2012. The units were all based on microelectromechanical technology (MEMS) and included the SiIMU02 and MinIM from Goodrich Atlantic Inertial Systems, HG1930 from Honeywell, STIM300 from Sensonor, MTI-300 and MTI-30 from XSens.

The units were subjected to a range of tests to determine their stability over time, noise and bias properties, repeatability and performance when subjected to temperature variations. Parameters outside the specifications were found for all sensors, especially for accelerometer and gyro biases and random walk. All units were found to have acceptable temperature sensitivity and repeatability performance between power-ons.

Sammendrag

Denne rapporten sammenfatter resultatene fra en rekke tester av lavkost treghetssensorenheter gjennomført ved FFI i slutten av 2012. Følgende enheter ble testet, alle basert på mikroelektromekanisk teknologi (MEMS): SiIMU02 og MinIM fra Goodrich Atlantic Inertial Systems, HG1930 fra Honeywell, STIM300 fra Sensonor, MTI-300 og MTI-30 fra XSens.

Enhetene ble testet med henblikk på stabilitet over tid, støy- og biasegenskaper, repeterbarhet og ytelse under varierende temperaturforhold. For alle enhetene ble det funnet parametere utenfor spesifikasjonene, særlig for akselerometer- og gyrobiaser og random walk. Alle enhetene hadde aksepterbar temperatursensitivitet og repeterbarhet mellom påslag.

Contents

1 Introduction

As part of the CDE «Kompakte Navigasjonssystemer» a series of rate table tests of several different MEMS-based IMUs (inertial measurement units) was conducted at FFI in late 2012 / early 2013. This report summarizes the results from these experiments.

An inertial measurement unit (IMU) consists of 3 gyroscopes, measuring angular rate, and 3 accelerometers, measuring linear acceleration. During the last decade or so, MEMS IMUs have become accurate enough to be used in many applications where one earlier had to rely on conventional, larger and more expensive sensors. In order to be able to use these sensors in applications, e.g. in navigation systems, it is important to model the error components of the sensors and how these vary with time and under different environmental conditions. In the sensor specifications provided by the different manufacturers, many different error parameters are given, which makes it difficult to compare the sensors directly. The goal of these experiments was therefore twofold. Firstly, we wanted to check whether the sensors satisfied the specifications. Secondly, we wanted to obtain more knowledge about the nature of the errors present in MEMS inertial sensors.

The following sensors were tested: SiIMU02 and MinIM from Goodrich Atlantic Inertial Systems, HG1930 from Honeywell, STIM300 from Sensonor, MTI-300 and MTI-30 from XSens.

2 Test Descriptions

The following tests were conducted for the different sensors:

2.1 Long term static test

The sensor was placed on a stable surface, and the output was logged for a long period (more than 6 hours), in order to determine the nature of the output from the gyros and accelerometers over time. The following characteristics were investigated:

- Stability over time
- Distribution and spectral properties of the output signals
- Allan variance and corresponding angular/velocity random walk and bias instability
- Output during self-warming, after the unit has been powered on.

2.2 Repeatability tests

To check whether the output varied significantly from turn-on to turn-on, the sensors were turned on several times and the output was logged. The orientation of the sensors was the same from turn-on to turn-on.

2.3 Temperature tests

The sensor was placed in a temperature chamber, where it was subjected to different temperature conditions. The IMU was kept at constant orientation during the tests, and both constant temperatures over extended time periods as well as rapidly varying temperature were used.

2.4 Up-down tests

In order to measure accelerometer biases and scale factors, as well as gyro biases, up-down tests were performed. In these tests, the IMU was first placed on the rate table, with one of the axes pointing down, and the output was logged for a period of about 15 minutes. The sensor was then turned around, such that the axis that previously was pointing down was now pointing up. The two accelerometers measuring in the horizontal plane would then measure an acceleration close to zero, and after the sensor was turned around, the direction of the measurement bias would be reversed. Likewise, the output of the downward pointing accelerometer would change signs after the turn. The accelerometer bias can then be computed as

$$f_0 = (\tilde{f}_w + \tilde{f}_e)/2, \tag{2.1}$$

where $\tilde{f}_w$ and $\tilde{f}_w$ denote the measured output from one of the horizontal accelerometers in each position, averaged over the measurement period.

Likewise, the accelerometer scale factor error can be computed as

$$\varepsilon = (\tilde{f}_u - \tilde{f}_d)/2g - 1, \tag{2.2}$$

where $\tilde{f}_u$ and $\tilde{f}_d$ denote the output from the accelerometer pointing up and down.

Similarly, the gyro bias from the gyro in the up/down direction can be computed as

$$\Theta_0 = \left(\tilde{\Theta}_u - \tilde{\Theta}_d\right)\Big/2. \tag{2.3}$$

3 Test results

3.1 SiIMU02

The SiIMU02 is a MEMS-based sensor manufactured by Goodrich/Atlantic Inertial Systems. The specifications of this IMU are given in Table 3.1. These values are listed by the manufacturer as “typical performance” [1].

Figure 3.1 SiIMU02

***Table** 3.1 Typical performance for the SiIMU02.*

	Gyros	Accelerometers
Bias repeatability	≤ 50 deg/hr 1σ	≤ 10 mg 1σ
Bias instability	≤ 1.5 deg/hr	≤ 0.5 mg
Random walk	≤ 0.1 deg/√hr	≤ 0.5 m/s/√hr
Scale factor repeatability	≤ 500 ppm 1σ	≤ 1500 ppm 1σ

3.1.1 Long term static test

In this test, the unit was placed on a stable table, with the x-accelerometer pointing down. The unit was powered on, after having been turned off for an extended period. Thus, potential effects due to self-warming would be visible in the data.

3.1.1.1 Accelerometers

Figure 3.2 to Figure 3.4 show the output from the accelerometers during the static test. As the output is given as delta velocity measurements, the values plotted are divided by delta t (0.0050 s in this case), to obtain accelerations. As seen in Figure 3.2, the x-accelerometer was oriented vertically, measuring gravity. Notice the high measurement value from the x-accelerometer (9.9854 m/s^2 averaged over the whole test), which indicates a high accelerometer bias. There is also a drift in the data from all three accelerometers. This is particularly obvious when the output is averaged over 1 minute intervals; see Figure 3.5 to Figure 3.7. There seems to be some kind of random walk component present in the acceleration data, i.e. an acceleration random walk or acceleration ramp.

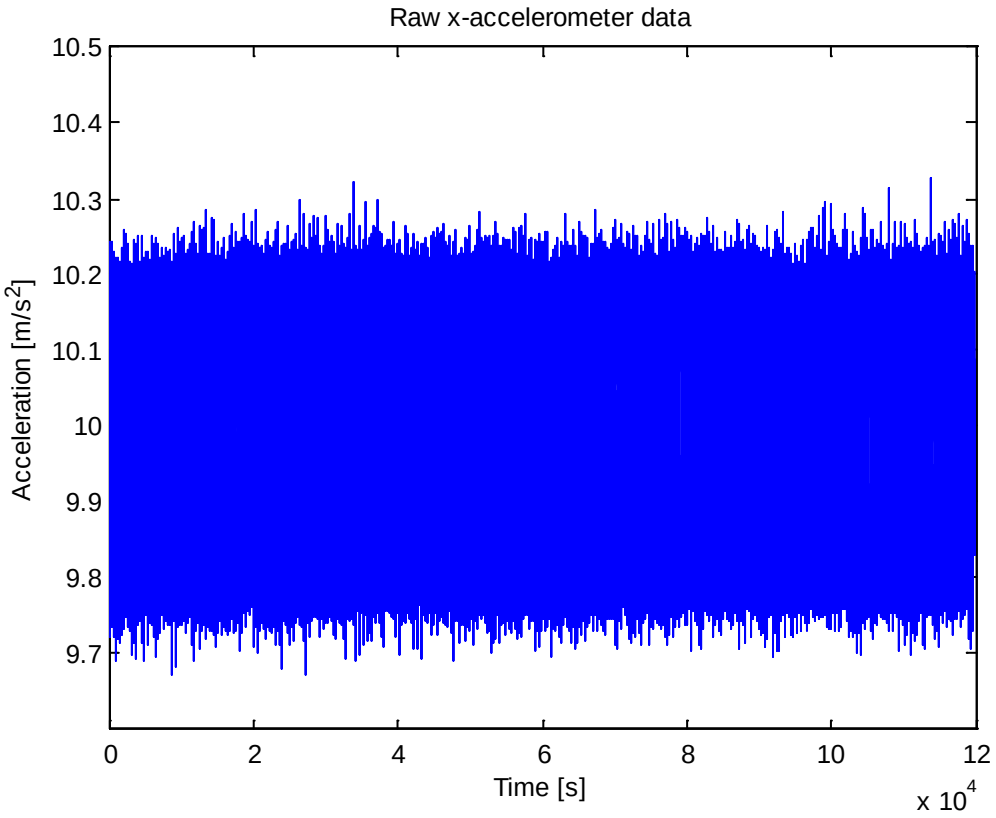

Figure 3.2 Raw data from the SiIMU02 x-accelerometer.

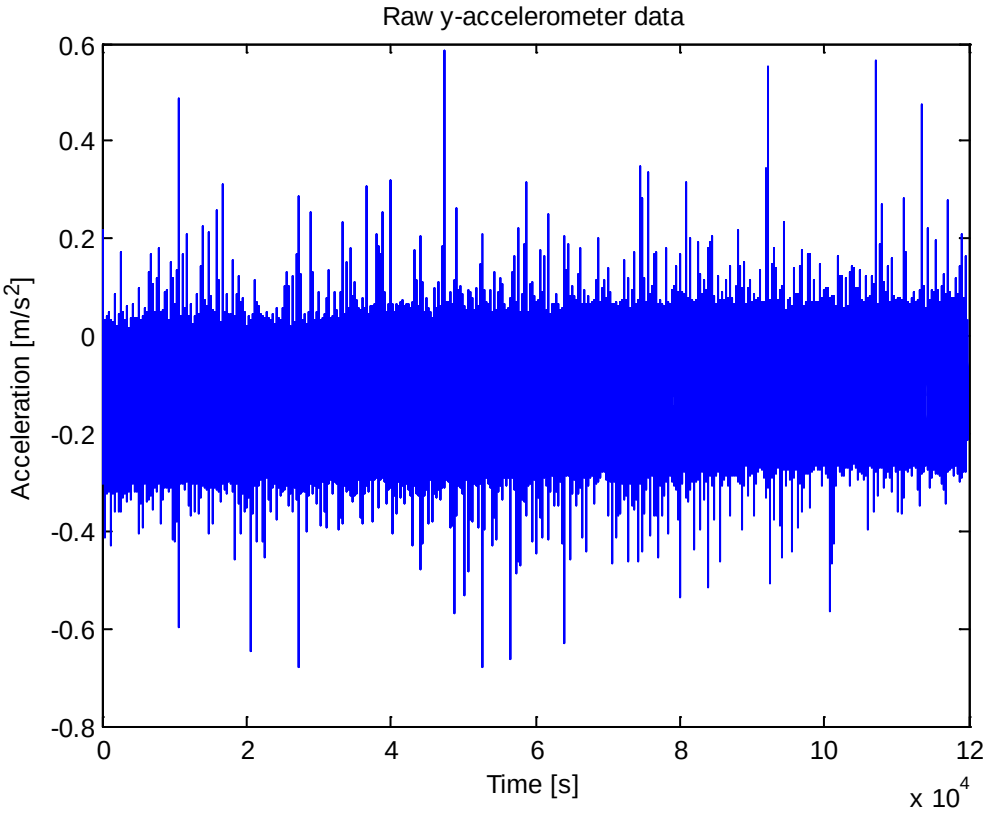

Figure 3.3 Raw data from the SiIMU02 y-accelerometer.

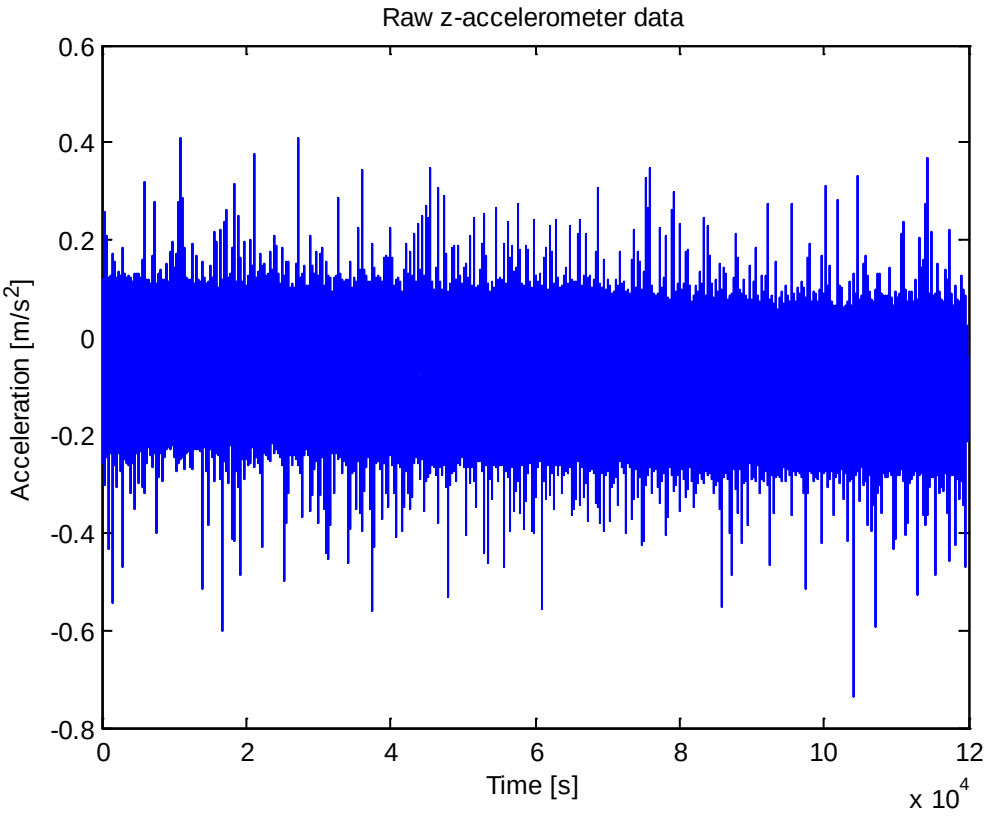

Figure 3.4 Raw data from the SiIMU02 z-accelerometer.

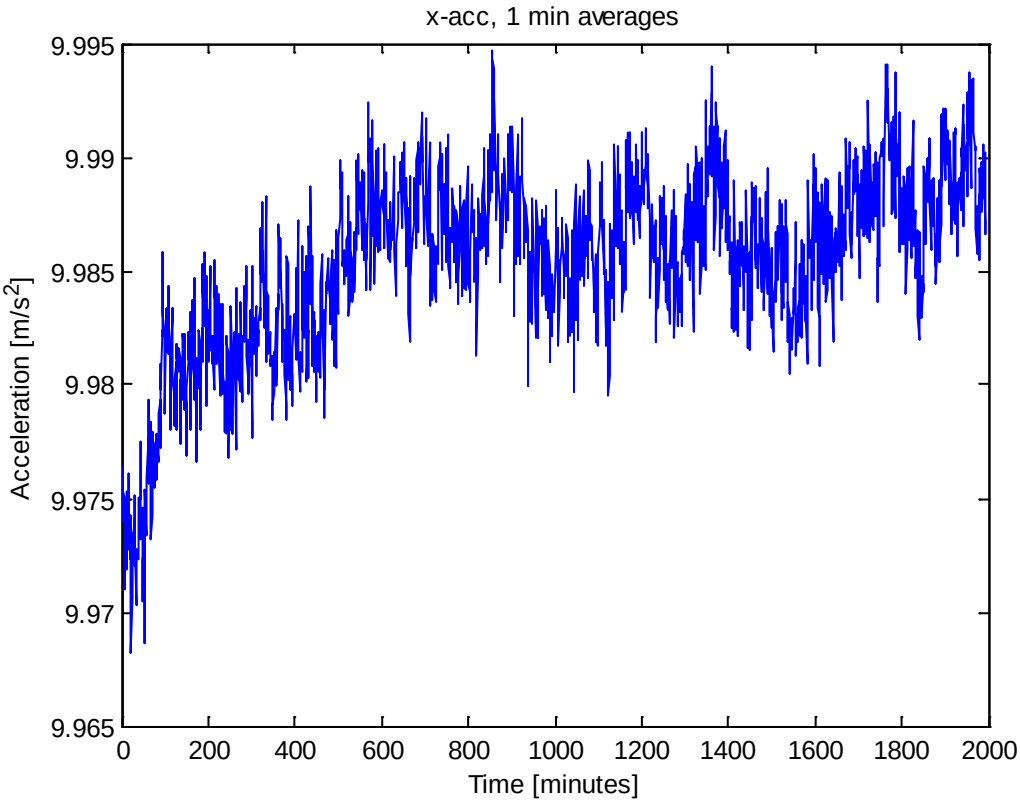

Figure 3.5 SiIMU02 x-accelerometer averaged over 1 minute intervals.

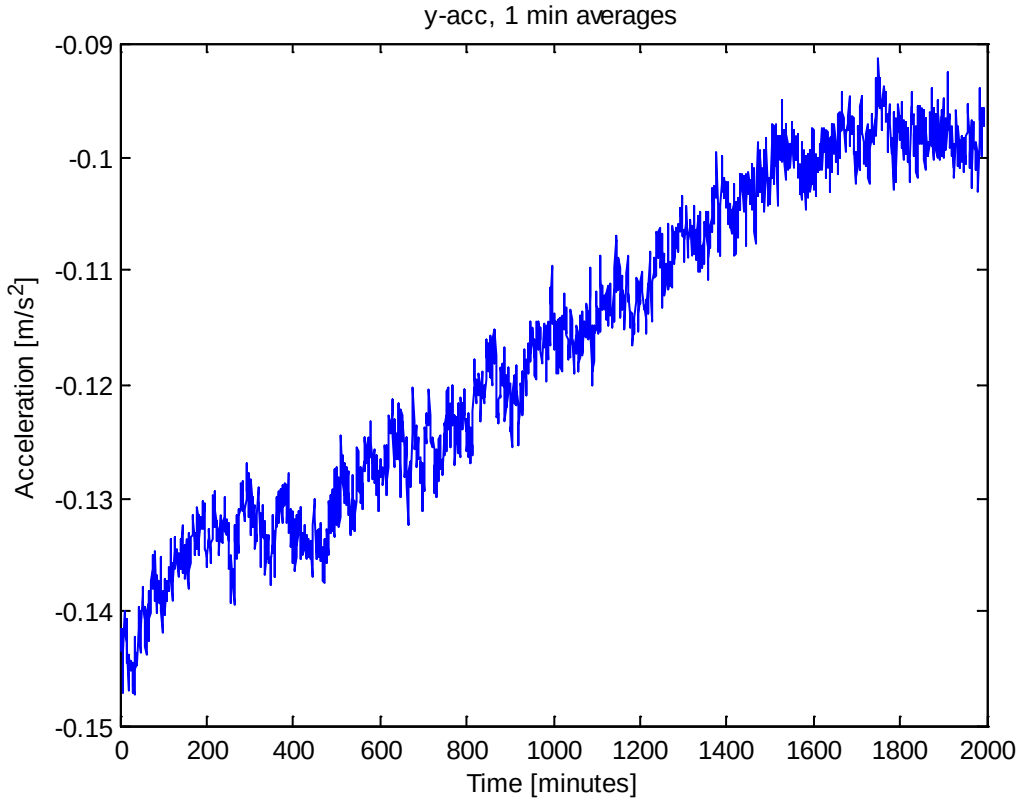

Figure 3.6 SiIMU02 y-accelerometer averaged over 1 minute intervals.

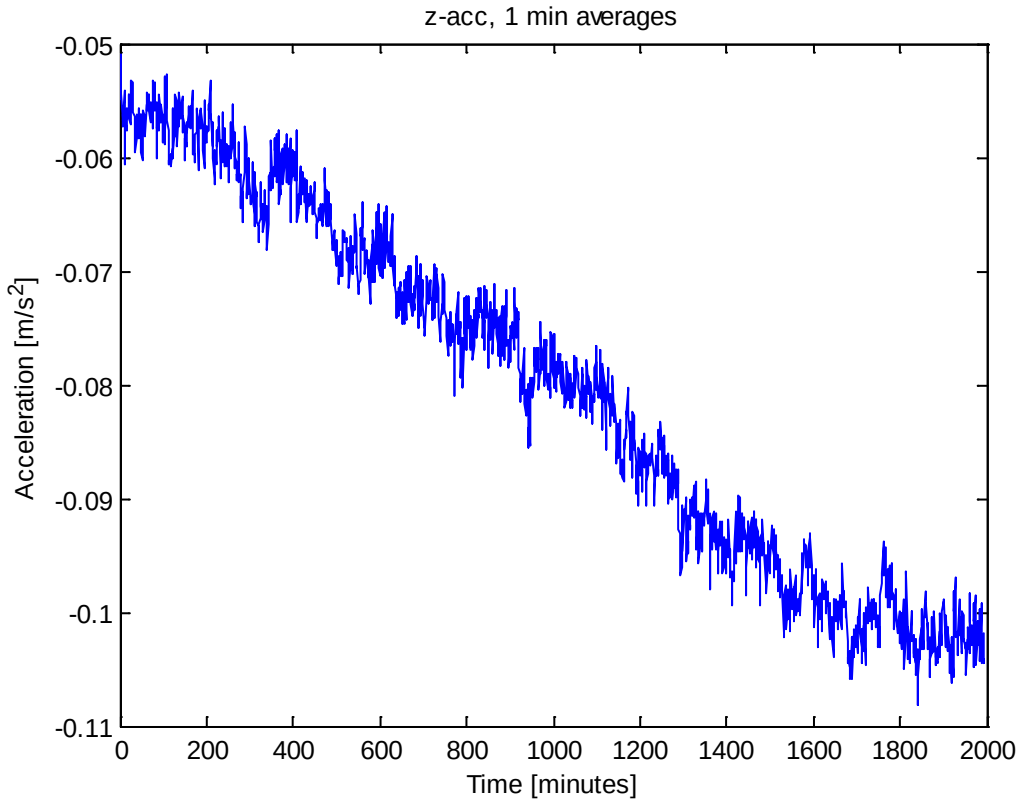

Figure 3.7 SiIMU02 z-accelerometer averaged over 1 minute intervals.

Figure 3.8 shows computed root Allan variance from the three accelerometers from the entire test interval. To simplify the computation of the Allan variance, the delta v measurements from the accelerometers were pre summed over 1 second intervals. Based on the Allan variance plots, the velocity random walk and bias instability values were estimated. The velocity random walk estimates were 0.32, 0.24 and 0.24 m/s/sqrt(h) for the x, y and z accelerometer, respectively, well within the specified value of 0.5 m/s/sqrt(h). The bias instability estimates (i.e. the minimum value of the root Allan variance curves) were 0.1 mg for all axes, again well within the specified value of 0.1 mg.

In the log-log plot of the root Allan variance, different error components will dominate the Allan variance curve for different averaging intervals, τ. The most common error types are quantization noise (slope -1 in the log-log root variance plot), velocity random walk (slope -1/2), bias instability (slope 0), acceleration random walk (slope +1/2) and acceleration ramp (slope +1), [2].

In Figure 3.8, the regions corresponding to velocity random walk, bias instability and acceleration ramp, are the most predominant in the y and z accelerometer, whereas the rate ramp is not that visible in the x accelerometer data.

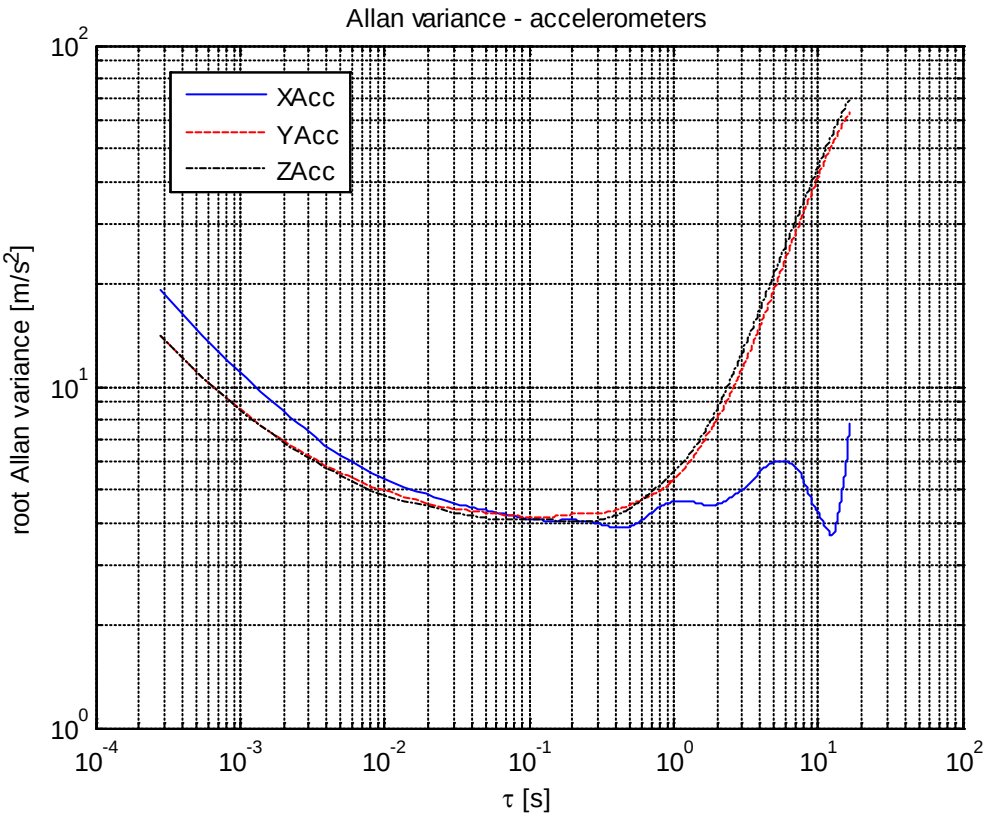

Figure 3.8 Computed root Allan variances SiIMU02 accelerometers.

Figure 3.9 to Figure 3.11show the computed spectral densities of the accelerometers. The frequencies seem to be rather evenly distributed. There are a few local maxima for certain frequencies, but these are too small to be of any significance.

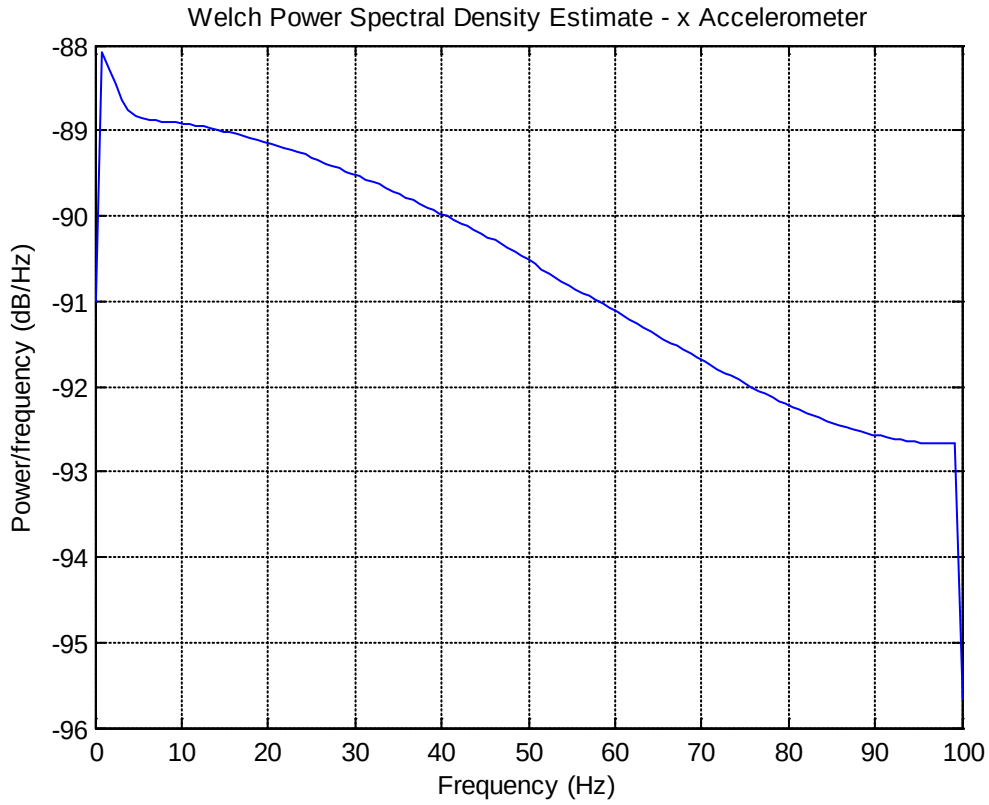

Figure 3.9 Spectral density plot, SiIMU02 x-accelerometer.

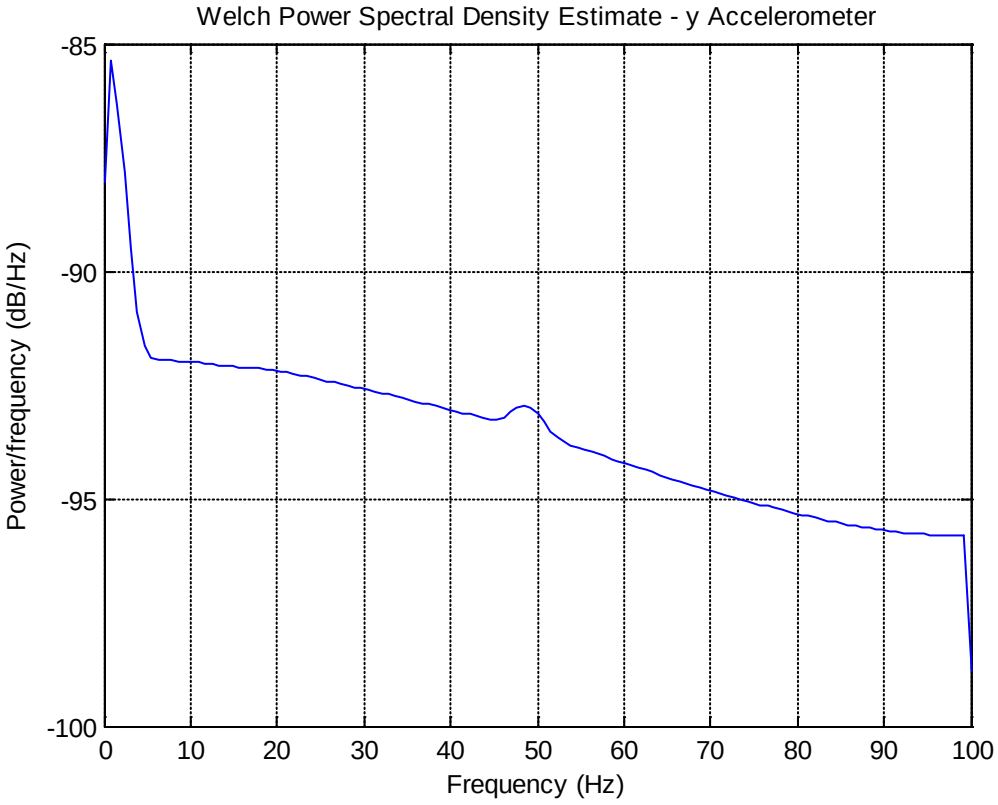

Figure 3.10 Spectral density plot, SiIMU02 y-accelerometer.

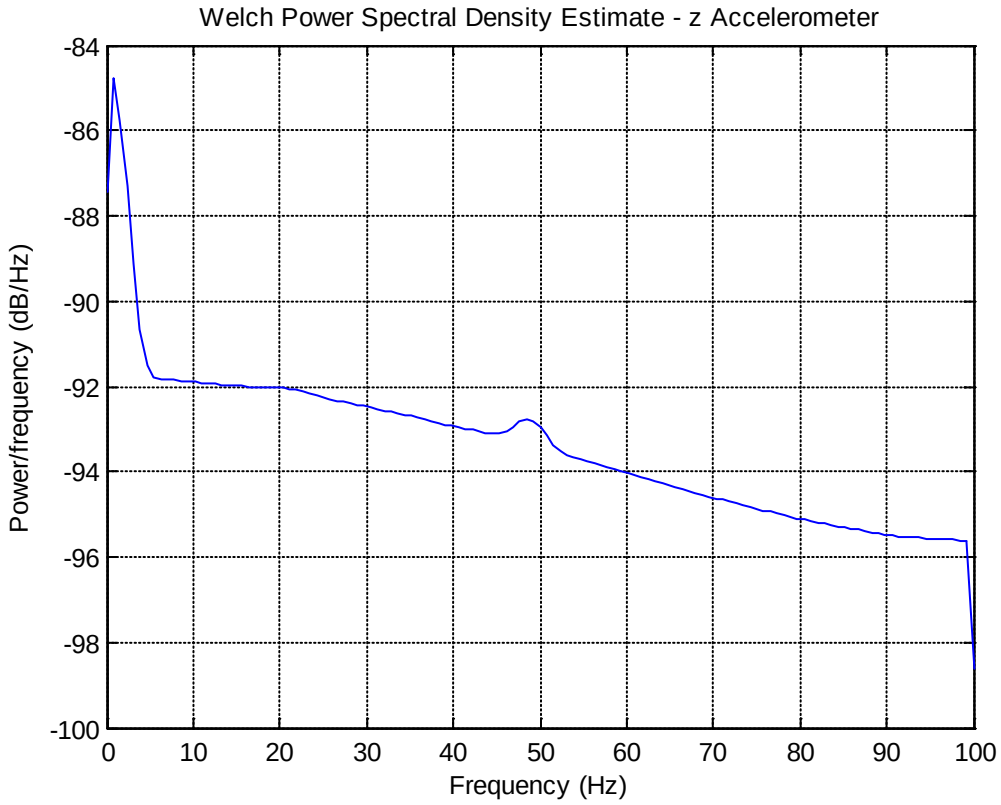

Figure 3.11 Spectral density plot, SiIMU02 z-accelerometer.

Figure 3.12 to Figure 3.14 show histograms for the raw accelerometer measurements. All histograms show a Gaussian-like distribution. The standard deviations of the measured accelerations (delta velocity divided by delta time) are (0.0603, 0.0447, 0.0459) m/s^2 for the x, y and z accelerometer, respectively.

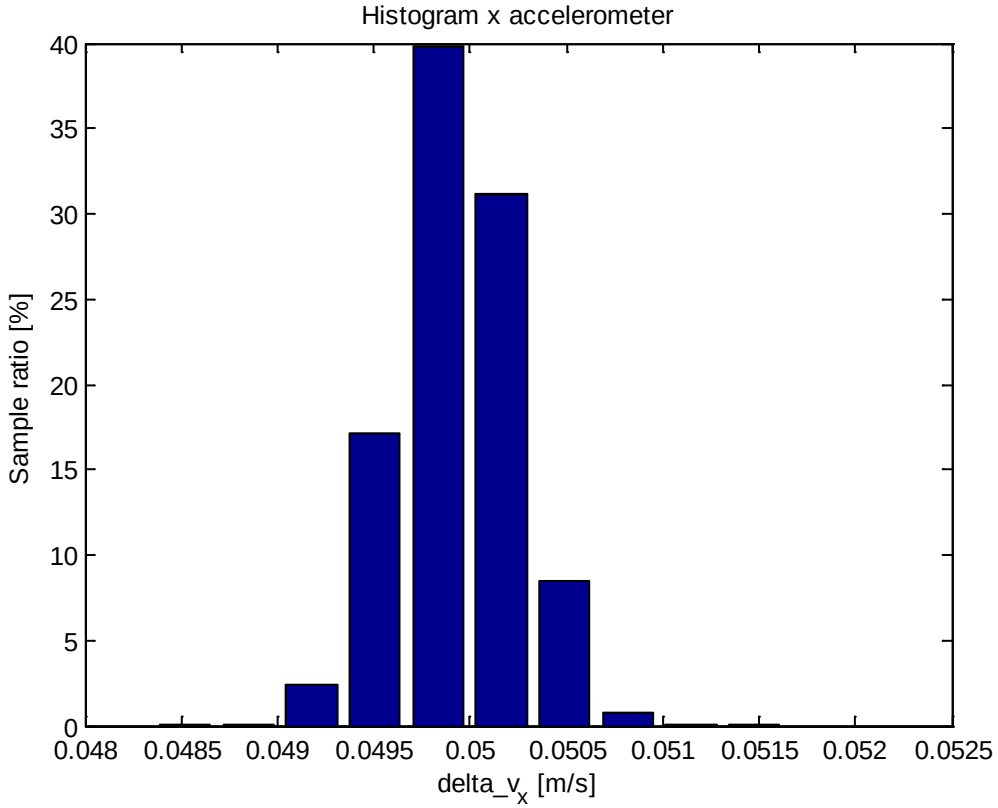

Figure 3.12 SiIMU x accelerometer histogram.

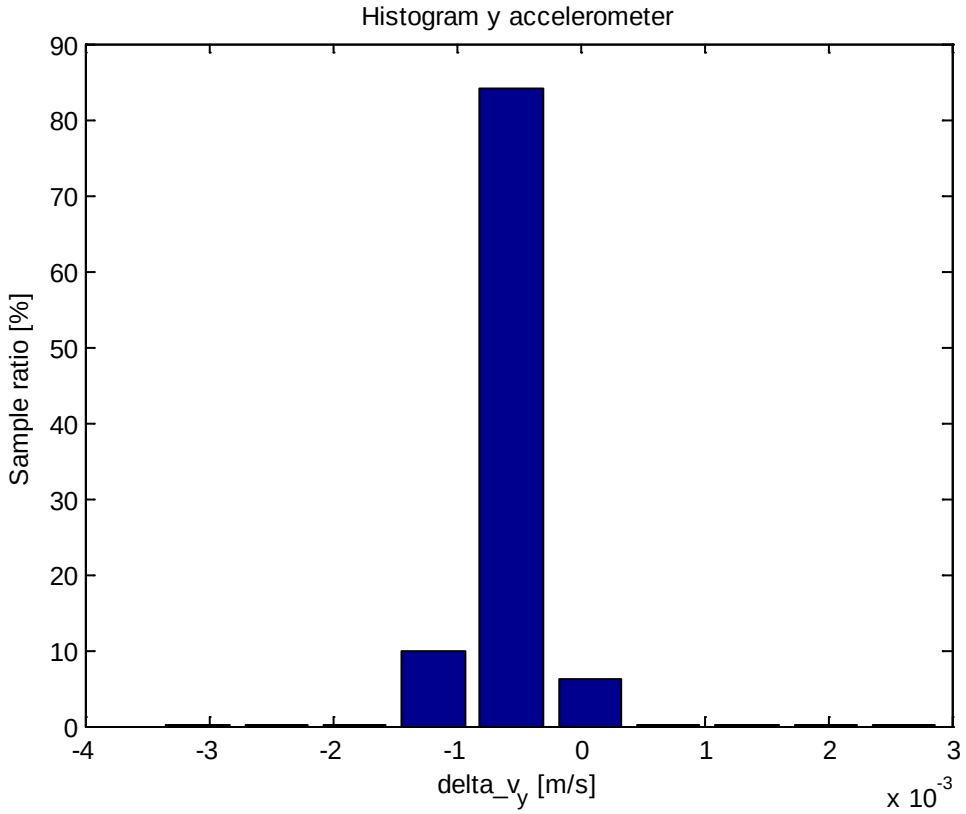

Figure 3.13 SiIMU y accelerometer histogram.

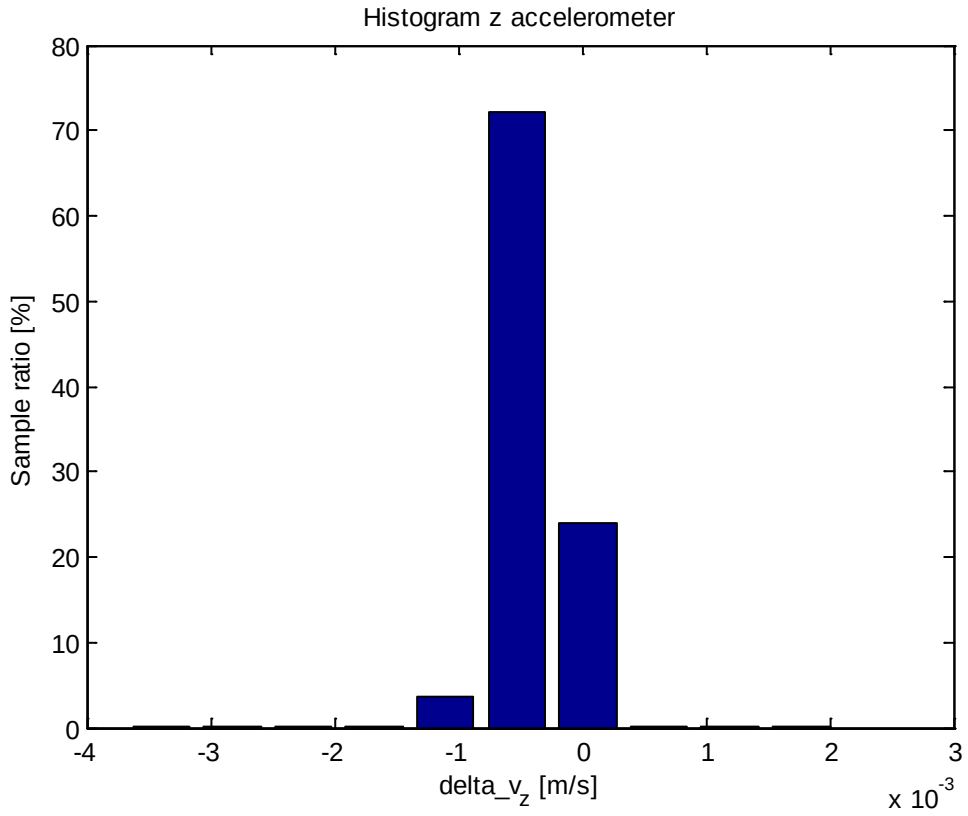

Figure 3.14 SiIMU z accelerometer histogram.

3.1.1.2 Gyroscopes

Figure 3.15 to Figure 3.17 show raw data from the SiIMU02 gyroscopes throughout the static test. As was also the case for the accelerometers, there seems to be a drift in the angular rate data, i.e. a rate random walk or rate ramp. This is particularly evident when the data are averaged over 1 minute intervals, cf. Figure 3.18 - Figure 3.20.

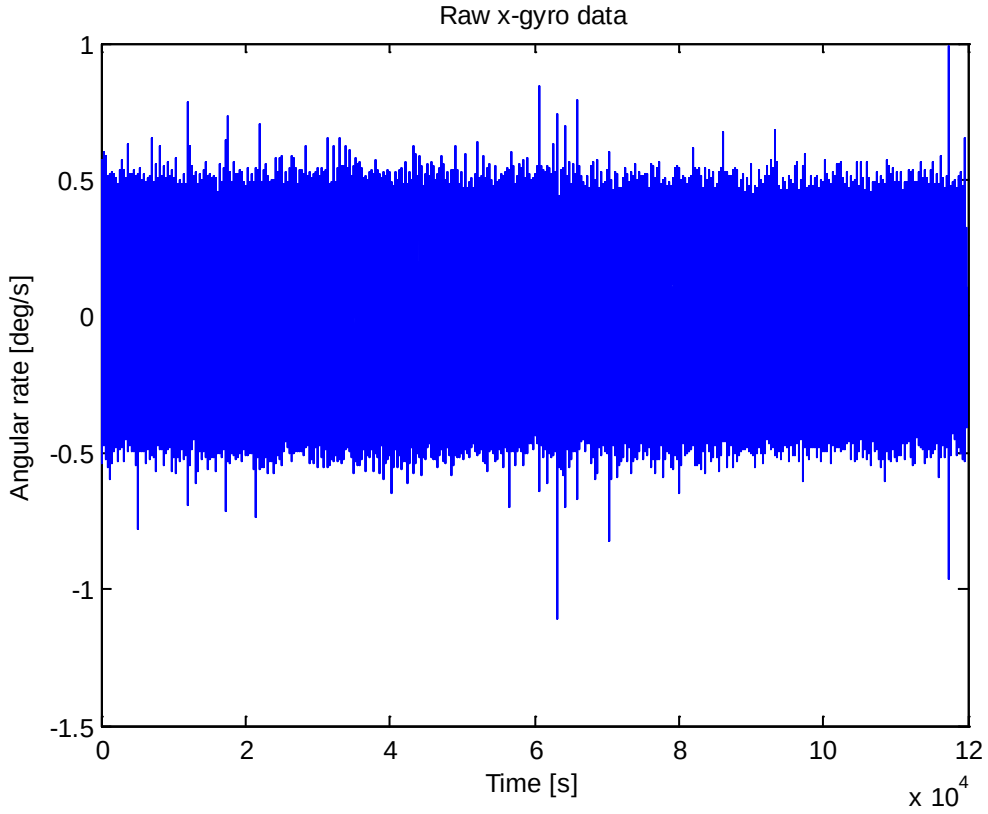

Figure 3.15 Raw data from the SiIMU02 x-gyro.

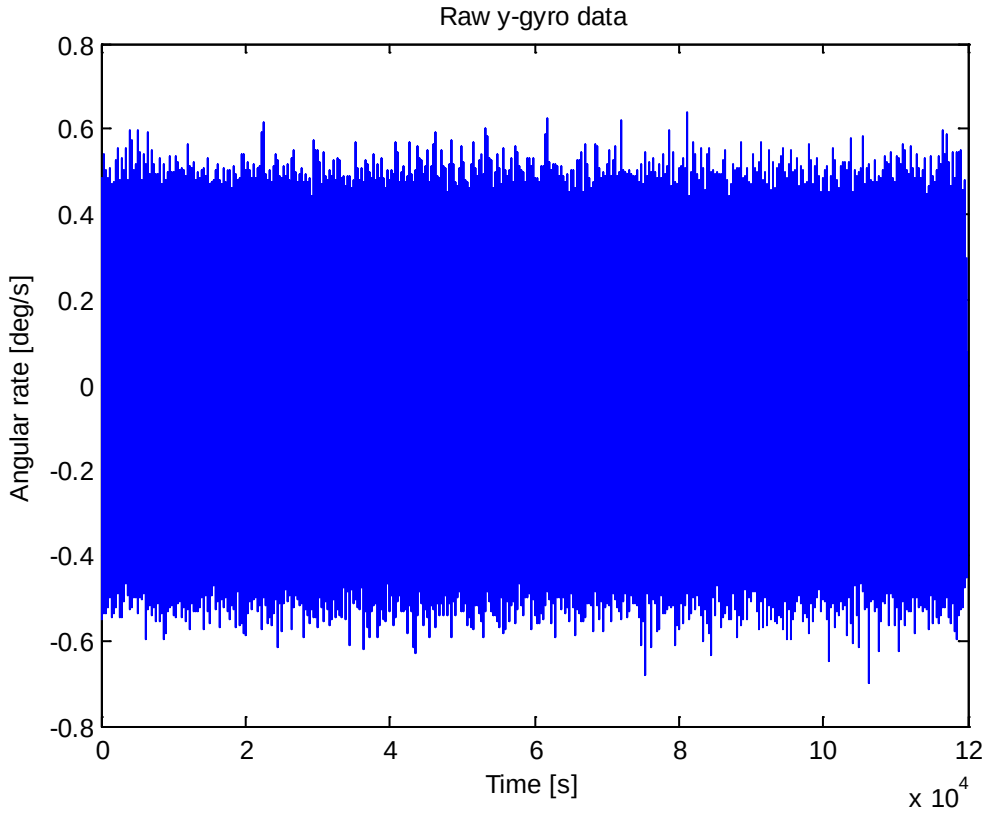

Figure 3.16 Raw data from the SiIMU02 y-gyro.

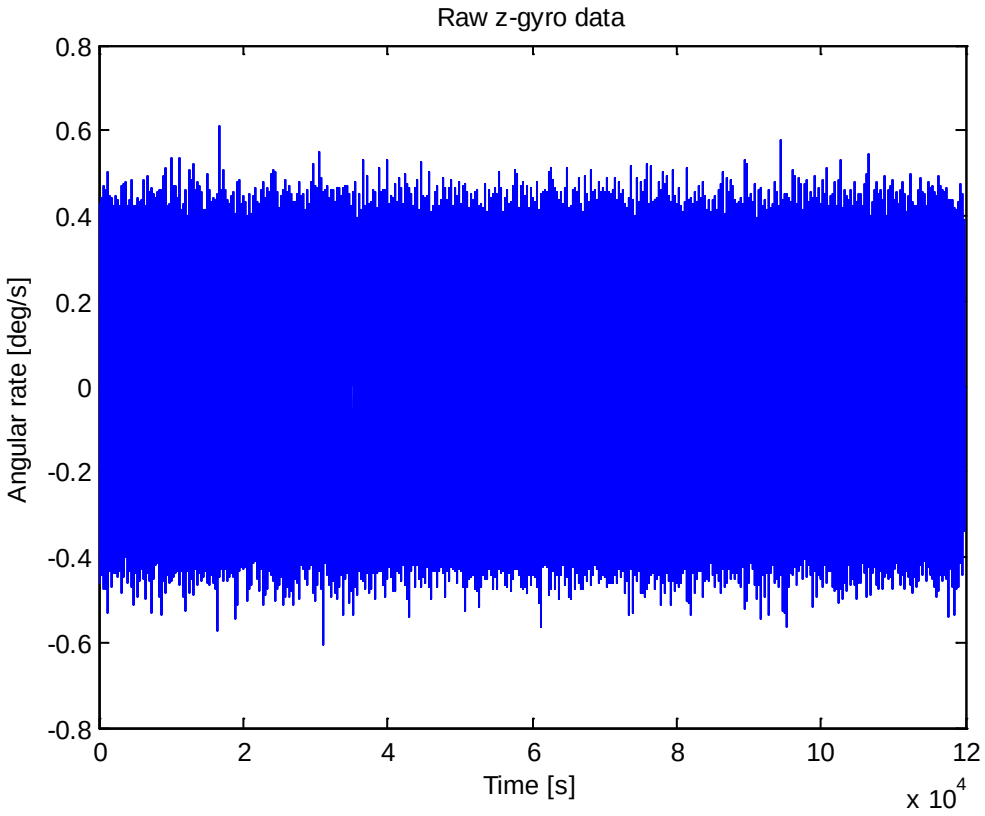

Figure 3.17 Raw data from the SiIMU02 z-gyro.

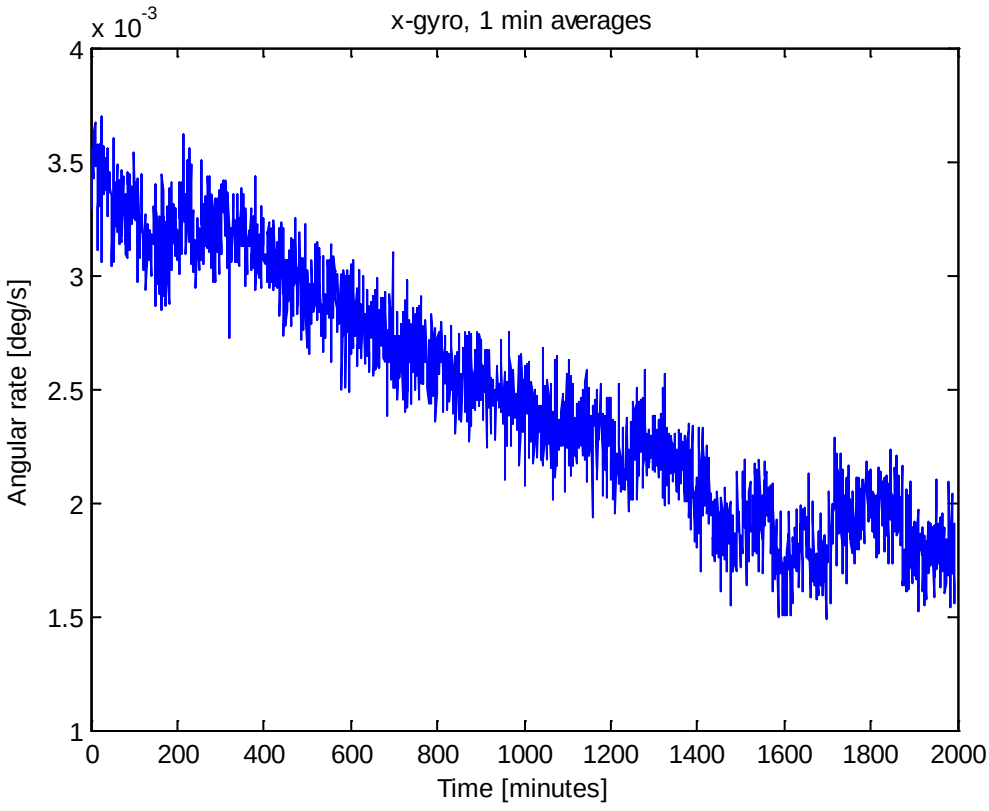

Figure 3.18 SiIMU02 x-gyro averaged over 1 minute intervals.

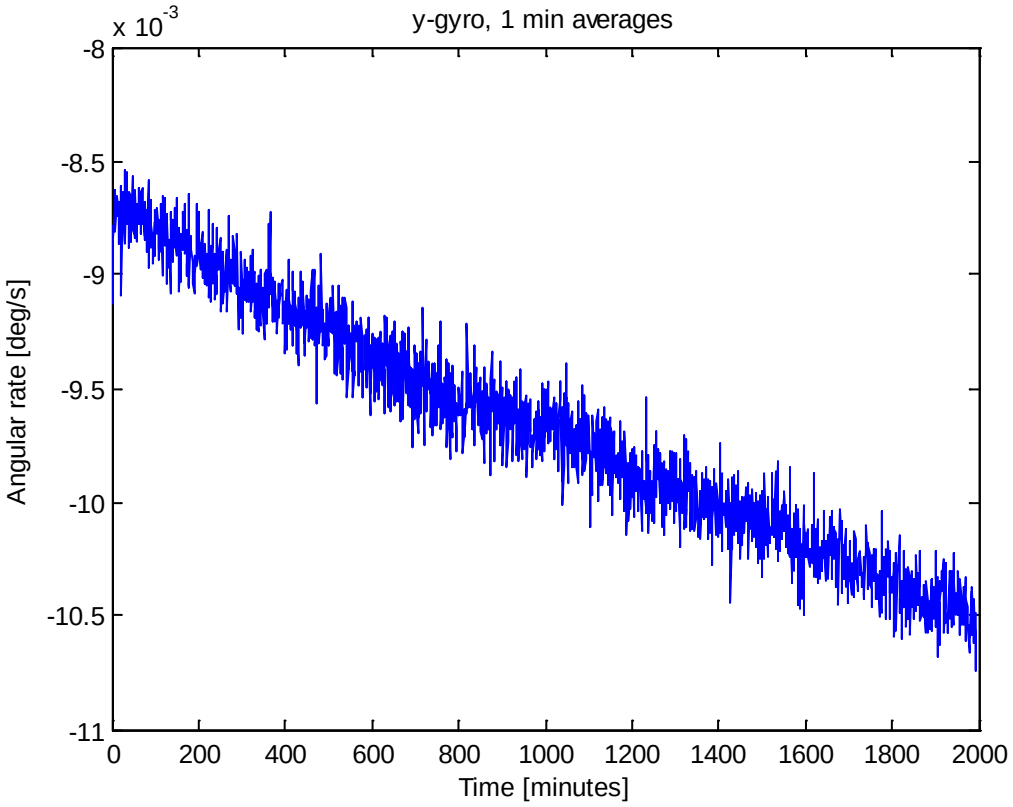

Figure 3.19 SiIMU02 y-gyro averaged over 1 minute intervals.

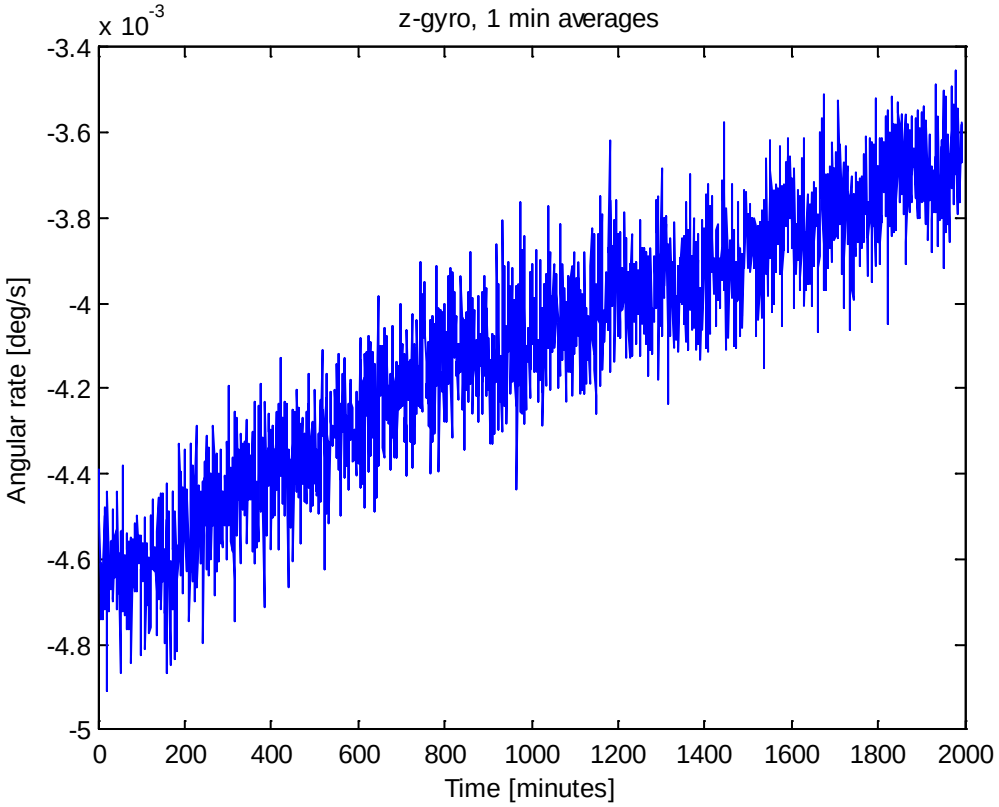

Figure 3.20 SiIMU02 z-gyro averaged over 1 minute intervals.

Figure 3.21 shows computed root Allan variance for the three gyros. As before, the delta v measurements from the accelerometers were pre summed over 1 second intervals before computing the Allan variance. Based on the Allan variance plots, the angular random walk and bias instability values were estimated. The angular random walk estimates were 0.0065, 0.0057 and 0.021 deg/sqrt(h) for the x, y and z gyro, respectively, well within the specified value of 0.1 deg/sqrt(h). The bias instability estimates (i.e. the minimum value of the root Allan variance curves) were 0.2, 0.1 and 0.1 deg/h, again well within the specified value of 1.5 deg/h.

The Allan variance curves also have a distinct positive slope for long averaging times, indicating the presence of rate random walk (slope +1/2), and rate ramp (slope +1) errors. This is also in correspondence with the drift in the angular rate visible in Figure 3.18 to Figure 3.20.

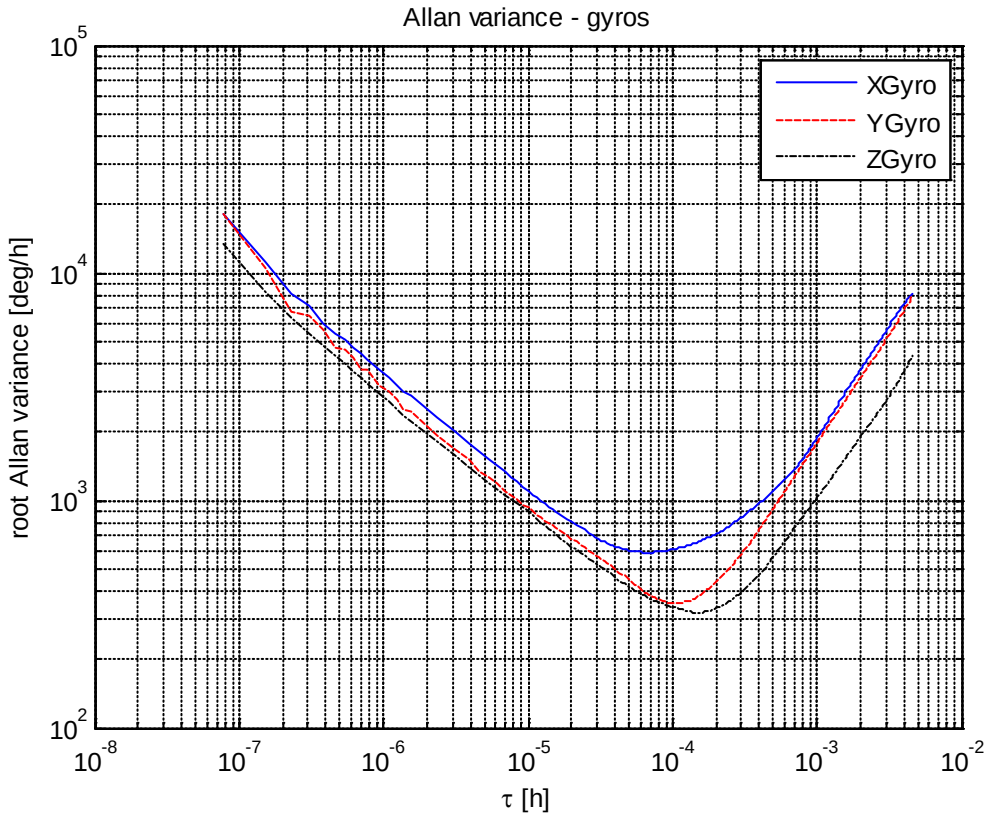

Figure 3.21 Computed root Allan variances - SiIMU02 gyros.

Figure 3.22 through Figure 3.24 show spectral density plots for the gyro measurements. Each gyro has a small maximum at a frequency between 20 and 30 Hz, slightly different between the different gyros.

Figure 3.22 Spectral density plot, SiIMU02 x-gyro.

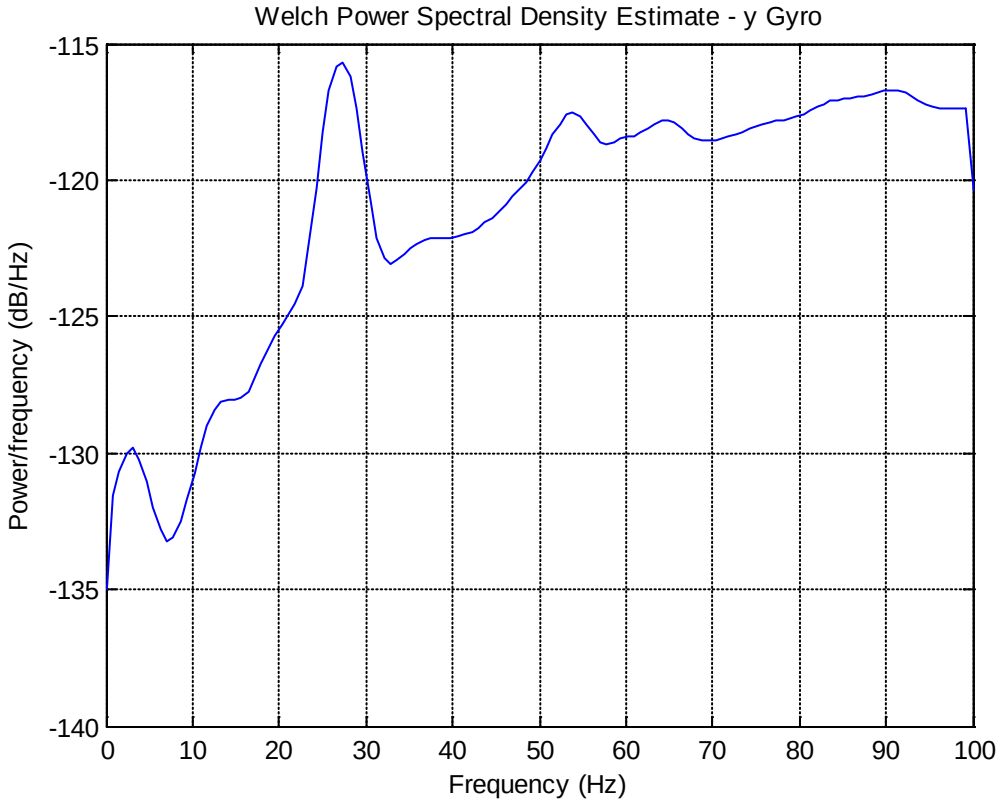

Figure 3.23 Spectral density plot, SiIMU02 y-gyro.

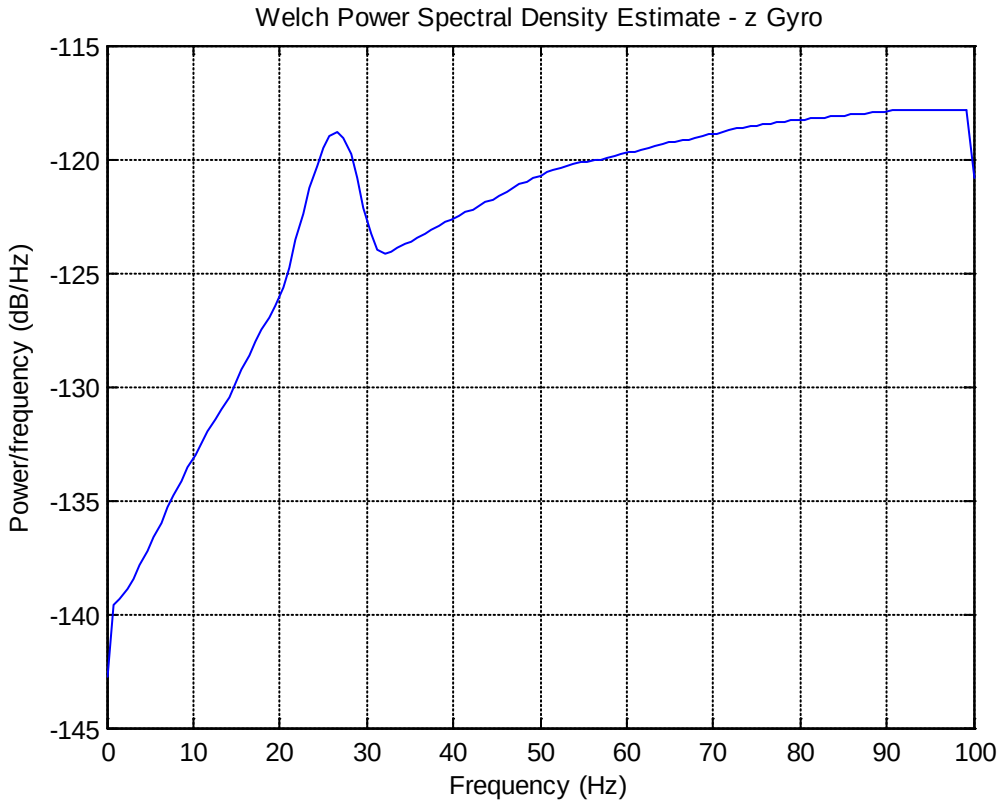

Figure 3.24 Spectral density plot, SiIMU02 z-gyro.

Figure 3.25 through Figure 3.27 show histograms of the gyro measurements. The distributions here are also Gaussian-like. The standard deviations of the angular rates (delta theta divided by delta time) were (0.1216, 0.1226, 0.1078) deg/s, for the x, y, and z gyro, respectively.

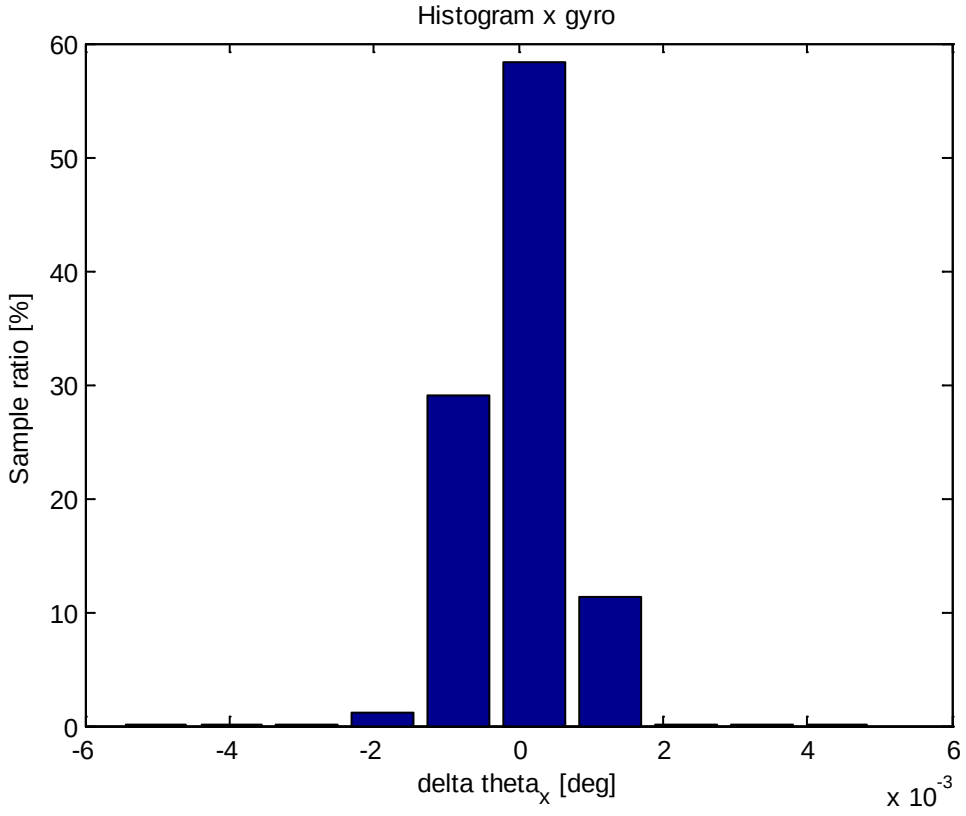

Figure 3.25 SiIMU x gyro histogram.

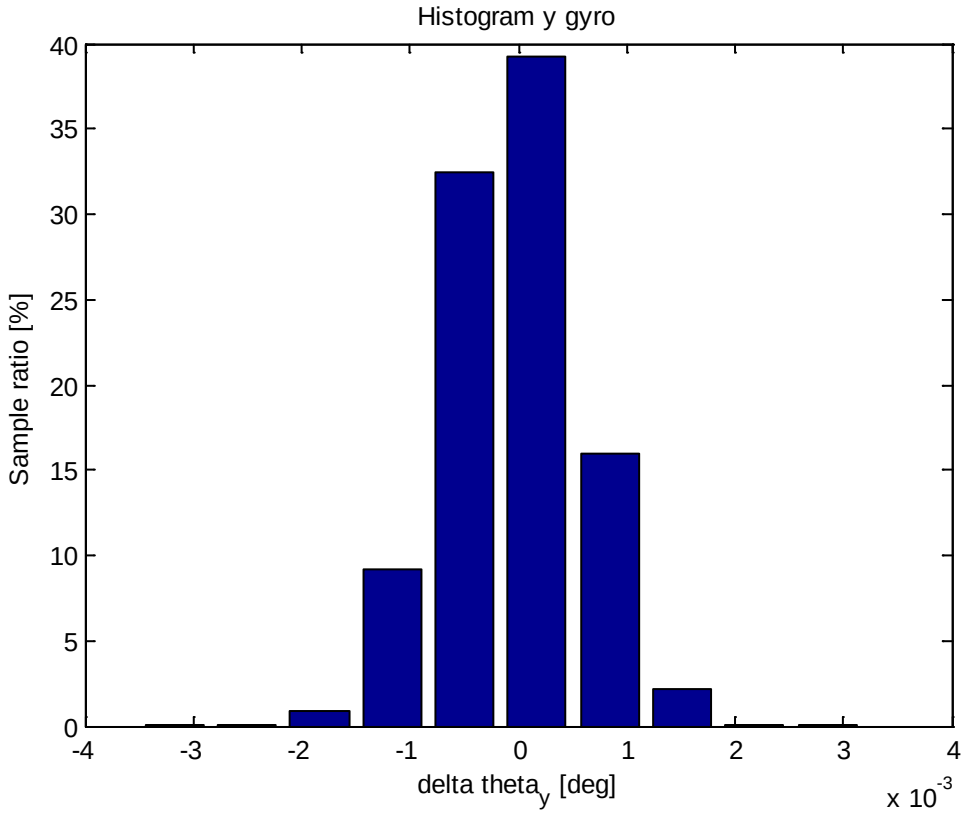

Figure 3.26 SiIMU y gyro histogram.

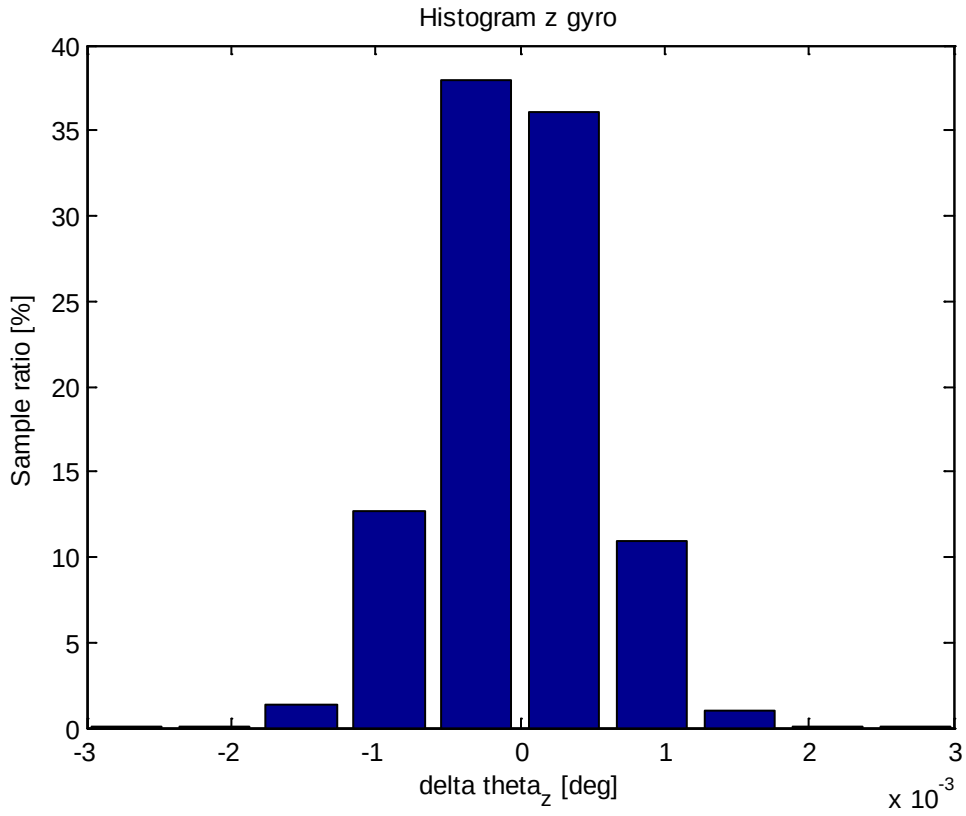

Figure 3.27 SiIMU z gyro histogram.

3.1.2 Repeatability and temperature tests

To check how the output of the gyros varies from power-on to power-on, static data from a number of different power-ons was logged. In addition, to test the sensitivity to temperature variations, the unit was placed in a temperature chamber, and the output was logged both at constant temperatures at different temperature levels, and during temperature variations.

The norms of the mean 3-dimensional accelerometer and gyro measurement vectors in the different tests, together with the standard deviations for the different axes are shown in Table 3.2 and Table 3.3. Notice the high values of the accelerometer measurements, significantly higher than the true acceleration of gravity. This suggests large accelerometer biases. Except for two of the tests (TempTest_10_grader and TempTest_-30_grader), in which the measured value is smaller than standard g, the output is rather stable throughout all the tests. The same is true for the standard deviations. The gyro output seems to be more sensitive to temperature variations. This is particularly evident for the mean output at low temperatures (-20 and -30 ˚C) and at high temperatures (40 and 50 ˚C). The standard deviations do not vary significantly throughout the tests.

Table 3.2 Mean SiIMU02 accelerometer measurements and standard deviations in repeatability and temperature tests.

Test name	norm(mean(f)) [m/s^2]	std f_x [m/s^2]	std f_y [m/s^2]	std f_z [m/s^2]
Langtidstest	9.9864	0.0603	0.0447	0.0459
OppstartsTest	9.8545	0.0673	0.0415	0.0417
Repeterbarhet_1	9.9887	0.06	0.0421	0.044
Repeterbarhet_2	9.9896	0.0603	0.0415	0.0433
Repeterbarhet_3	9.9901	0.0601	0.0408	0.0425
TempTest_0_grader	9.7961	0.0627	0.0394	0.0424
TempTest_-10_grader	9.9731	0.0641	0.0404	0.0464
TempTest_10_grader	9.7925	0.063	0.0382	0.0416
TempTest_-20_grader	9.9749	0.0664	0.0402	0.0465
TempTest_20_til_-20_grader	9.9674	0.0644	0.0696	0.044
TempTest_20grader	9.9736	0.0625	0.0364	0.0396
TempTest_-30_grader	9.7976	0.064	0.0446	0.0498
TempTest_30_grader	9.9799	0.0604	0.0352	0.0353
TempTest_40_grader	9.9776	0.0582	0.0339	0.0351
TempTest_50_grader	9.964	0.0582	0.0327	0.0324

Table 3.3 Mean SiIMU02 gyro measurements and standard deviations in repeatability and temperature tests.

Test name	norm(mean(ω)) [deg/s]	std ω_x [deg/s]	std ω_y [deg/s]	std ω_z [deg/s]
Langtidstest	0.0108	0.1216	0.1226	0.1078
OppstartsTest	0.013	0.1307	0.1219	0.1084
Repeterbarhet_1	0.0121	0.1177	0.1232	0.1078
Repeterbarhet_2	0.0123	0.1176	0.1235	0.1077
Repeterbarhet_3	0.0122	0.1168	0.1233	0.1077
TempTest_0_grader	0.0274	0.1129	0.1172	0.0984
TempTest_-10_grader	0.0299	0.1154	0.1121	0.0984
TempTest_10_grader	0.0196	0.1204	0.1191	0.1019
TempTest_-20_grader	0.0298	0.1178	0.1062	0.095
TempTest_20_til_-20_grader	0.0193	0.1163	0.1128	0.0977
TempTest_20grader	0.0179	0.1194	0.1237	0.1055
TempTest_-30_grader	0.0429	0.1175	0.1043	0.0945
TempTest_30_grader	0.0146	0.1154	0.1214	0.1113
TempTest_40_grader	0.028	0.1207	0.1242	0.1144
TempTest_50_grader	0.027	0.1228	0.1269	0.1186

3.1.3 Up/down tests

The results from the up/down tests are shown in Table 3.4 and Table 3.5. The results are color coded, such that values within the specifications are coded as green, values outside 1 sigma, but within 3 sigma are codes as yellow, whereas values outside 3 sigma are coded in red. In cases where the specification is given as a maximum value, green is used for values less than the maximum value, whereas red is used when the value exceeds the maximum value. This color convention is used throughout the report.

As previously suggested, the up/down tests show that the accelerometer biases are high both for the x and z accelerometer, which both exceed the 1 sigma specification, but are still within 2 sigma. In addition, the accelerometer scale factor errors for the y and z accelerometers are between 2 and 3 sigma. The gyro biases are within the specifications.

Table 3.4 SiIMU02 accelerometer parameters computed from up/down tests

Test	x acc. bias (mg)	x acc. scale factor (ppm)	y acc. bias (mg)	y acc. scale factor (ppm)	z acc. bias (mg)	z acc. scale factor (ppm)
1/2 (x up)	15.6	317				
3/4 (z up)					12.5	3883
5/6 (y up)			6.8	3935		
Spec.	10	1500	10	1500	10	1500

Table 3.5 SiIMU02 gyro parameters computed from up/down test.

Test	x gyro bias (deg/h)	y gyro bias (deg/h)	z gyro bias (deg/h)
1/2 (x up)	39.5		
3/4 (z up)		-11.1	
5/6 (y up)			-13.4
Spec.	50	50	50

3.2 Sensonor STIM300

Figure 3.28 Sensonor STIM300 IMU

The STIM300 [3] is a MEMS-based IMU manufactured by the Norwegian company Sensonor. It contains 3 gyroscopes, 3 accelerometers and 3 inclinometers. The inclinometers were not evaluated in these tests.

Table 3.6 Specifications of the Sensonor STIM300.

	Gyros	Accelerometers
Bias range	±250 deg/hr	
Bias on/off repeatability		±0.75 mg
Bias instability	0.5 deg/hr	0.05 mg
Random walk	0.15 deg/√hr	0.06 m/s/√hr
Scale factor accuracy	± 500 ppm	±300 ppm

3.2.1 Long term static test

In this test, the unit was placed on a stable table, with the x-accelerometer pointing down. The unit was powered on, after having been turned off for an extended period. Thus, potential effects due to self-warming would be visible in the data.

3.2.1.1 Accelerometers

Figure 3.29 to Figure 3.31show the output from the accelerometers during the static test. As the output is given as delta velocity measurements, the values plotted are divided by delta t (0.0020 s in this case), to obtain accelerations. As seen in Figure 3.31 the z-accelerometer was oriented vertically, measuring gravity. Notice the low measurement value from this accelerometer compared to standard gravity (9.7655 m/s^2, when averaged over the whole test), indicating a large accelerometer bias. Contrary to what was the case for the SiIMU accelerometer data, there is no obvious drift in the data. Figure 3.32 to Figure 3.34 show the accelerometer output averaged over 1 minute intervals. No significant startup effects are visible.

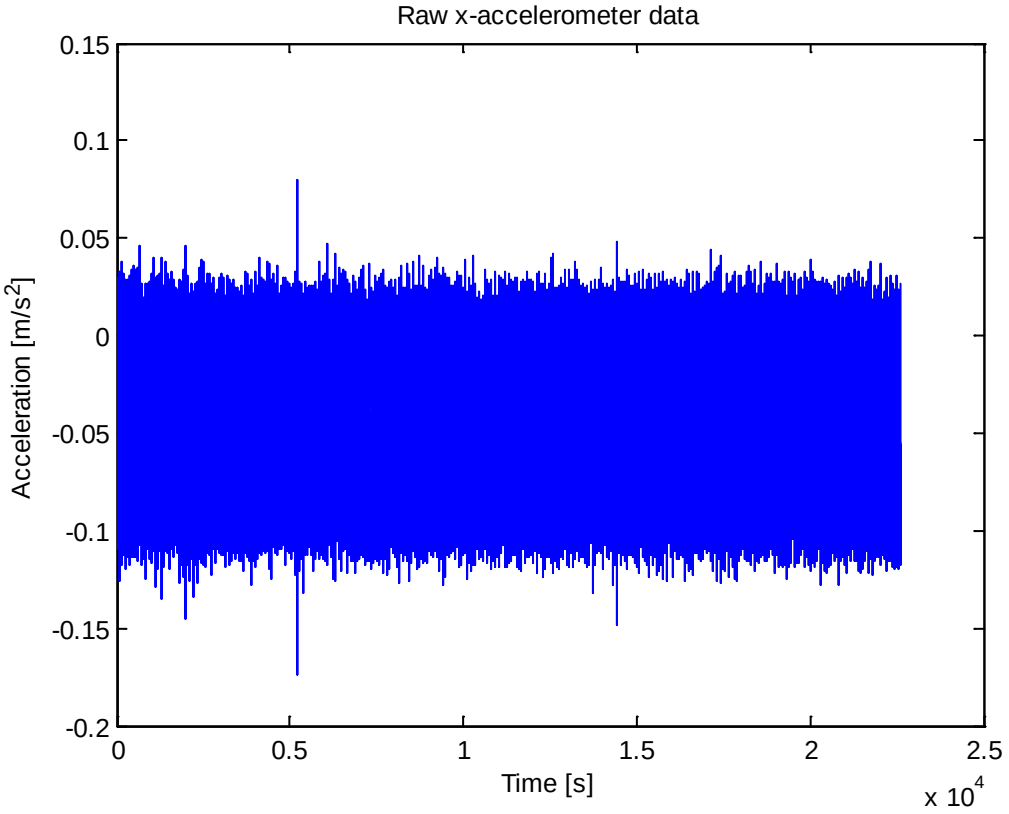

Figure 3.29 Raw data from the STIM300 x accelerometer.

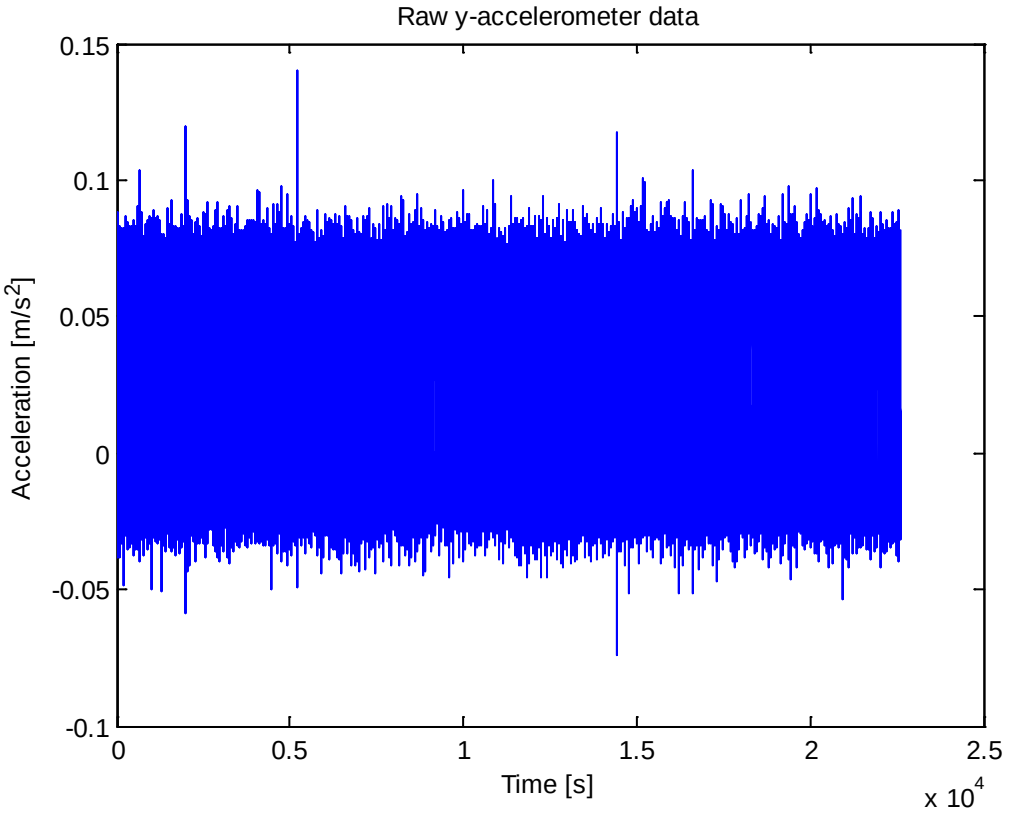

Figure 3.30 Raw data from the STIM300 y accelerometer.

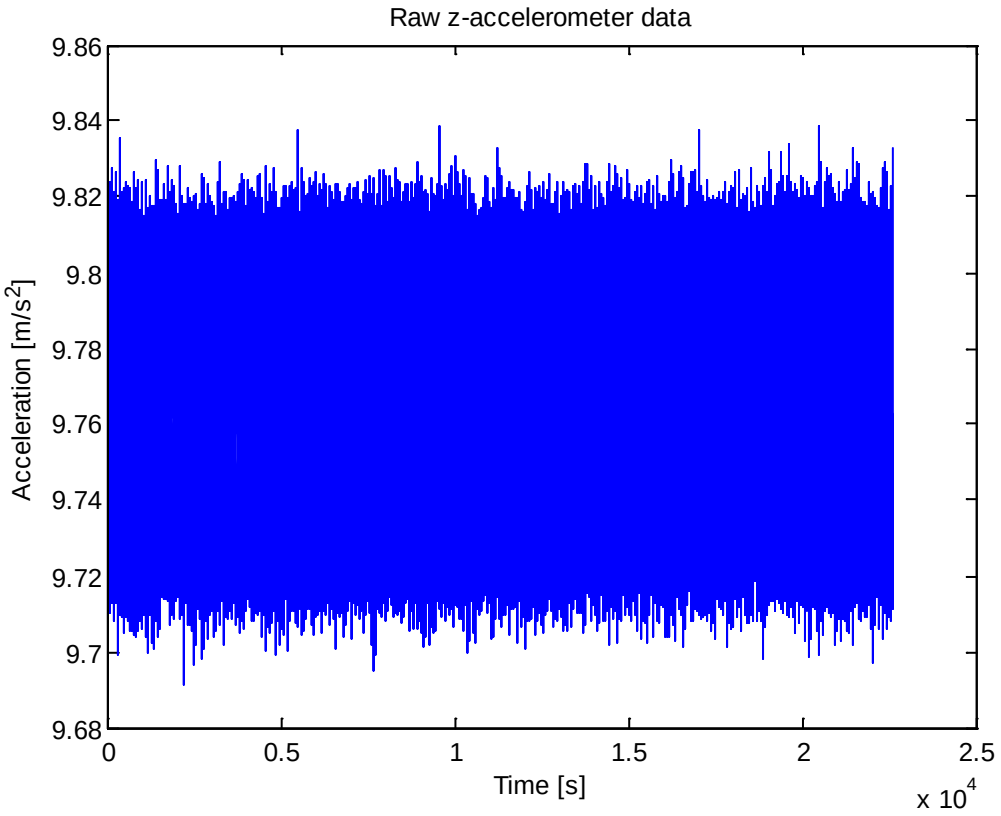

Figure 3.31 Raw data from the STIM300 z accelerometer.

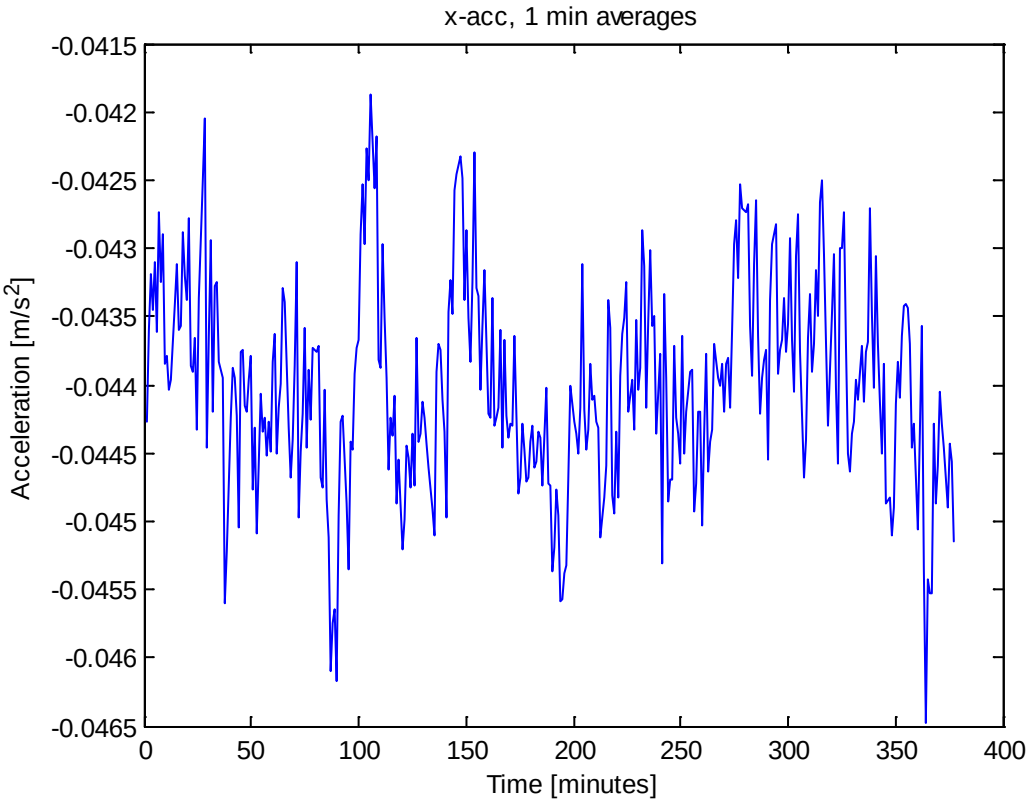

Figure 3.32 STIM 300 x accelerometer data averaged over 1 minute intervals.

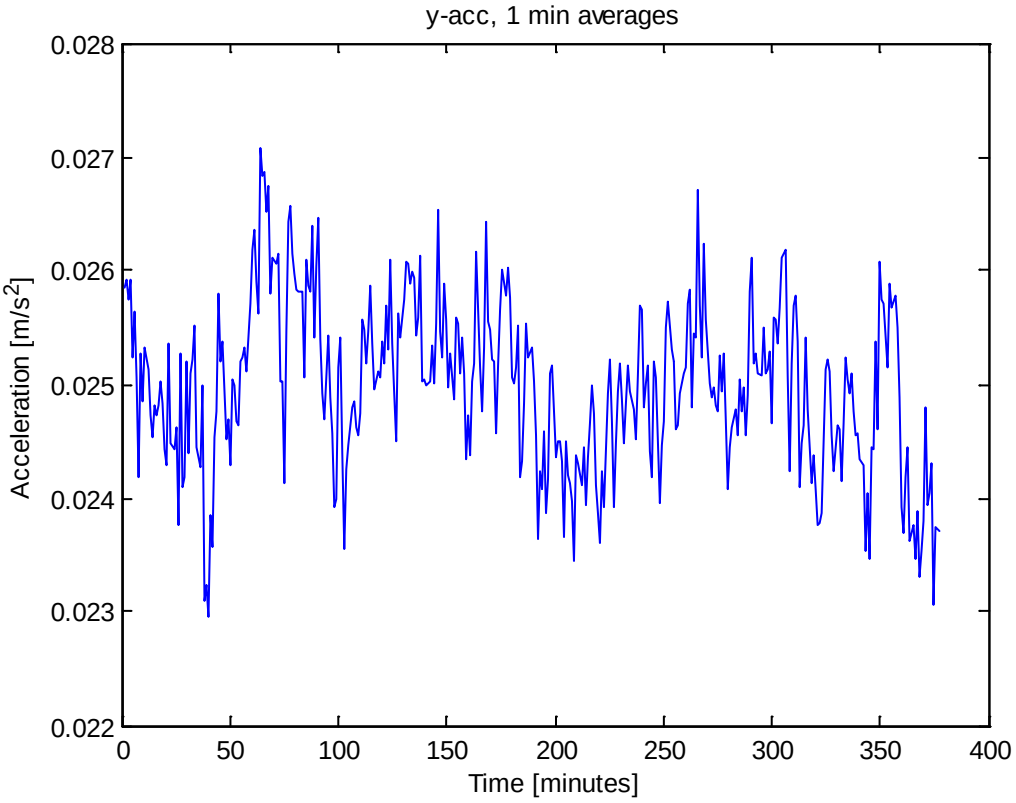

Figure 3.33 STIM 300 y accelerometer data averaged over 1 minute intervals.

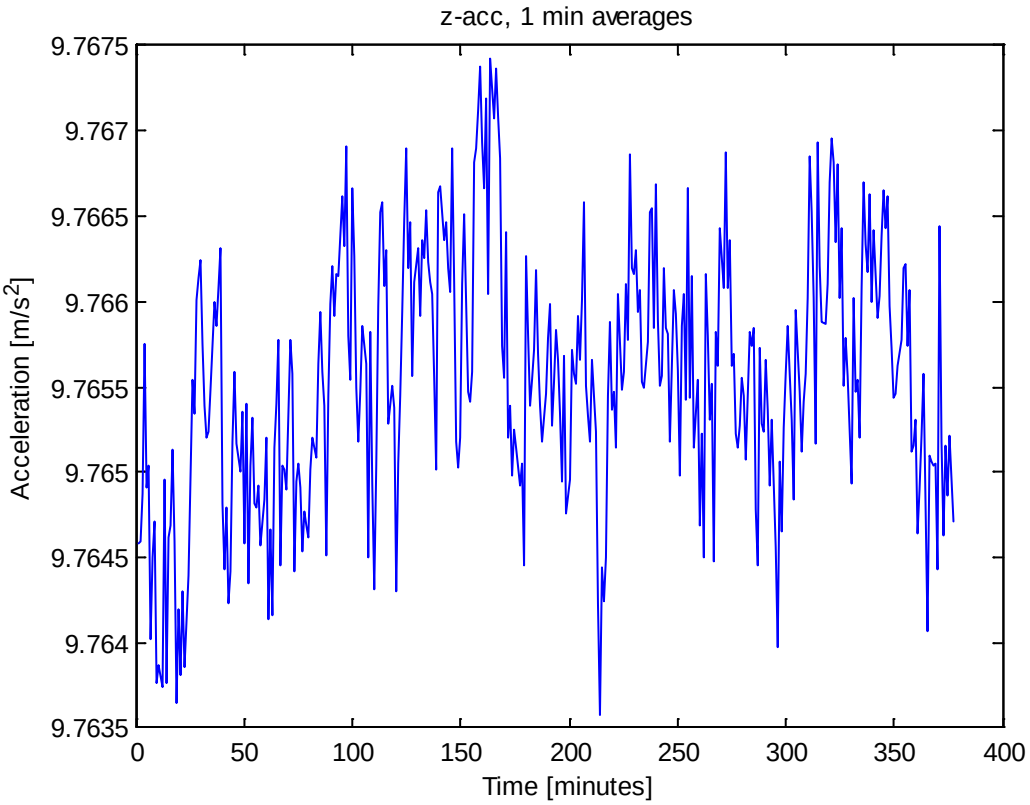

Figure 3.34 STIM 300 z accelerometer data averaged over 1 minute intervals.

Figure 3.35 shows computed root Allan variance from the three accelerometers from the entire test interval. The same pre summing over 1 second intervals as before was used. Based on the Allan variance plots, the velocity random walk and bias instability values were estimated. The velocity random walk estimates were 0.083, 0.067 and 0.069 m/s/sqrt(h) for the x, y and z accelerometer, respectively, all slightly above the specified value of 0.06 m/s/sqrt(h). The bias instability estimates (i.e. the minimum value of the root Allan variance curves) were 0.03, 0.04 and 0.02 mg for the three axes, all within the specification of 0.05 mg.

The accelerometer Allan variance plots are dominated by velocity random walk (slope -1/2) for $\tau < 10^2$ seconds and bias instability (slope 0) for $\tau > 10^2$ seconds. For longer averaging times, the number of samples that are averaged over is low, leading to poor Allan variance estimates, seen as negative slopes in the Allan variance curve.

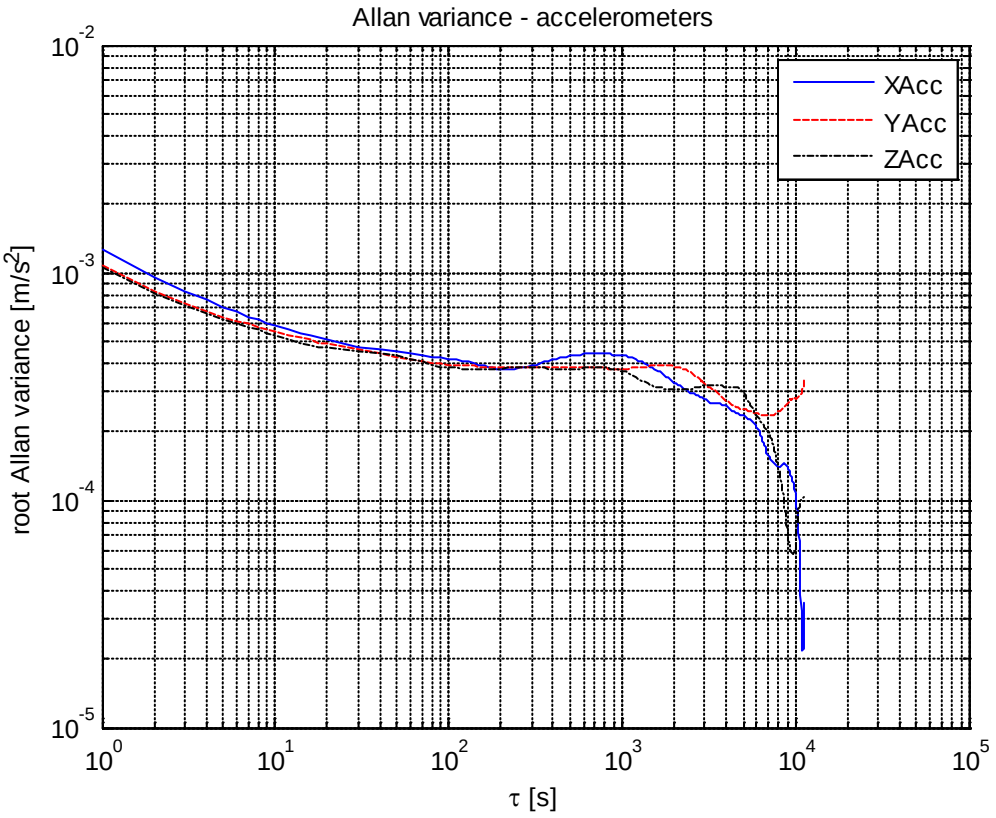

Figure 3.35 Computed Allan variances from the STIM300 accelerometers.

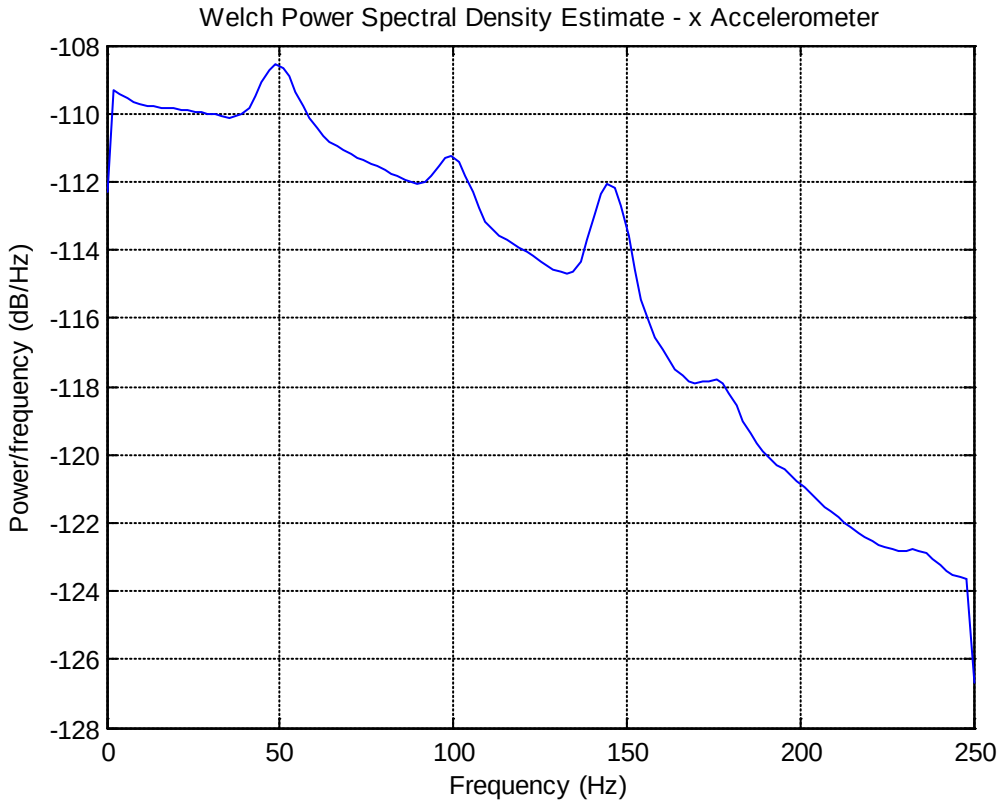

Figure 3.36 Spectral density plot, SiIMU02 x accelerometer.

Figure 3.36 to Figure 3.38 show the computed spectral densities of the accelerometers. The frequencies seem to be rather evenly distributed. There are a few local maxima for certain frequencies, but these are too small to be of any significance.

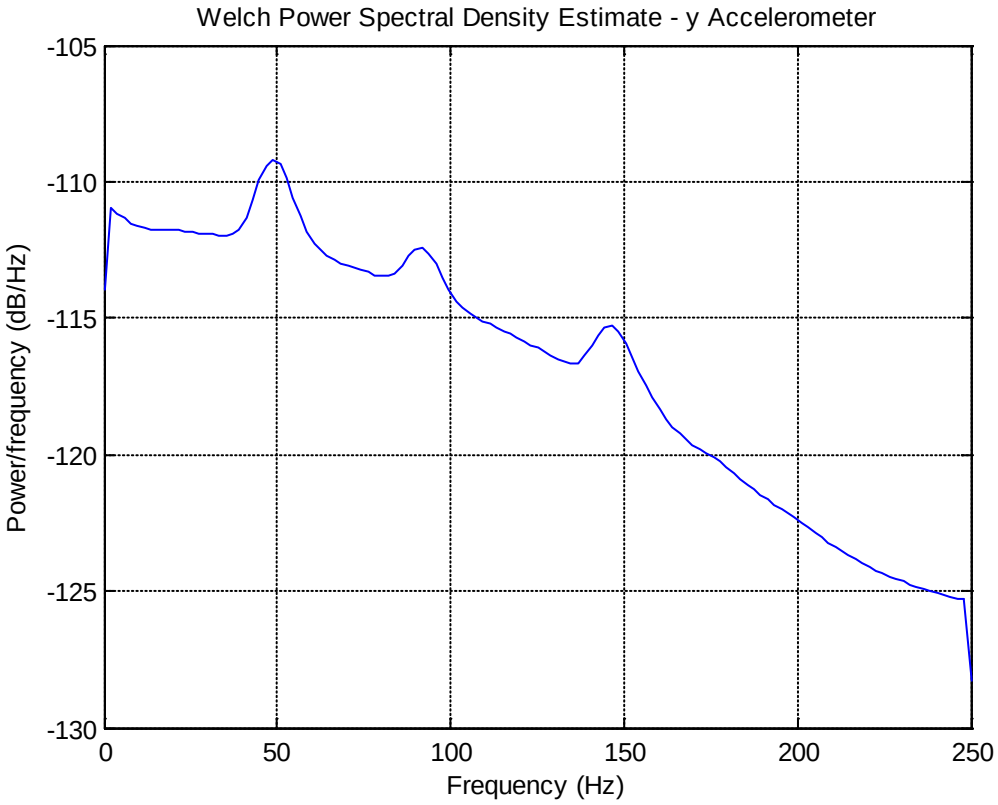

Figure 3.37 Spectral density plot, SiIMU02 y accelerometer.

Figure 3.38 Spectral density plot, SiIMU02 z accelerometer.

Figure 3.39 to Figure 3.41 show histograms for the raw accelerometer measurements. All histograms show a Gaussian-like distribution. The standard deviations of the measured accelerations (delta velocity divided by delta time) are (0.0096, 0.0086, 0.0072) m/s^2 for the x, y and z accelerometer, respectively.

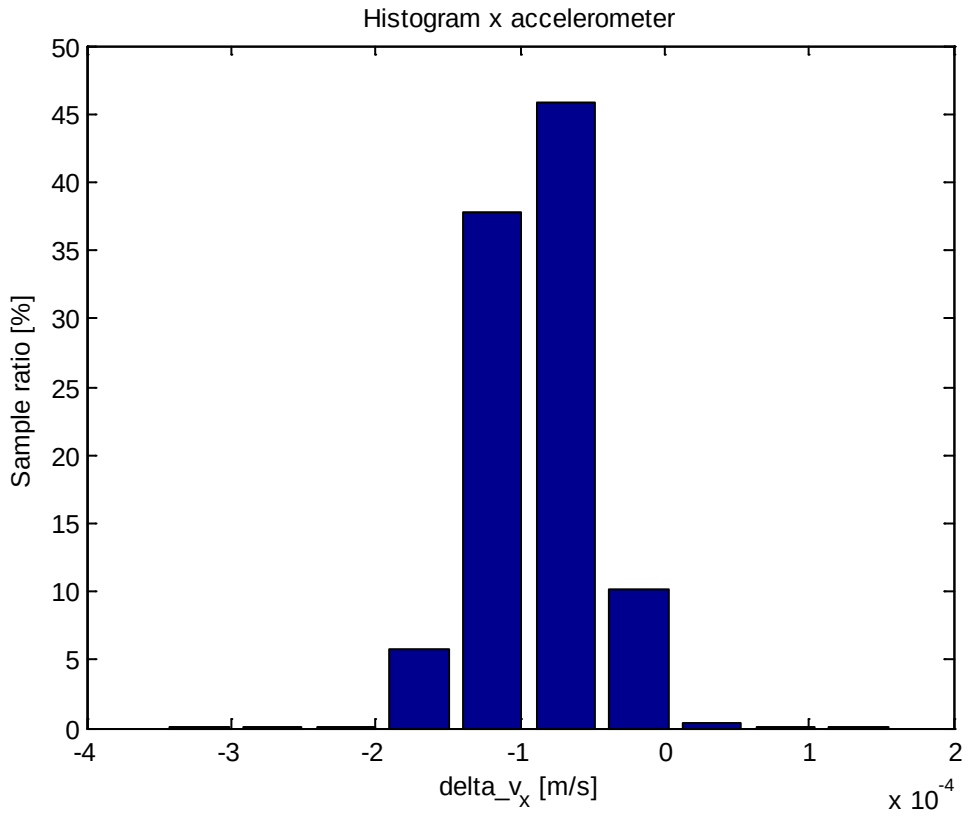

Figure 3.39 STIM300 x accelerometer histogram.

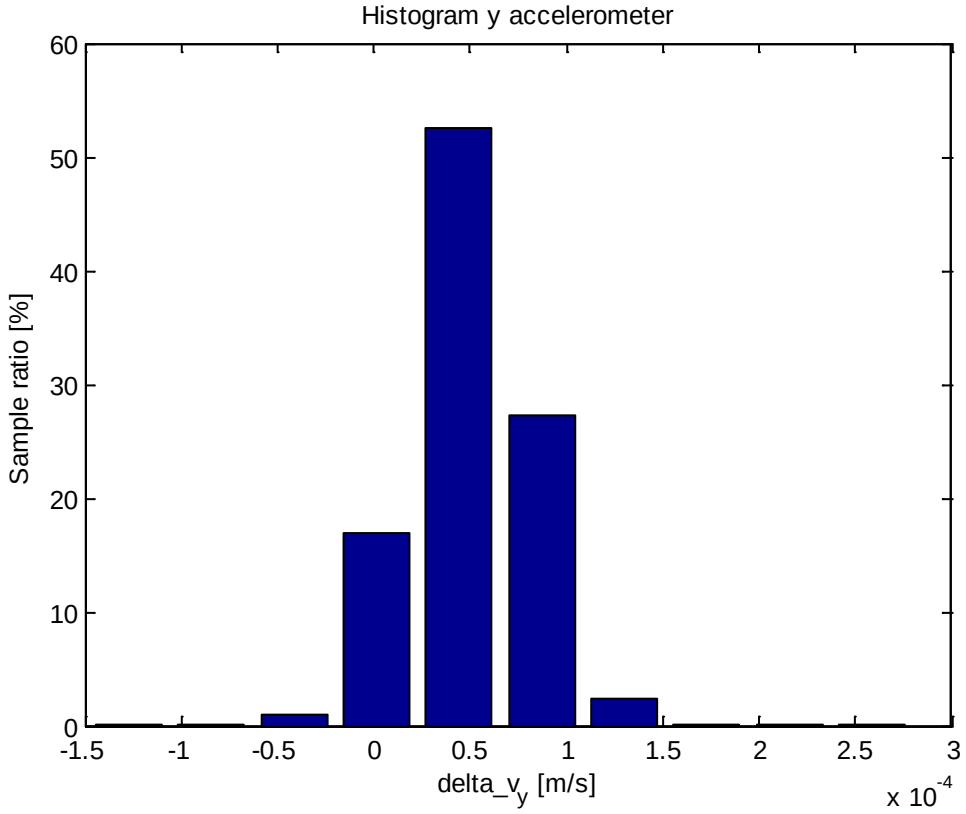

Figure 3.40 STIM300 y accelerometer histogram.

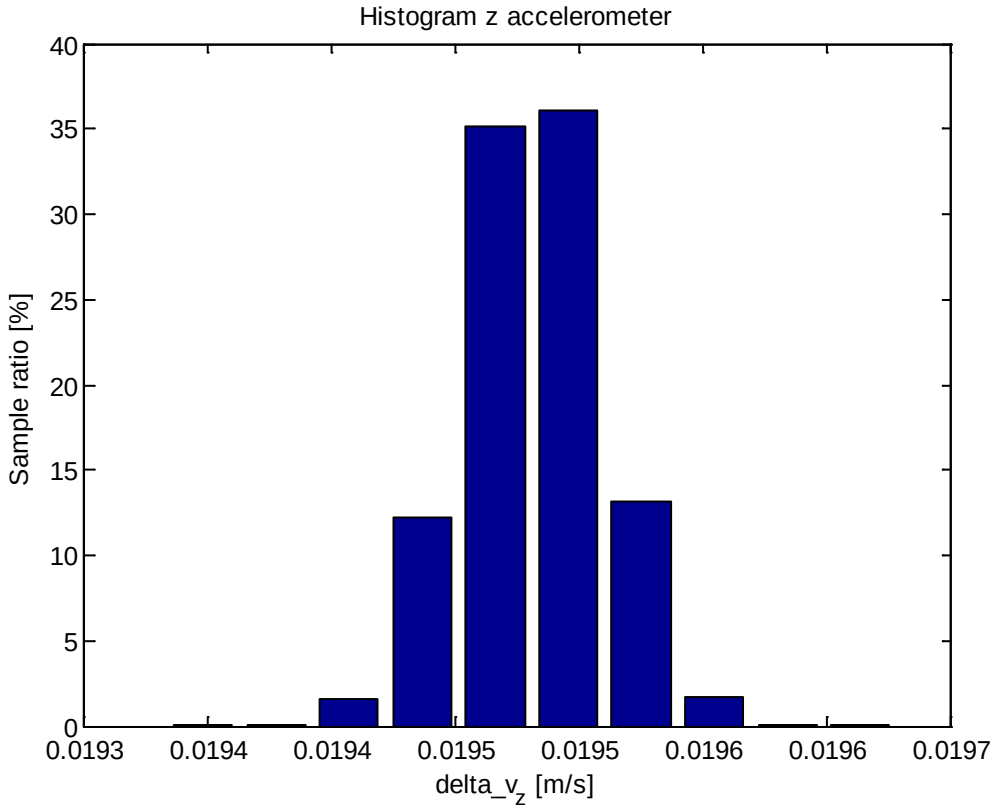

Figure 3.41 STIM300 z accelerometer histogram.

3.2.1.2 Gyroscopes

Figure 3.42 to Figure 3.44 show raw data from the STIM300 gyroscopes throughout the static test. The same data averaged over 1 minute intervals are shown in Figure 3.45 to Figure 3.47. A small drift in the rate data (a rate random walk, or possibly a rate ramp) can be seen in the z gyro data.

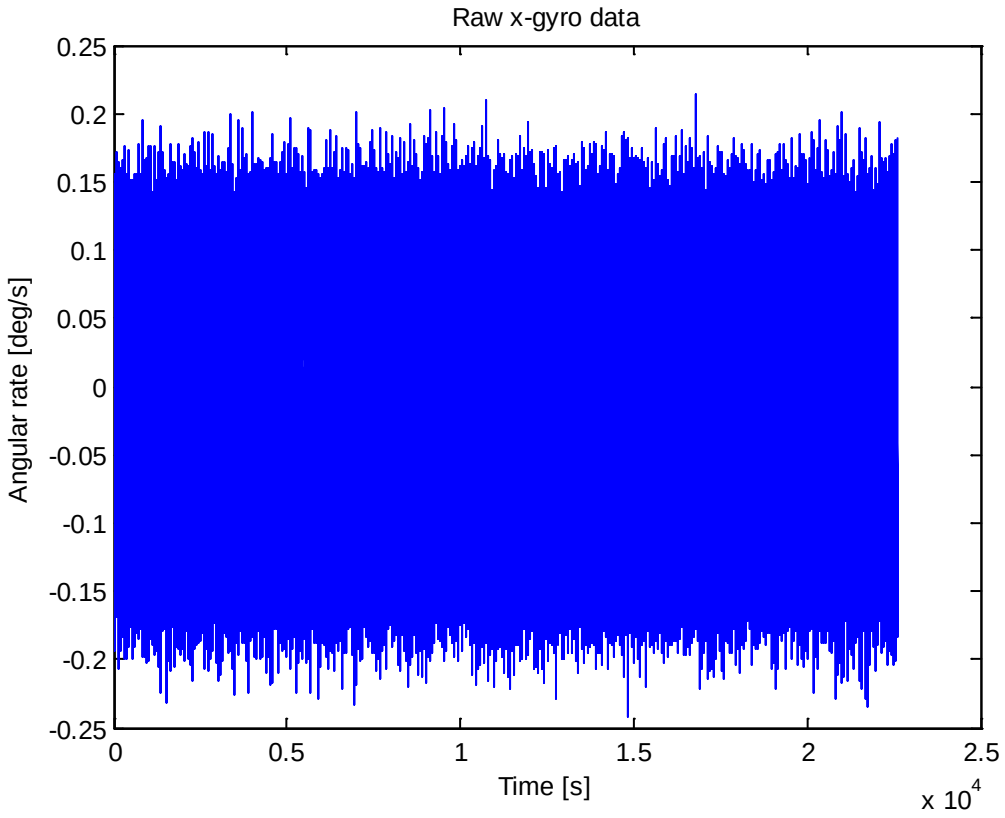

Figure 3.42 Raw data from the STIM300 x gyro.

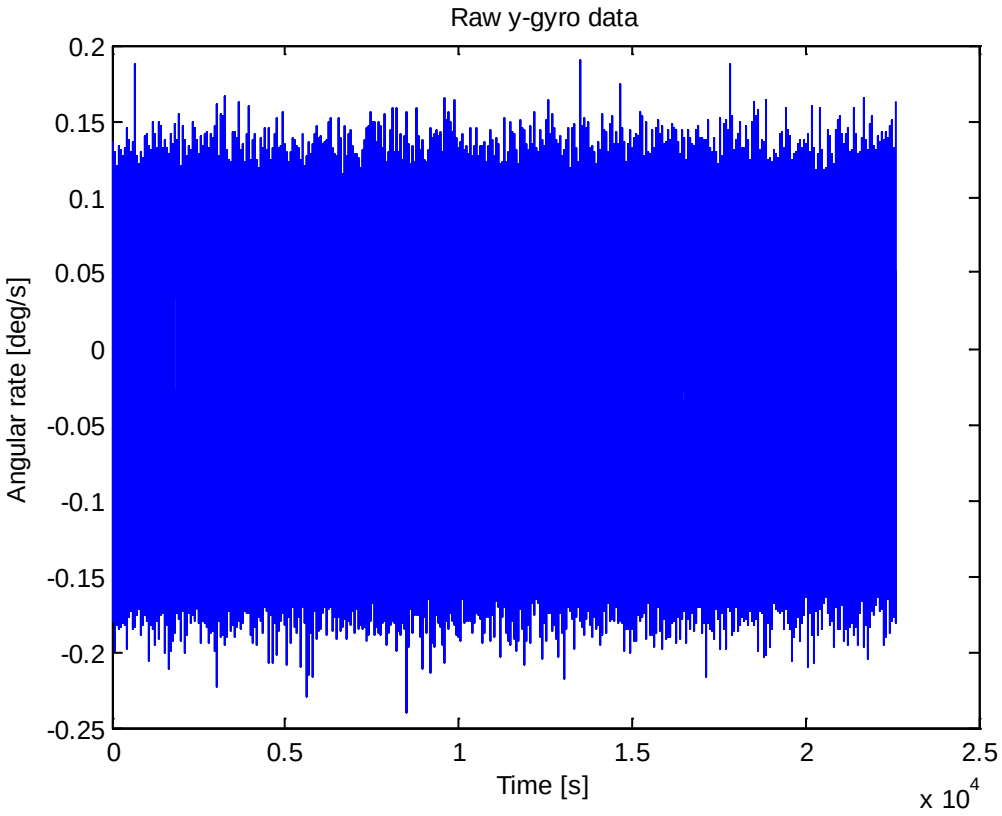

Figure 3.43 Raw data from the STIM300 y gyro.

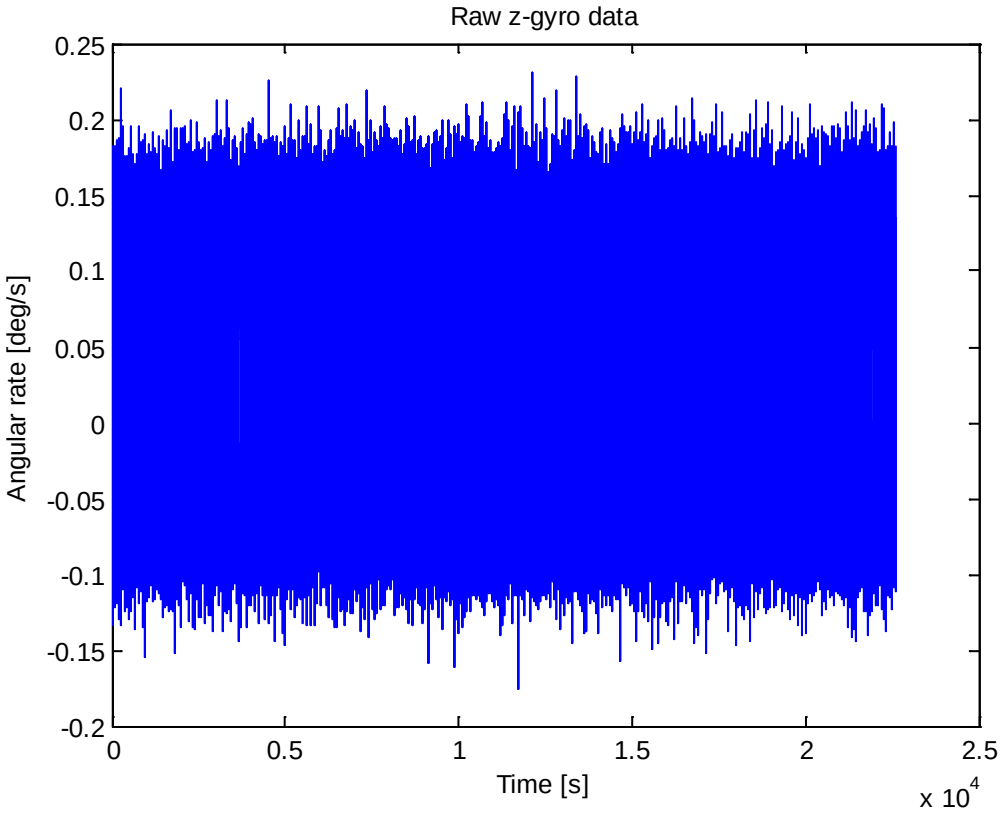

Figure 3.44 Raw data from the STIM300 z gyro.

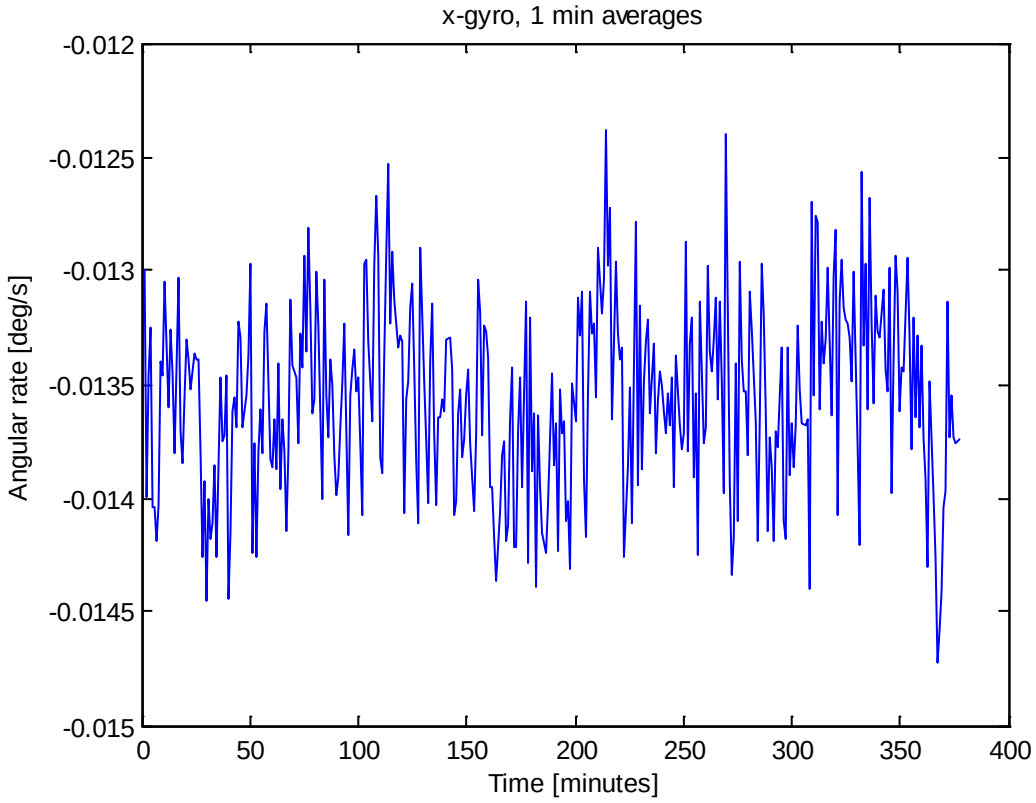

Figure 3.45 STIM 300 x gyro data averaged over 1 minute intervals.

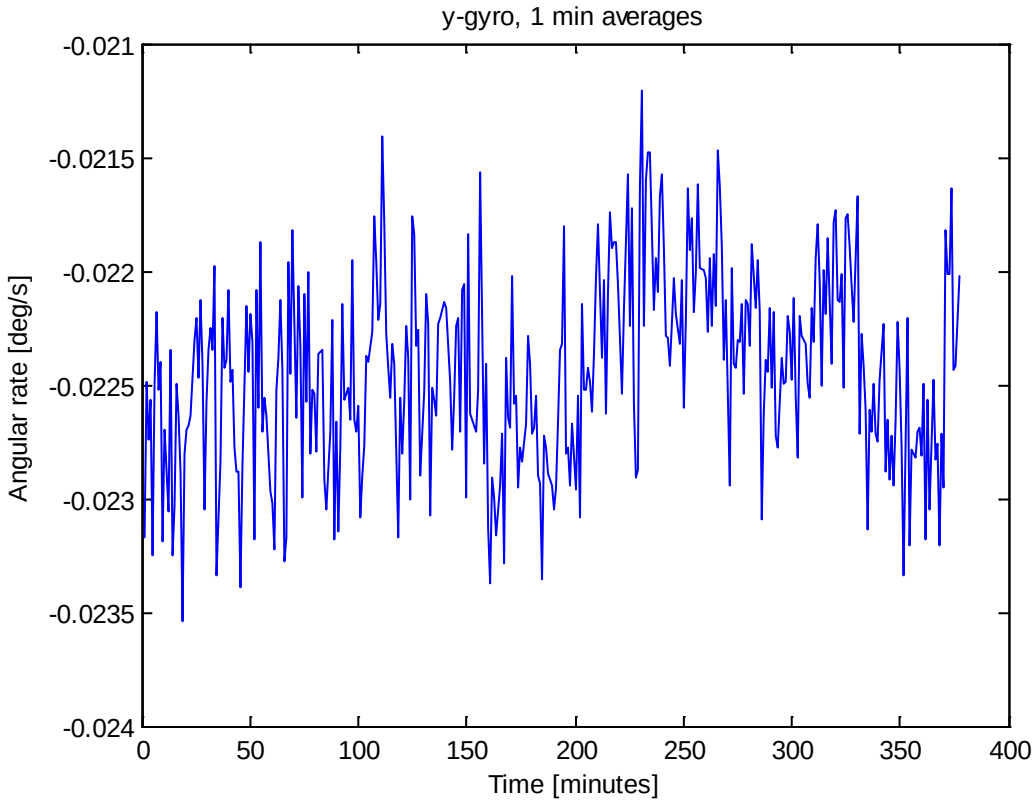

Figure 3.46 STIM 300 y gyro data averaged over 1 minute intervals.

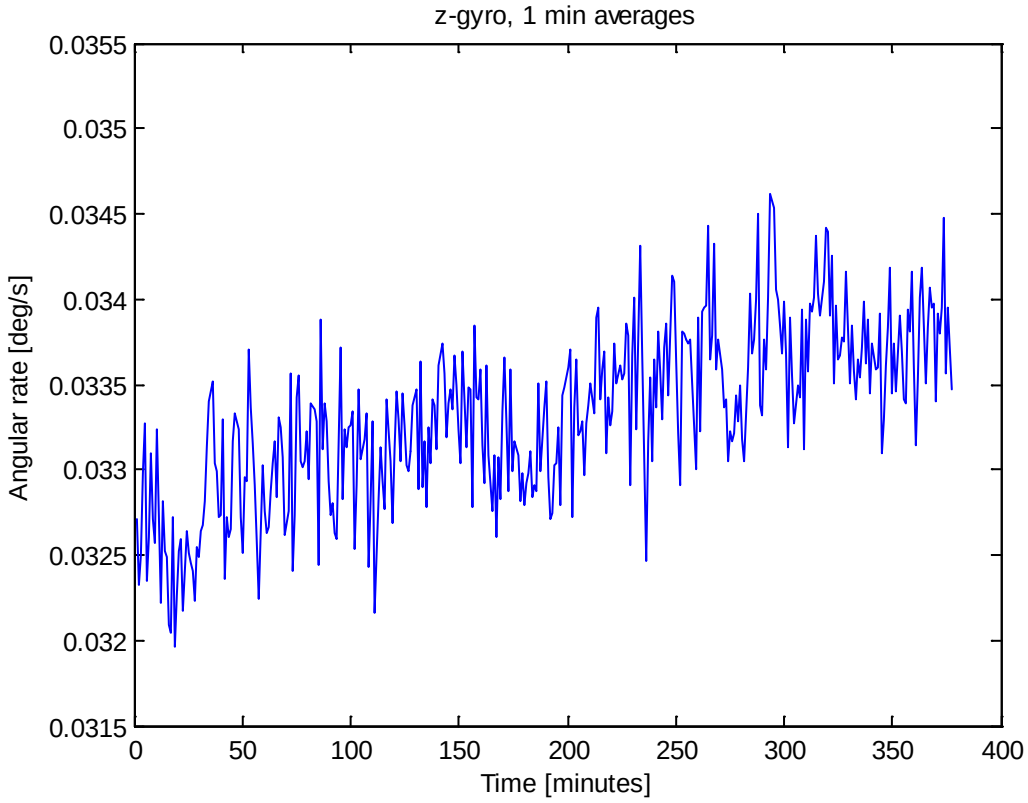

Figure 3.47 STIM 300 z gyro data averaged over 1 minute intervals.

Figure 3.48 shows computed Allan variance for the three gyros, again after 1 second interval pre summing. Based on the Allan variance plots, the angular random walk and bias instability values were estimated. The angular random walk estimates were 0.141, 0.120 and 0.109 deg/sqrt(h) for the x, y and z gyro, respectively, all within the specified value of 0.15 deg/sqrt(h). The bias instability estimates (i.e. the minimum value of the root Allan variance curves) were 0.7, 0.6 and 0.6 deg/h, slightly more than the specified value of 1.5 deg/h.

The Allan variance curves contain the usual regions of angular random walk (slope -1/2) and bias instability (slope 0). The curve for the z gyro also has positive a slope (+1) for long averaging times, indicating the presence of a rate ramp error component.

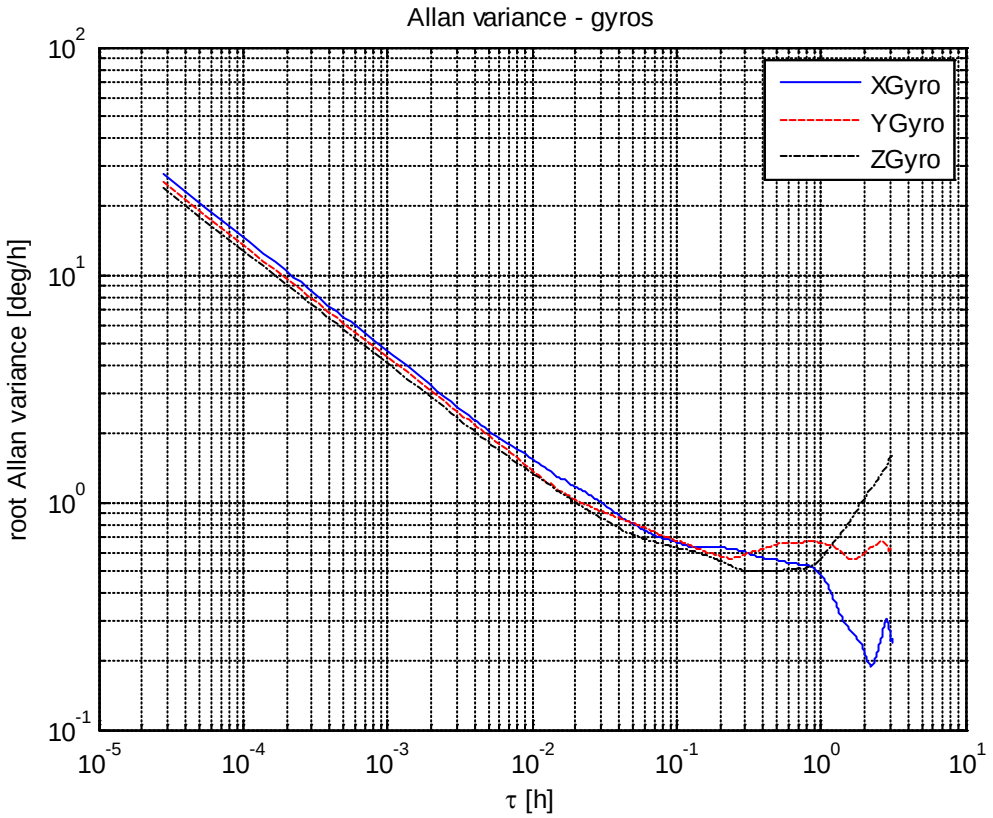

Figure 3.48 Computed Allan variance from STIM300 gyro data.

Figure 3.49 through Figure 3.51 show spectral density plots for the gyro measurements. No significant peaks are present.

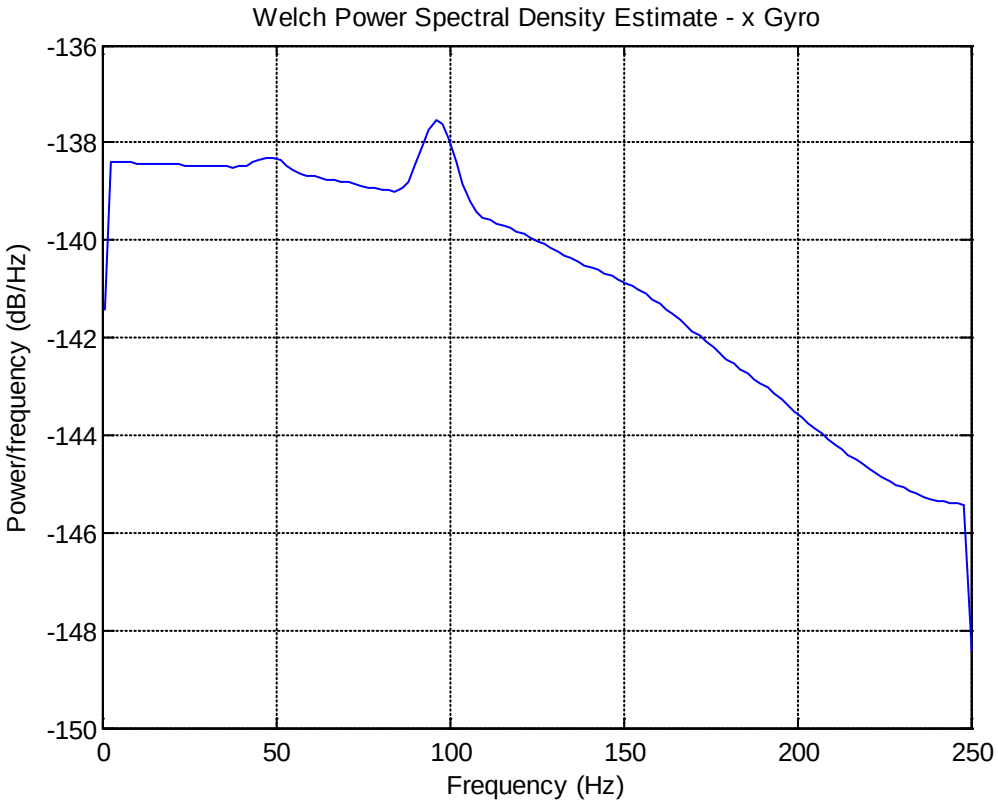

Figure 3.49 Spectral density plot, STIM300 x gyro.

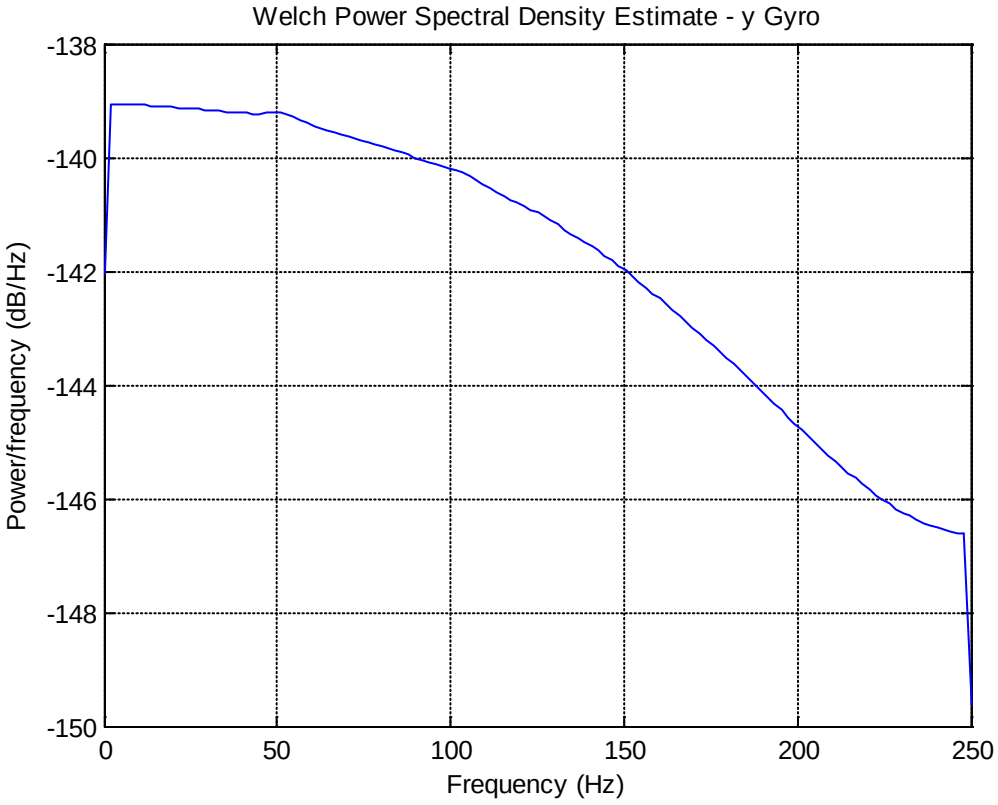

Figure 3.50 Spectral density plot, STIM300 y gyro.

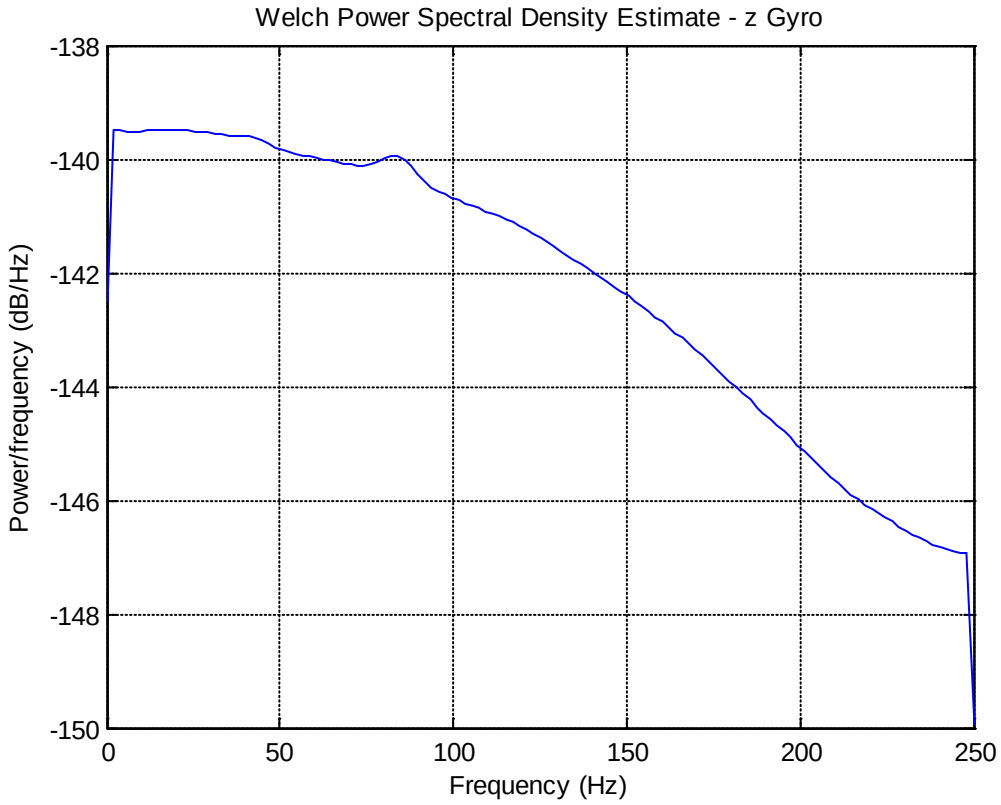

Figure 3.51 Spectral density plot, STIM300 z gyro.

Figure 3.52 to Figure 3.54 show histograms of the STIM300 gyro measurements. The distributions here are also Gaussian-like. The standard deviations of the angular rates (delta theta divided by delta time) were (0.0437, 0.0391, 0.0377) deg/s, for the x, y, and z gyro, respectively.

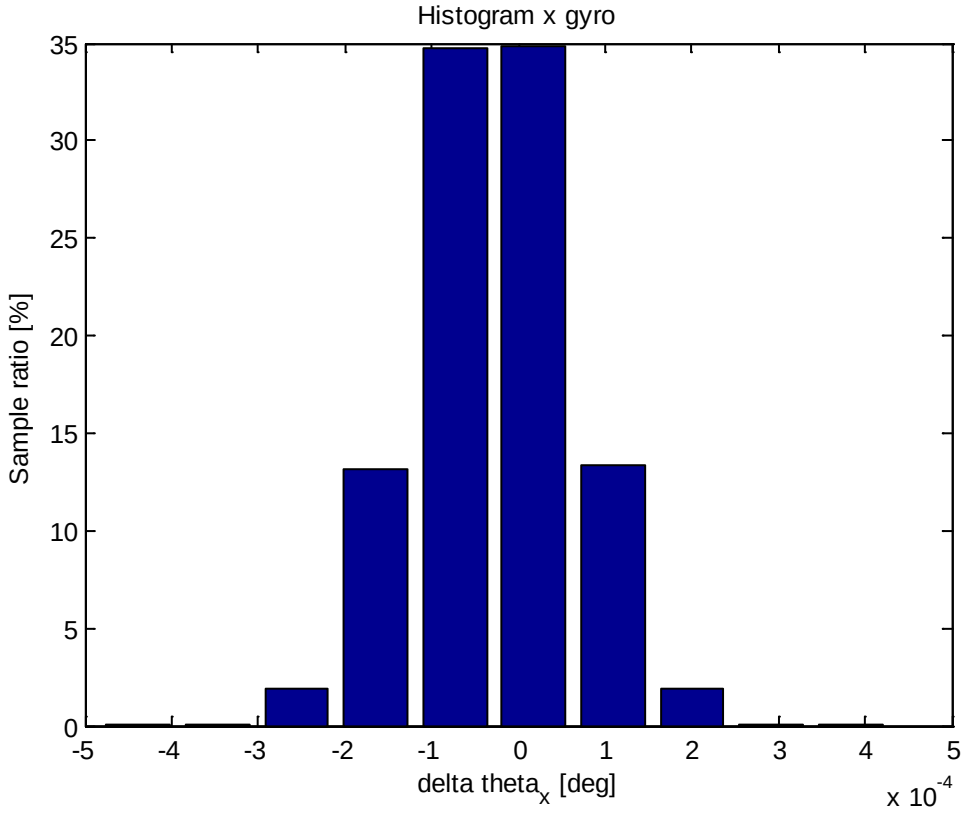

Figure 3.52 STIM300 x gyro histogram.

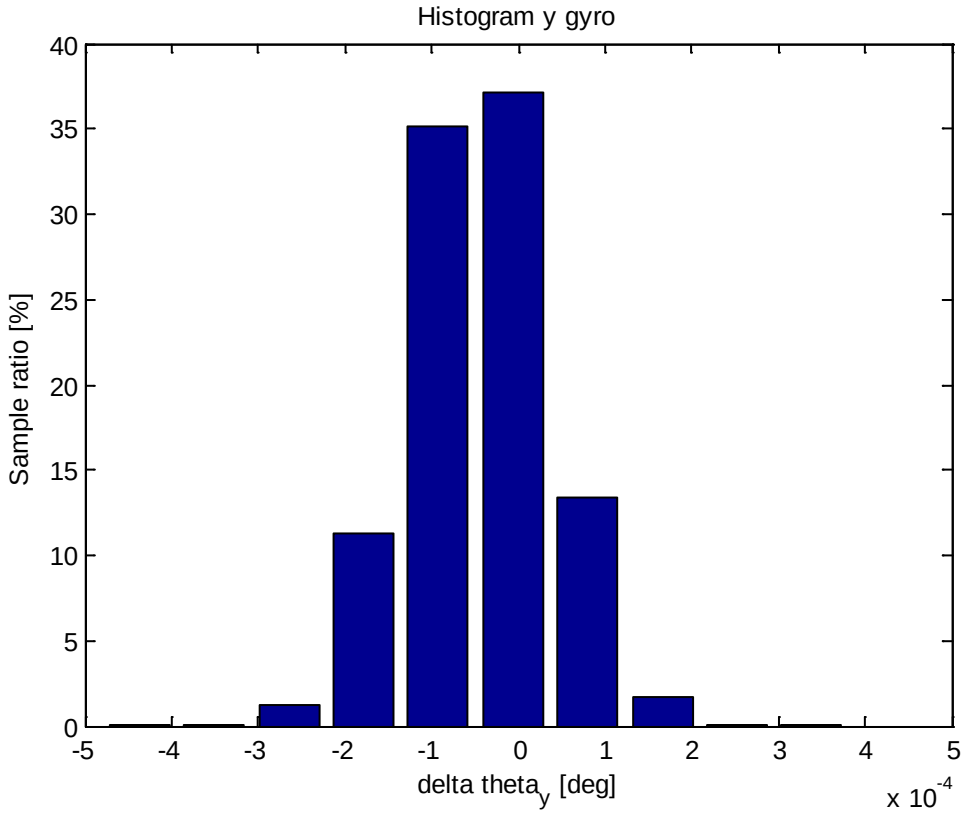

Figure 3.53 STIM300 y gyro histogram.

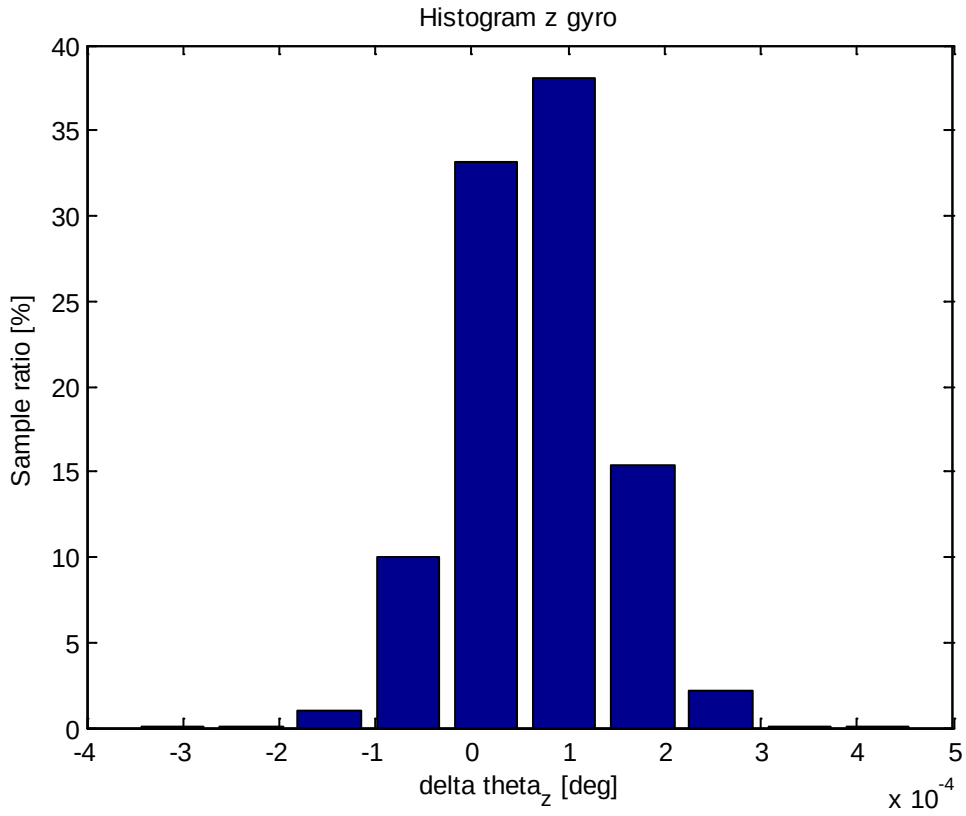

Figure 3.54 STIM300 z gyro histogram.

3.2.2 Repeatability and temperature tests

The results from the repeatability and temperature tests are shown in Table 3.7 and Table 3.8. As was also the case for the SiIMU02 data, the STIM300 accelerometer data also give a too small value compared to standard gravity, indicating large accelerometer biases. The accelerometer output does not vary significantly between different power-ons and temperatures. The standard deviations seem to increase slightly at low temperatures. The gyros are slightly more sensitive to temperature deviations, both in the output and standard deviations.

Table 3.7 Mean STIM300 accelerometer measurements and standard deviations in repeatability and temperature tests.

Test name	norm(mean(f)) [m/s^2]	std f_x [m/s^2]	std f_y [m/s^2]	std f_z [m/s^2]
Langtidstest2	9.773	0.0196	0.0158	0.015
Oppstarts Langtidstest2	9.7753	0.019	0.0172	0.0144
Repeterbarhet 1	9.7697	0.0191	0.0154	0.0147
Repeterbarhet 2	9.7699	0.0192	0.0155	0.0157
Repeterbarhet 3	9.7696	0.0191	0.0154	0.0147
TempTest 0 grader	9.7685	0.0304	0.0294	0.0154
TempTest -10 grader	9.7707	0.0373	0.0369	0.0169
TempTest 10 grader	9.7699	0.0305	0.0303	0.0149
TempTest -20 grader	9.7577	0.0407	0.0433	0.0172
TempTest 20 til -20 grader	9.7665	0.0347	0.0359	0.0167
TempTest 20 grader	9.7743	0.0251	0.0238	0.0161
TempTest -30 grader	9.7636	0.0666	0.0729	0.018
TempTest 30 grader	9.7716	0.0178	0.0146	0.6016
TempTest 40 grader	9.7769	0.0221	0.0182	0.176
TempTest 50 grader	9.7809	0.0259	0.0224	0.0134

Table 3.8 Mean STIM300 gyro measurements and standard deviations in repeatability and temperature tests.

Test name	norm(mean(ω)) [deg/s]	std ω_x [deg/s]	std ω_y [deg/s]	std ω_z [deg/s]
Langtidstest2	0.0375	0.0437	0.0391	0.0377
Oppstarts Langtidstest2	0.0358	0.0429	0.0382	0.0725
Repeterbarhet 1	0.0405	0.0437	0.0391	0.0377
Repeterbarhet 2	0.0409	0.0438	0.039	0.0378
Repeterbarhet 3	0.0406	0.0438	0.0392	0.0378
TempTest 0 grader	0.0333	0.044	0.0433	0.0577
TempTest -10 grader	0.0427	0.0455	0.0454	0.0694
TempTest 10 grader	0.0329	0.0462	0.045	0.0672
TempTest -20 grader	0.047	0.0471	0.0466	0.0764
TempTest 20 til -20 grader	0.0442	0.0471	0.0424	0.0681
TempTest 20 grader	0.0443	0.0455	0.0422	0.0572
TempTest -30 grader	0.0408	0.0821	0.0971	0.0754
TempTest 30 grader	0.0277	0.0464	0.0412	0.0382
TempTest 40 grader	0.0354	0.0531	0.0553	1.2169
TempTest 50 grader	0.0441	0.0574	0.0559	0.0511

Up/down testsTable 3.9 and Table 3.10, using the same color coding as before. As the repeatability tests indicated, all the accelerometer biases are outside the specification. The gyro biases are within the min./max. specification of 200 deg/h. However, large biases (~100 deg/h) are present, and according to the repeatability tests, they are fairly constant over time. When using these measurements in an INS, a large slowly varying error model should preferably be used to model this error component.

Table 3.9 STIM300 accelerometer parameters computed from up/down tests

Test	x acc. bias (mg)	x acc. scale factor (ppm)	y acc. bias (mg)	y acc. scale factor (ppm)	z acc. bias (mg)	z acc. scale factor (ppm)
1/2 (z up)					4.7	21
3/4 (y up)			3.2	134		
5/6 (x up)	3.2	86				
Spec.	0.75	300	0.75	300	0.75	300

Table 3.10 STIM300 gyro parameters computed from up/down test.

Test	x gyro bias (deg/h)	y gyro bias (deg/h)	z gyro bias (deg/h)
1/2 (z up)			101
3/4 (y up)		-85.6	
5/6 (x up)	-69.2		
Spec. (max)	250	250	250

3.3 XSens MTI300

The MTI300 [4] is a MEMS-bases IMU manufactured by the Dutch company XSens. It is part of the so-called MTI 100-series, and in addition to the inertial sensors, it also contains a magnetometer and a barometer (which were not tested). The specifications of the inertial sensors are given in Table 3.11.

Figure 3.55 The XSens MTI300 IMU.

Table 3.11 Specifications of the XSens MTI300.

	Gyros	Accelerometers
Bias repeatability (Max, 1yr)	0.5 deg/s	0.05 m/s^2
Bias instability (typical)	10 deg/hr	40 µg
Random walk (max.)	0.015 deg/s/sqrt(Hz)	150 µg/sqrt(Hz)
Scale factor accuracy	Not specified	Not specified

3.3.1 Long term static test

As before, the unit was placed on a stable table, with the z-accelerometer pointing down. The unit was powered on, after having been turned off for an extensive period. Thus, potential effects due to self-warming would be visible in the data.

3.3.1.1 Accelerometers

Figure 3.56 to Figure 3.58 show the output from the accelerometers during the static test. As the output is given as delta velocity measurements, the values plotted are divided by delta time to obtain accelerations. The same data averaged over 1 minute intervals are shown in Figure 3.59 through Figure 3.61. A small drift in these data can be seen, possibly due to a random walk in these data, i.e. a rate random walk. No significant startup effects are visible.

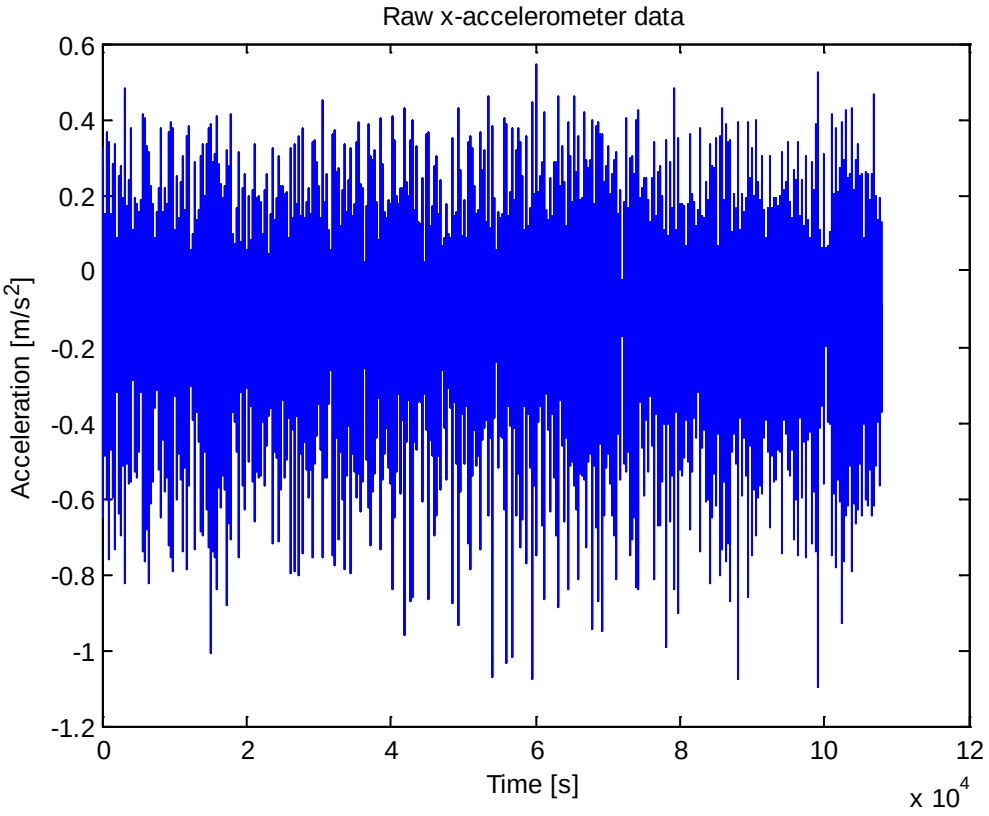

Figure 3.56 Raw data from theMTI300 x accelerometer.

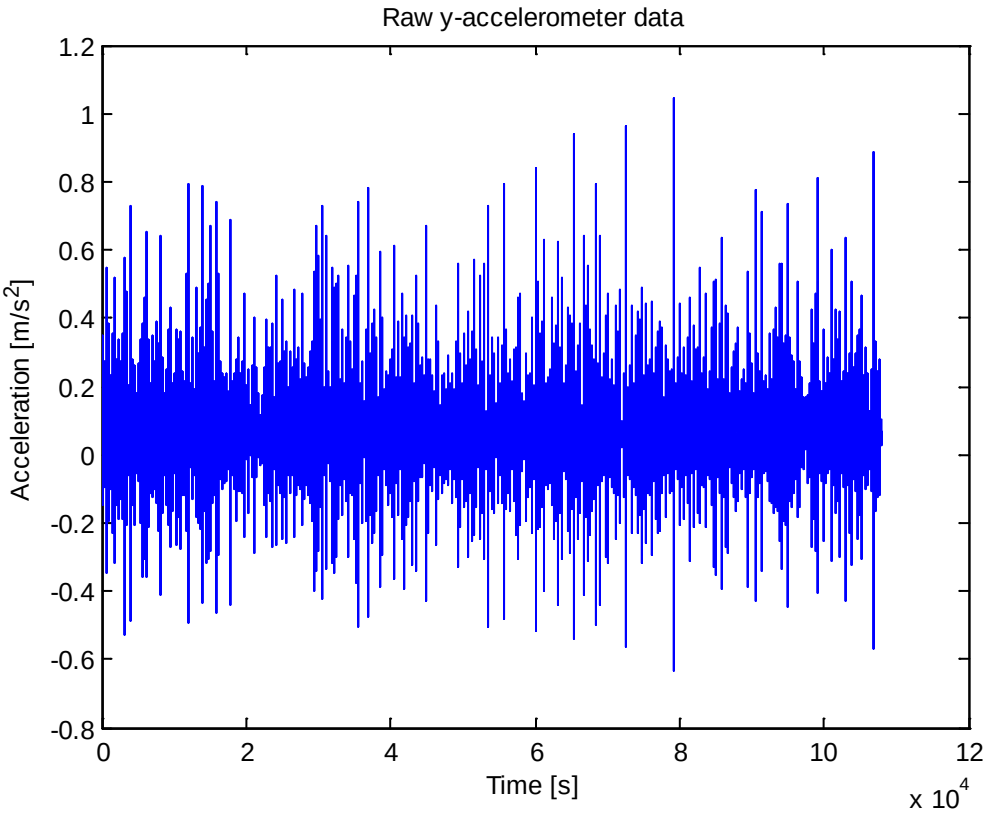

Figure 3.57 Raw data from the MTI300 y accelerometer.

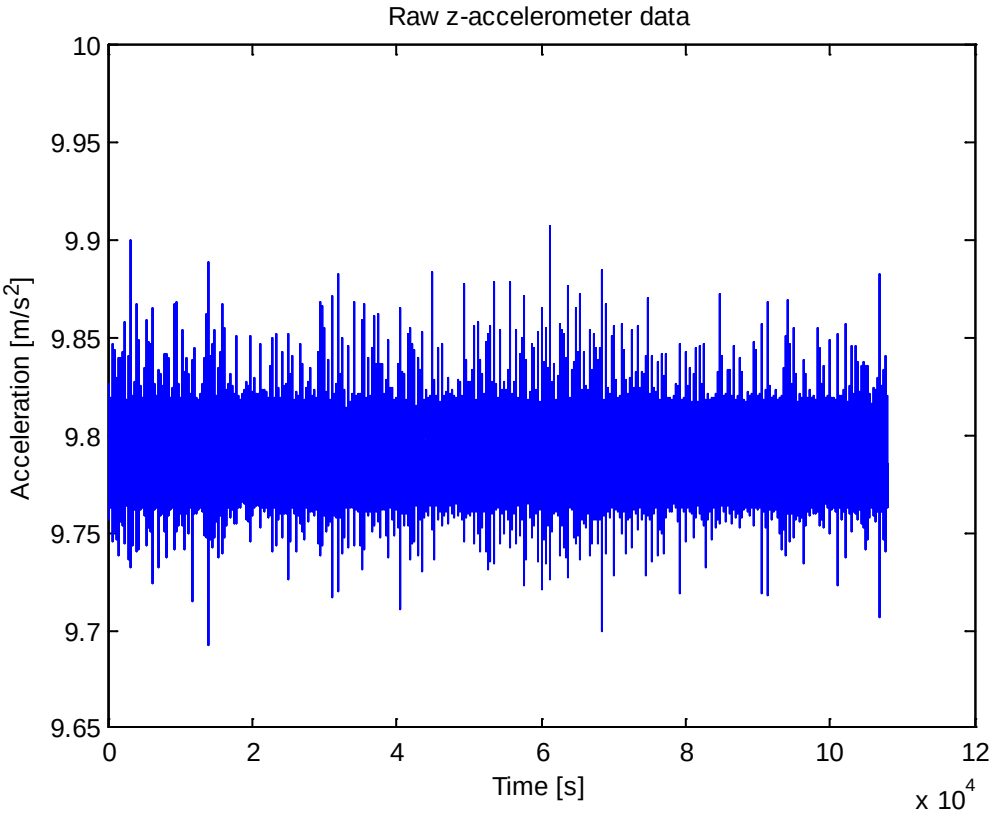

Figure 3.58 Raw data from the MTI300 z accelerometer.

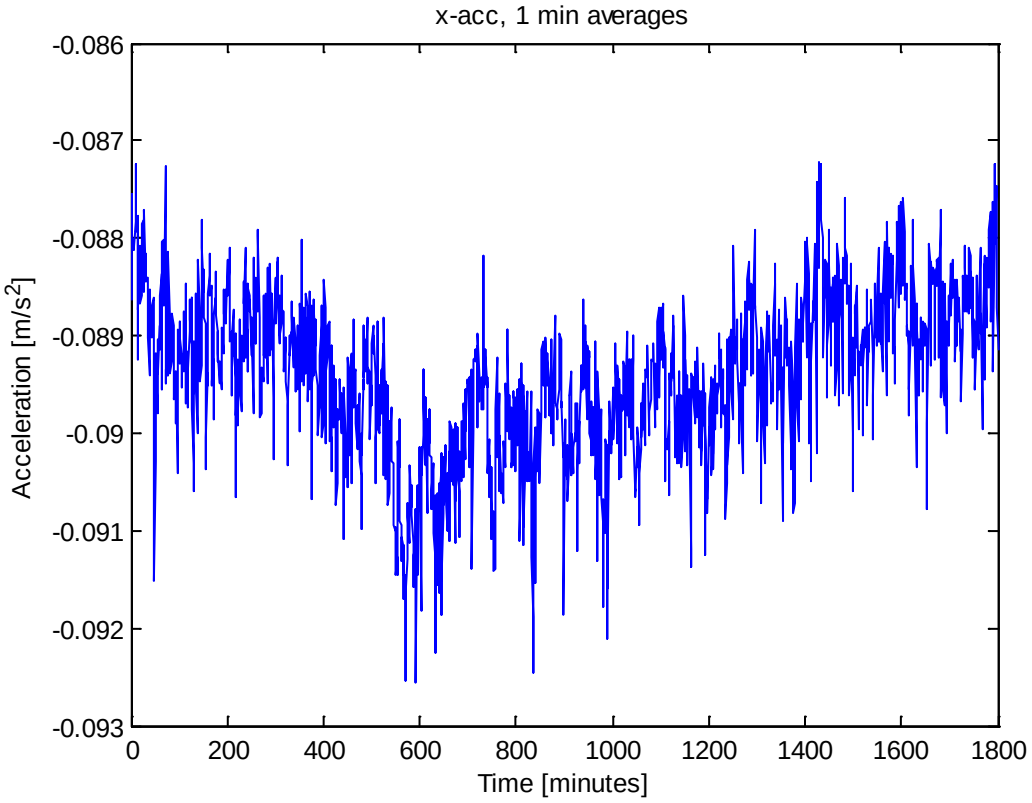

Figure 3.59 MTI300 x accelerometer data averaged over 1 minute intervals.

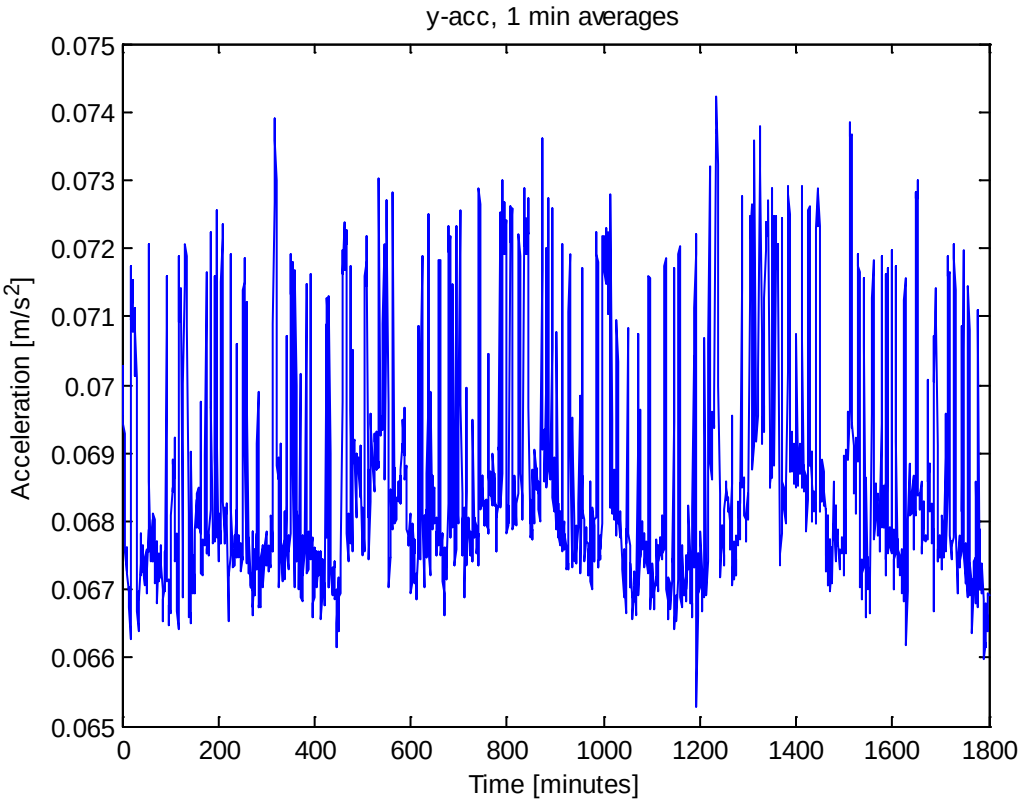

Figure 3.60 MTI300 y accelerometer data averaged over 1 minute intervals.

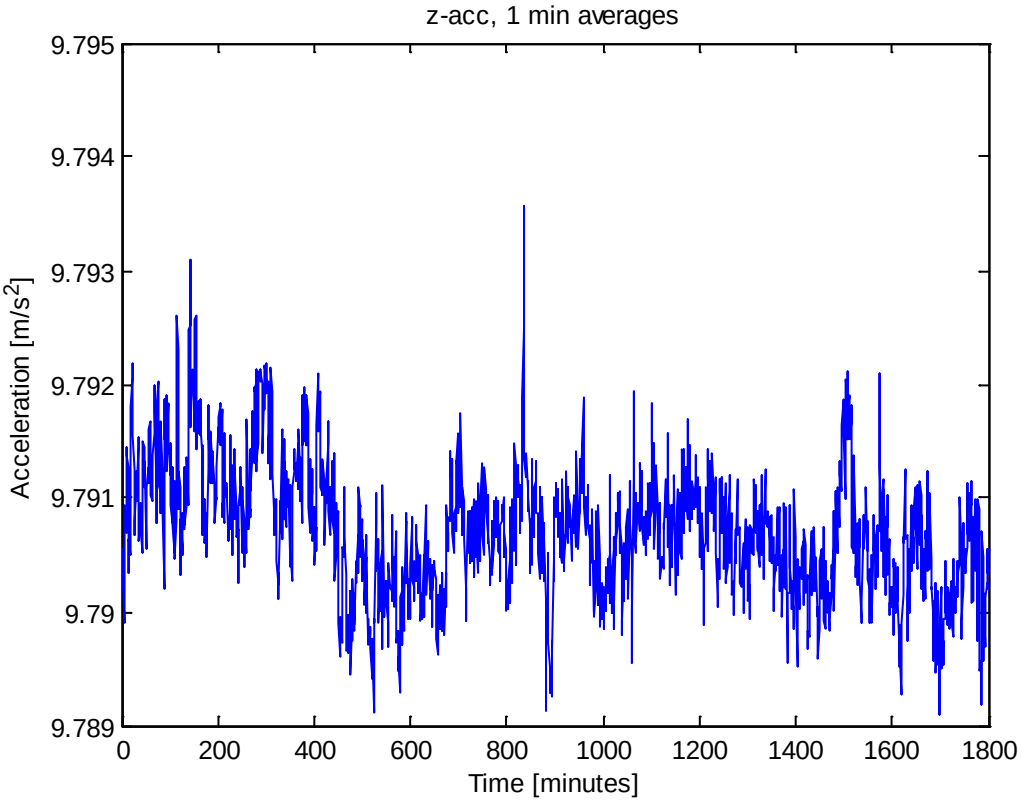

Figure 3.61 MTI300 z accelerometer data averaged over 1 minute intervals.

Figure 3.62 shows computed root Allan variance from the three accelerometers from the entire test interval. The same pre summing over 1 second intervals as before was used. The quality of the estimated Allan variance curves is poor, especially for the y accelerometer. Based on the Allan variance plots, the velocity random walk and bias instability values were estimated. The velocity random walk estimates were 16.3, 131.3, 56.6 µg/sqrt(Hz) for the x, y and z accelerometer, respectively, all within the specified value of 150 µg/sqrt(Hz). The bias instability estimates (i.e. the minimum value of the root Allan variance curves) were 30, 40 and 20 µg for the three axes, all within the specification of 40 µg.

The slopes of the Allan variance plot are quite unusual, especially for the y accelerometer data. The velocity random walk component clearly dominates for low averaging times ($\tau > 10^1$ seconds). For longer averaging times the logarithmic Allan variance curves have a flat or even positive slope, indicating that there are contributions from several different error sources in this range of averaging times. The bias instability estimates given above are therefore possibly not very accurate.

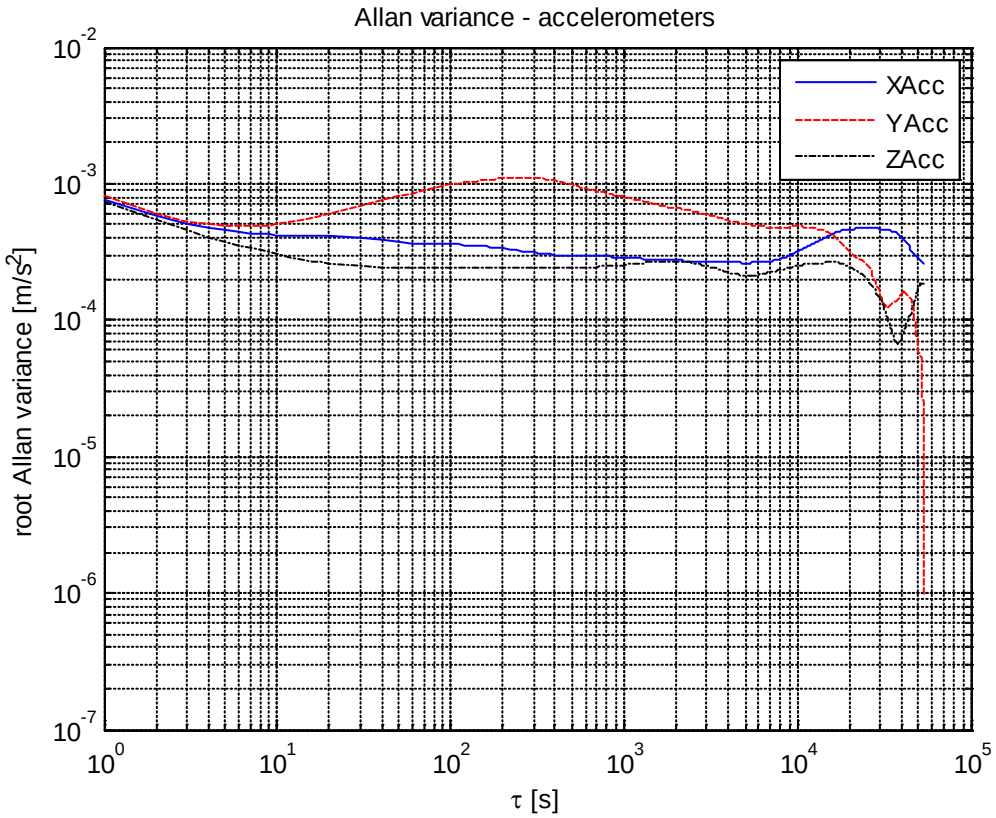

Figure 3.62 Computed Allan variance from MTI300 accelerometer data.

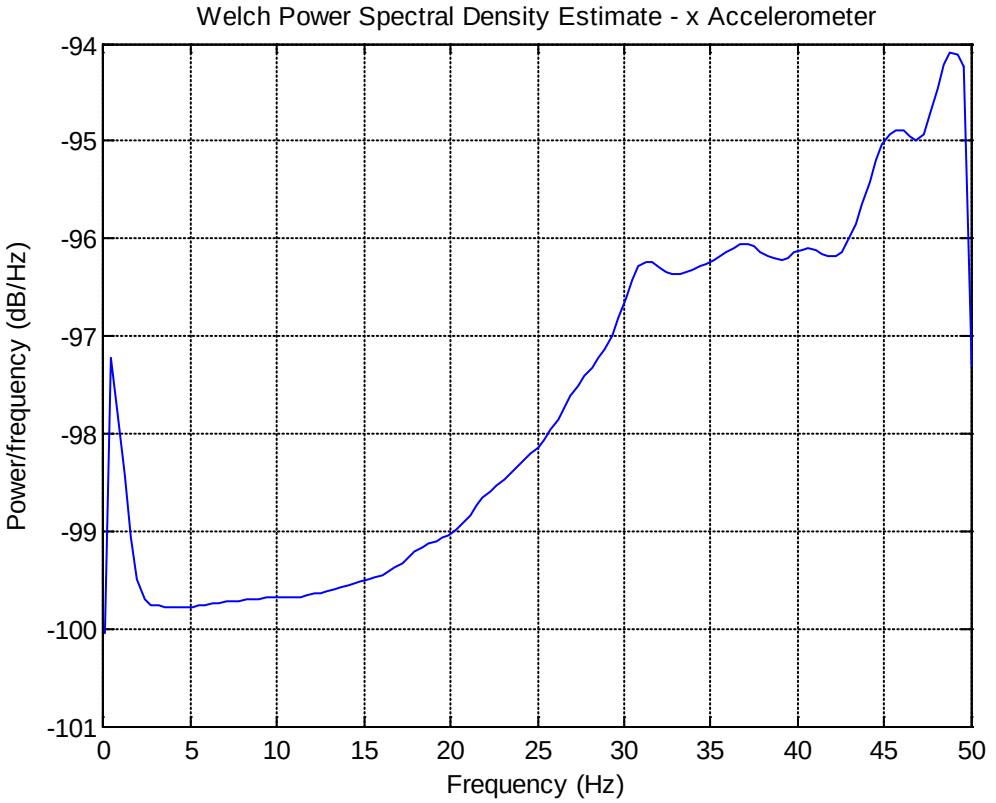

Figure 3.63 Spectral density plot - MTI300 x accelerometer.

Figure 3.63 through Figure 3.65 show the computed spectral densities of the accelerometers. The frequencies seem to be rather evenly distributed. There are a few local maxima for certain frequencies, but these are too small to be of significance.

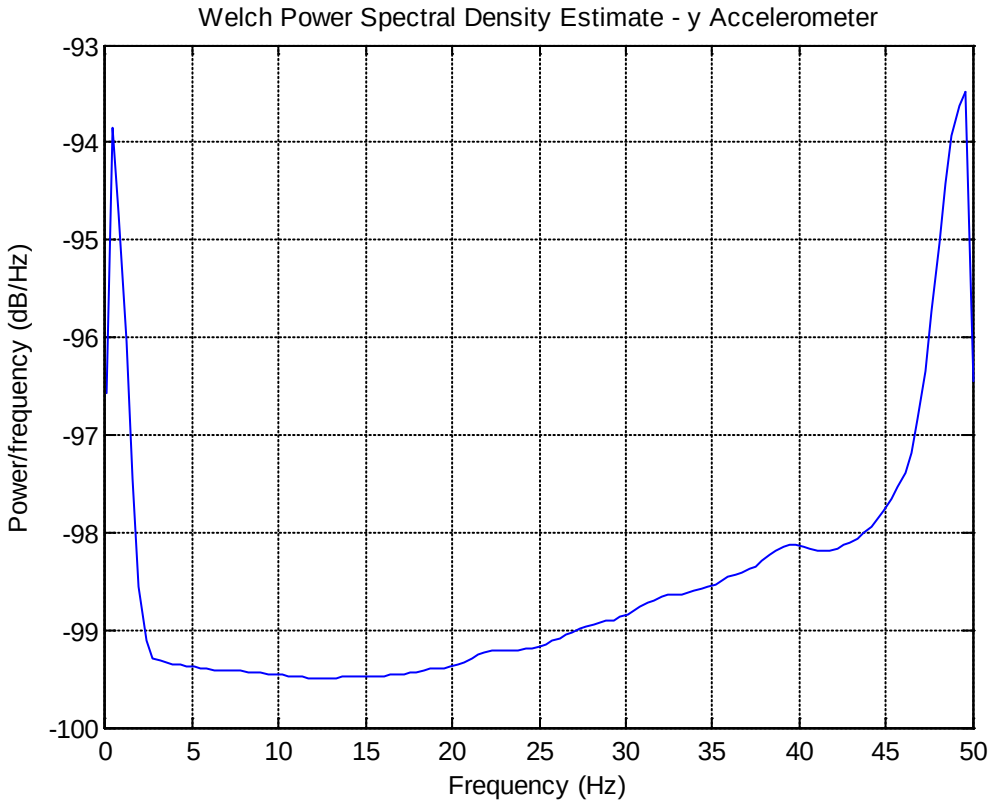

Figure 3.64 Spectral density plot - MTI300 y accelerometer.

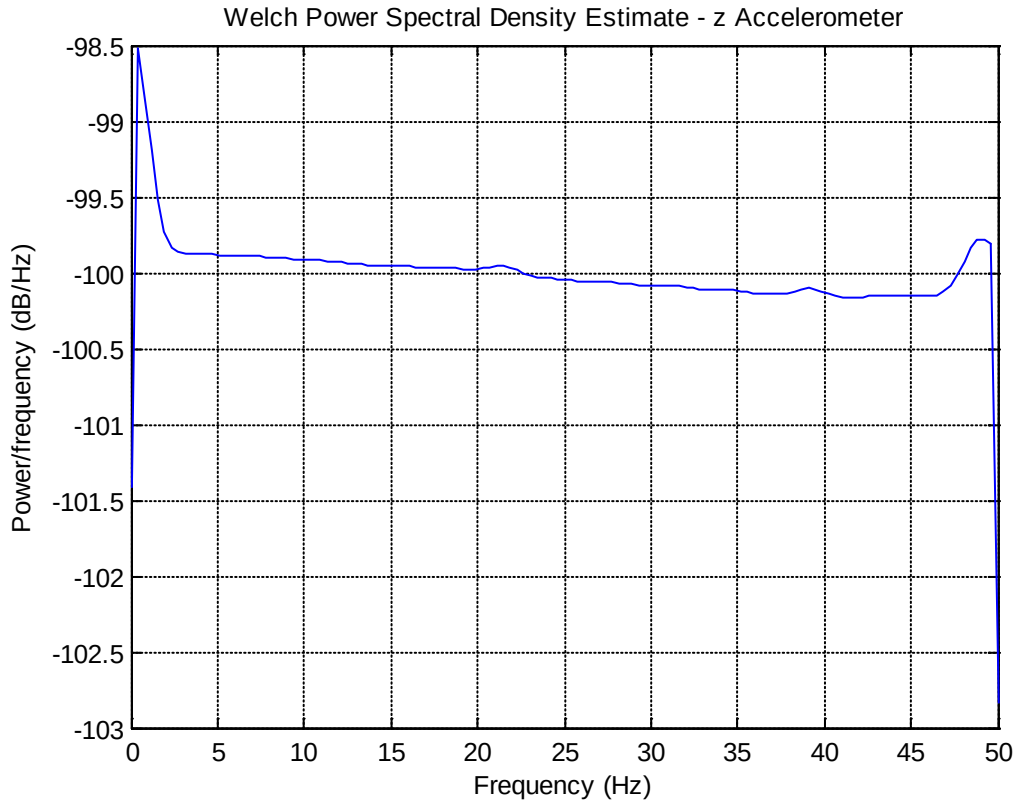

Figure 3.65 Spectral density plot - MTI300 z accelerometer.

Figure 3.66 through Figure 3.68 show histograms for the raw accelerometer measurements. All histograms show a Gaussian-like distribution, with very sharp peaks. The standard deviations of the measured accelerations (delta velocity divided by delta time) are (0.0196, 0.0158, 0.015) m/s^2 for the x, y and z accelerometer, respectively.

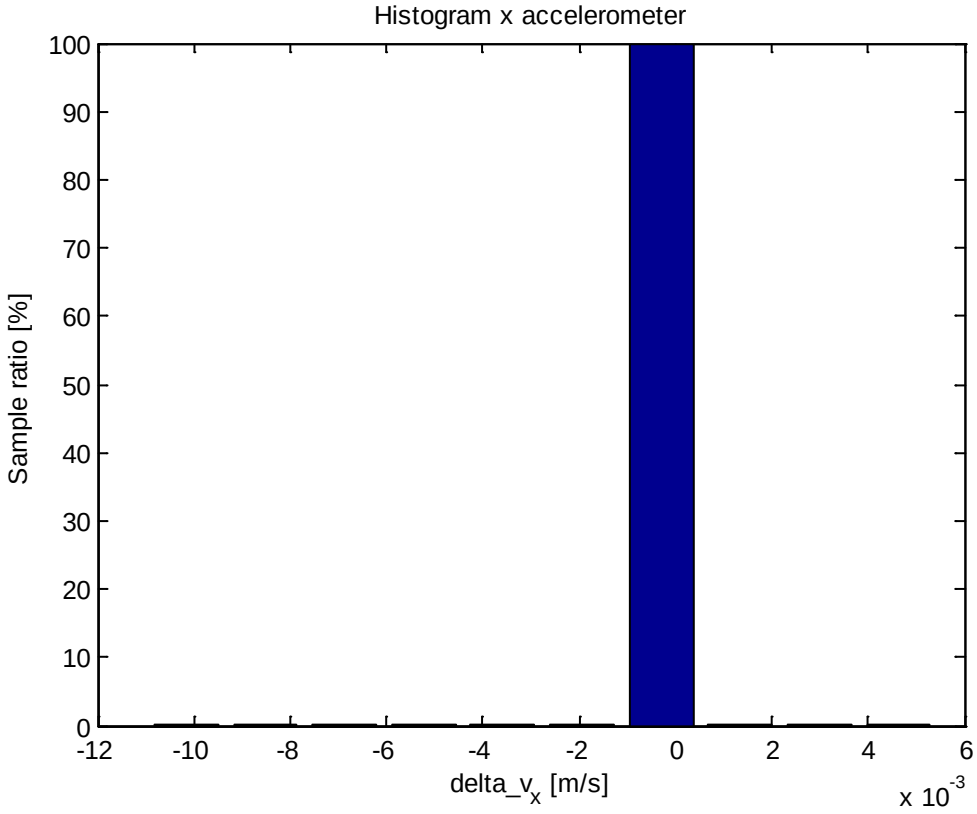

Figure 3.66 MTI300 x accelerometer histogram.

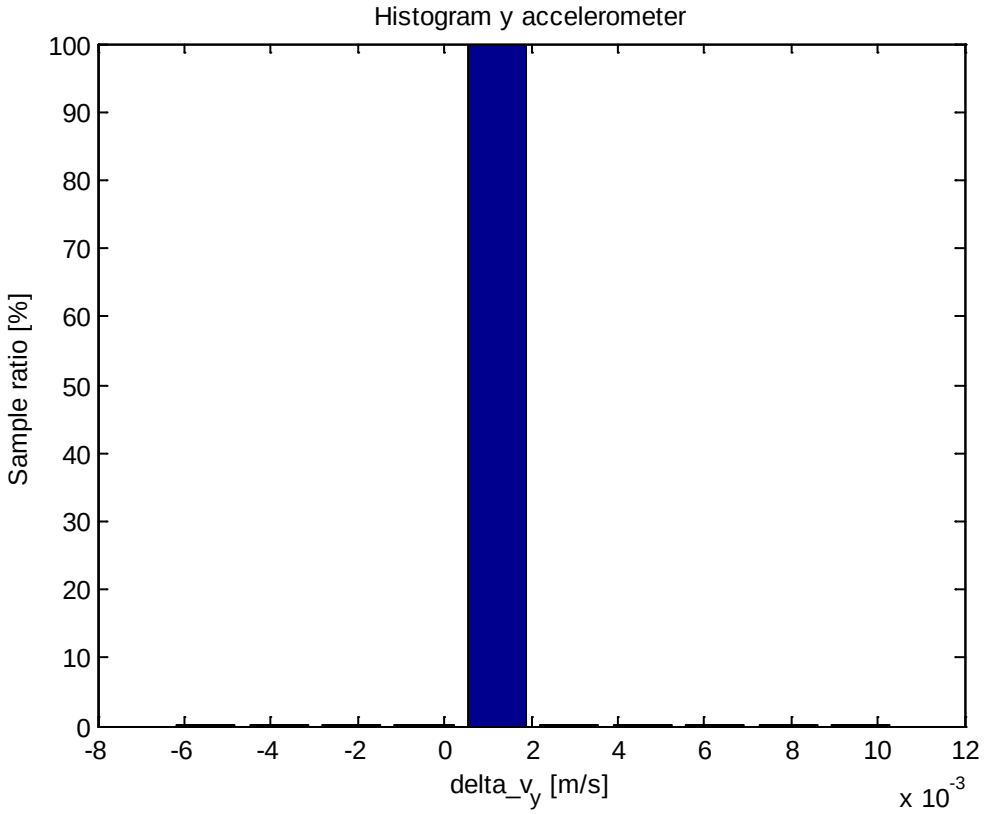

Figure 3.67 MTI300 y accelerometer histogram.

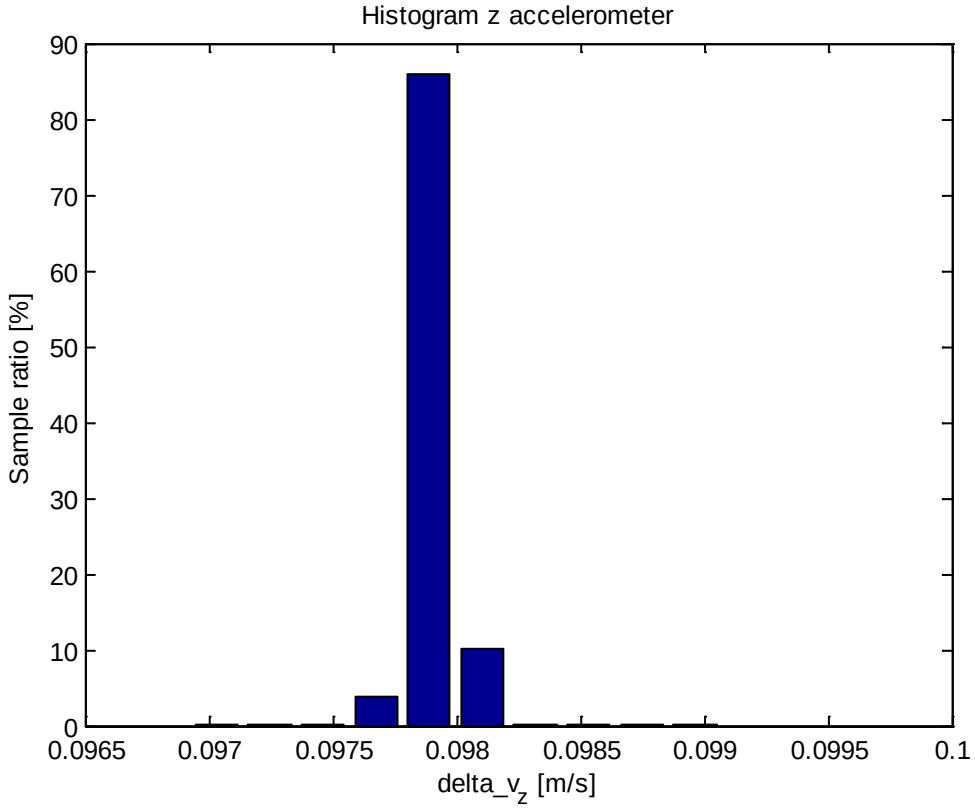

Figure 3.68 MTI300 z accelerometer histogram.

3.3.1.2 Gyroscopes

Figure 3.69 through Figure 3.71 show raw data from the MTI300 gyroscopes throughout the static test. The same data averaged over 1 minute intervals are shown in Figure 3.72 through Figure 3.74 . No significant startup effects are present.

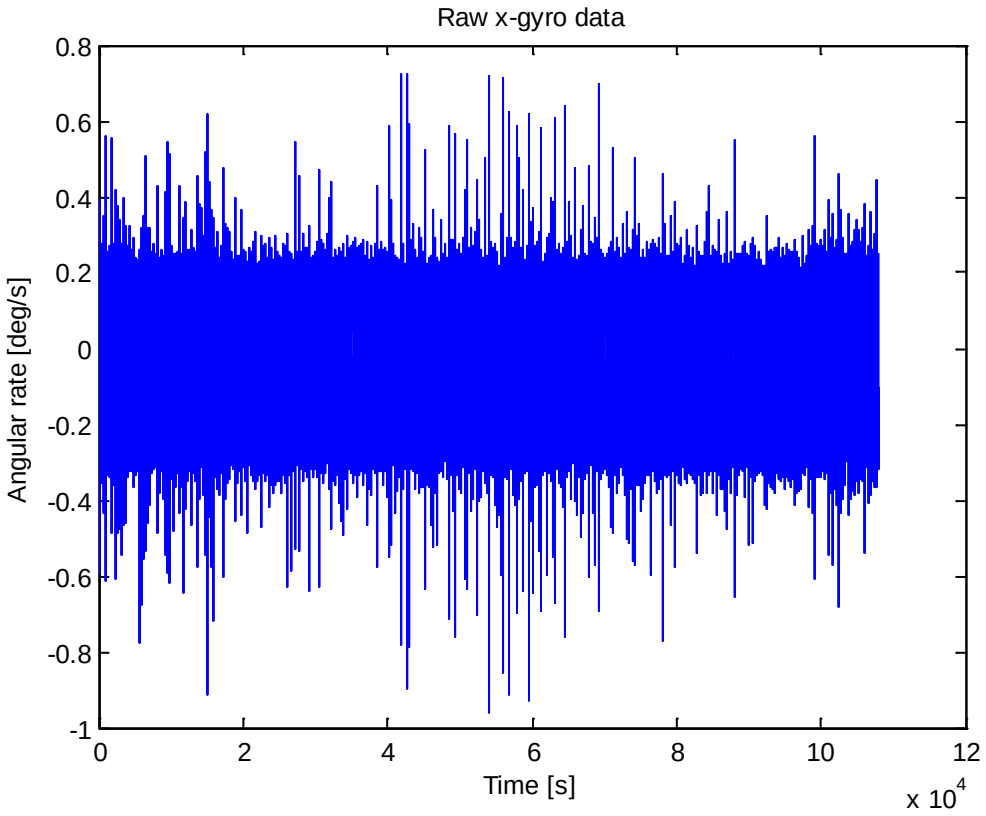

Figure 3.69 Raw data from theMTI300 x gyro.

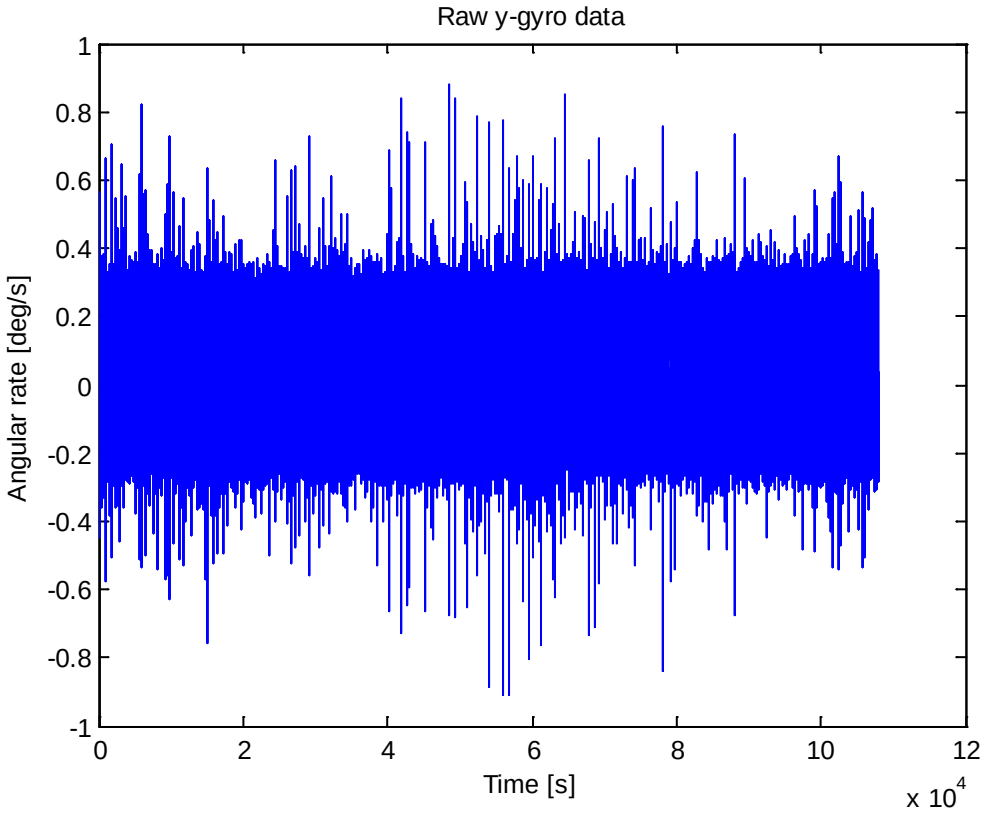

Figure 3.70 Raw data from theMTI300 y gyro.

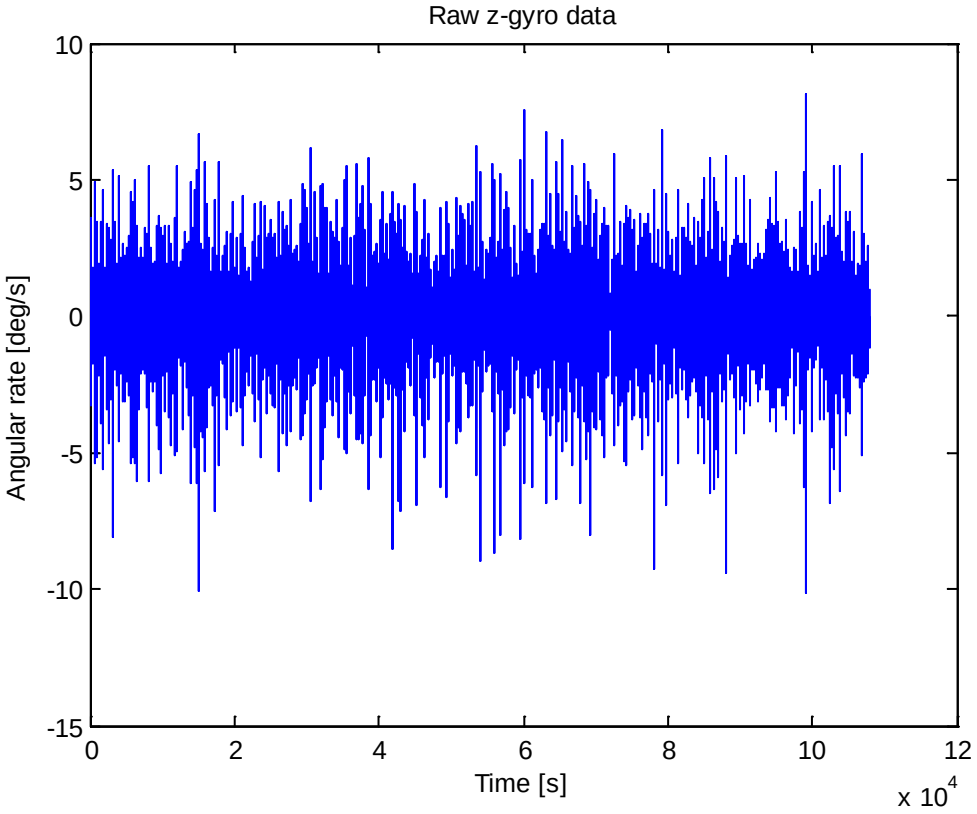

Figure 3.71 Raw data from theMTI300 z gyro.

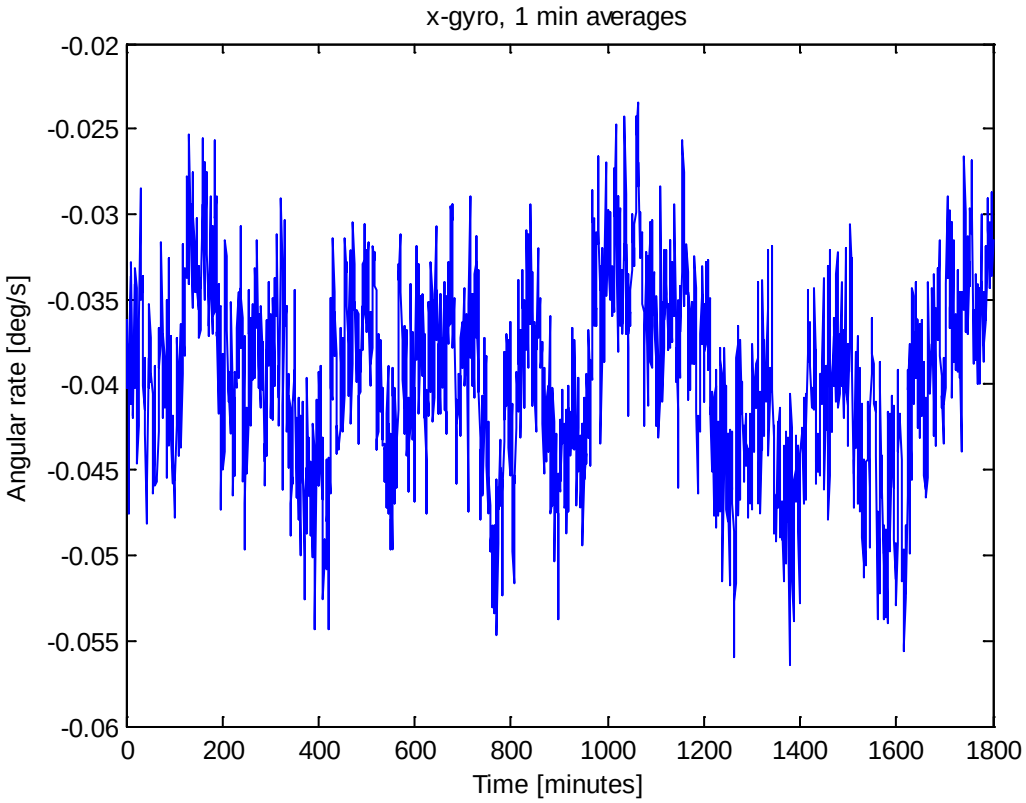

Figure 3.72 MTI300 x gyro data averaged over 1 minute intervals.

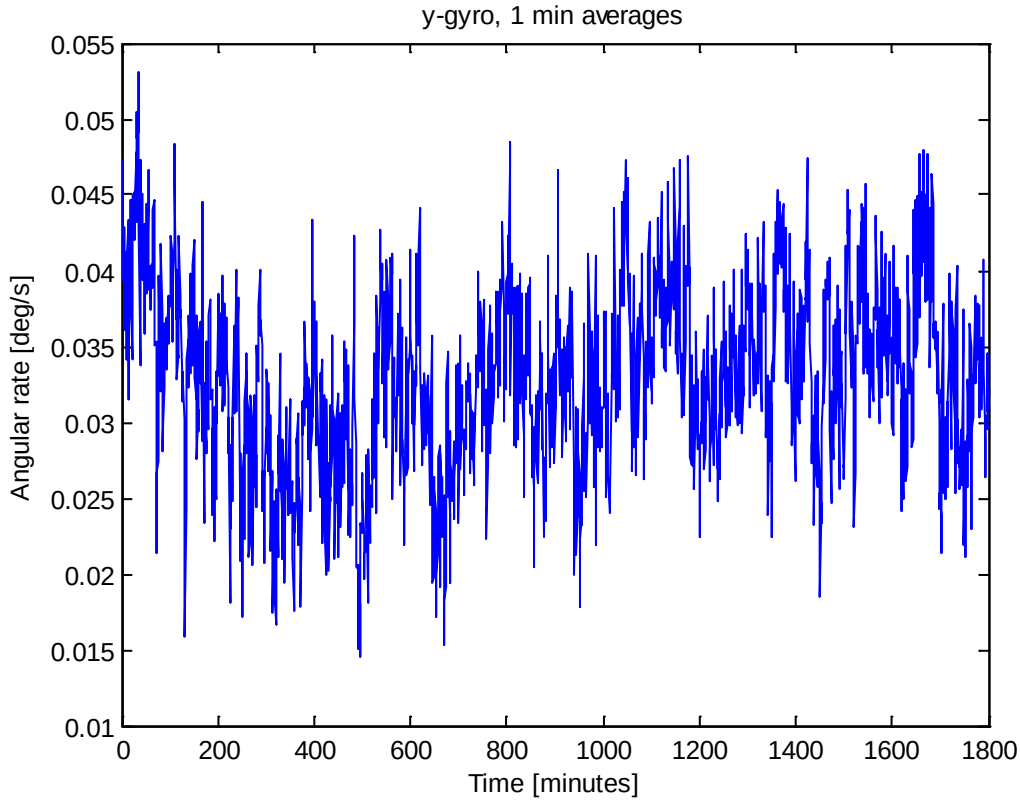

Figure 3.73 MTI300 y gyro data averaged over 1 minute intervals.

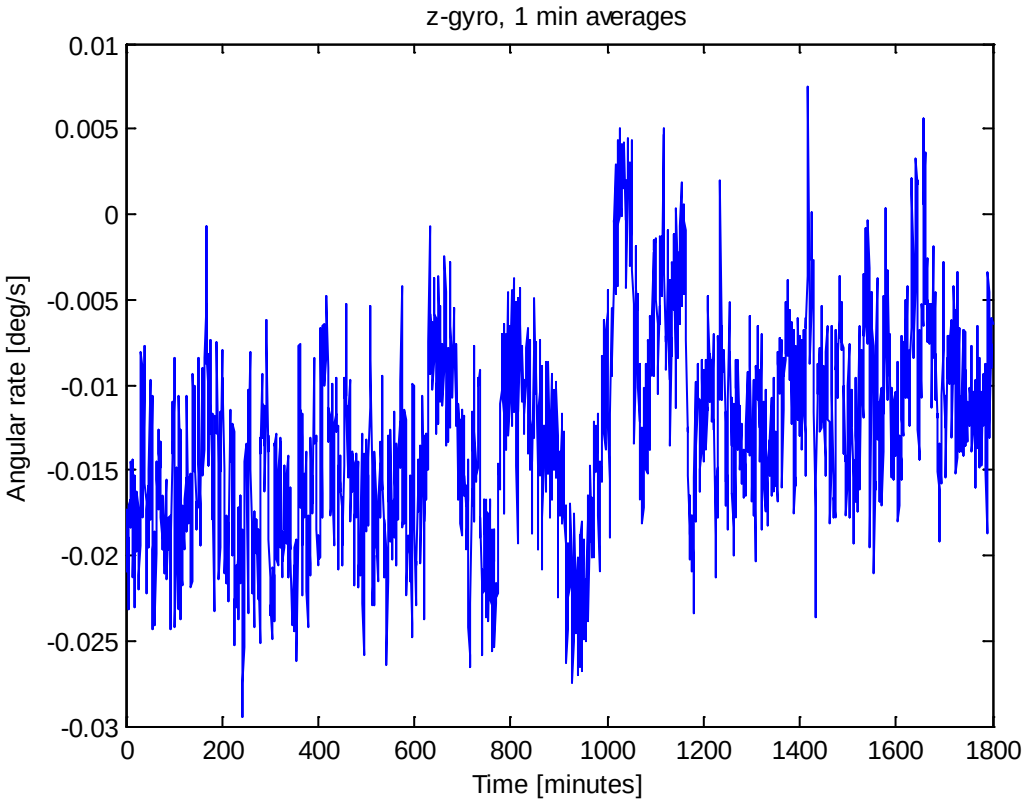

Figure 3.74 MTI300 z gyro data averaged over 1 minute intervals.

Figure 3.75 shows computed Allan variance for the three gyros, again after 1 second interval pre summing. Based on the Allan variance plots, the angular random walk and bias instability values were estimated. The angular random walk estimates were 0.415, 0.356 and 0.215 deg/sqrt(h) for the x, y and z gyro, respectively, all within the specified value of 0.9 deg/sqrt(h). The bias instability estimates (i.e. the minimum value of the root Allan variance curves) were 8.4, 9.7 and 9.2 deg/h, all within the specified value of 10 deg/h.

The Allan variance curves contain the usual regions of angular random walk (slope -1/2) and bias instability (slope 0). The curves for the y and z gyro also have positive slopes (+1) for long averaging times, indicating the presence of a rate ramp error component. However, this may also be the result of inaccurate estimates due to few samples in this region.

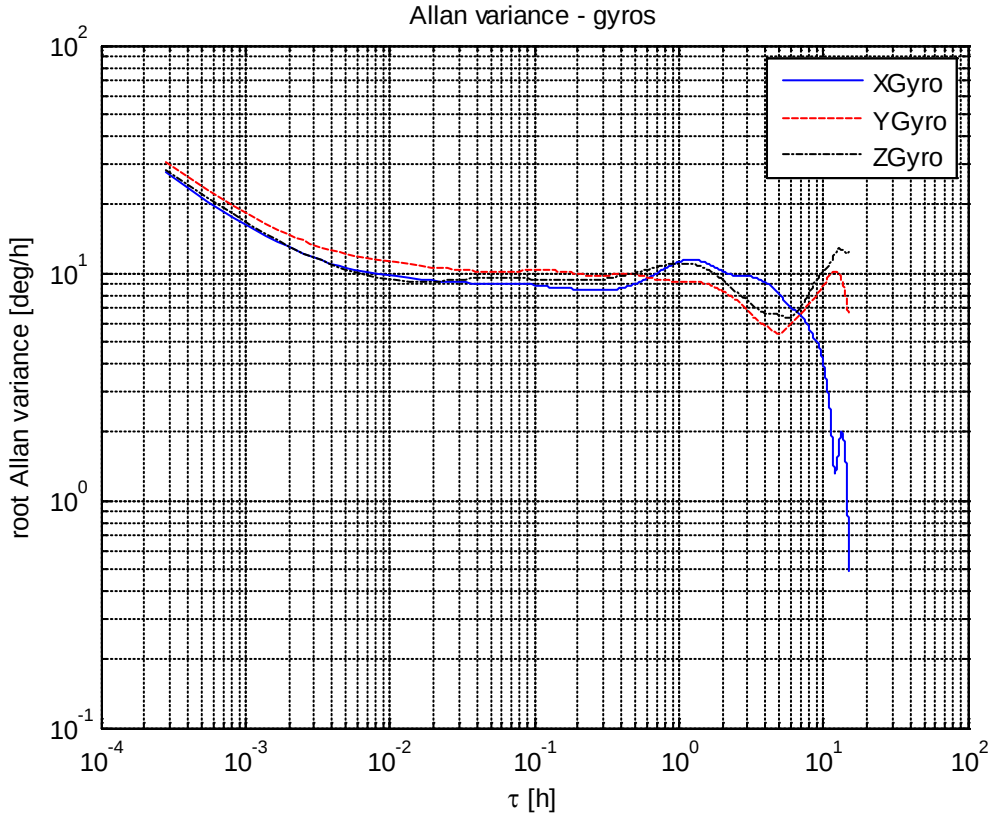

Figure 3.75 Computed Allan variance from MTI300 gyro data.

Figure 3.76 through Figure 3.78 show spectral density plots for the gyro measurements. No significant peaks are present.

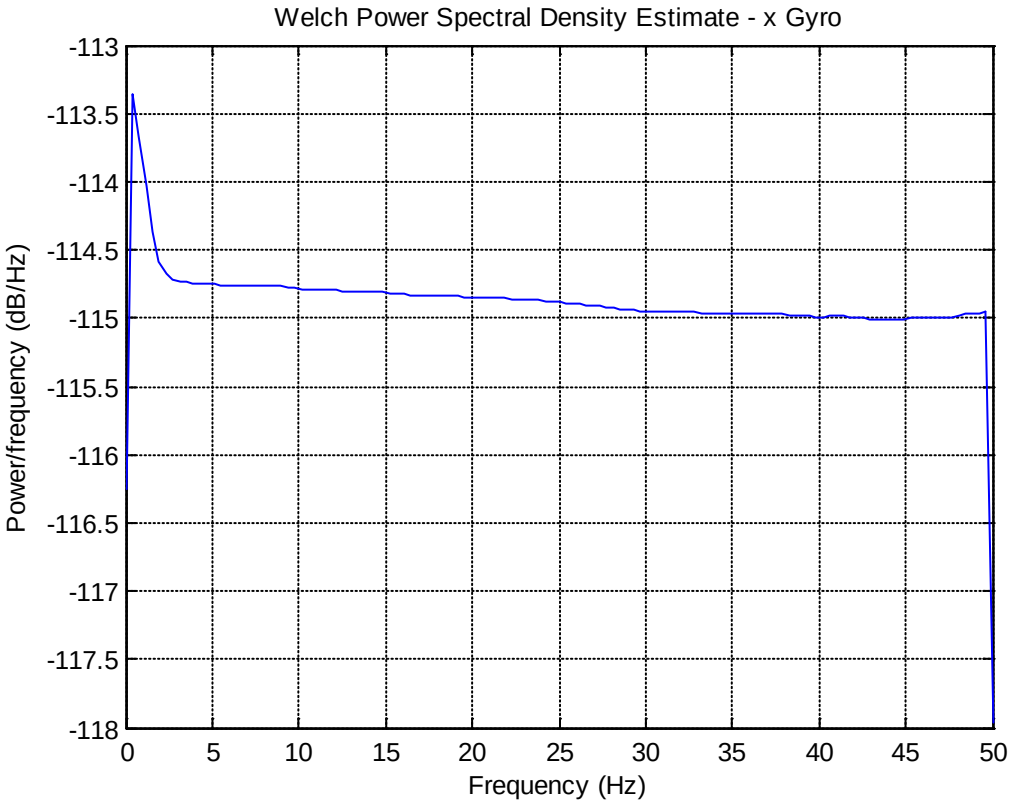

Figure 3.76 Spectral density plot - MTI300 x gyro.

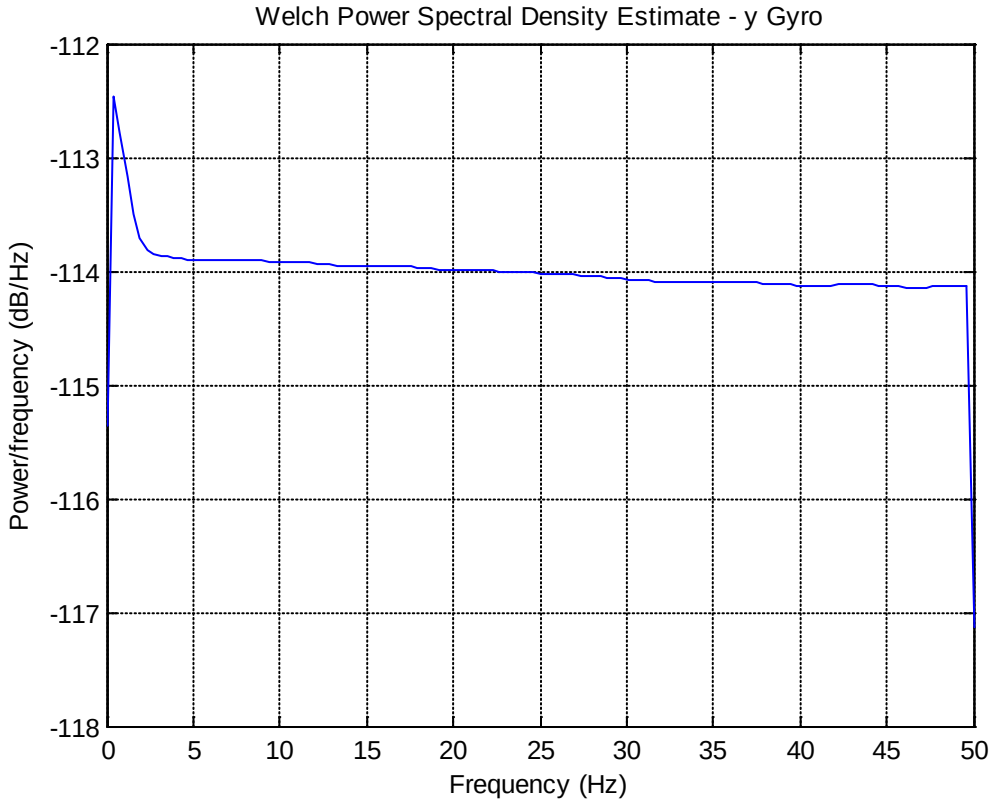

Figure 3.77 Spectral density plot - MTI300 y gyro.

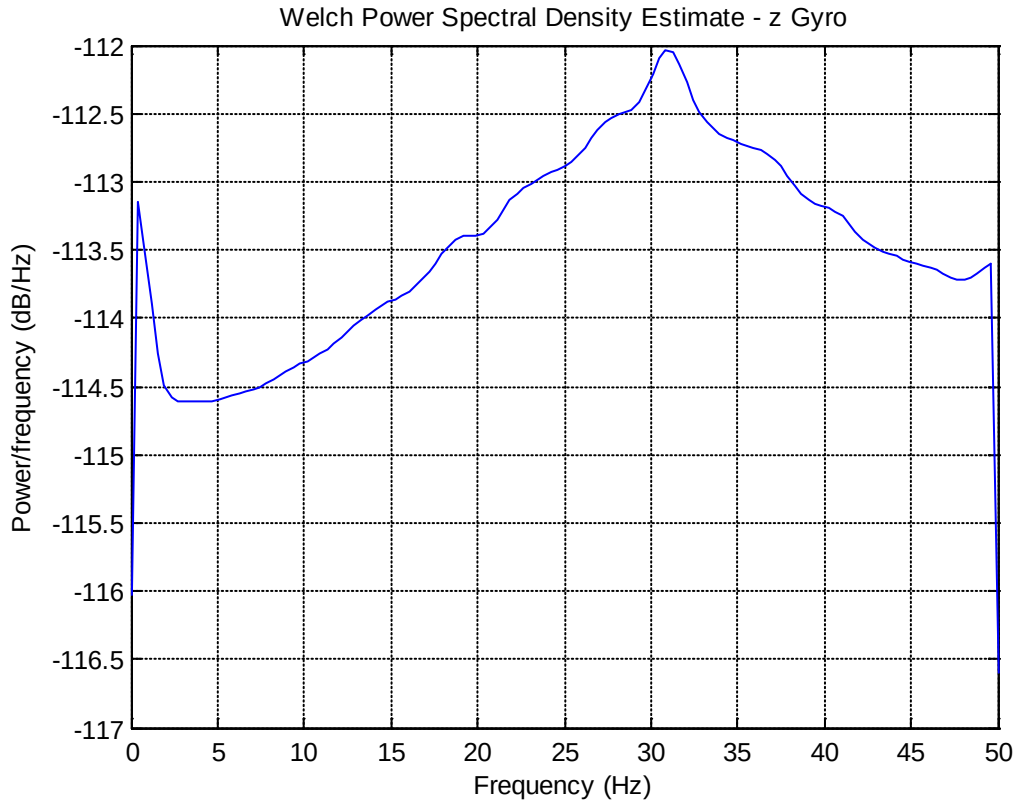

Figure 3.78 Spectral density plot - MTI300 z gyro.

Figure 3.76 through Figure 3.78 show histograms of the MTI300 gyro measurements. Again, the distributions are Gaussian-like. The standard deviations of the angular rates (delta theta divided by delta time) were (0.074, 0.071, 0.087) deg/s, for the x, y, and z gyro, respectively.

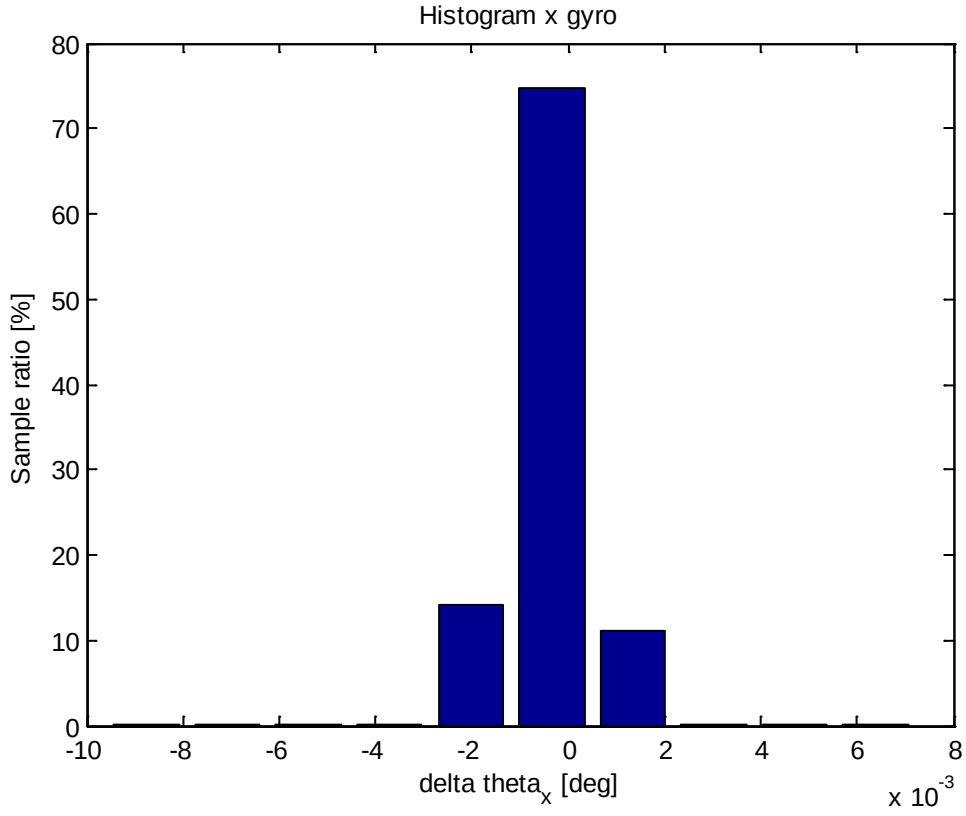

Figure 3.79 MTI300 x gyro histogram.

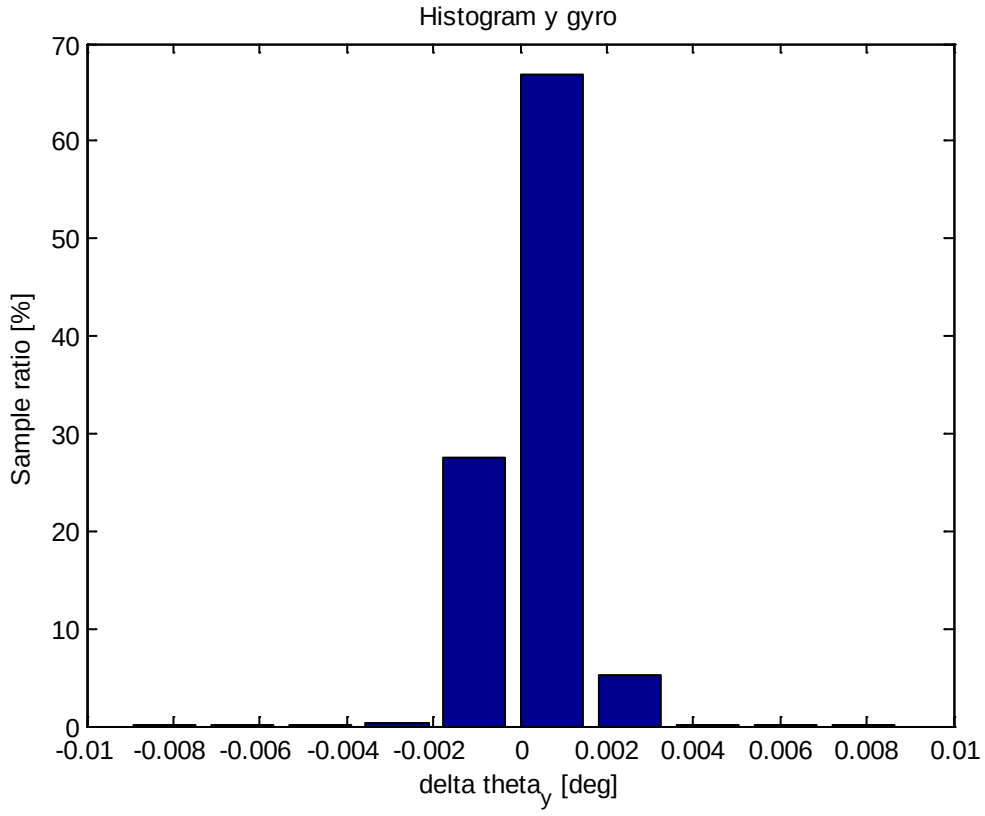

Figure 3.80 MTI300 y gyro histogram.

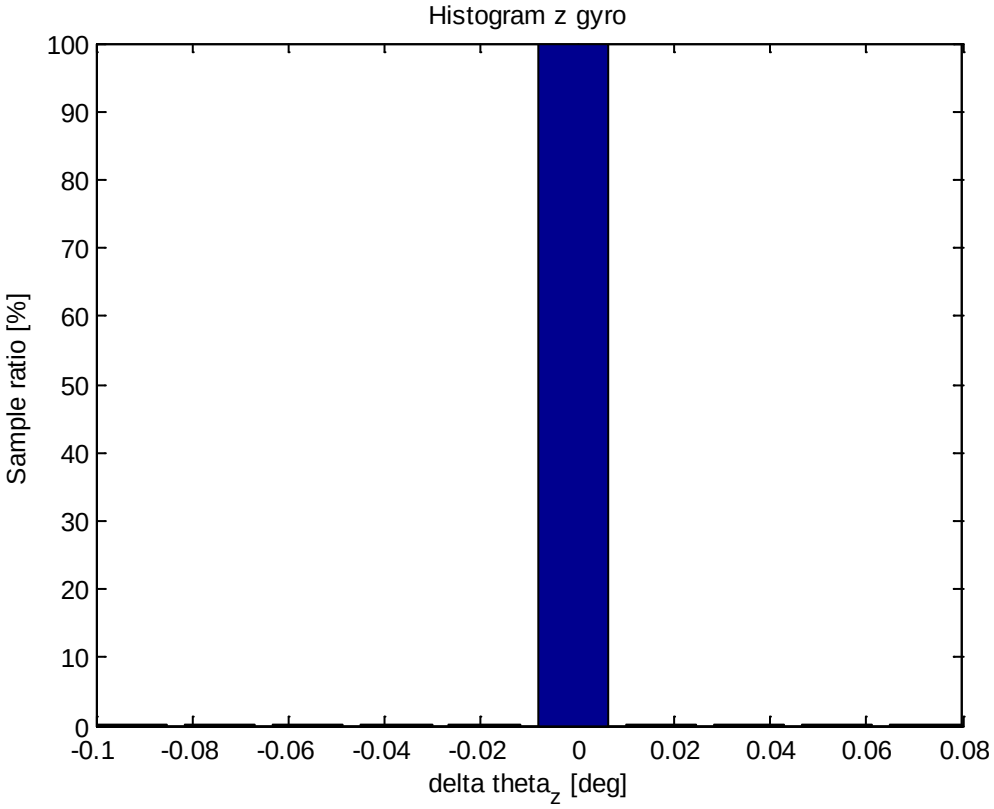

Figure 3.81 MTI300 z gyro histogram.

3.3.2 Repeatability and temperature tests

The results from the repeatability and temperature tests are shown in Table 3.12 and table 3.13, for the accelerometers and gyroscopes, respectively. Again, the accelerometers give a too small value compared to standard gravity, indication large accelerometer biases. The accelerometer output does not vary significantly between different power-ons and temperatures. As for STIM300, we see a slight increase in the accelerometer standard deviations at low temperatures. The gyro means vary slightly more between power-ons and the means are again more sensitive to temperature changes. However, the standard deviations are less affected by the temperature variations.

Table 3.12 Mean MTI-300 accelerometer measurements and standard deviations in repeatability and temperature tests.

Test name	norm(mean(f)) [m/s^2]	std f_x [m/s^2]	std f_y [m/s^2]	std f_z [m/s^2]
Langtidstest_1	9.7914	0.0096	0.0086	0.0072
Oppstartstest	9.7821	0.0098	0.008	0.0071
Repeterbarhetstest_1	9.7907	0.0089	0.0092	0.0071
Repeterbarhetstest_2	9.7914	0.0074	0.0088	0.0073
Repeterbarhetstest_3	9.7925	0.0075	0.0087	0.0071
TemperaturTest_+0grader	9.7873	0.013	0.0085	0.0069
TemperaturTest_+10grader	9.7874	0.011	0.0081	0.0069
TemperaturTest_+20grader	9.7855	0.011	0.008	0.0071
TemperaturTest_+20Til+50grader	9.7826	0.0077	0.0082	0.0074
TemperaturTest_+30grader	9.7836	0.0089	0.0081	0.0072
TemperaturTest_+40grader	9.7835	0.0076	0.0079	0.0075
TemperaturTest_+50grader	9.7845	0.0078	0.008	0.0076
TemperaturTest_-10grader	9.7784	0.013	0.011	0.0068
TemperaturTest_-20grader	9.7863	0.016	0.023	0.0074
TemperaturTest_-30grader	9.7836	0.021	0.019	0.01
TemperaturTest_-30Til+20grader	9.8134	0.0089	0.0085	0.0076

Table 3.13 Mean MTI-300 gyro measurements and standard deviations in repeatability and temperature tests.

Test name	norm(mean(ω)) [deg/s]	std ω_x [deg/s]	std ω_y [deg/s]	std ω_z [deg/s]
Langtidstest_1	0.0531	0.074	0.081	0.087
Oppstartstest	0.047	0.073	0.081	0.087
Repeterbarhetstest_1	0.0536	0.074	0.082	0.091
Repeterbarhetstest_2	0.0678	0.073	0.081	0.089
Repeterbarhetstest_3	0.0552	0.073	0.081	0.086
TemperaturTest_+0grader	0.0336	0.066	0.075	0.098
TemperaturTest_+10grader	0.04374	0.07	0.077	0.093
TemperaturTest_+20grader	0.0761	0.073	0.081	0.089
TemperaturTest_+20Til+50grader	0.0587	0.082	0.089	0.082
TemperaturTest_+30grader	0.093	0.077	0.085	0.086
TemperaturTest_+40grader	0.0986	0.08	0.088	0.081
TemperaturTest_+50grader	0.0586	0.083	0.092	0.085
TemperaturTest_-10grader	0.0322	0.064	0.072	0.095
TemperaturTest_-20grader	0.1091	0.064	0.069	0.1
TemperaturTest_-30grader	0.07182	0.058	0.066	0.13
TemperaturTest_-30Til+20grader	0.0525	0.073	0.08	0.079

3.3.3 Up-down tests

The results from the up/down tests are shown in Table 3.14 and Table 3.15 using the same color coding as before. The only sensor that exceeds the specified maximum bias is the y accelerometer, which has a slightly too high bias value.

Table 3.14 MTI300 accelerometer parameters computed from up/down tests

Test	x acc. bias (m/s^2)	x acc. scale factor (ppm)	y acc. bias (m/s^2)	y acc. scale factor (ppm)	z acc. bias (m/s^2)	z acc. scale factor (ppm)
1/2 (z up)					0.027	363
3/4 (y up)			0.059	344		
5/6 (x up)	0.0051	571				
Spec. (max)	0.05	N/A	0.05	N/A	0.05	N/A

Table 3.15 MTI300 gyro parameters computed from up/down test.

Test	x gyro bias (deg/h)	y gyro bias (deg/h)	z gyro bias (deg/h)
1/2 (z up)			95.9
3/4 (y up)		147	
5/6 (x up)	140		
Spec. (max)	180	180	180

3.4 XSens MTI-30

The MTI30 [5] is a MEMS-based IMU also manufactured by the Dutch company XSens. It is part of the so-called MTI 10-series, which has slightly lower performance than the MTI 100-series. The specifications of the inertial sensors are given in Table 3.16.

Figure 3.82 The XSens MTI30 IMU.

Table 3.16 Specifications of the XSens MTI30.

	Gyros	Accelerometers
Bias repeatability (Max, 1yr)	0.5 deg/s	0.05 m/s^2
Bias instability (typical)	10 deg/hr	40 µg
Random walk (max.)	0.05 deg/s/sqrt(Hz)	150 µg/sqrt(Hz)
Scale factor accuracy	Not specified	Not specified

3.4.1 Long term static test

As in the previous tests, the unit was placed on a stable table, with the z-accelerometer pointing down. The unit was powered on, after having been turned off for an extensive period. Thus, potential effects due to self-warming would be visible in the data.

3.4.1.1 Accelerometers

Figure 3.83 through Figure 3.85 show the output from the accelerometers during the static test. As the output is given as delta velocity measurements, the values plotted are divided by delta time to obtain accelerations. The same data averaged over 1 minute intervals are shown in Figure 3.99 through Figure 3.101. Some sudden steps are visible both in the x and z accelerometer data. In the y data, we see a sudden change in the magnitude of the noise after around 2000 seconds. This behavior may be due to startup effects.

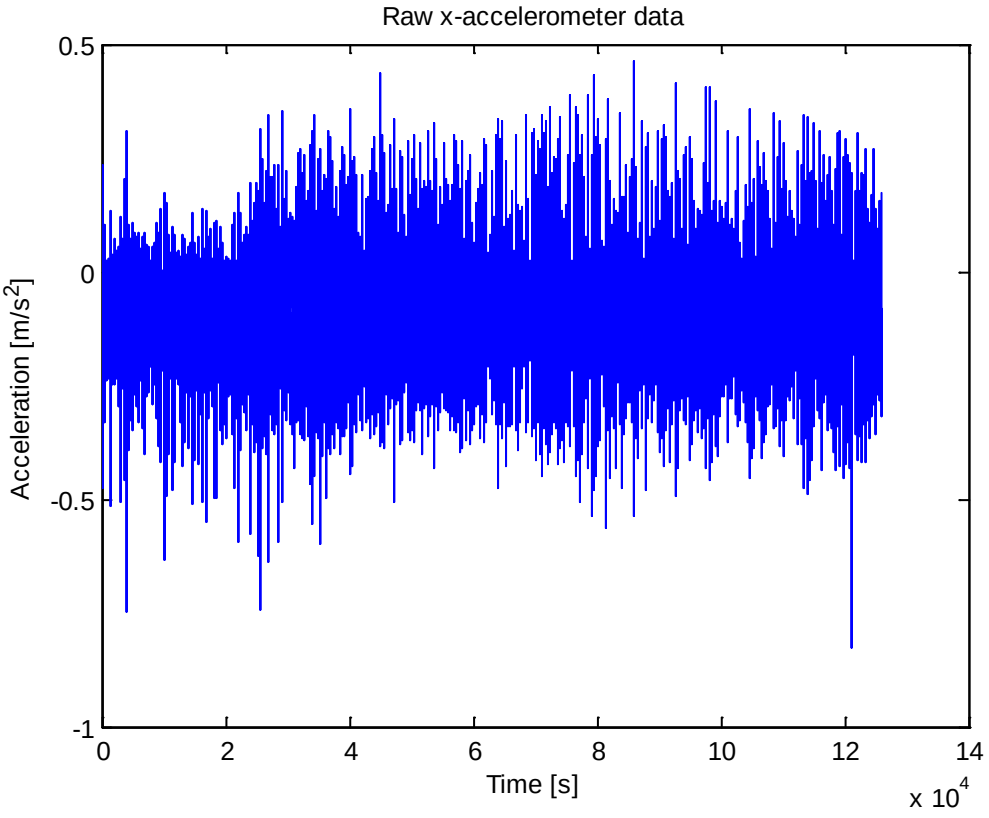

Figure 3.83 Raw data from theMTI30 x accelerometer.

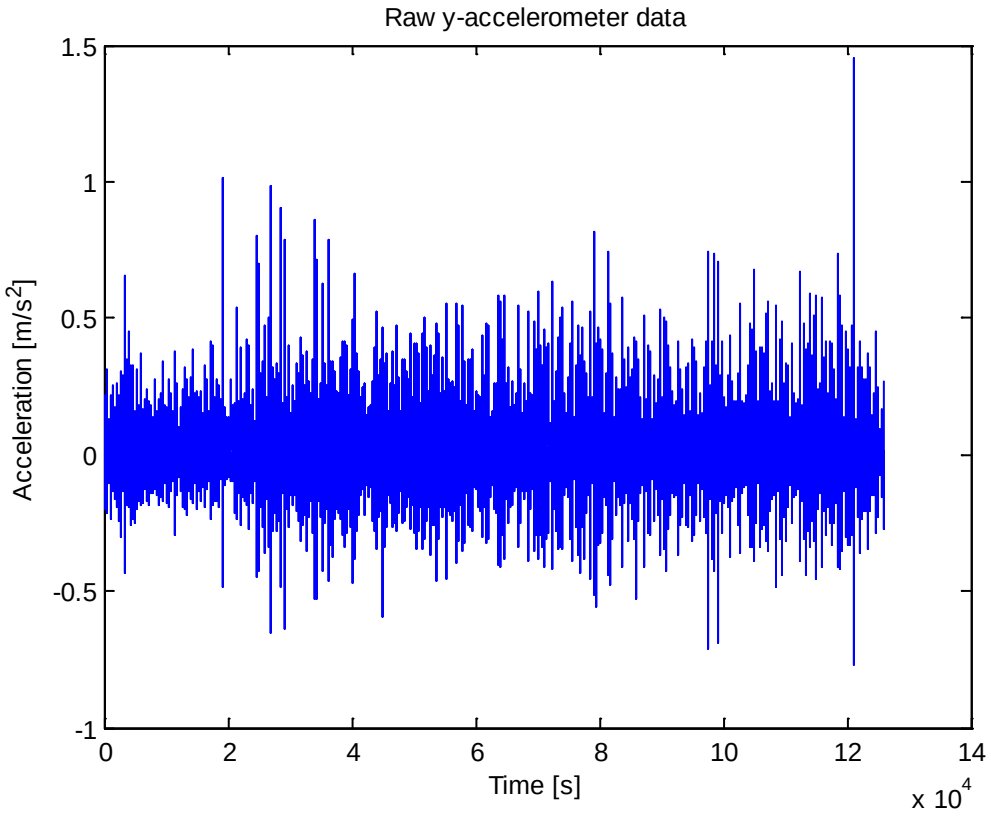

Figure 3.84 Raw data from theMTI30 y accelerometer.

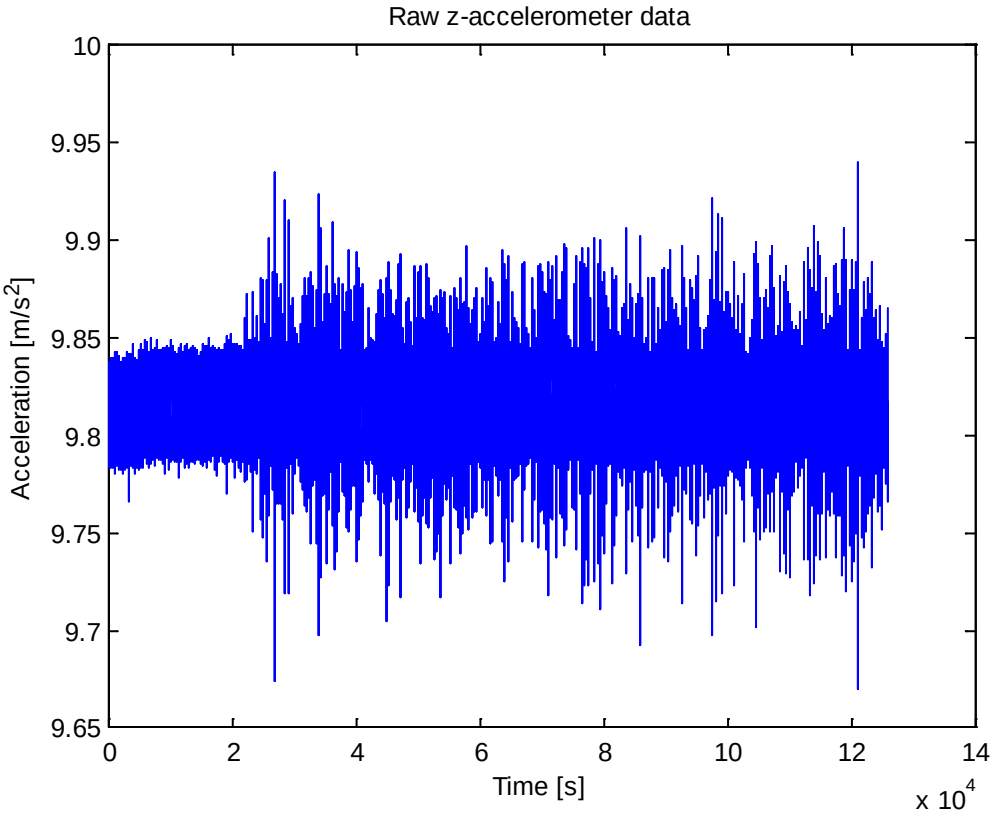

Figure 3.85 Raw data from theMTI30 z accelerometer.

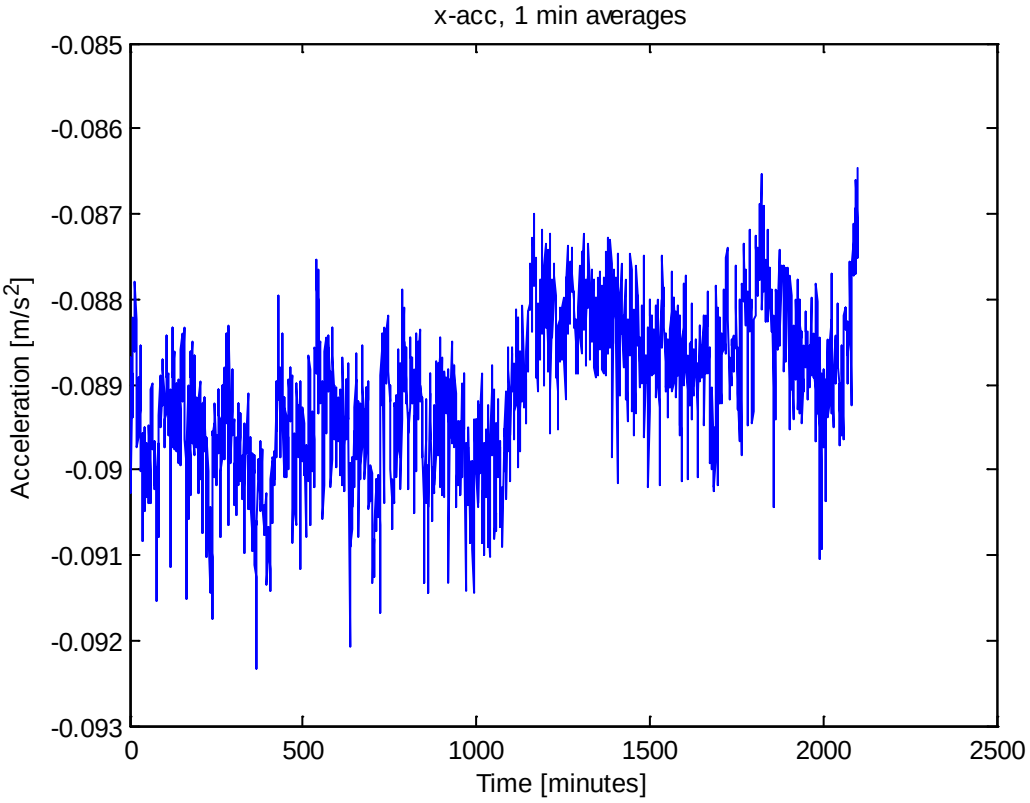

Figure 3.86 MTI30 x accelerometer data averaged over 1 minute intervals.

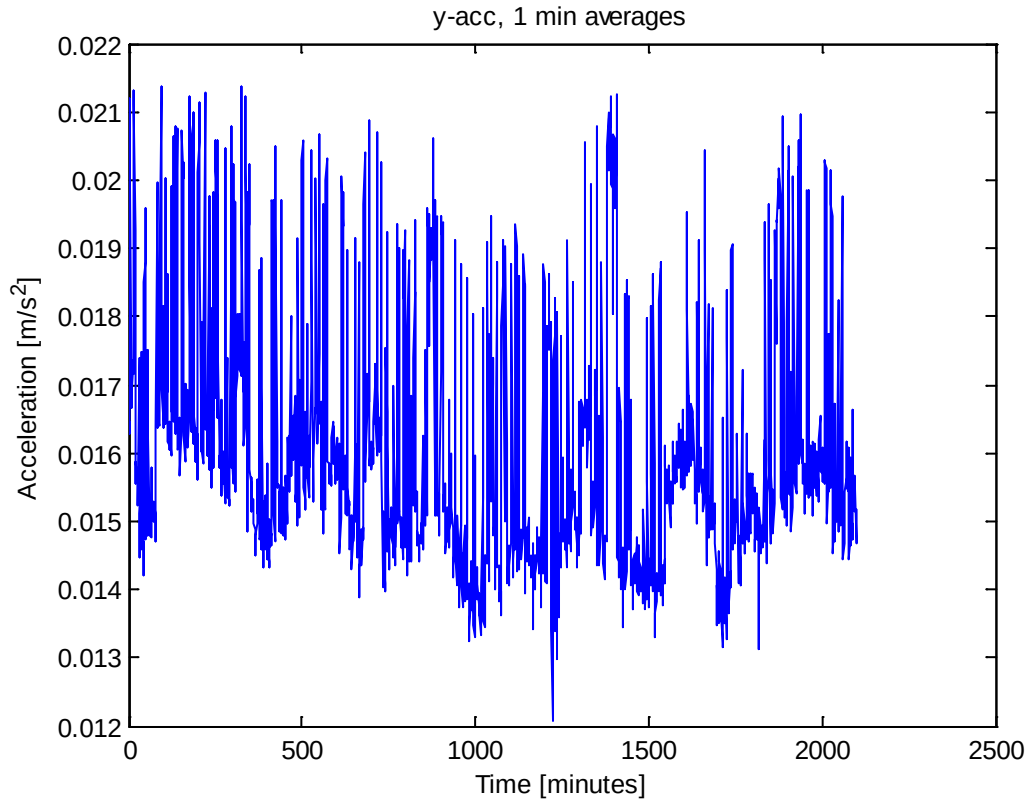

Figure 3.87 MTI30 y accelerometer data averaged over 1 minute intervals.

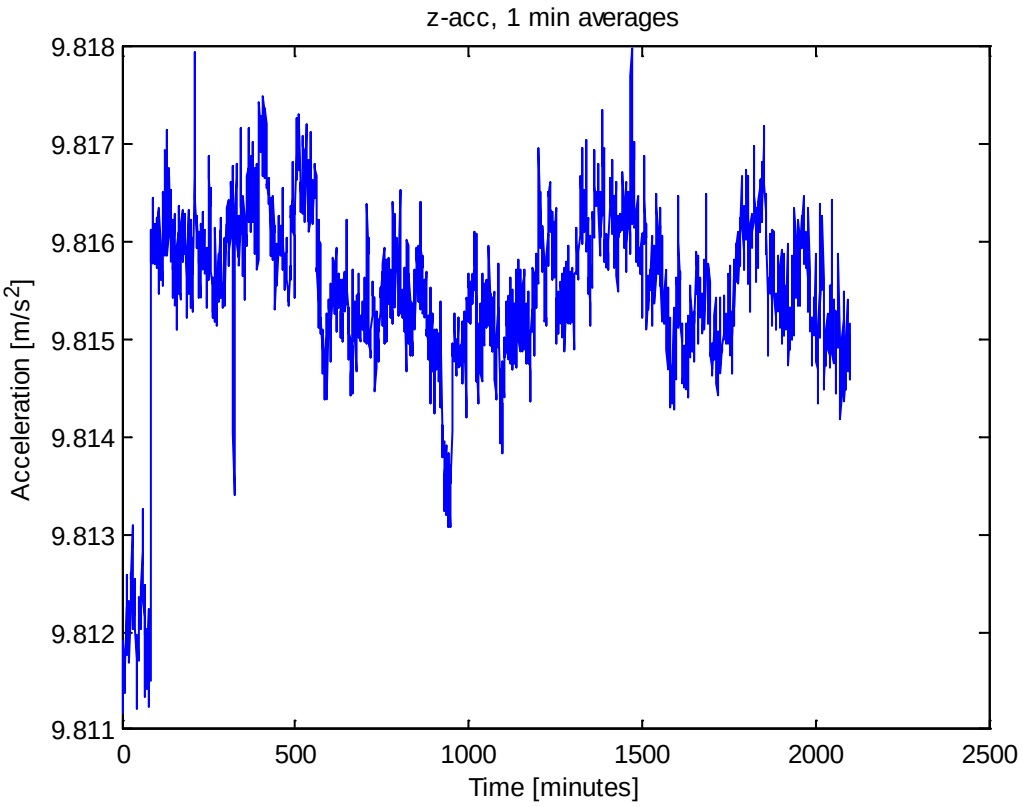

Figure 3.88 MTI30 z accelerometer data averaged over 1 minute intervals.

Figure 3.89 shows computed root Allan variance from the three accelerometers from the entire test interval. The same pre summing over 1 second intervals as before was used. As was the case for the MTI300 accelerometer data, the quality of the estimated Allan variance curve is poor. Based on the Allan variance plots, the velocity random walk and bias instability values were estimated. The velocity random walk estimates were 77.9, 82.5, 75.2 µg/sqrt(Hz) for the x, y and z accelerometer, respectively, all within the specified value of 150 µg/sqrt(Hz). The bias instability estimates (i.e. the minimum value of the root Allan variance curves) were 30, 50 and 30 µg for the three axes, the y accelerometer being above the specification of 40 µg. However, due to the unusual shape of the Allan variance curve, this estimate may be inaccurate.

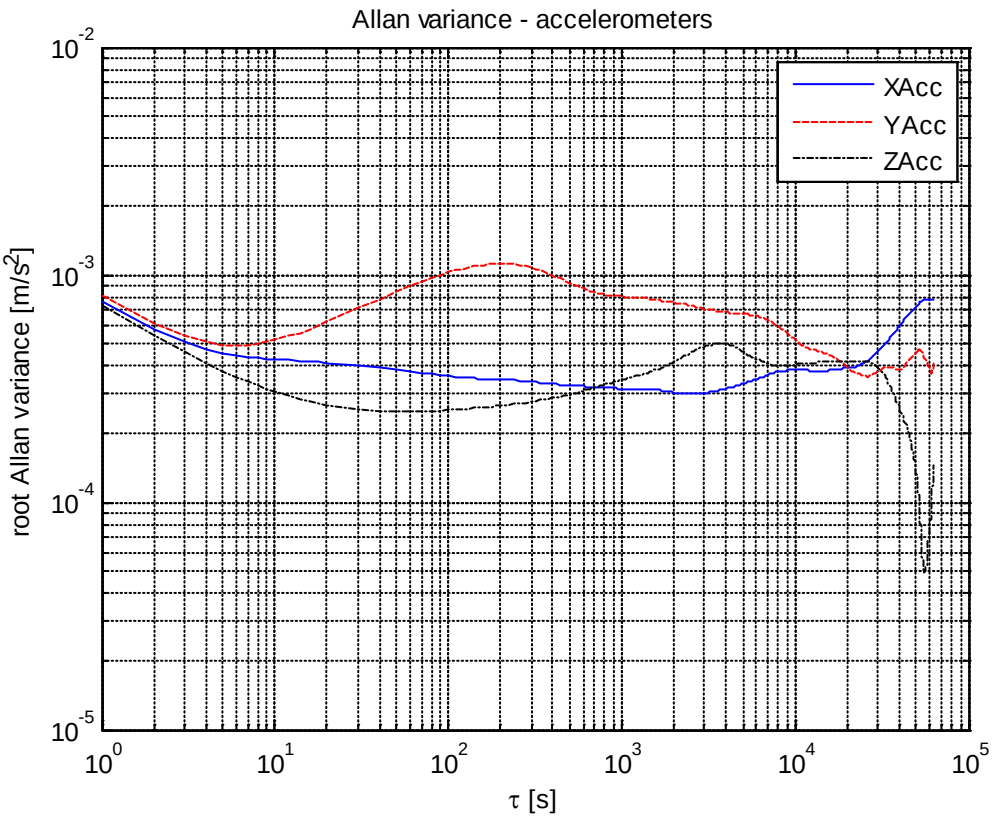

Figure 3.89 Computed Allan variance from the MTI30 accelerometer data.

Figure 3.90 through Figure 3.92 show the computed spectral densities of the accelerometers. The frequencies seem to be rather evenly distributed. There are a few local maxima for certain frequencies, but these are too small to be of significance. The plots are almost identical to those from the MTI300 unit, which is natural since the accelerometers in these units probably are identical.

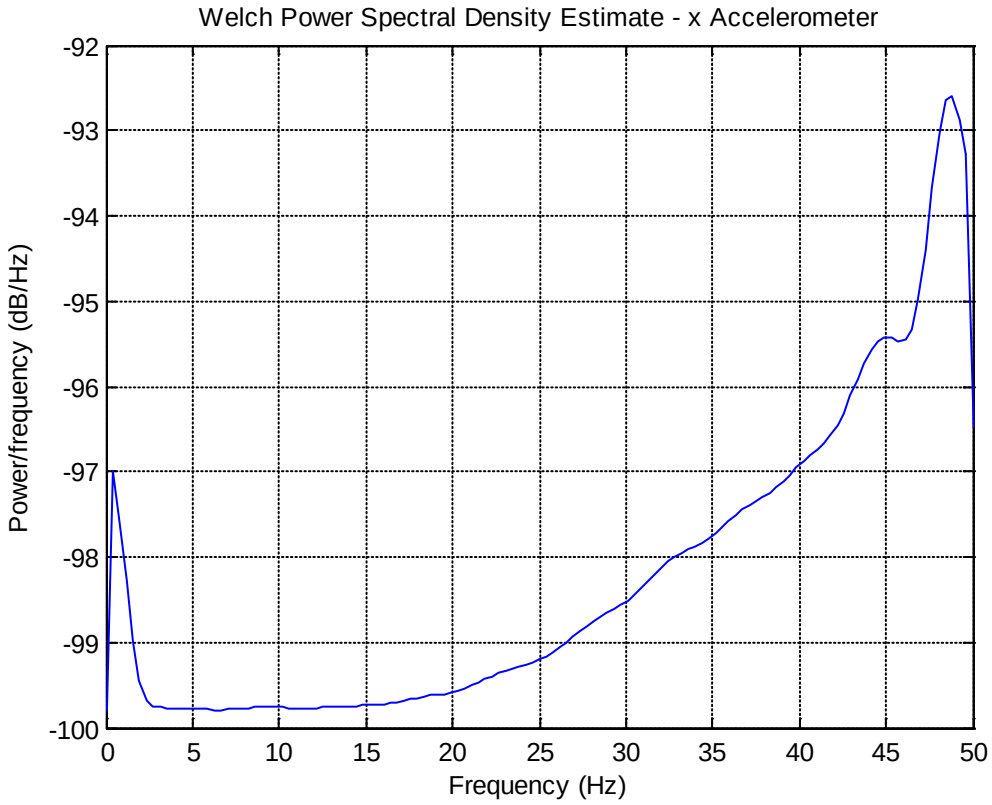

Figure 3.90 Spectral density plot - MTI30 x accelerometer.

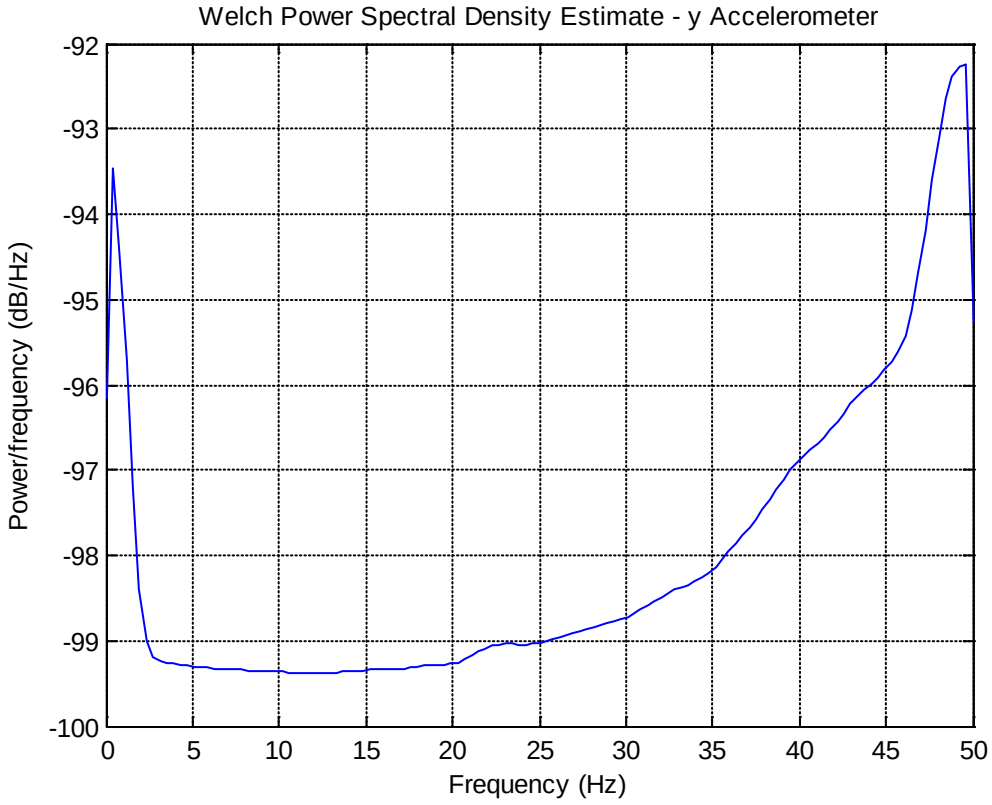

Figure 3.91 Spectral density plot - MTI30 y accelerometer.

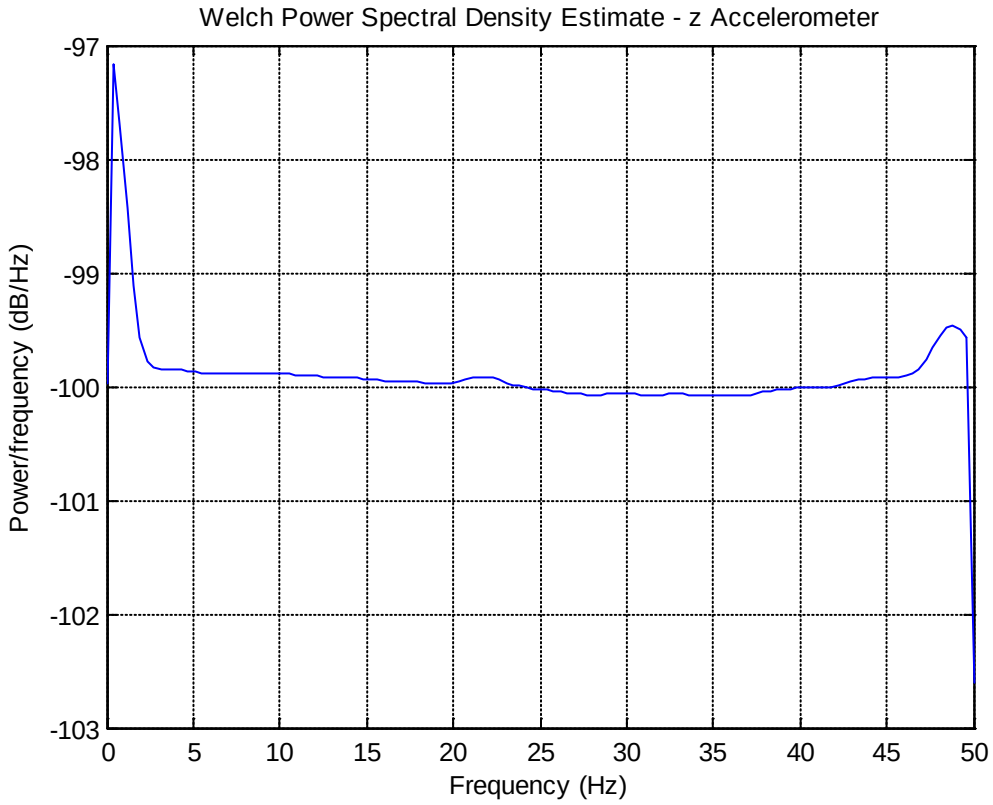

Figure 3.92 Spectral density plot - MTI30 z accelerometer.

Figure 3.93 through Figure 3.95show histograms for the raw accelerometer measurements. All histograms show a Gaussian-like distribution, with very sharp peaks. The standard deviations of the measured accelerations (delta velocity divided by delta time) are (0.0092, 0.0094, 0.0072) m/s^2 for the x, y and z accelerometer, respectively.

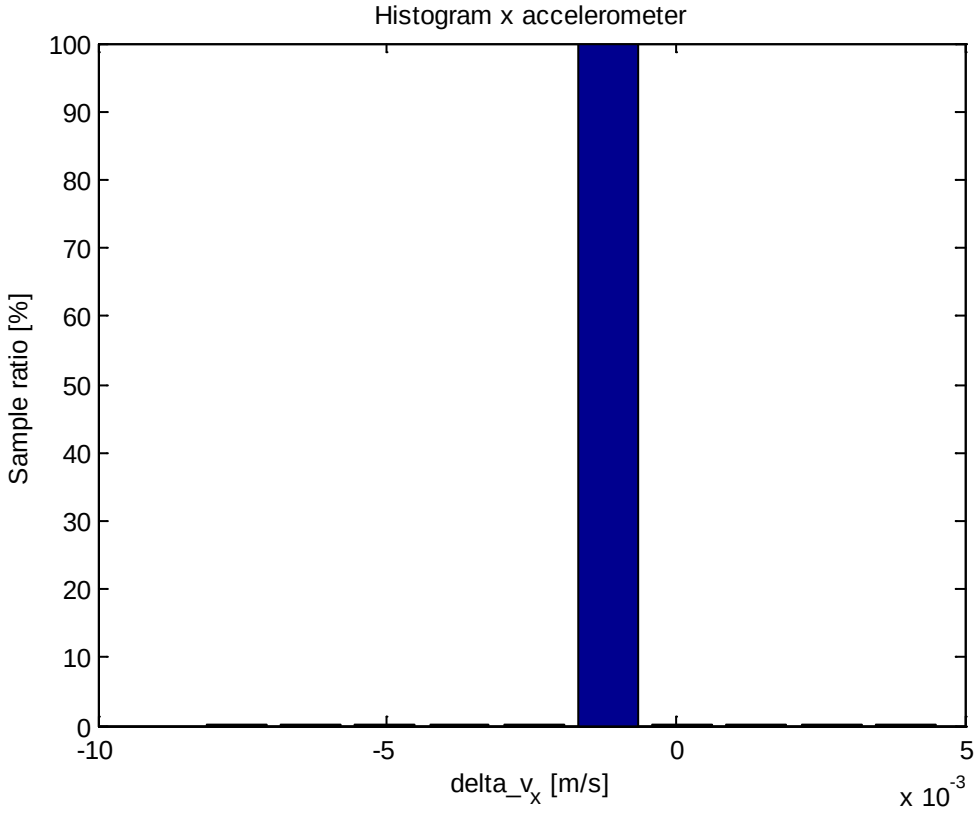

Figure 3.93 MTI30 x accelerometer histogram.

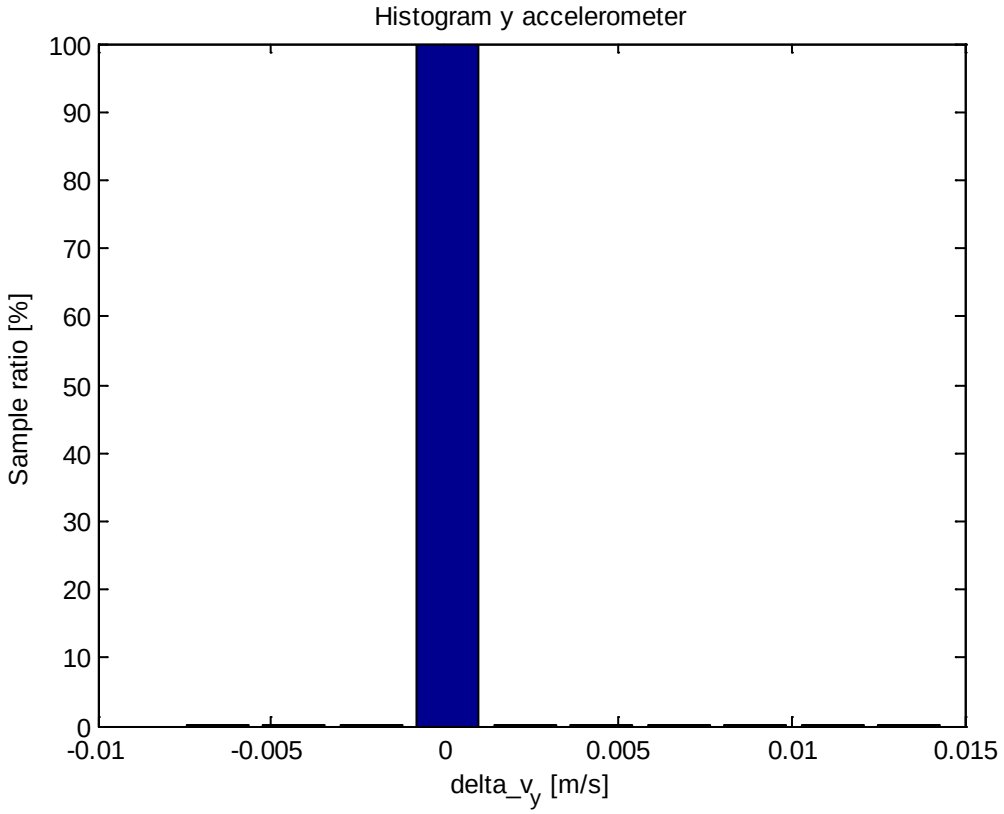

Figure 3.94 MTI30 y accelerometer histogram.

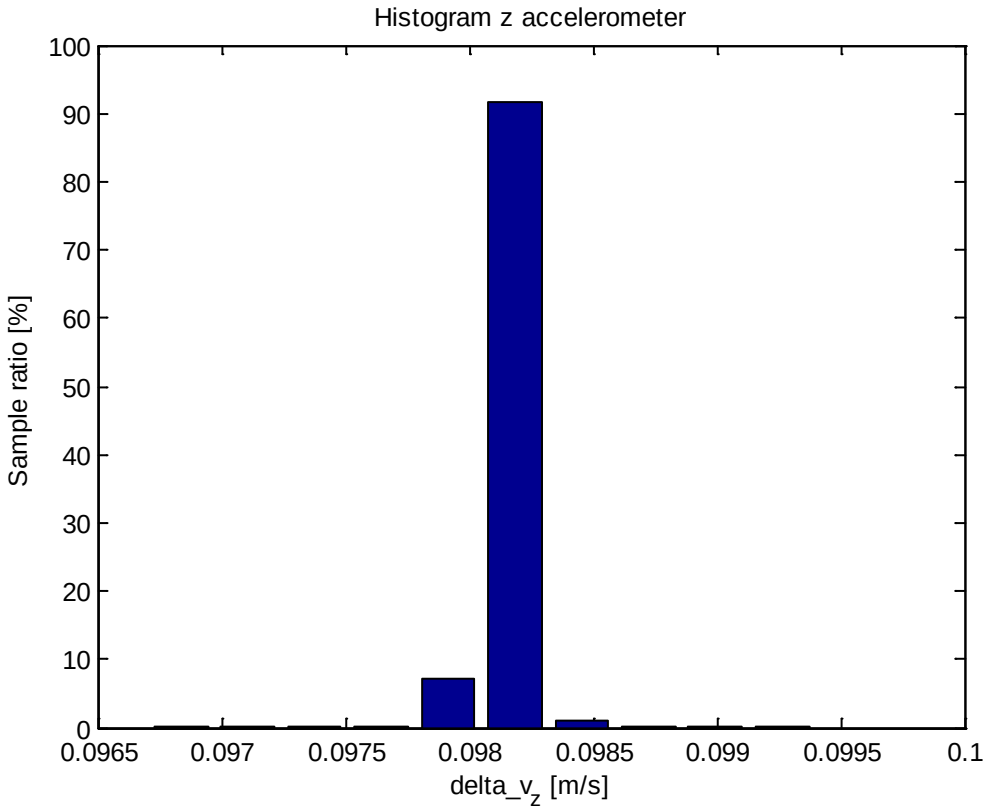

Figure 3.95 MTI30 z accelerometer histogram.

3.4.1.2 Gyroscopes

Figure 3.96 through Figure 3.98 show raw data from the MTI30 gyroscopes throughout the static test. The same data averaged over 1 minute intervals are shown in Figure 3.99 through Figure 3.101. The same change in noise level as was seen in one of the accelerometers is also visible in the x and y gyro data. Apart from this no significant startup effects are present.

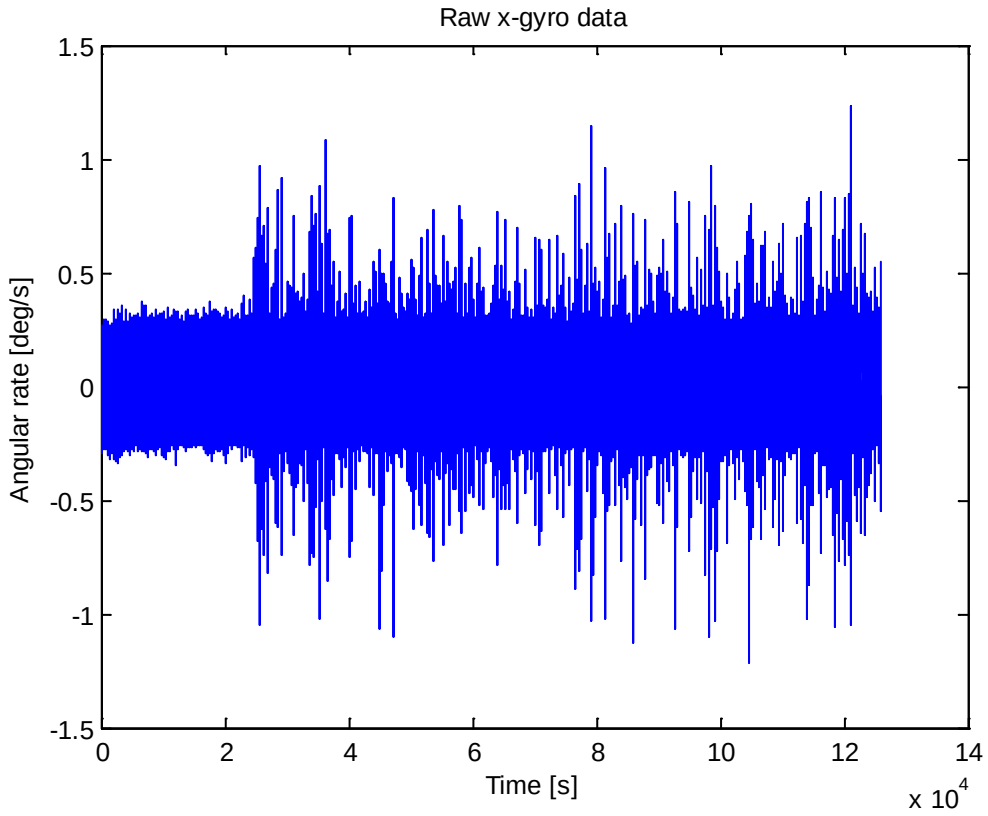

Figure 3.96 Raw data from the MTI30 x gyro.

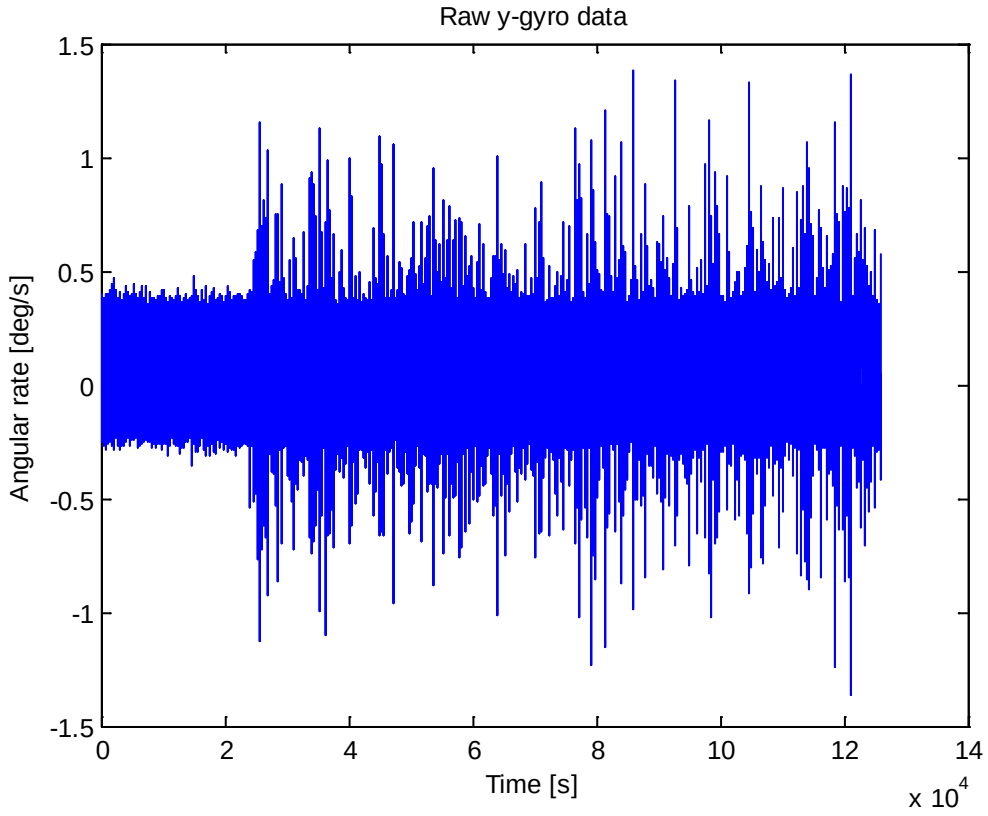

Figure 3.97 Raw data from theMTI30 y gyro.

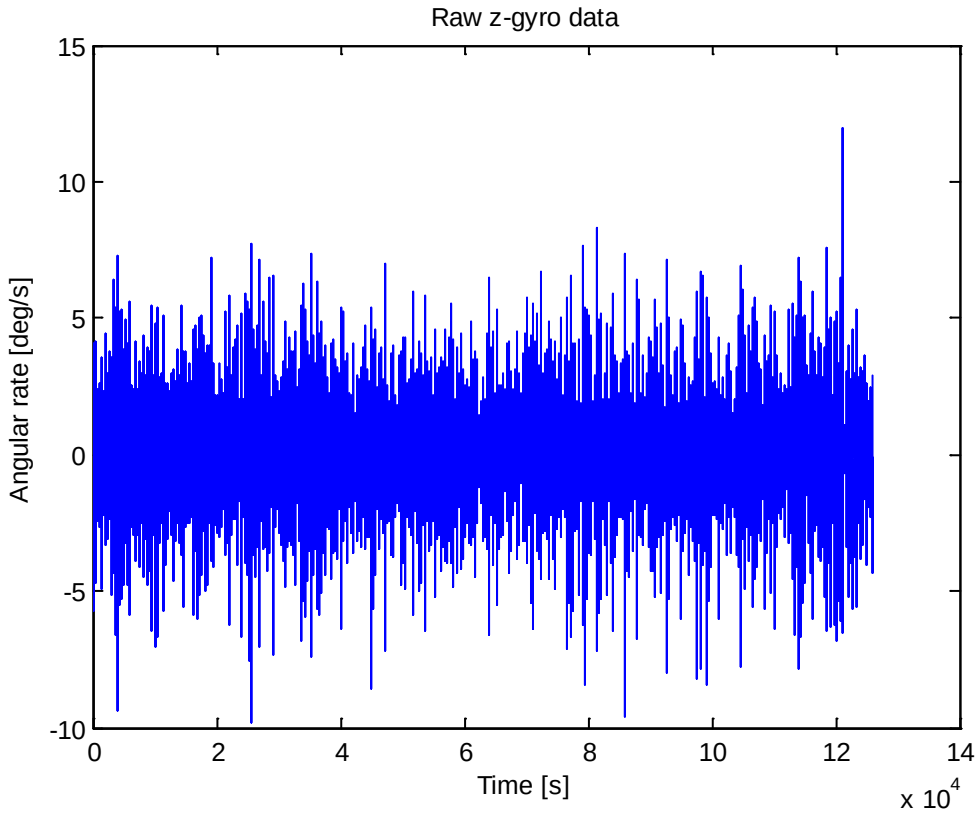

Figure 3.98 Raw data from theMTI30 z gyro.

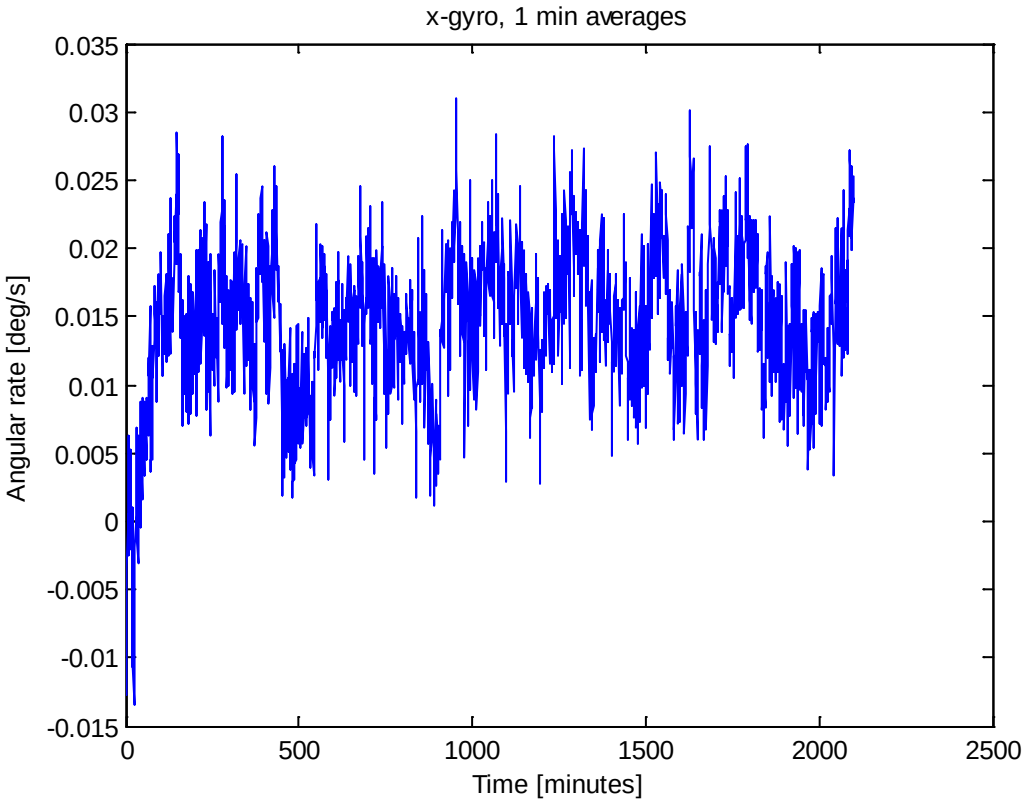

Figure 3.99 MTI30 x gyro data averaged over 1 minute intervals.

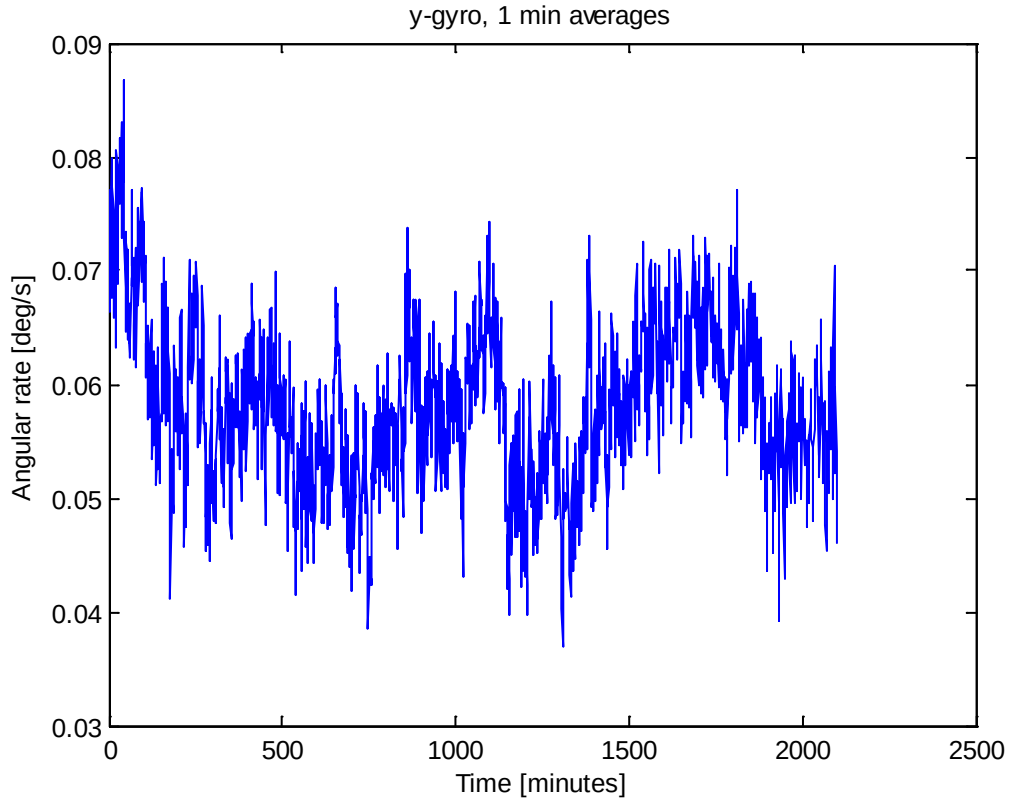

Figure 3.100 MTI30 y gyro data averaged over 1 minute intervals.

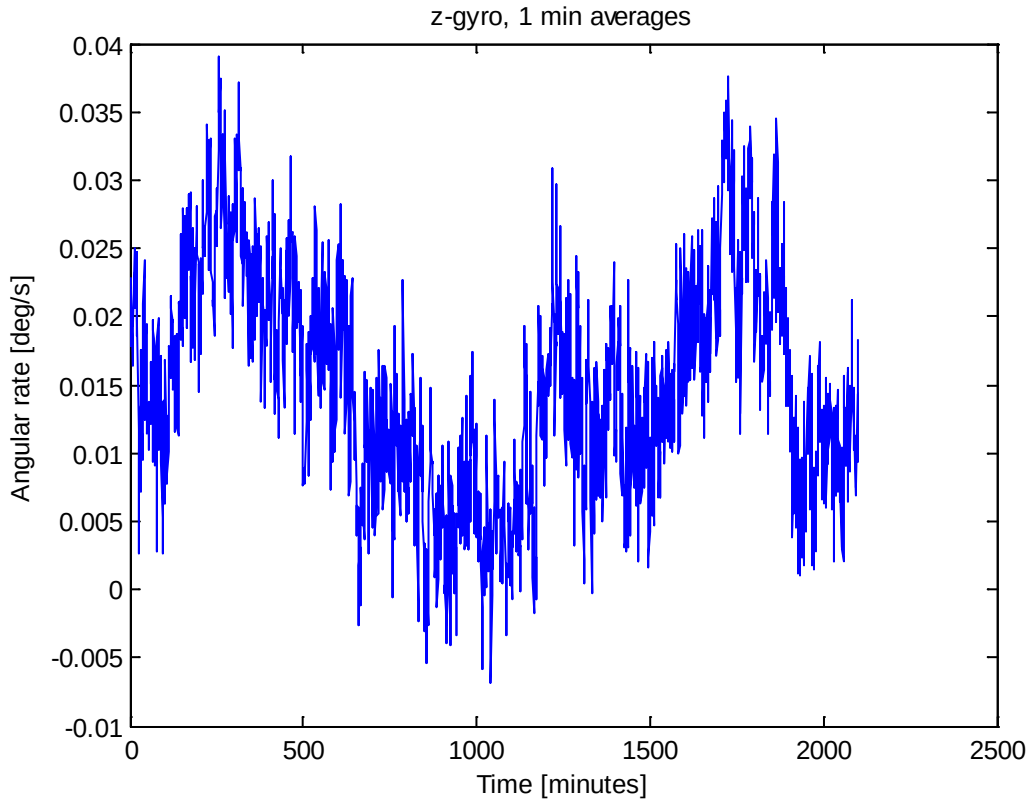

Figure 3.101 MTI30 z gyro data averaged over 1 minute intervals.

Figure 3.102 shows computed Allan variance for the three gyros, again after 1 second interval pre summing. Based on the Allan variance plots, the angular random walk and bias instability values were estimated. The angular random walk estimates were 0.439, 0.406 and 0.014 deg/sqrt(h) for the x, y and z gyro, respectively, all within the specified value of 3 deg/sqrt(h) (0.05 deg/s/sqrt(Hz)). The bias instability estimates (i.e. the minimum value of the root Allan variance curves) were 8.3, 10.0 and 9.3 deg/h, all within the specified value of 10 deg/h.

The Allan variance curves contain the usual regions of angular random walk (slope -1/2) and bias instability (slope 0). The curves for the y and z gyro also have positive slopes (+1) for long averaging times, indicating the presence of a rate ramp error component. However, this may also be the result of inaccurate estimates due to few samples in this region.

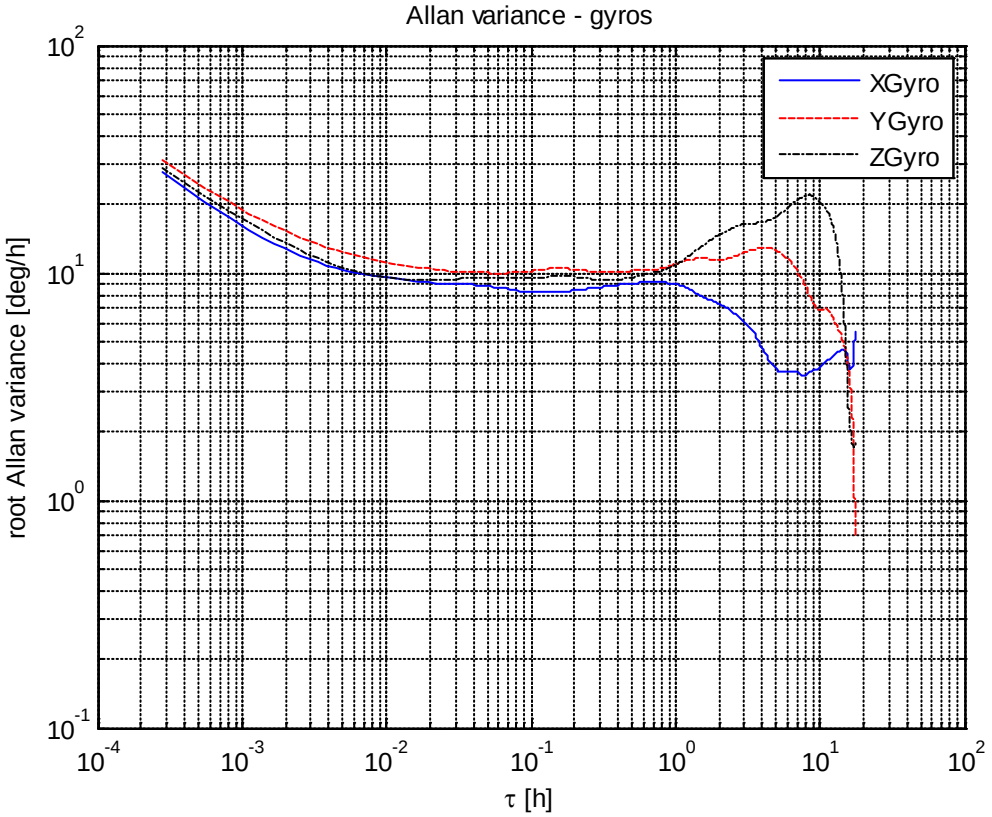

Figure 3.102 Computed Allan variance from MTI30 gyro data.

Figure 3.103 through Figure 3.105 show spectral density plots for the gyro measurements. Again, the plots are very similar to those of the MTI300. No significant peaks are present.

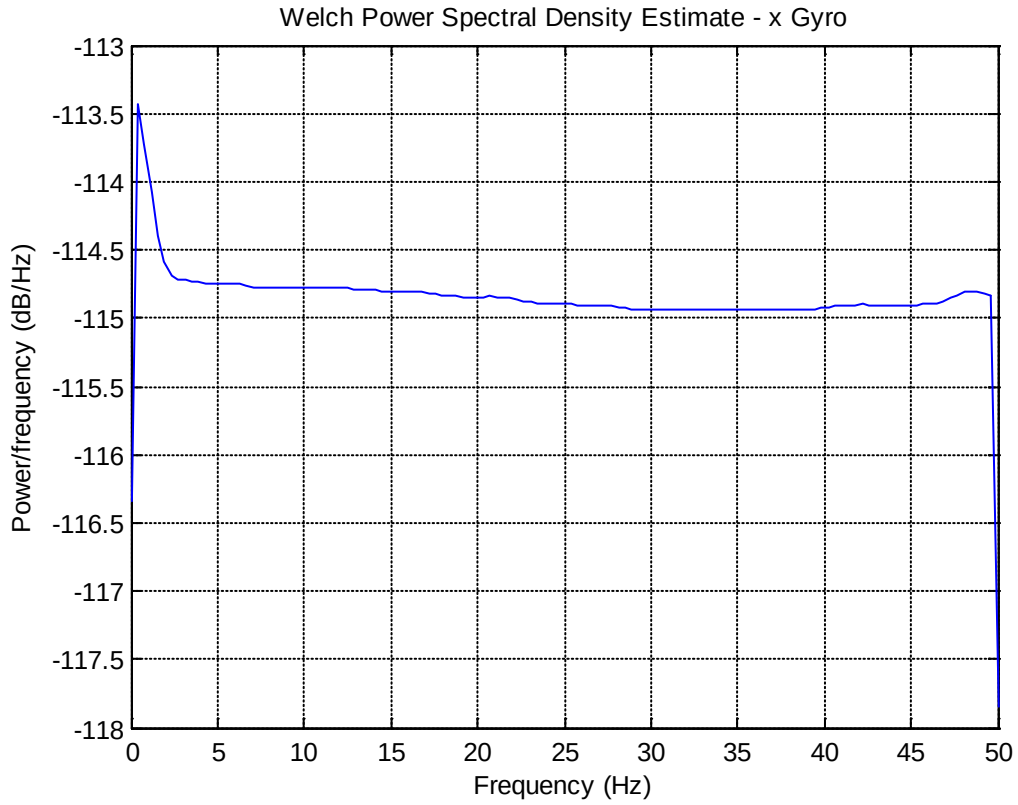

Figure 3.103 Spectral density plot - MTI30 x gyro.

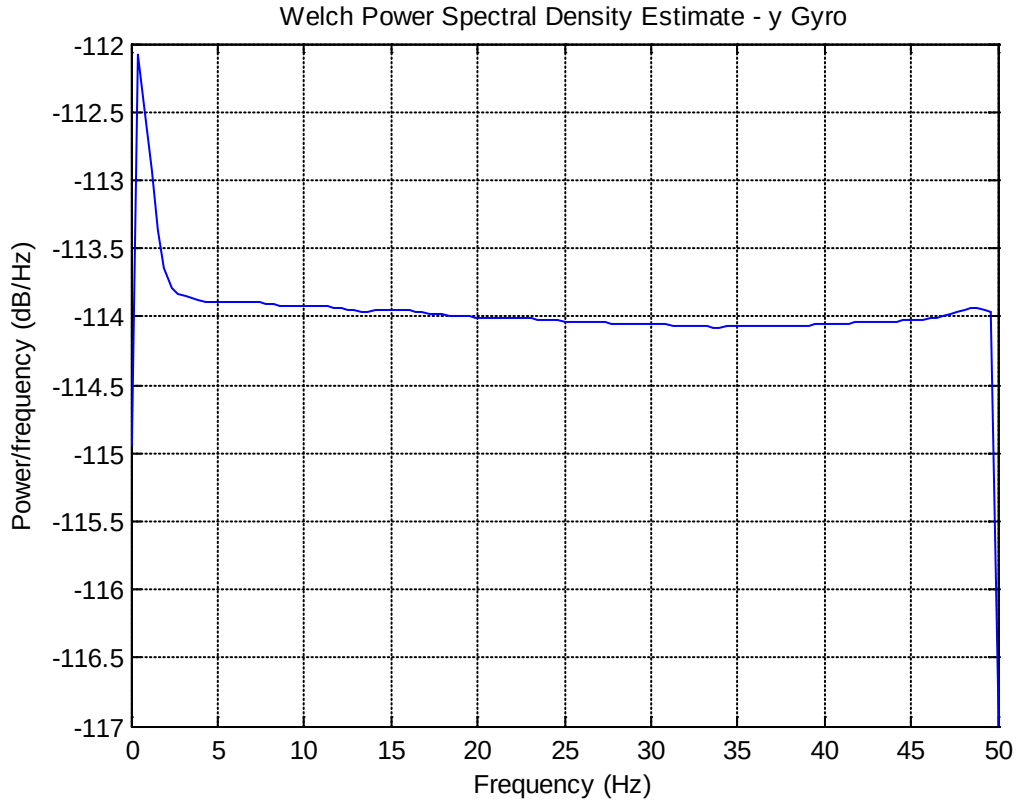

Figure 3.104 Spectral density plot - MTI30 y gyro.

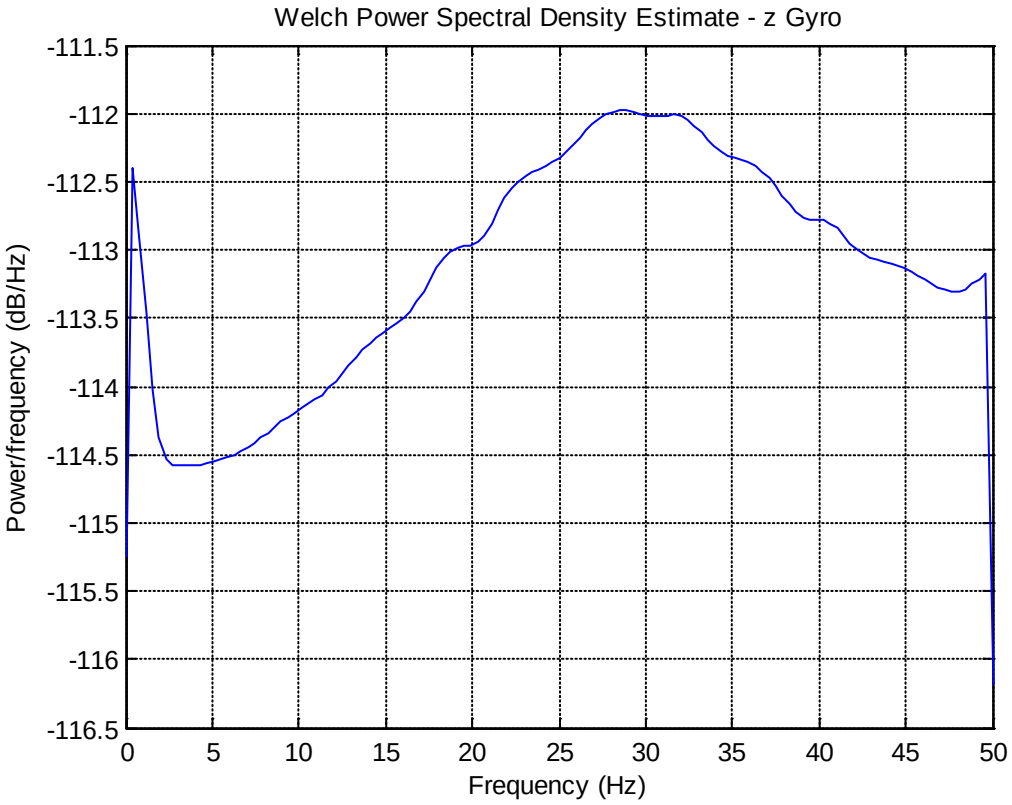

Figure 3.105 Spectral density plot - MTI30 z gyro.

Figure 3.106 through Figure 3.108 show histograms of the MTI30 gyro measurements. Again, the distributions are Gaussian-like, and very similar to the MTI300 data. The standard deviations of the angular rates (delta theta divided by delta time) were (0.074, 0.081, 0.090) deg/s, for the x, y, and z gyro, respectively.

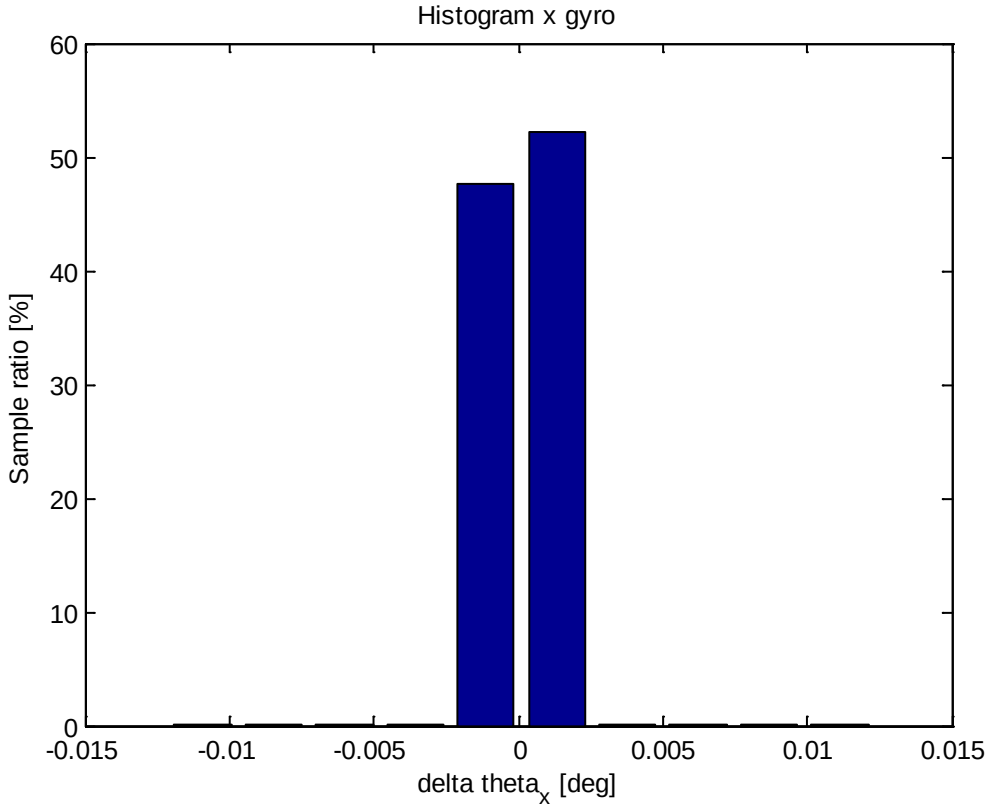

Figure 3.106 MTI30 x gyro histogram.

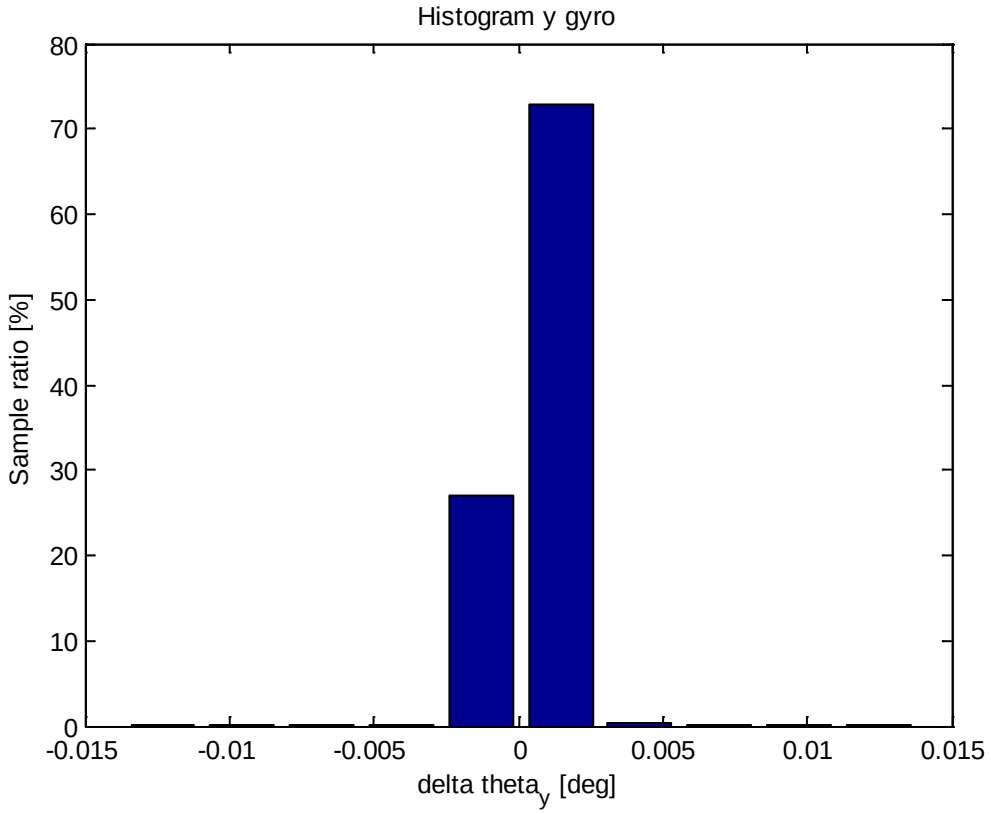

Figure 3.107 MTI30 y gyro histogram.

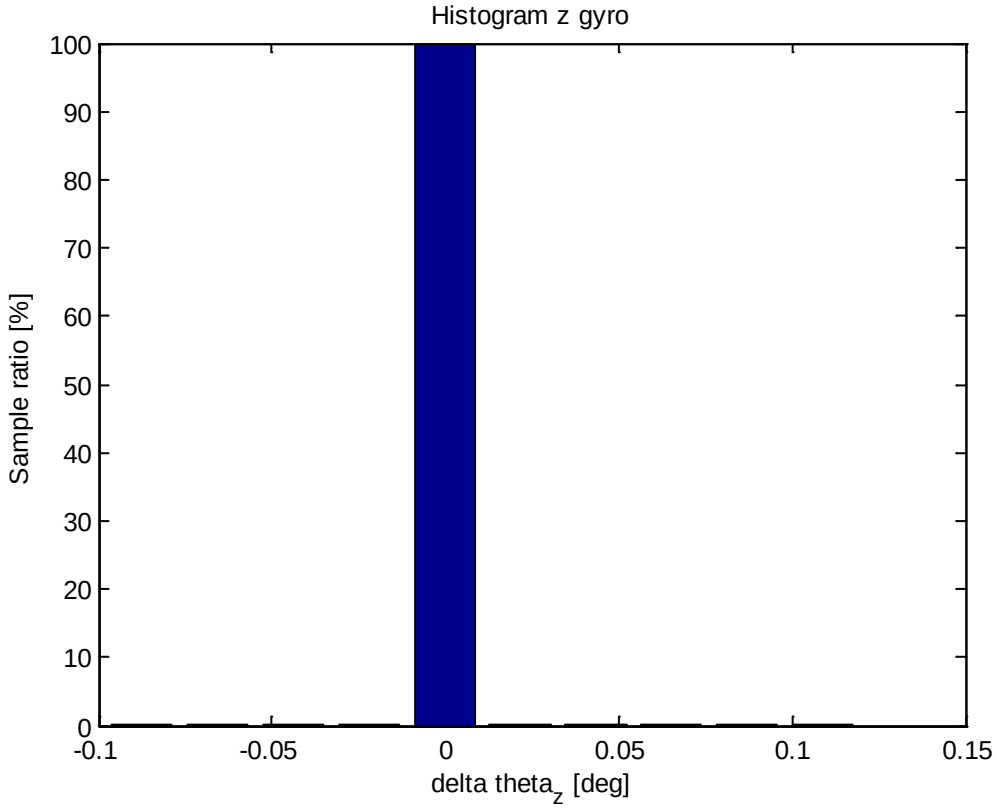

Figure 3.108 MTI300 z gyro histogram.

3.4.2 Repeatability and temperature tests

The results from the repeatability and temperature tests are shown in Table 3.17 and Table 3.18, for the accelerometers and gyroscopes, respectively. In this case, the measurements from the accelerometers are much closer to standard gravitation. The same trends as in the MTI300 data are present, i.e. the output is fairly consistent between power-ons, and the gyros are more sensitive to temperature variations than the accelerometers. However, the gyro standard deviations are less affected by temperature changes than what has been the case in the IMUs from the other manufacturers tested in this report.

Table 3.17 Mean MTI-30 accelerometer measurements and standard deviations in repeatability and temperature tests.

Test name	norm(mean(f)) [m/s^2]	std f_x [m/s^2]	std f_y [m/s^2]	std f_z [m/s^2]
Oppstart_Og_LangtidsTest	9.8159	0.0092	0.0094	0.0072
Repiterbarhetstest_1	9.8099	0.0089	0.0087	0.0071
Repiterbarhetstest_2	9.8099	0.0088	0.0087	0.0071
Repiterbarhetstest_3	9.8095	0.0086	0.0085	0.0071
TemperaturTest_+0grader	9.814	0.0081	0.0083	0.0068
TemperaturTest_+10grader	9.8167	0.0082	0.0087	0.007
TemperaturTest_+20grader	9.8093	0.0087	0.0094	0.0071
TemperaturTest_+30grader	9.8157	0.0086	0.0087	0.0073
TemperaturTest_+40grader	9.8137	0.0079	0.0082	0.0074
TemperaturTest_+50grader	9.8144	0.0083	0.009	0.0076
TemperaturTest_-10grader	9.812	0.0086	0.0101	0.0067
TemperaturTest_-20grader	9.7934	0.0138	0.0176	0.0068
TemperaturTest_-30grader	9.7822	0.0208	0.021	0.0068
TemperaturTest_+20graderTil+50	9.8116	0.0088	0.0092	0.0079
TemperaturTest_+40 til +10 grader	9.8158	0.0093	0.0099	0.0075
TemperaturTest_-30 til +20 grader	9.8034	0.0082	0.0088	0.0077

Table 3.18 Mean MTI-30 gyro measurements and standard deviations in repeatability and temperature tests.

Test name	norm(mean(ω)) [deg/s]	std ω_x [deg/s]	std ω_y [deg/s]	std ω_z [deg/s]
Oppstart_Og_LangtidsTest	0.06177	0.0736	0.0814	0.0904
Repiterbarhetstest_1	0.05305	0.0732	0.0811	0.0904
Repiterbarhetstest_2	0.07505	0.0732	0.0809	0.0899
Repiterbarhetstest_3	0.0713	0.0734	0.0809	0.0876
TemperaturTest_+0grader	0.04424	0.0661	0.0742	0.0757
TemperaturTest_+10grader	0.01724	0.0696	0.0776	0.079
TemperaturTest_+20grader	0.04859	0.0733	0.0807	0.0854
TemperaturTest_+30grader	0.0335	0.077	0.0846	0.0855
TemperaturTest_+40grader	0.01517	0.0803	0.0878	0.0812
TemperaturTest_+50grader	0.03191	0.0838	0.0913	0.0848
TemperaturTest_-10grader	0.04952	0.0628	0.0707	0.0781
TemperaturTest_-20grader	0.04705	0.0604	0.0682	0.0748
TemperaturTest_-30grader	0.05448	0.0579	0.0655	0.0876
TemperaturTest_+20graderTil+50	0.05545	0.0827	0.0908	0.0836
TemperaturTest_+40 til +10 grader	0.0146	0.0723	0.0805	0.0955
TemperaturTest_-30 til +20 grader	0.009054	0.0728	0.0798	0.076

3.4.3 Up-down tests

The results from the up/down tests are shown in Table 3.19 and Table 3.20, using the same color coding as before. All the sensors are within the specifications.

Table 3.19 MTI30 accelerometer parameters computed from up/down tests.

Test	x acc. bias (m/s^2)	x acc. scale factor (ppm)	y acc. bias (m/s^2)	y acc. scale factor (ppm)	z acc. bias (m/s^2)	z acc. scale factor (ppm)
1/2 (z up)					0.012	1000
3/4 (y up)			0.0058	1000		
5/6 (x up)	0.0037	1000				
Spec. (max)	0.05		0.05		0.05	

Table 3.20 MTI30 gyro parameters computed from up/down test.

Test	x gyro bias (deg/h)	y gyro bias (deg/h)	z gyro bias (deg/h)
1/2 (z up)			7.4
3/4 (y up)		141	
5/6 (x up)	91		
Spec. (max)	180	180	180

3.5 MinIM

The MinIM [6] is a MEMS-based IMU manufactured by the British company Goodrich Atlantic Inertial Systems. The specifications of the inertial sensors are given in Table 3.21.

Figure 3.109 The Goodrich Atlantic Inertial Systems MinIM.

Table 3.21 MinIM specifications.

	Gyros	Accelerometers
Bias repeatability	100 deg/hr	20 mg
Bias instability (typical)	8 deg/hr	0.7 mg
Random walk (max.)	1.2 deg/sqrt(h)	0.6 m/s/sqrt(hr)
Scale factor accuracy	1000 ppm	1800 ppm

3.5.1 Static long term test

As in the previous tests, the unit was placed on a stable table, with the x-accelerometer pointing down. The unit was powered on, after having been turned off for an extensive time period. Thus, potential effects due to self-warming would be visible in the data.

3.5.1.1 Accelerometers

Figure 3.110 through Figure 3.112 show the output from the accelerometers during the static test. As the output is given as delta velocity measurements, the values plotted are divided by delta time to obtain accelerations. The same data averaged over 1 minute intervals are shown in Figure 3.113 through Figure 3.115. The measured acceleration is low compared to standard gravity. No significant drift or startup effects are visible.

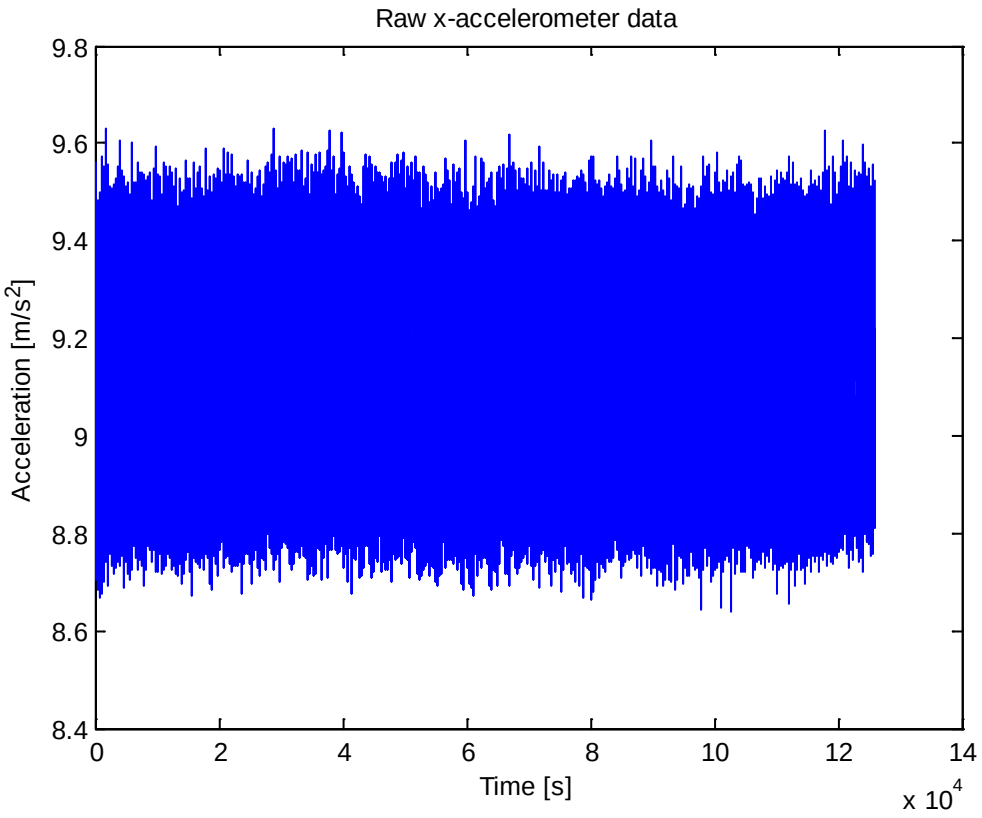

Figure 3.110 Raw data from the MinIM x accelerometer.

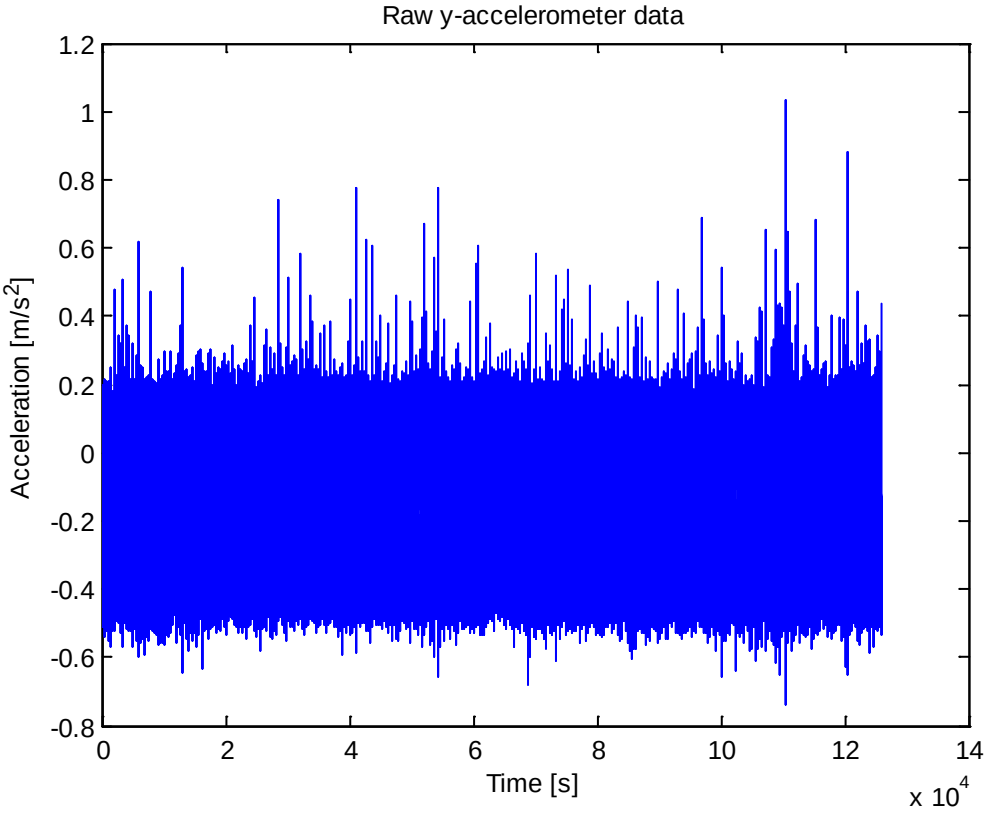

Figure 3.111 Raw data from the MinIM y accelerometer.

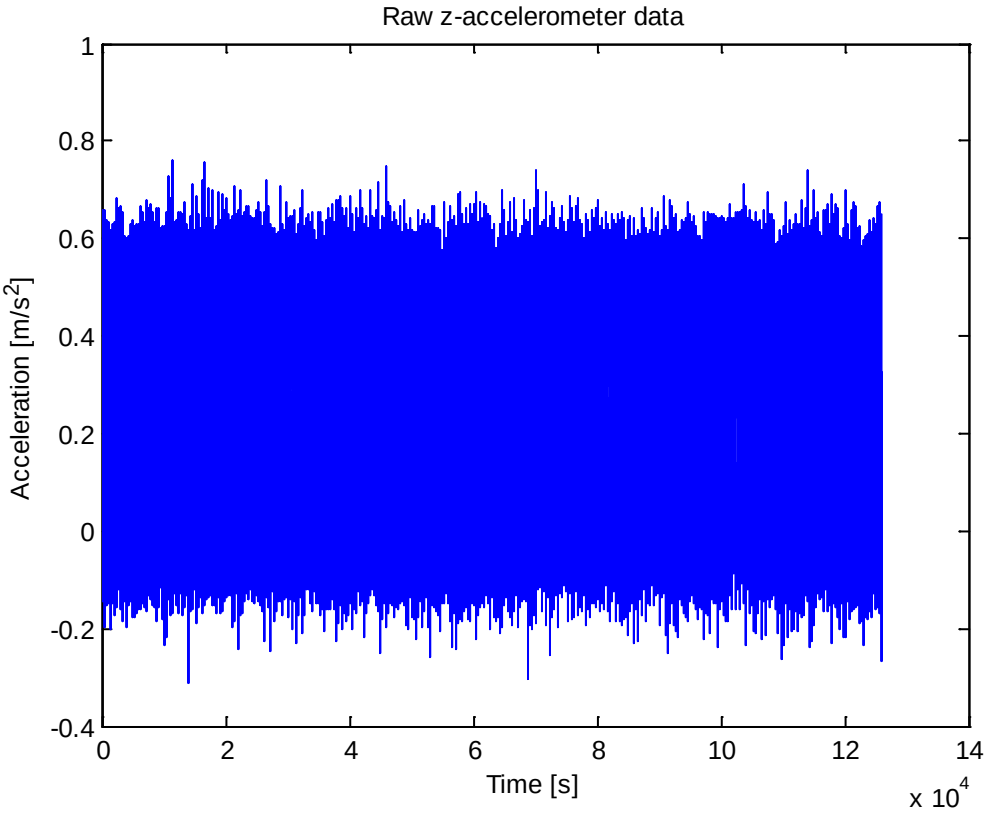

Figure 3.112 Raw data from the MinIM z accelerometer.

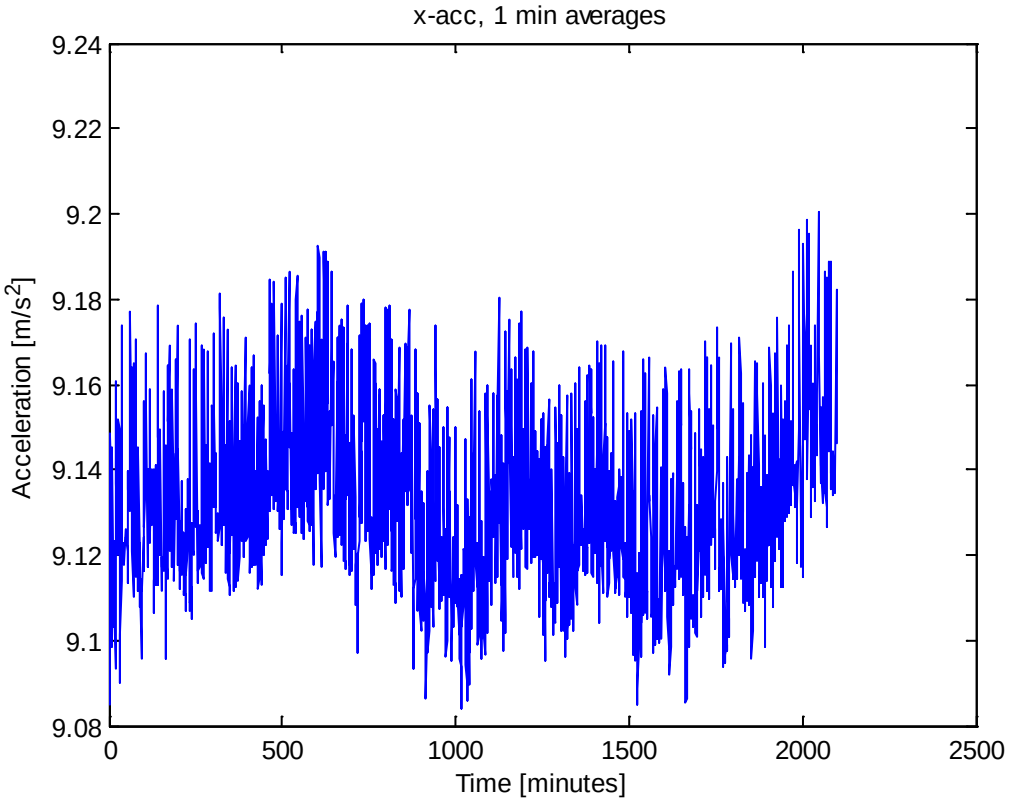

Figure 3.113 MinIM x accelerometer data averaged over 1 minute intervals.

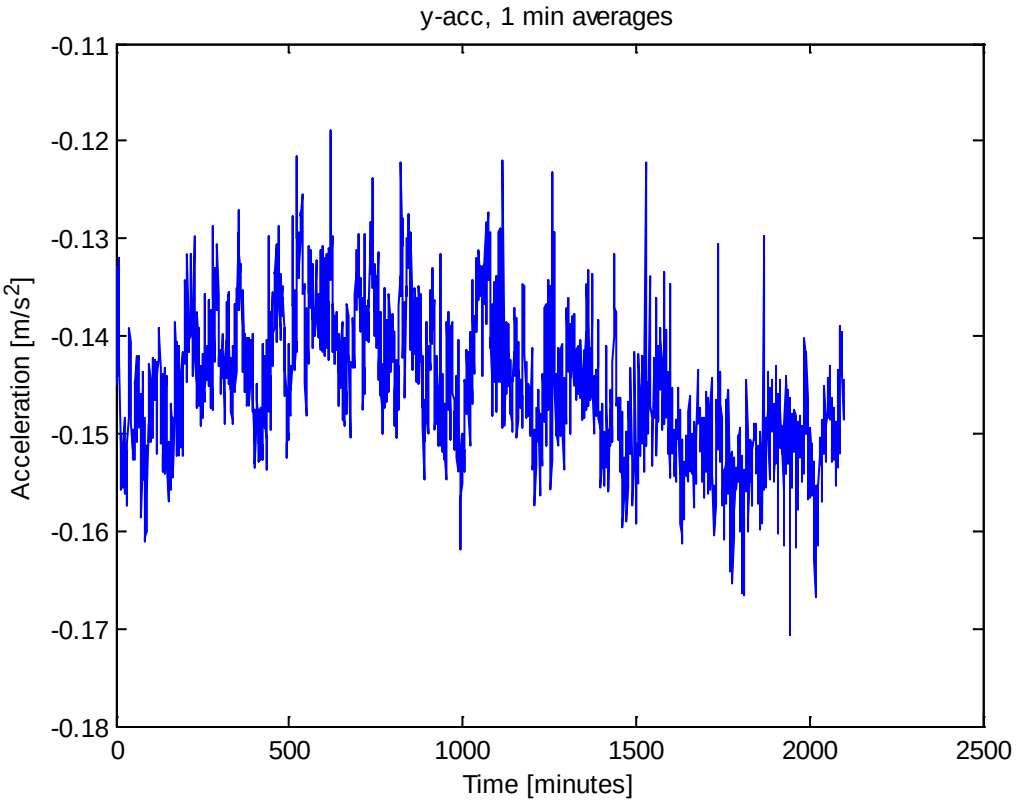

Figure 3.114 MinIM y accelerometer data averaged over 1 minute intervals.

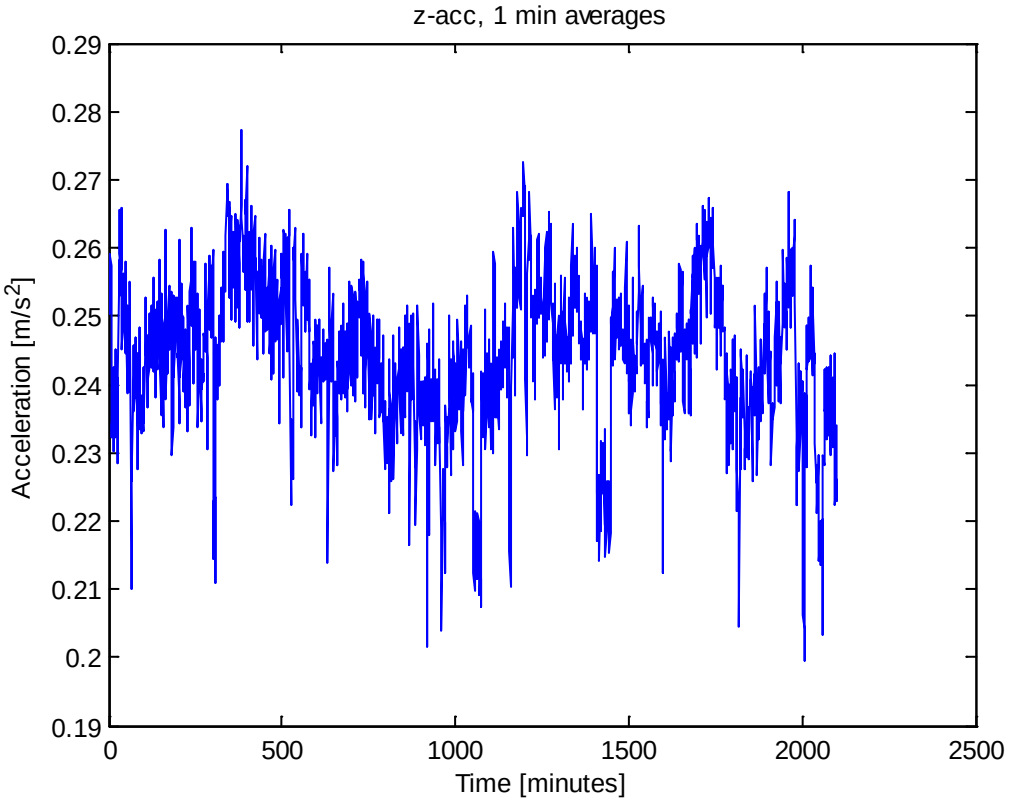

Figure 3.115 MinIM z accelerometer data averaged over 1 minute intervals.

Figure 3.116 shows computed root Allan variance from the three accelerometers from the entire test interval. The same pre summing over 1 second intervals as before was used. Again, the shapes of the Allan variance curves are unusual, especially for the x accelerometer. Based on the Allan variance plots, the velocity random walk and bias instability values were estimated. The velocity random walk estimates were 0.57, 0.57 and 0.57 m/s/sqrt(h) for the x, y and z accelerometer, respectively, all within the specified value of 0.6 m/s/sqrt(h) . The bias instability estimates (i.e. the minimum value of the root Allan variance curves) were 0.5, 0.5 and 0.5 mg for the three axes, all within the specification of 0.7 mg.

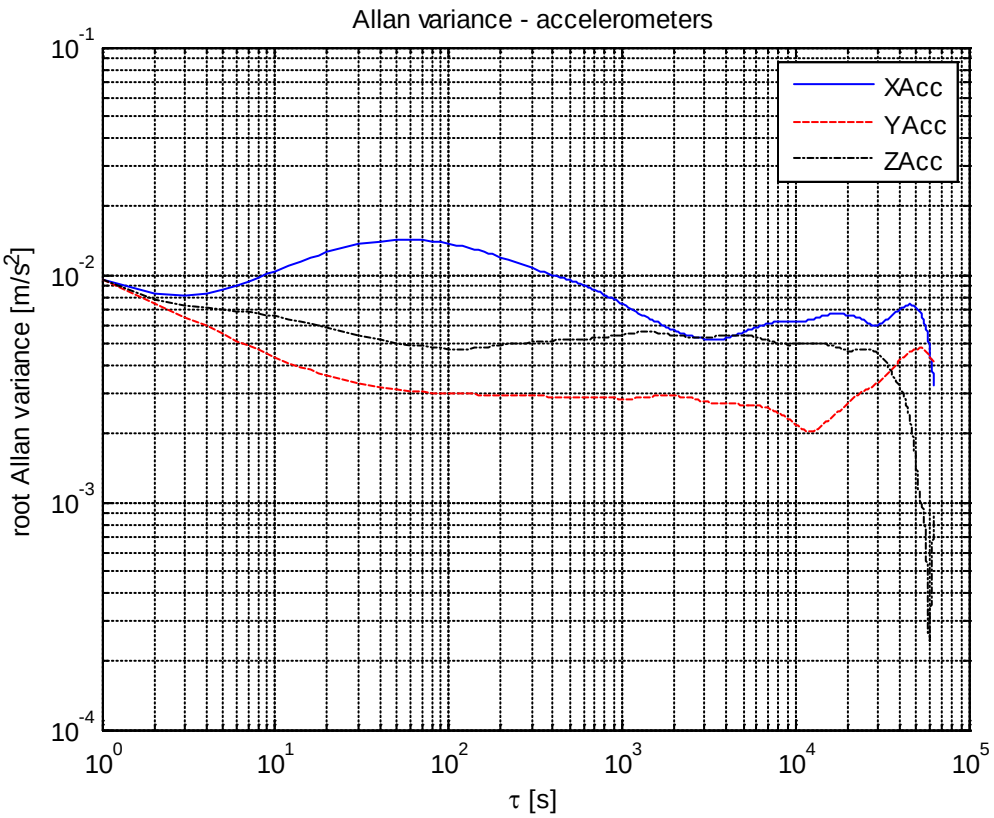

Figure 3.116 Computed Allan variance from the MinIM accelerometer data.

Figure 3.117 through Figure 3.119 show the computed spectral densities of the accelerometers. The spectral densities clearly fall off for higher frequencies.

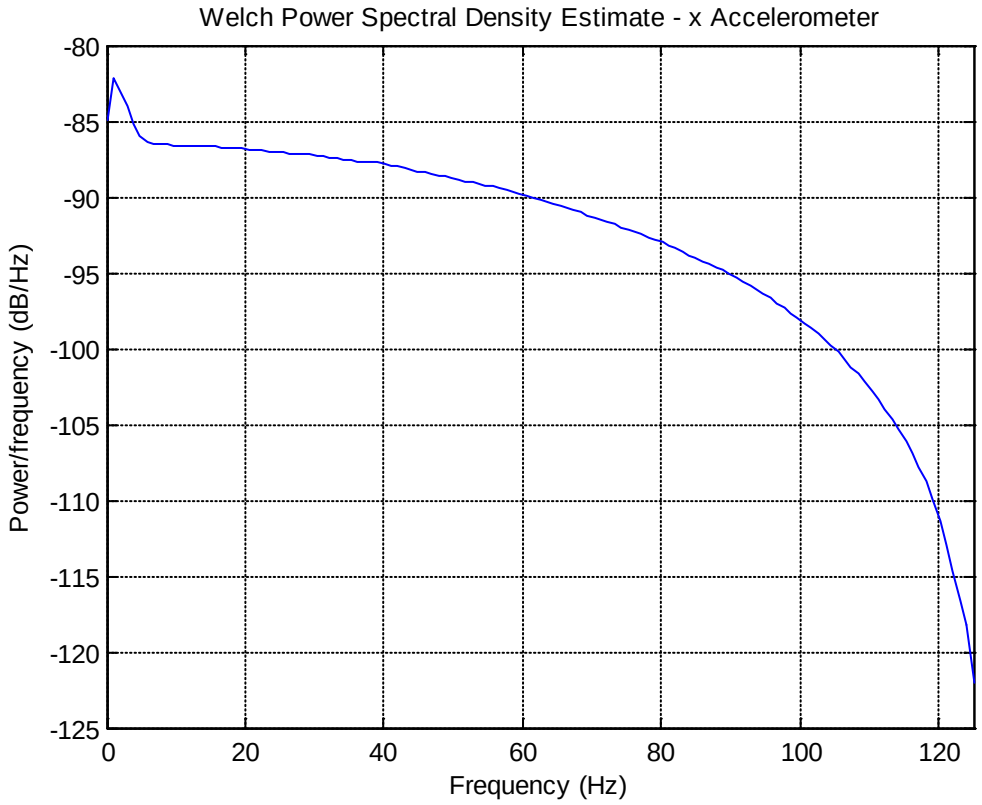

Figure 3.117 Spectral density plot - MinIM x accelerometer.

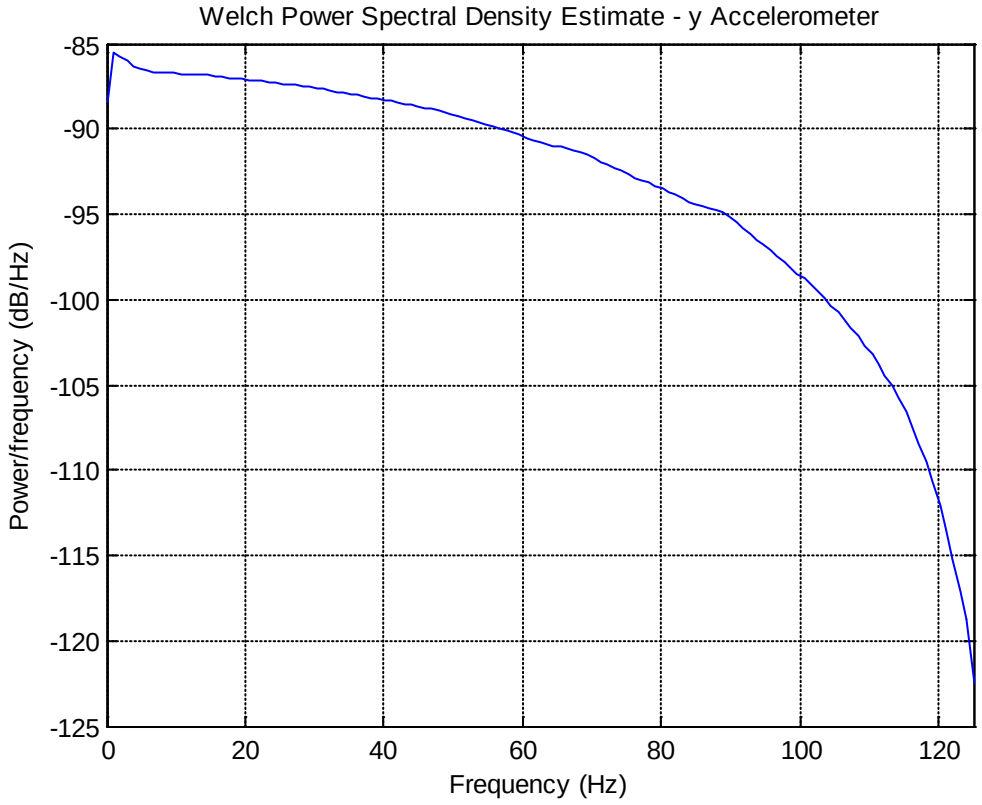

Figure 3.118 Spectral density plot - MinIM y accelerometer.

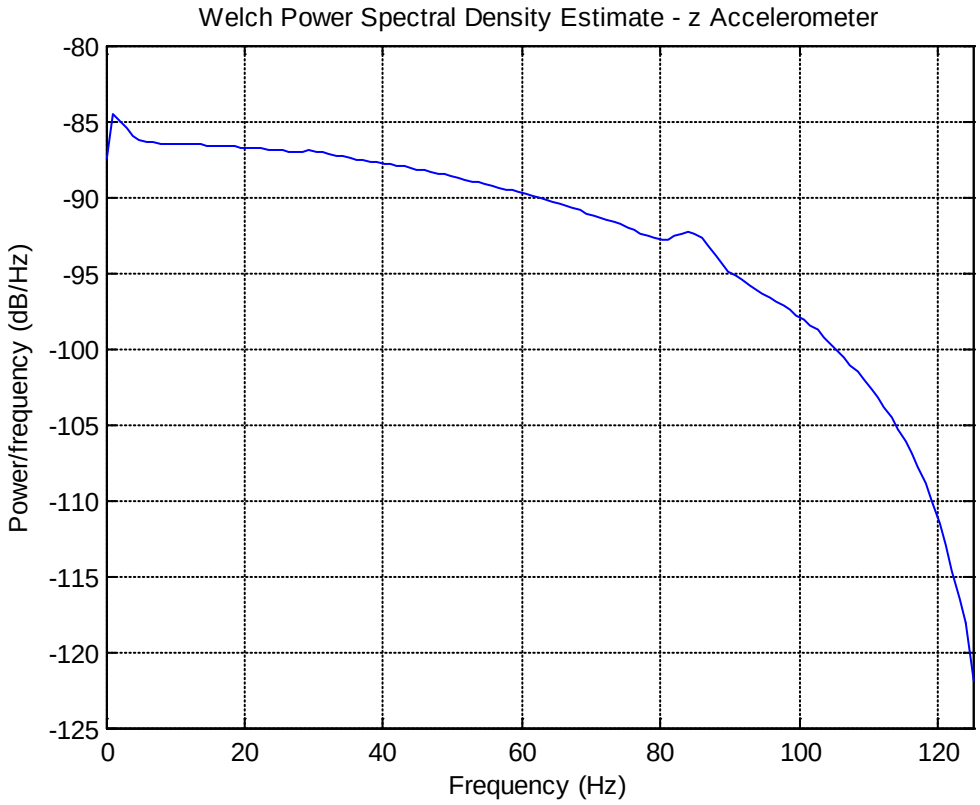

Figure 3.119 Spectral density plot – MinIM z accelerometer.

Figure 3.120 through Figure 3.122 show histograms for the raw accelerometer measurements. All histograms show a Gaussian-like distribution, with very sharp peaks. The standard deviations of the measured accelerations (delta velocity divided by delta time) are (0.094, 0.088, 0.093) m/s^2 for the x, y and z accelerometers, respectively.

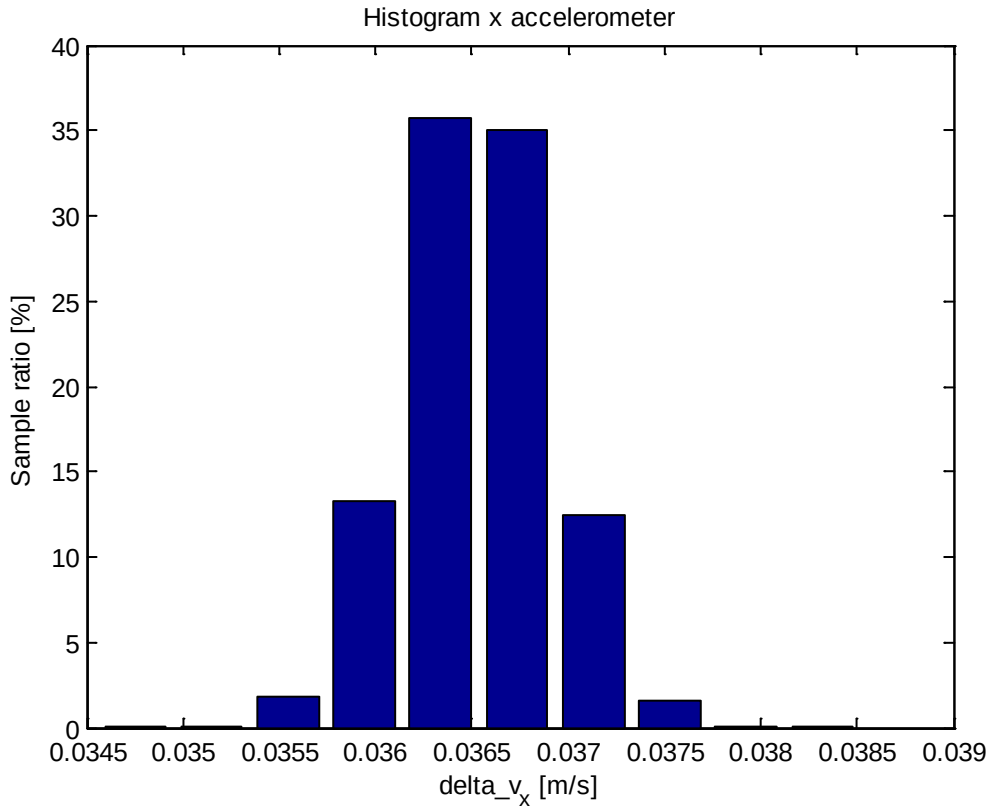

Figure 3.120 MinIM x accelerometer histogram.

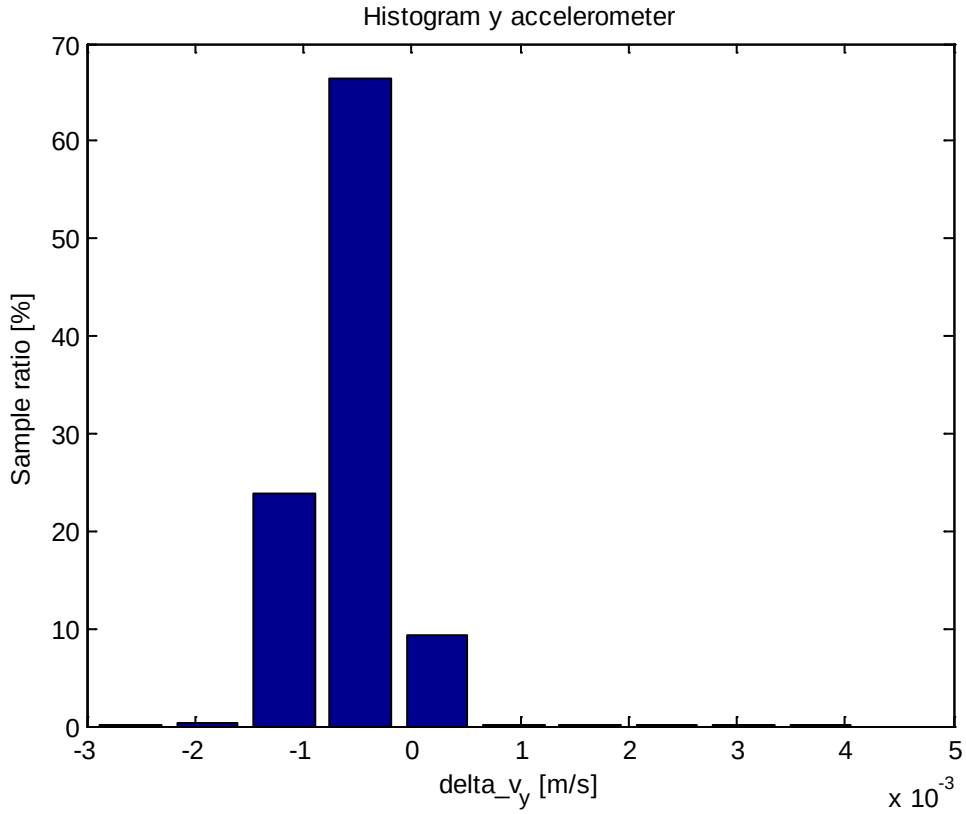

Figure 3.121 MinIM y accelerometer histogram.

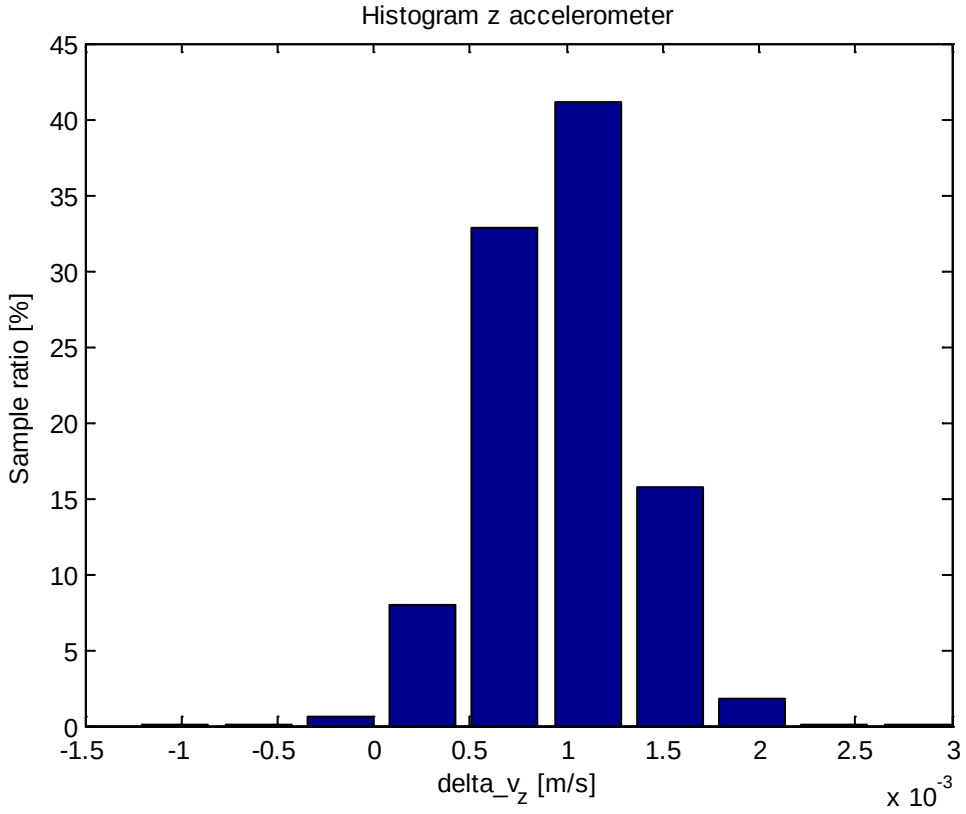

Figure 3.122 MinIM z accelerometer histogram.

3.5.1.2 Gyroscopes

Figure 3.123 through Figure 3.125show raw data from the MinIM gyroscopes throughout the static test. The same data averaged over 1 minute intervals are shown in Figure 3.126 through Figure 3.128. A small drift is visible in all three gyros in the start of the time series. This startup effect is quite persistent, and the output is not stable until around 500 minutes after power-on.

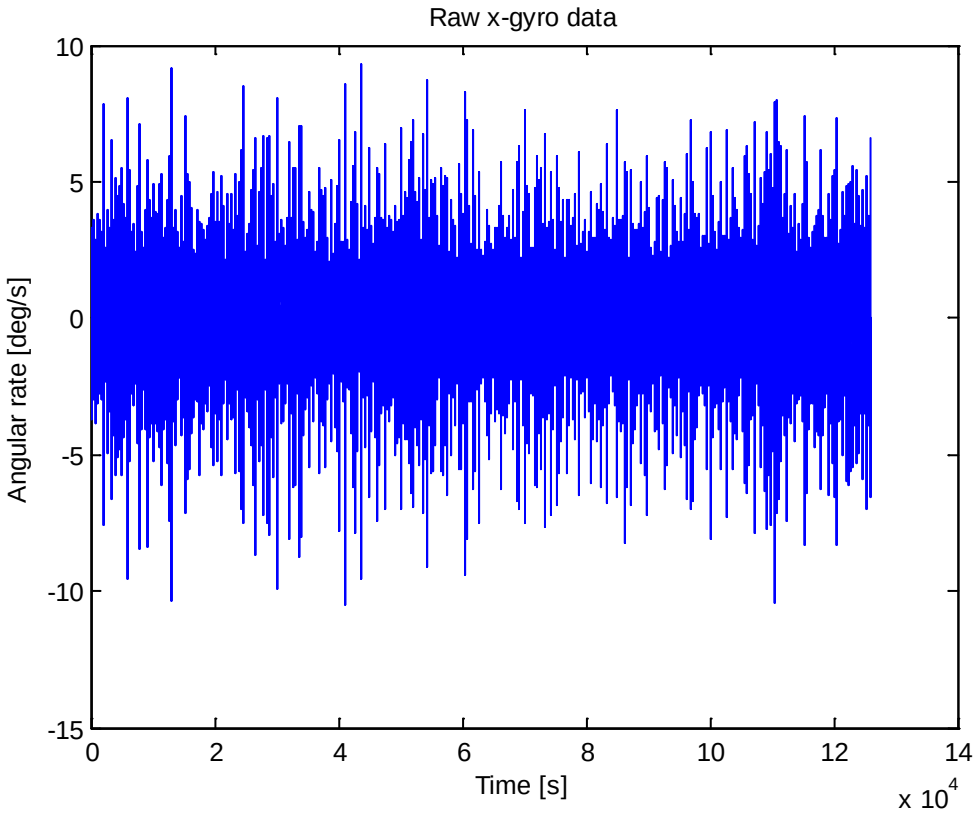

Figure 3.123 Raw data from the MinIM x gyro.

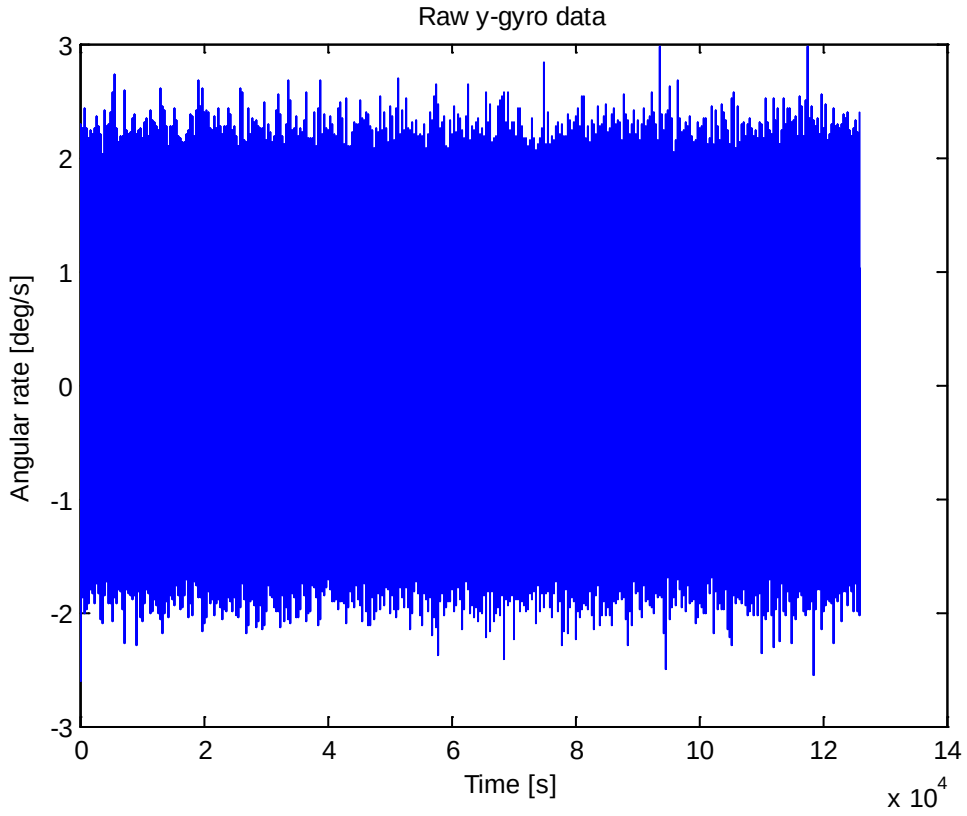

Figure 3.124 Raw data from the MinIM y gyro.

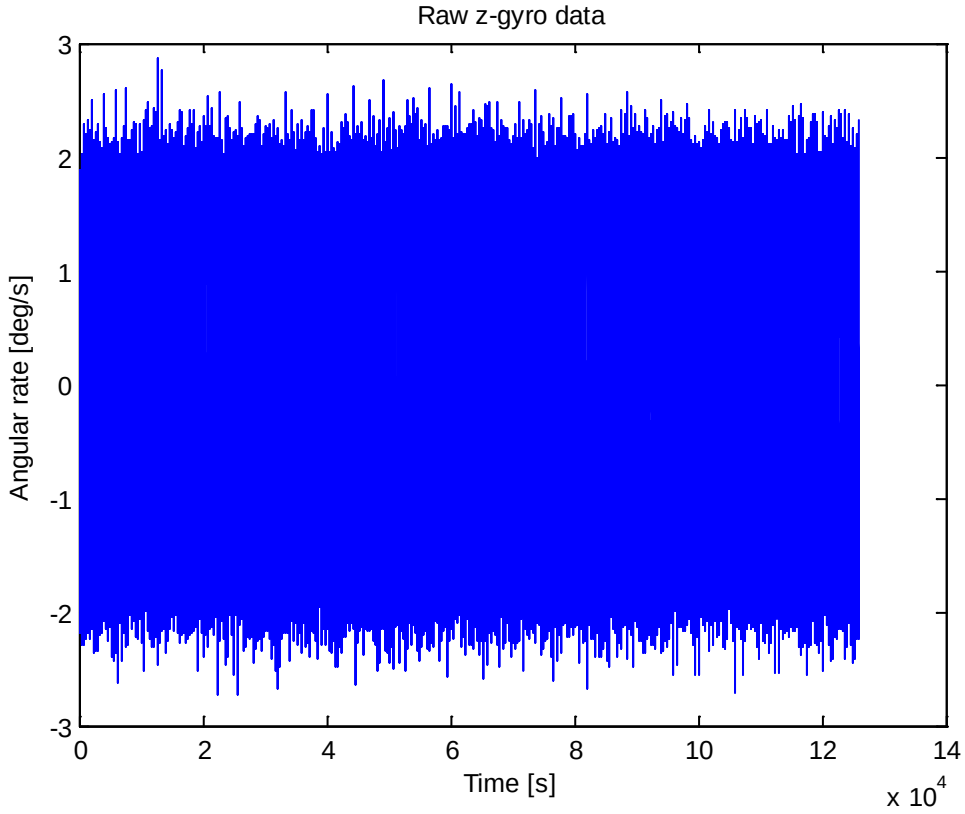

Figure 3.125 Raw data from the MinIM z gyro.

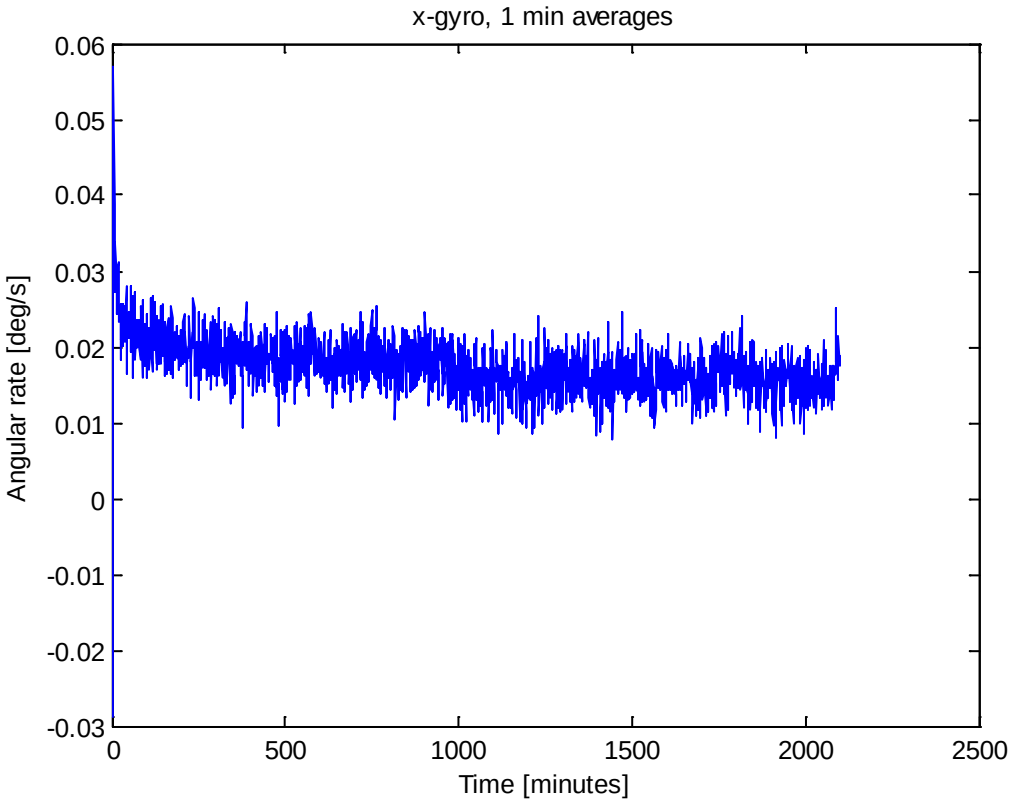

Figure 3.126 MinIM x gyro data averaged over 1 minute intervals.

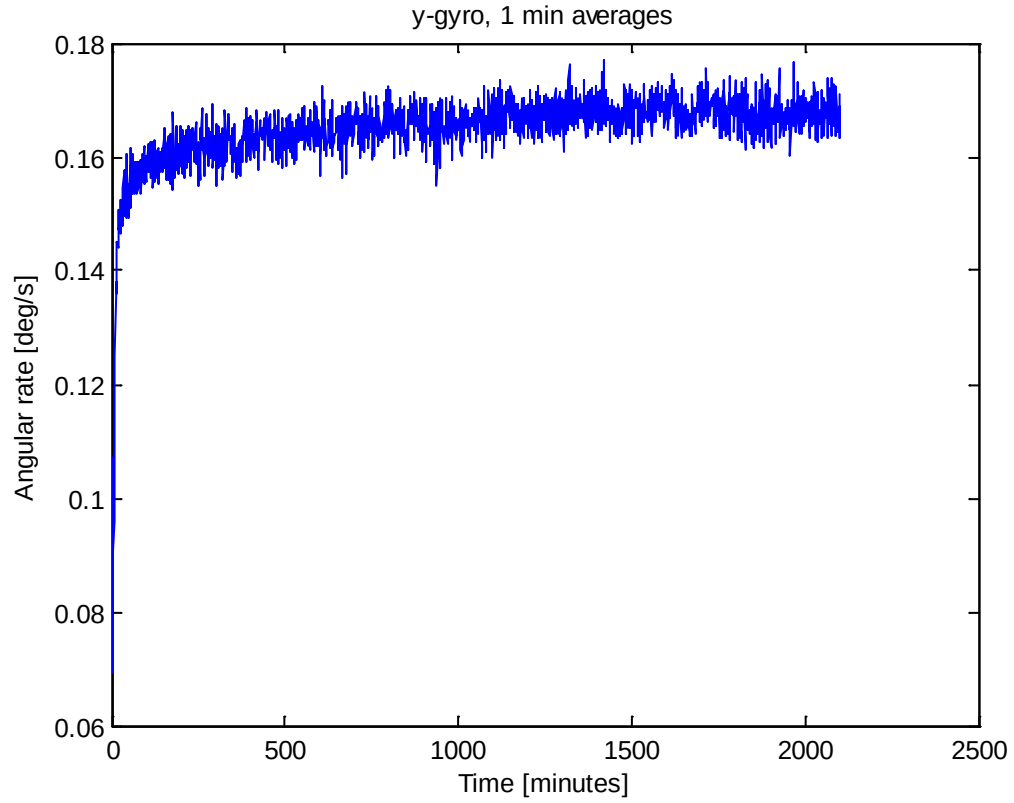

Figure 3.127 MinIM y gyro data averaged over 1 minute intervals.

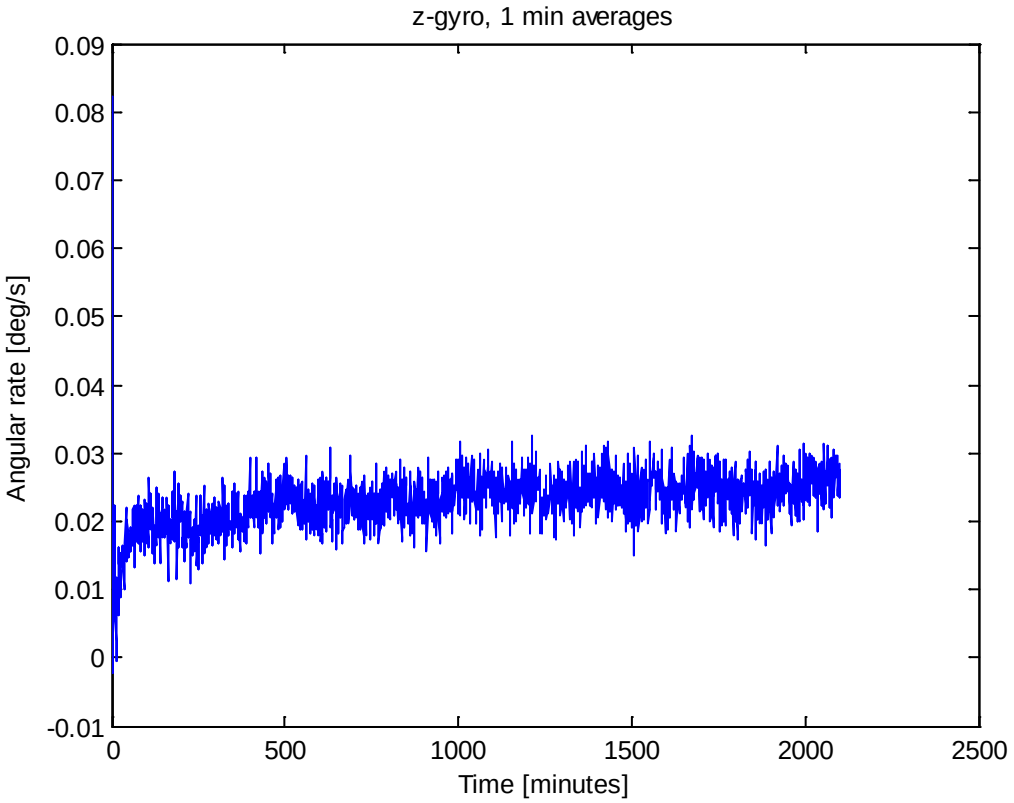

Figure 3.128 MinIM z gyro data averaged over 1 minute intervals.

Figure 3.129 shows computed Allan variance for the three gyros, again after 1 second interval pre summing. Based on the Allan variance plots, the angular random walk and bias instability values were estimated. The angular random walk estimates were 0.99, 0.92 and 0.96 deg/sqrt(h) for the x, y and z gyro, respectively, all within the specified value of 1.2 deg/sqrt(h). The bias instability estimates (i.e. the minimum value of the root Allan variance curves) were 2.1, 3.1 and 2.8 deg/h, all within the specified value of 8 deg/h.

The Allan variance curves contain the usual regions of angular random walk (slope -1/2) and bias instability (slope 0). The curves for the y and z gyro also have positive slopes (+1) for long averaging times, indicating the presence of a rate ramp error component. However, this may also be the result of inaccurate estimates due to few samples in this region.

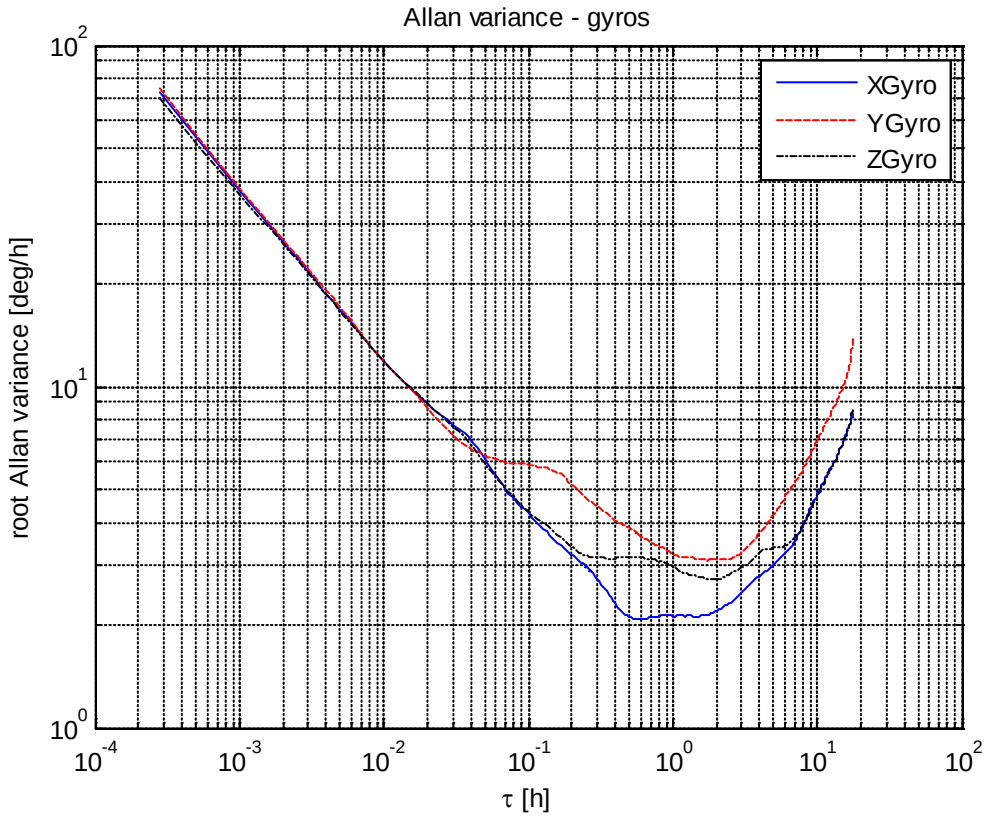

Figure 3.129 Computed Allan variance from MinIM gyro data.

Figure 3.117 through Figure 3.120 show spectral density plots for the gyro measurements. Similarly as in the accelerometer plots, the spectral densities clearly fall of for higher frequencies. There are also a few local maxima, but these are too small to be of any significance.

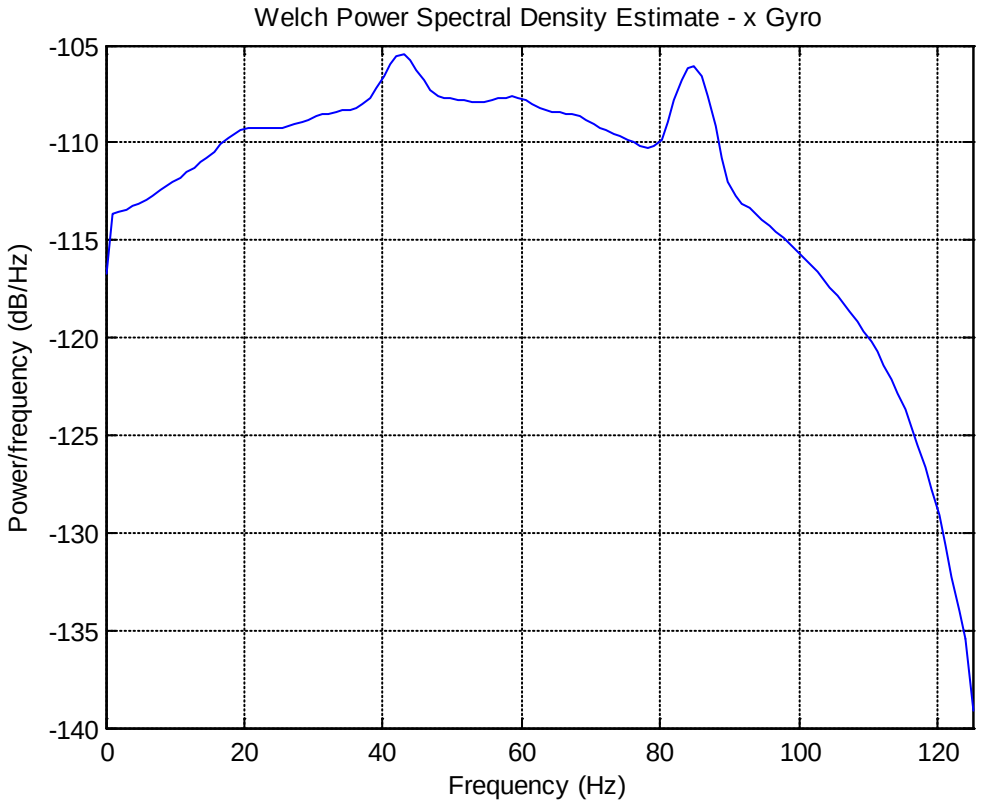

Figure 3.130 Spectral density plot - MinIM x gyro.

Figure 3.131 Spectral density plot - MinIM y gyro.

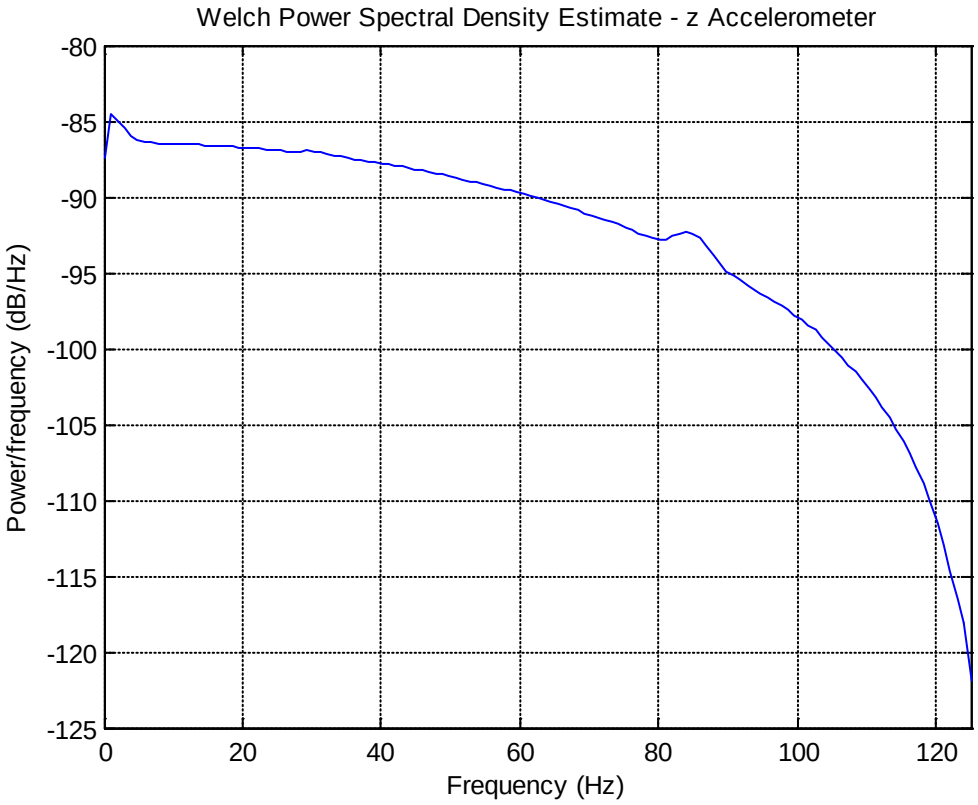

Figure 3.132 Spectral density plot - MinIM z gyro.

Figure 3.106 through Figure 3.108 show histograms of the MinIM gyro measurements. Again, the distributions are Gaussian-like. The standard deviations of the angular rates (delta theta divided by delta time) were (0.51, 0.49, 0.53) deg/s, for the x, y, and z gyro, respectively.

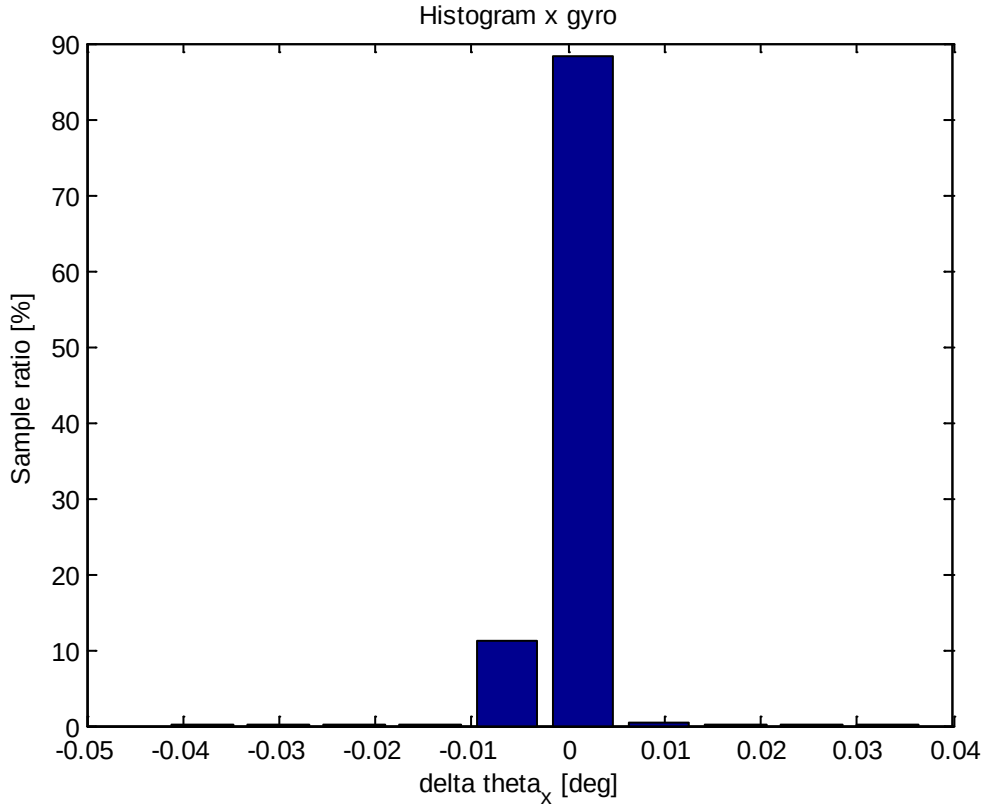

Figure 3.133 MinIM x gyro histogram.

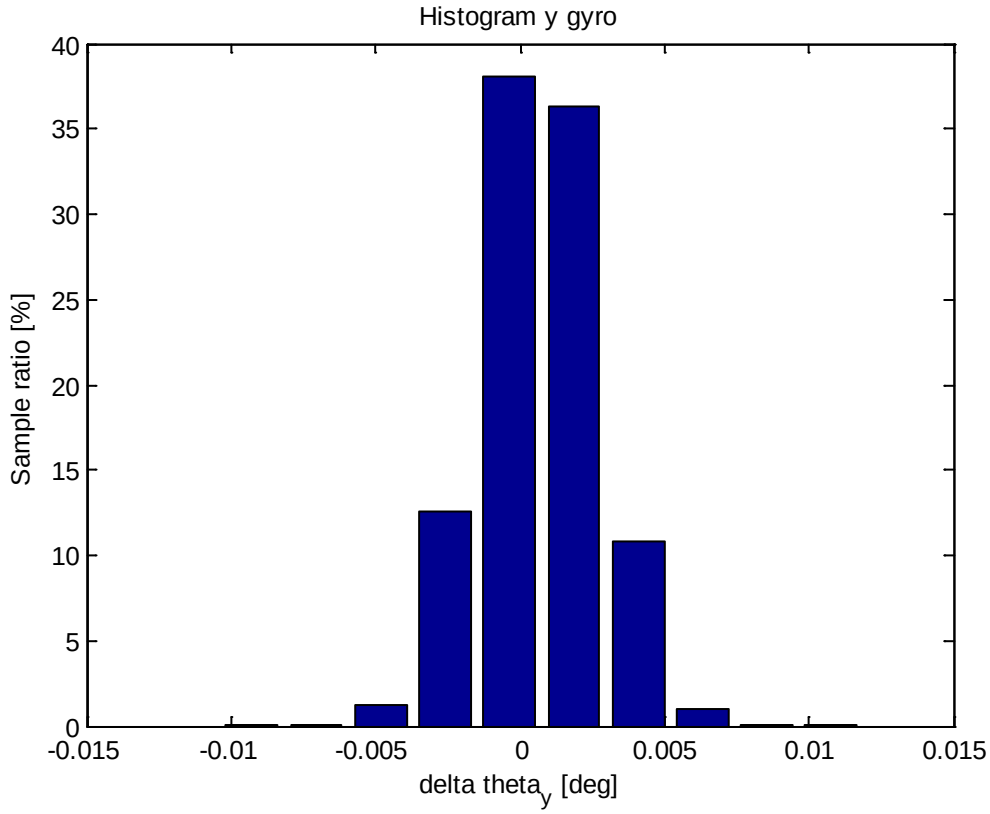

Figure 3.134 MinIM y gyro histogram.

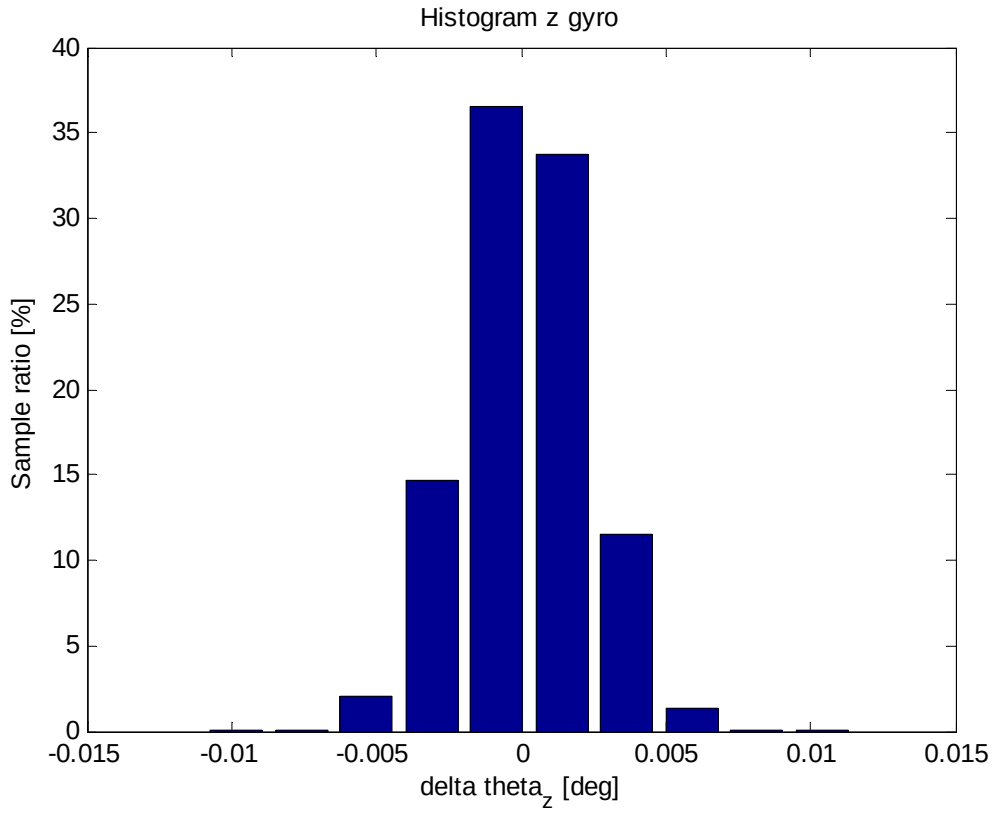

Figure 3.135 MinIM z gyro histogram.

3.5.2 Repeatability and temperature tests

The results from the repeatability and temperature tests are shown in Table 3.22 and Table 3.23, for the accelerometers and gyroscopes, respectively. Both accelerometers and gyros have fairly good repeatability between power-ons at room temperature, but are quite sensitive to temperature and temperature changes.

Table 3.22 Mean MinIM accelerometer measurements and standard deviations in repeatability and temperature tests.

Test name	norm(mean(f)) [m/s^2]	std f_x [m/s^2]	std f_y [m/s^2]	std f_z [m/s^2]
Oppstart Og Langtidstest	9.1364	0.094	0.0877	0.0929
repeterbarhet_1	9.1855	0.0921	0.0877	0.093
repeterbarhet_2	9.1936	0.0932	0.088	0.0936
repeterbarhet_3	9.2009	0.0922	0.0878	0.0928
TemperaturTest_+0grader	9.067	0.0901	0.0853	0.0864
TemperaturTest_+10grader	9.0744	0.0897	0.087	0.0893
TemperaturTest_+20grader	9.1826	0.0947	0.0904	0.0962
TemperaturTest_+30grader	9.2506	0.0947	0.0904	0.0962
TemperaturTest_+40grader	9.2207	0.0958	0.0927	0.0981
TemperaturTest_+50grader	9.2603	0.099	0.0957	0.1004
TemperaturTest_-10grader	9.09	0.0847	0.0829	0.0839
TemperaturTest_-20grader	8.9939	0.082	0.0841	0.0818
TemperaturTest_-30grader	9.1092	0.0763	0.0875	0.0802
TemperaturTest_-40 til + 20 grader	9.0763	0.0977	0.0889	0.0987
TemperaturTest_-40grader	9.1492	0.0833	0.087	0.0989

Table 3.23 Mean MinIM gyro measurements and standard deviations in repeatability and temperature tests.

Test name	norm(mean(ω)) [deg/s]	std ω_x [deg/s]	std ω_y [deg/s]	std ω_z [deg/s]
Oppstart Og Langtidstest	0.1662	0.5141	0.4895	0.5343
repeterbarhet_1	0.1599	0.5143	0.4895	0.5355
repeterbarhet_2	0.1623	0.5135	0.4896	0.5342
repeterbarhet_3	0.1663	0.5133	0.4889	0.5349
TemperaturTest_+0grader	0.2972	0.5292	0.4765	0.4769
TemperaturTest_+10grader	0.1807	0.5063	0.4873	0.4818
TemperaturTest_+20grader	0.1732	0.4848	0.5055	0.4722
TemperaturTest_+30grader	0.2252	0.4848	0.5055	0.4722
TemperaturTest_+40grader	0.1083	0.4744	0.4762	0.4797
TemperaturTest_+50grader	0.0893	0.4863	0.5112	0.4839
TemperaturTest_-10grader	0.2471	0.5324	0.4918	0.4749
TemperaturTest_-20grader	0.1212	0.5773	0.5524	0.4933
TemperaturTest_-30grader	0.0118	0.5581	0.547	0.5053
TemperaturTest_-40 til + 20 grader	0.1668	0.5118	0.4899	0.5114
TemperaturTest_-40grader	0.0628	0.6099	0.5375	0.5027

3.5.3 Up-down tests

The results from the up/down tests are shown in Table 3.24 and Table 3.25, using the same color coding as before. The scale factor in the y accelerometer exceeds the specification. However, the specification does not specify whether this value is to be interpreted as a maximum value, or a 1 sigma value. In the latter case, the measured value is between 1 and 2 sigma. The measured y gyro bias is almost 6 times the specified value.

Table 3.24 MinIM accelerometer parameters computed from up/down tests

Test	x acc. bias (mg)	x acc. scale factor (ppm)	y acc. bias (mg)	y acc. scale factor (ppm)	z acc. bias (mg)	z acc. scale factor (ppm)
1/2 (x up)	0.06	932				
3/4 (y up)			0.05	2377		
5/6 (z up)					0.03	1008
Spec.	20	1800	20	1800	20	1800

Table 3.25 MinIM gyro parameters computed from up/down test.

Test	x gyro bias (deg/h)	y gyro bias (deg/h)	z gyro bias (deg/h)
1/2 (x up)	56.6		
3/4 (y up)		590	
5/6 (z up)			86
Spec.	100	100	100

3.6 Honeywell HG1930

The HG1930 [7] is a MEMS IMU manufactured by the American company Honeywell. The specifications are given in Table 3.26.

Figure 3.136 The HG1930 IMU.

Table 3.26 Specifications of the Honeywell HG1930 IMU.

	Gyros	Accelerometers
Bias repeatability (1 σ)	60 deg/hr	15 mg
Bias instability (1 σ)	10 deg/hr	3 mg
Random walk (max.)	0.125 deg/sqrt(hr) (roll axis) 0.09 deg /sqrt(hr) (pitch , yaw axis)	0.12 m/s/sqrt(h)
Scale factor repeatability (1 σ)	700 ppm	700 ppm

3.6.1 Static long term test

As in the previous tests, the unit was placed on a stable table, with the x-accelerometer pointing down. The unit was powered on, after having been turned off for an extensive period. Thus, potential effects due to self-warming would be visible in the data.

3.6.1.1 Accelerometers

Figure 3.137 through Figure 3.139 show the output from the accelerometers during the static test. As the output is given as delta velocity measurements, the values plotted are divided by delta time to obtain accelerations. The same data averaged over 1 minute intervals are shown in Figure 3.148Figure 3.140 through Figure 3.142. A drift in these data is visible in all three accelerometers. In the x accelerometer the output stabilizes after around 50 000 seconds (~ 14 hours), whereas in the other two accelerometers the drift is present throughout the entire test period. This suggests the presence of a rate random walk or rate ramp error component.

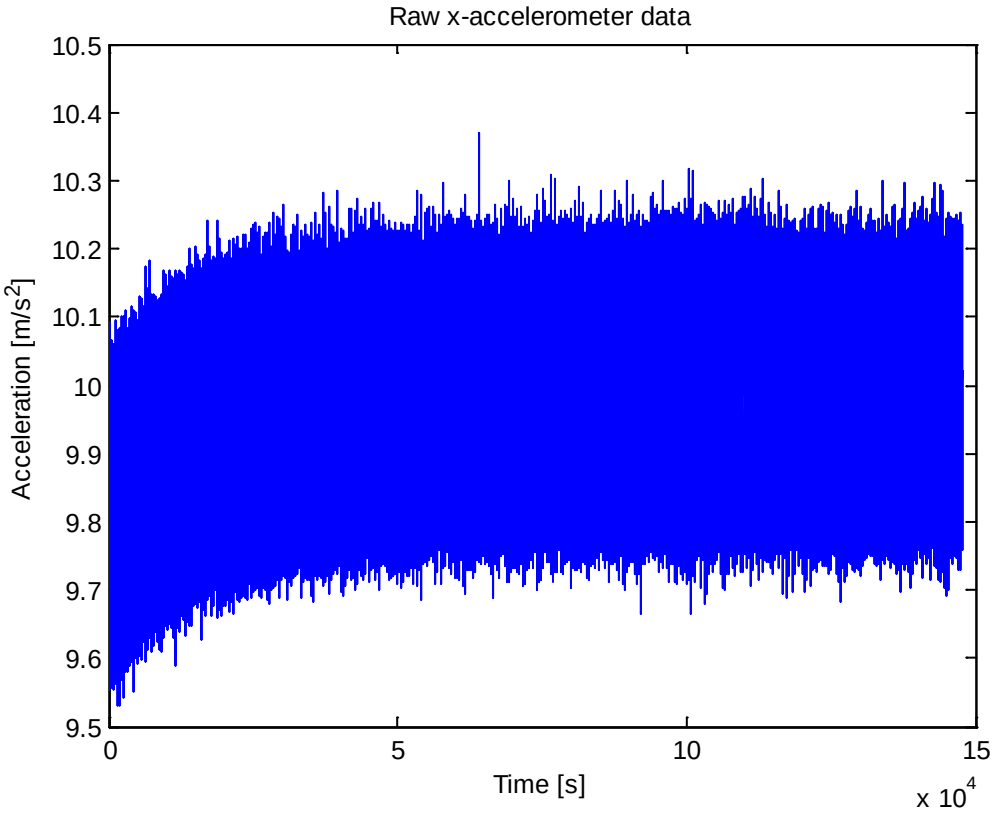

Figure 3.137 Raw data from the HG1930 x accelerometer.

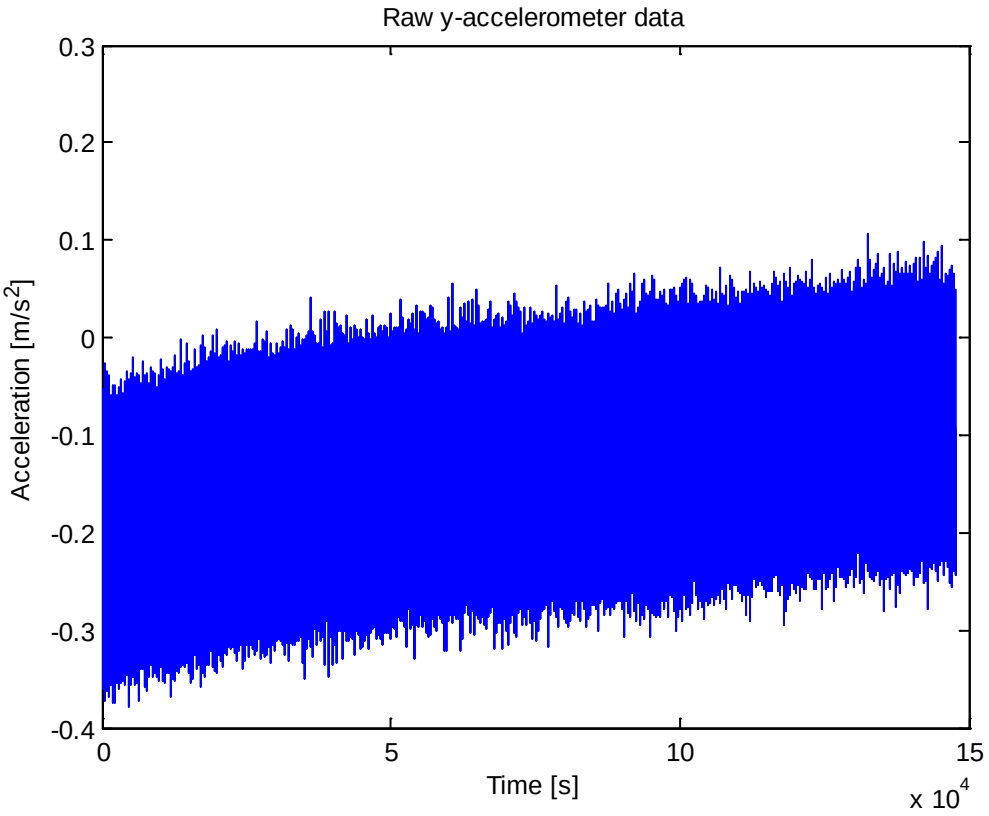

Figure 3.138 Raw data from the HG1930 y accelerometer.

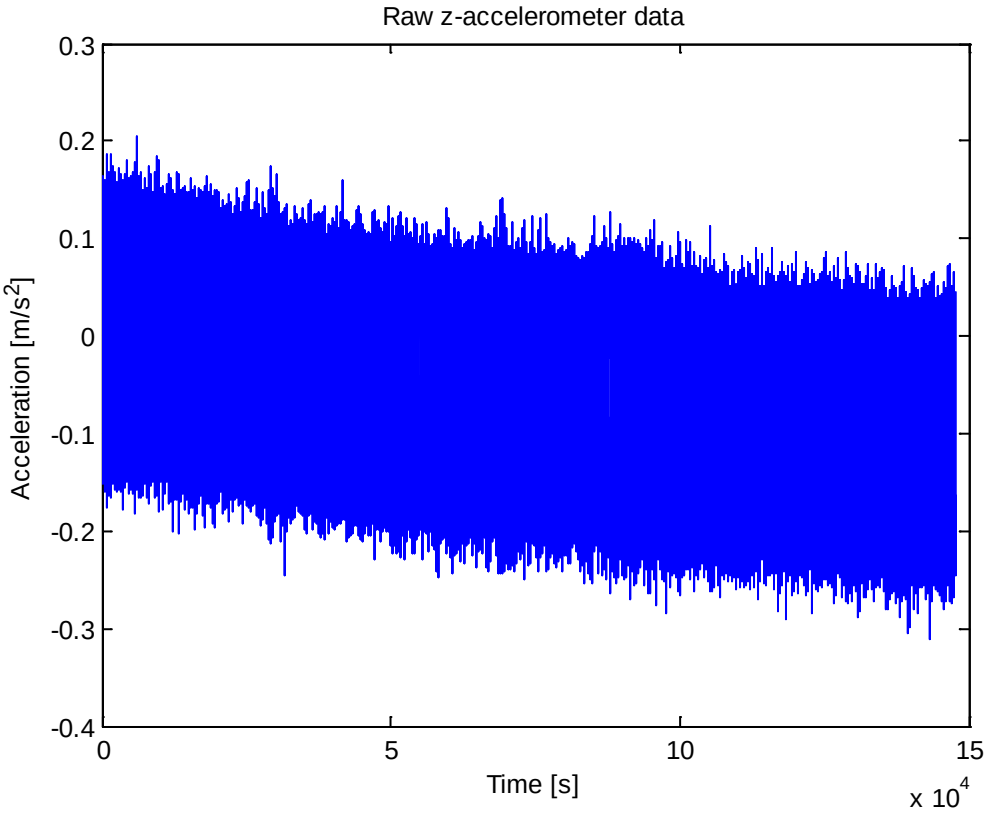

Figure 3.139 Raw data from the HG1930 z accelerometer.

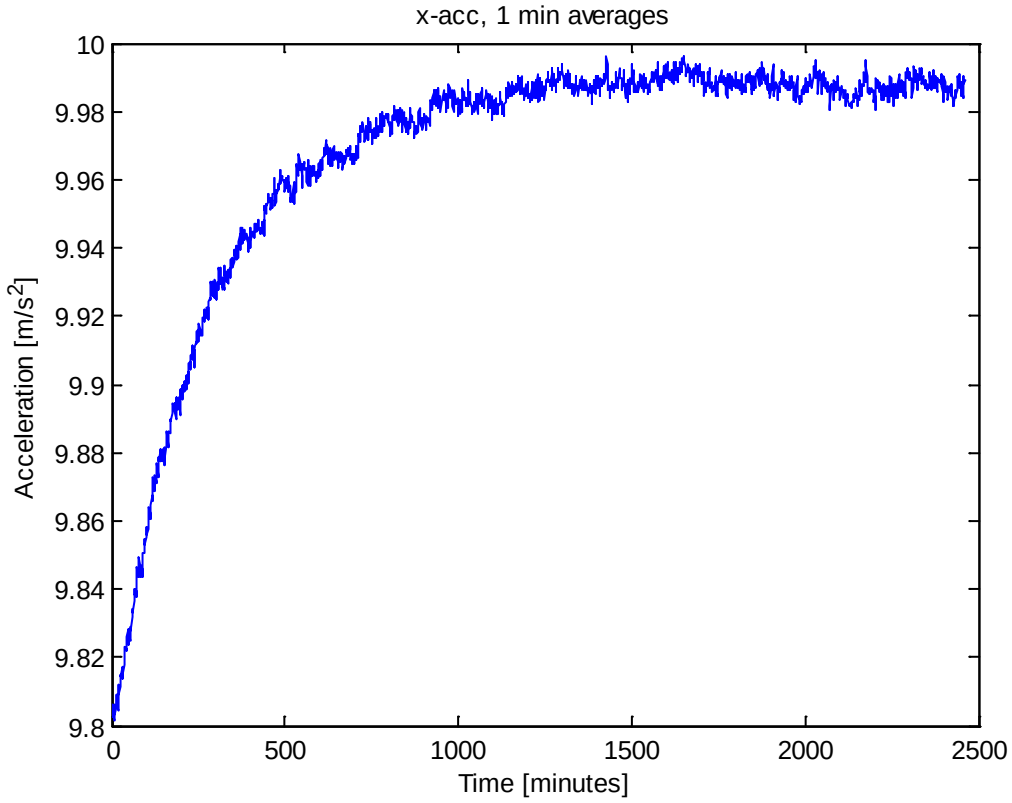

Figure 3.140 HG1930 x accelerometer data averaged over 1 minute intervals.

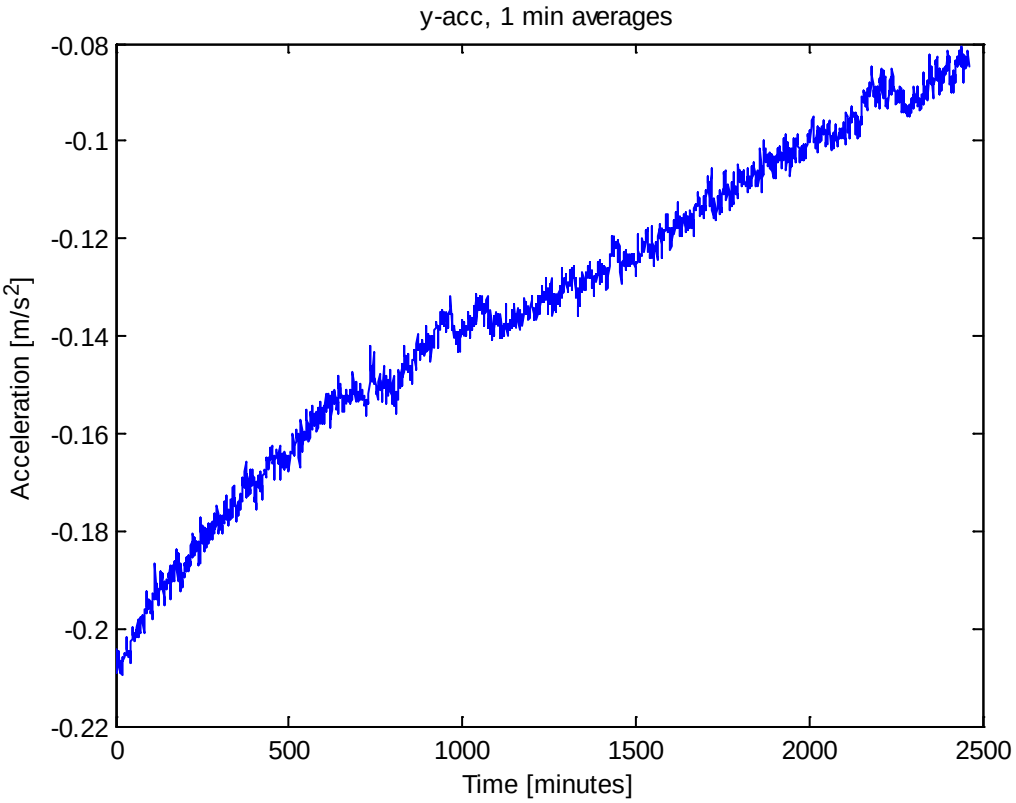

Figure 3.141 HG1930 y accelerometer data averaged over 1 minute intervals.

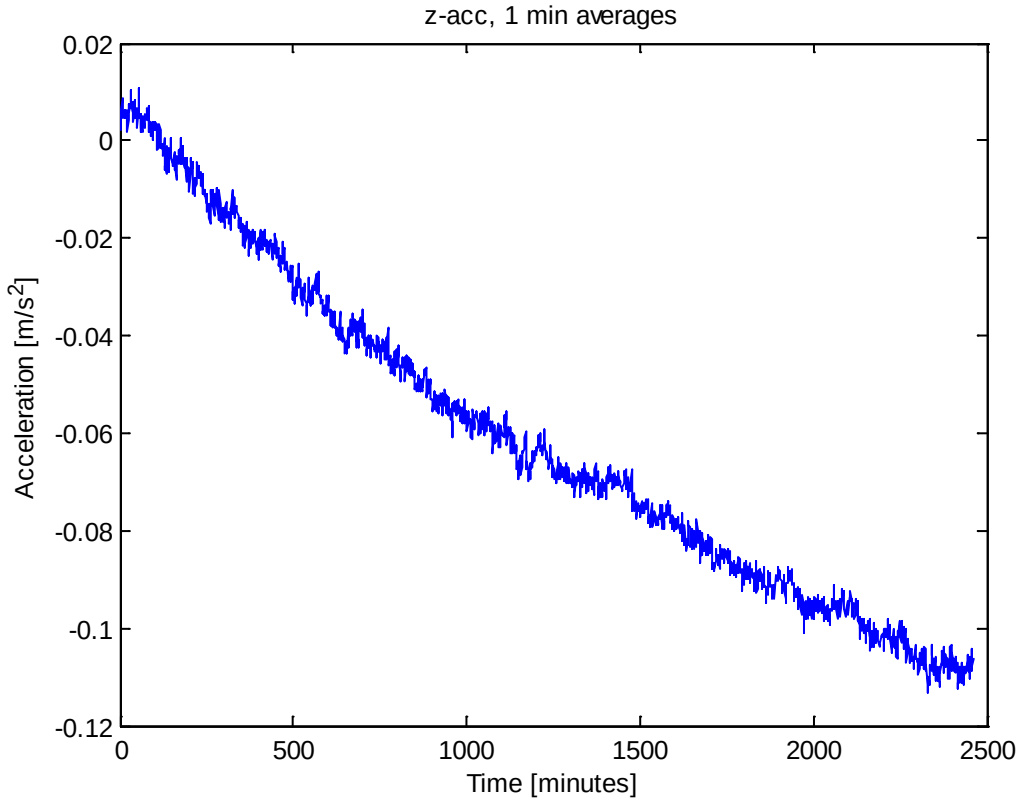

Figure 3.142 HG1930 z accelerometer data averaged over 1 minute intervals.

Figure 3.143 shows computed root Allan variance from the three accelerometers from the entire test interval. The same pre summing over 1 second intervals as before was used. Based on the Allan variance plots, the velocity random walk and bias instability values were estimated. The velocity random walk estimates were 0.28,0.14, and 0.19 m/s/sqrt(hr) for the x, y and z accelerometer, respectively, all well above the specified maximum value of 0.12 m/s/sqrt(hr). The bias instability estimates (i.e. the minimum value of the root Allan variance curves) were 0.15, 0.1, and 0.13 mg, for the x, y and z axis, well within the specification of 3 mg.

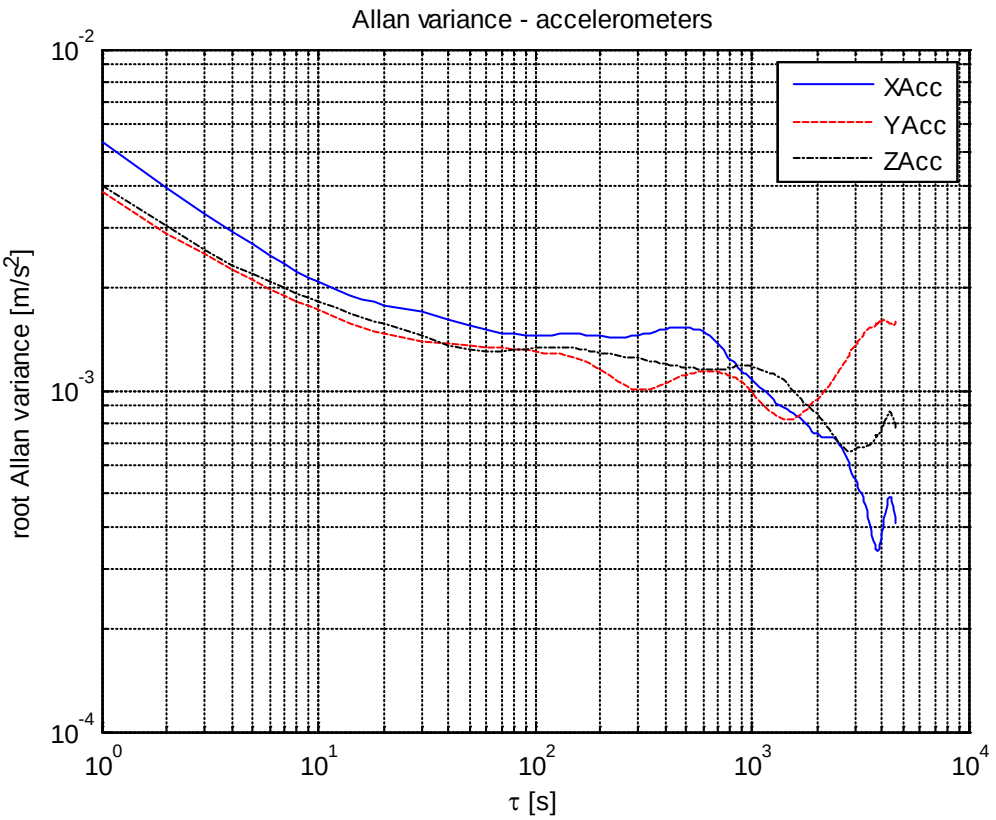

Figure 3.143 Computed Allan variance from the HG1930 accelerometer data.

Figure 3.144 through Figure 3.146 show the computed spectral densities of the accelerometers. Clear peaks are visible at low frequencies. Apart from this, the spectral densities fall of for higher frequencies.

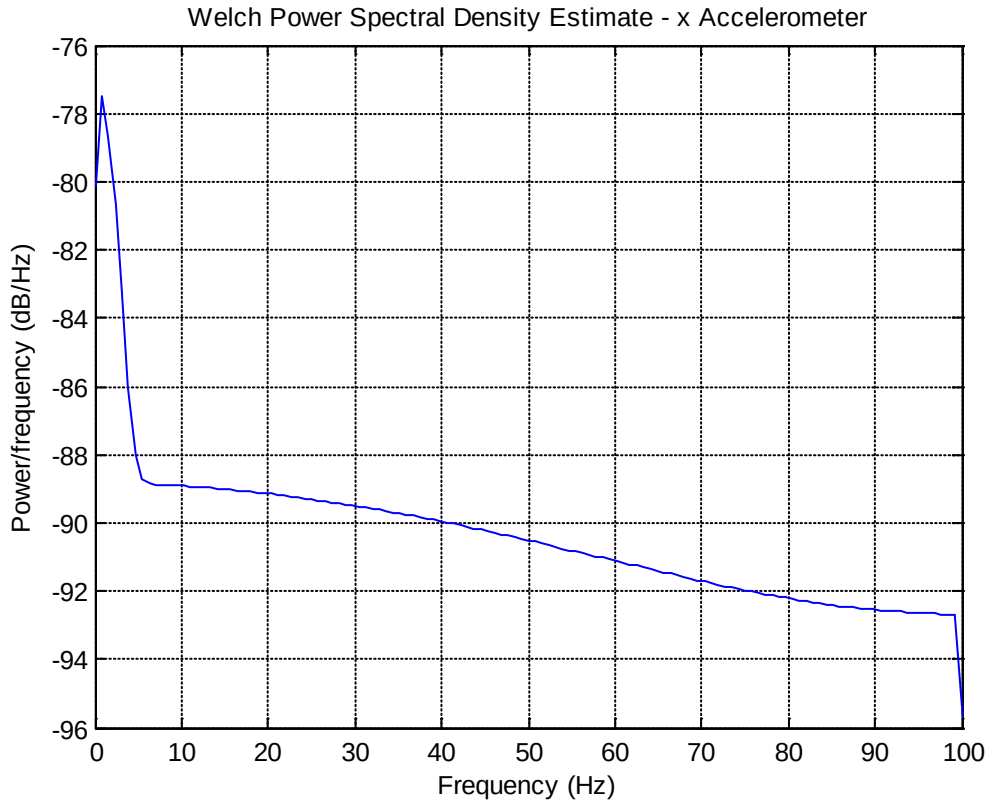

Figure 3.144 Spectral density plot - HG1930 x accelerometer.

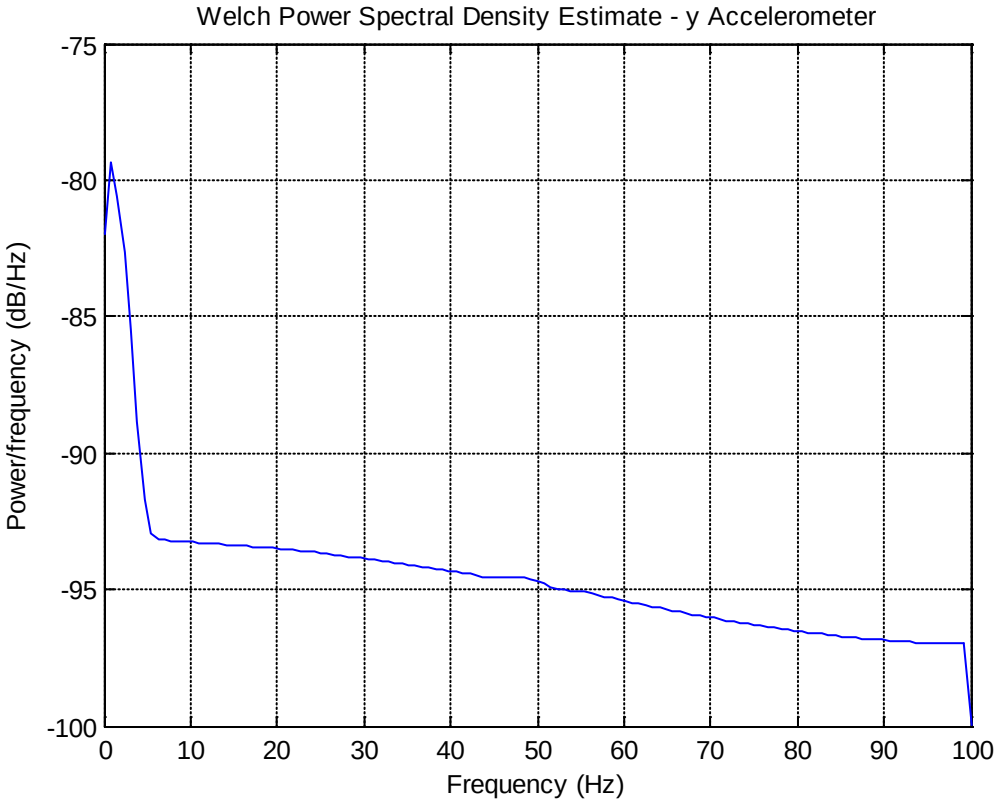

Figure 3.145 Spectral density plot - HG1930 y accelerometer.

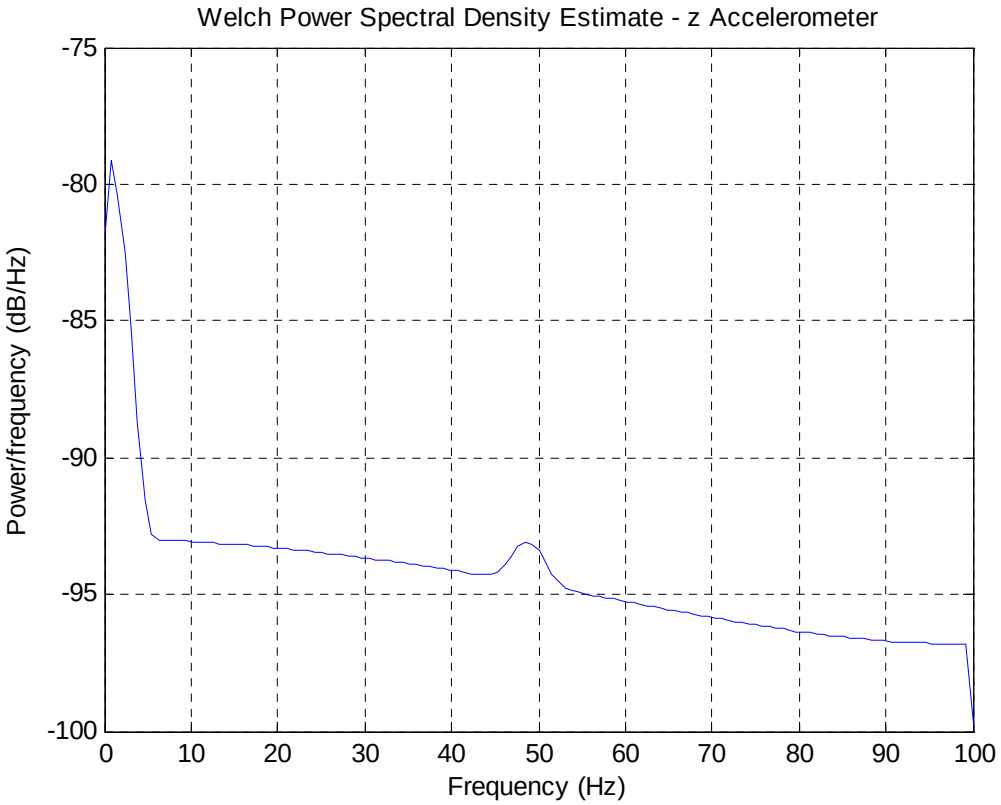

Figure 3.146 Spectral density plot - HG1930 z accelerometer.

Figure 3.144 to Figure 3.146 show histograms for the raw accelerometer measurements. All histograms show a Gaussian-like distribution. The standard deviations of the measured accelerations (delta velocity divided by delta time) are (0.072, 0.049, 0.050) m/s^2 for the x, y and z accelerometers, respectively.

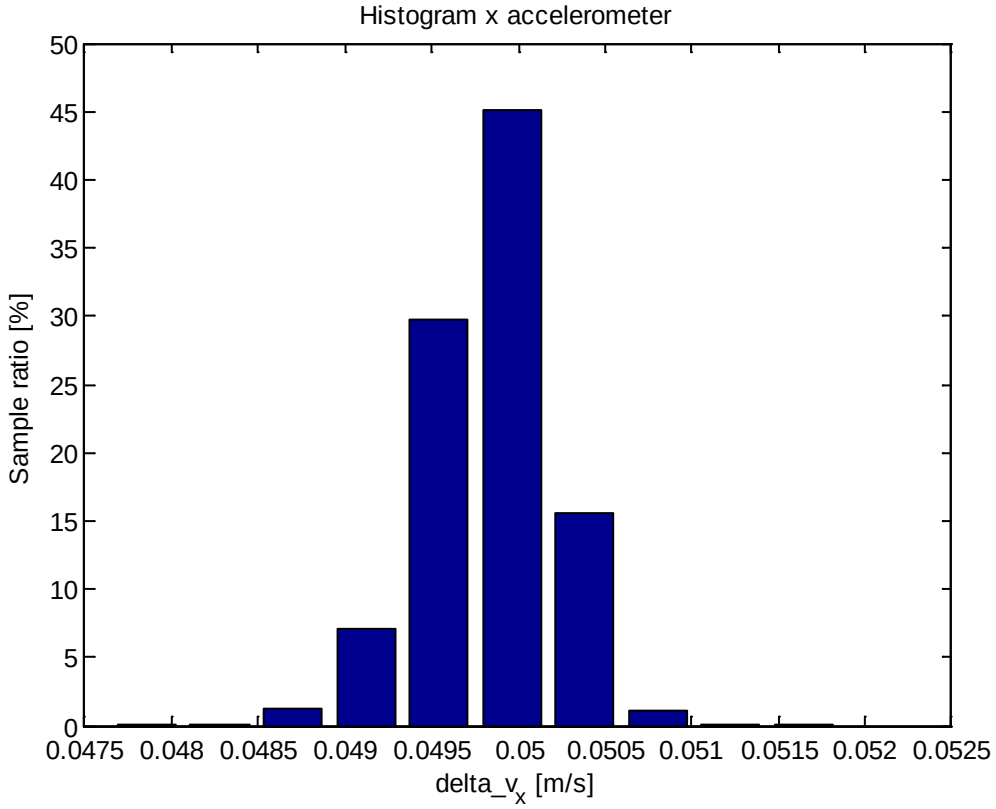

Figure 3.147 HG1930 x accelerometer histogram.

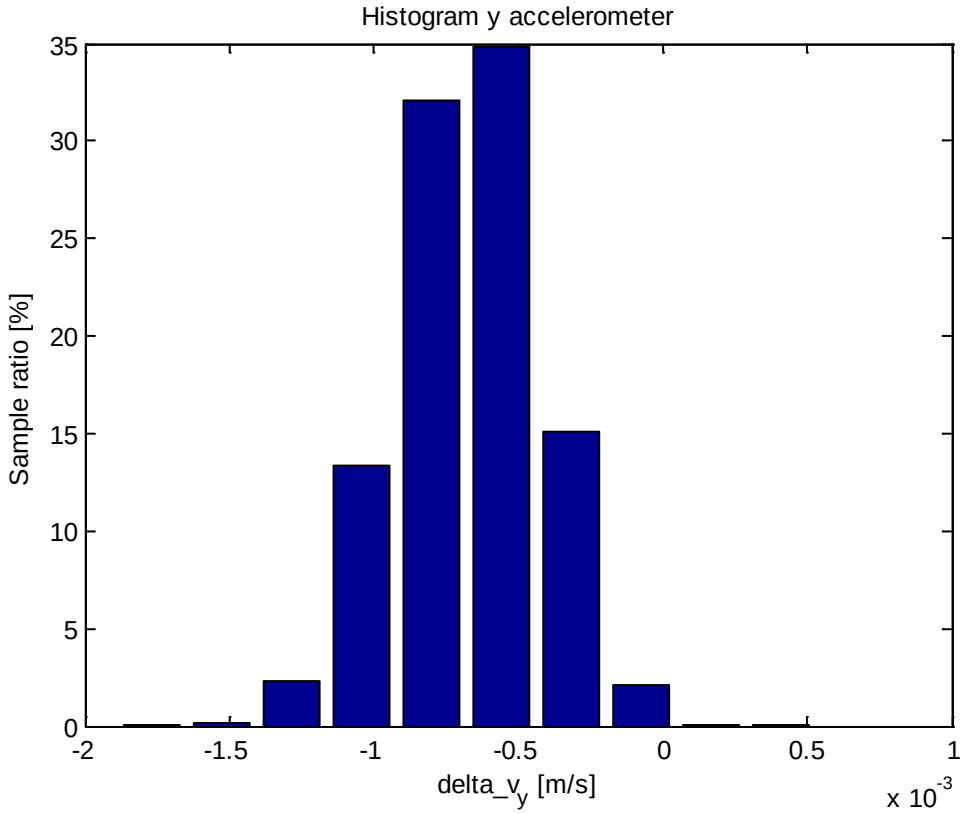

Figure 3.148 HG1930 y accelerometer histogram.

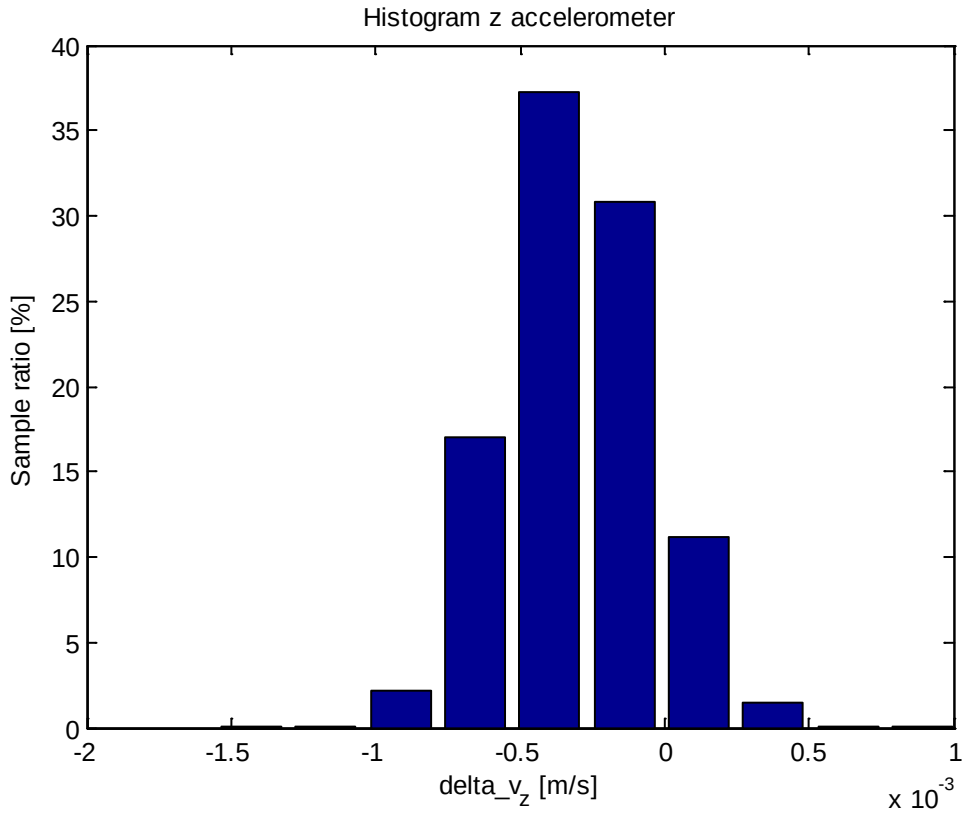

Figure 3.149 HG1930 z accelerometer histogram.

3.6.1.2 Gyroscopes

Figure 3.150 through Figure 3.152 show raw data from the MinIM gyroscopes throughout the static test. The same data averaged over 1 minute intervals are shown in Figure 3.153 through Figure 3.155. Both a startup effect and a persistent drift are clearly visible in the averaged data, indicating the presence of a rate random walk.

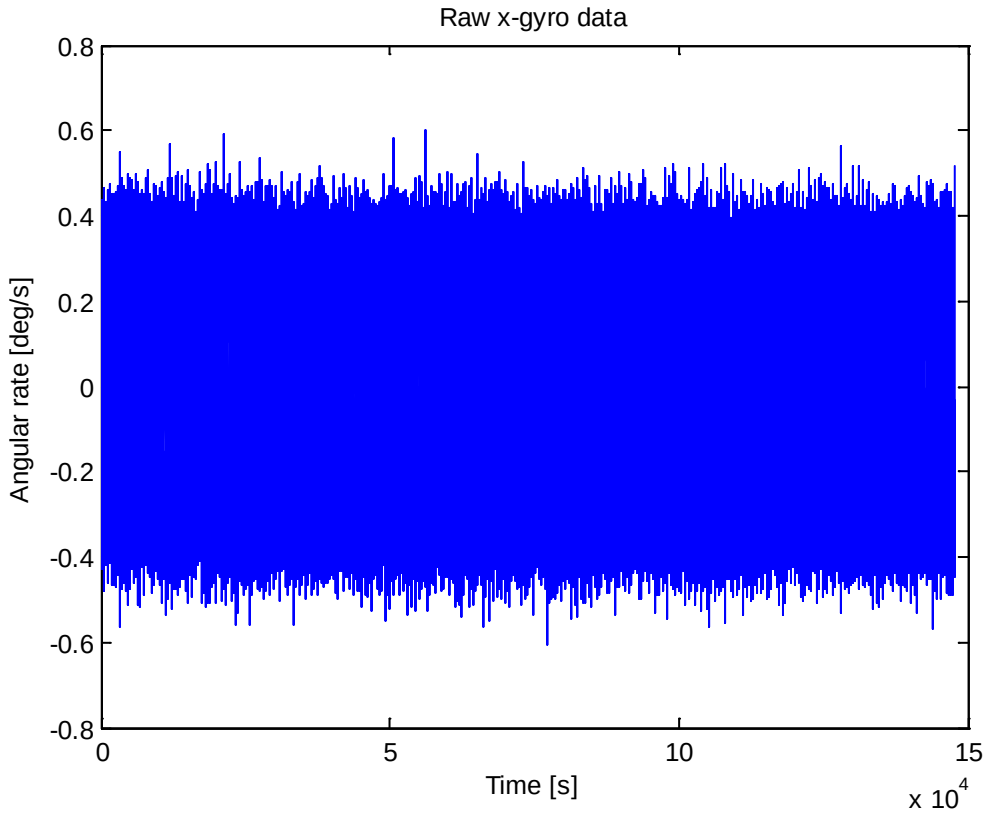

Figure 3.150 Raw data from the HG1930 x gyro.

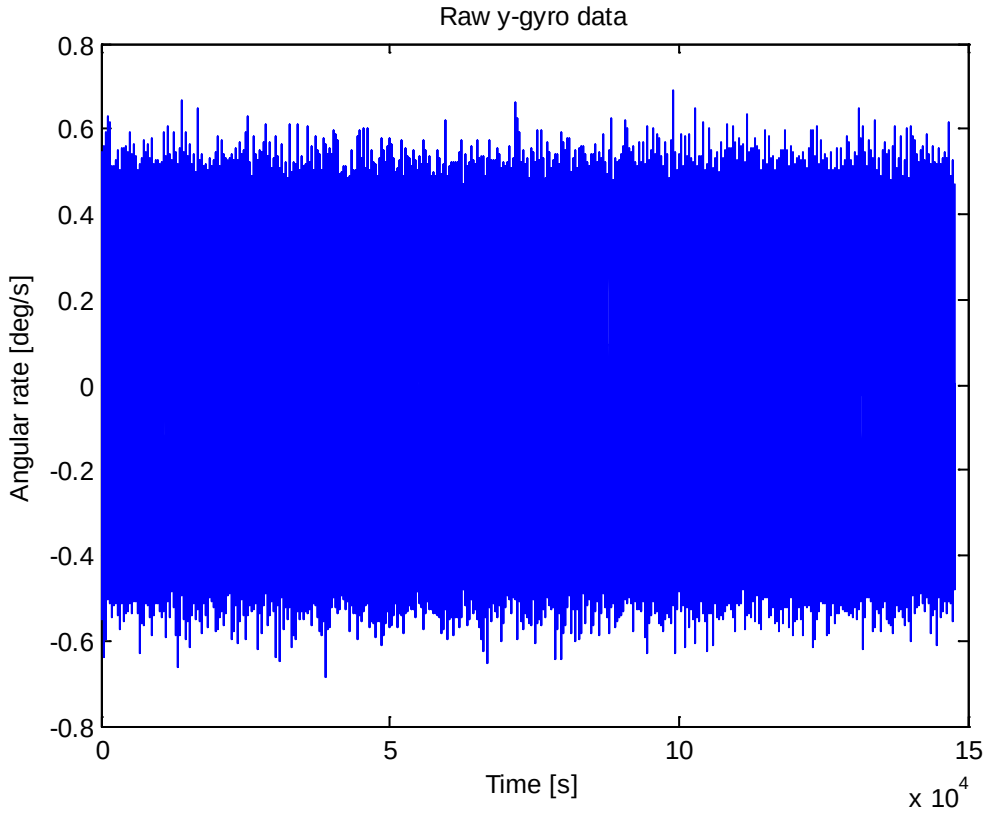

Figure 3.151 Raw data from the HG1930 y gyro.

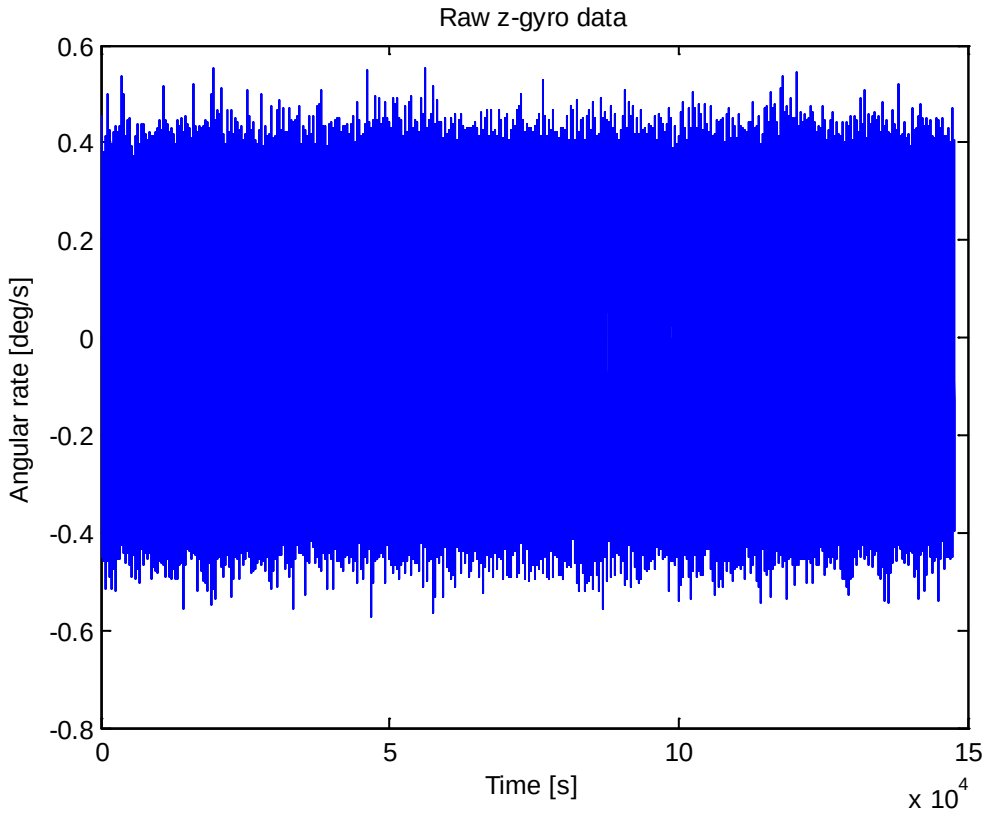

Figure 3.152 Raw data from the HG1930 z gyro.

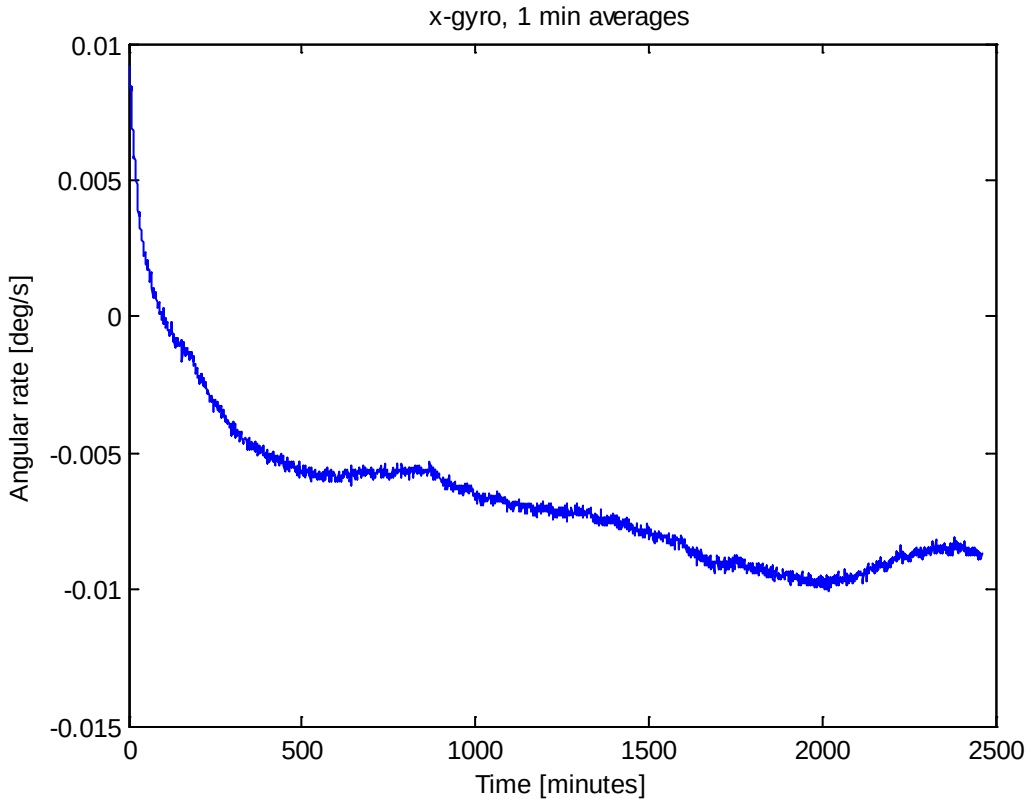

Figure 3.153 HG1930 x gyro data averaged over 1 minute intervals.

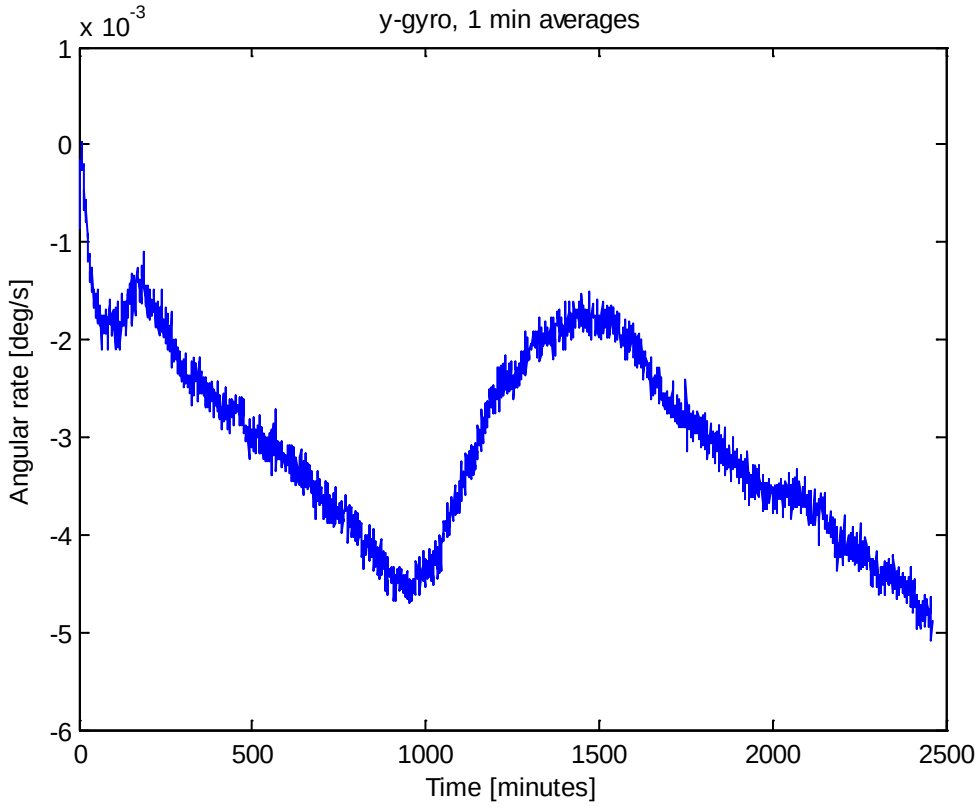

Figure 3.154 HG1930 y gyro data averaged over 1 minute intervals.

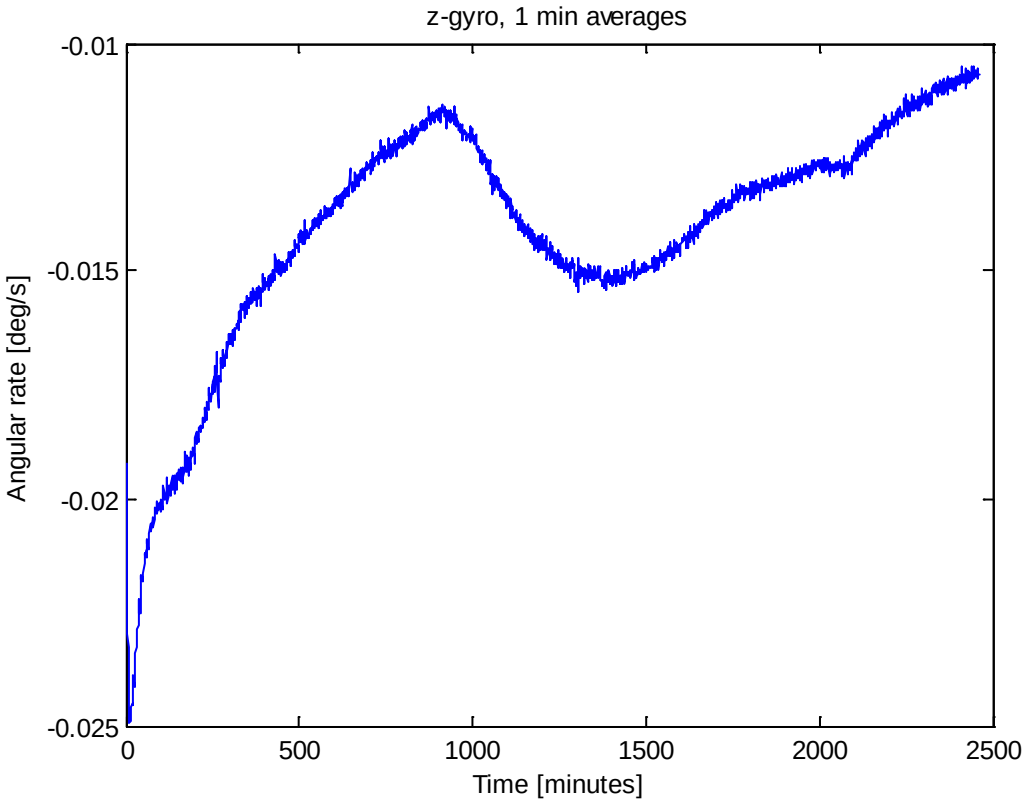

Figure 3.155 HG1930 z gyro data averaged over 1 minute intervals.

Figure 3.156 shows computed Allan variance for the three gyros, again after 1 second interval pre summing. Based on the Allan variance plots, the angular random walk and bias instability values were estimated. The angular random walk estimates were 0.069, 0.092 and 0.60 deg/sqrt(h) for the x, y and z gyro, respectively, all within the specified value of 0.09/0.125 deg/sqrt(h). The bias instability estimates (i.e. the minimum value of the root Allan variance curves) were 0.11, 0.070 and 0.084 deg/h, all well within the specified value of 10 deg/h.

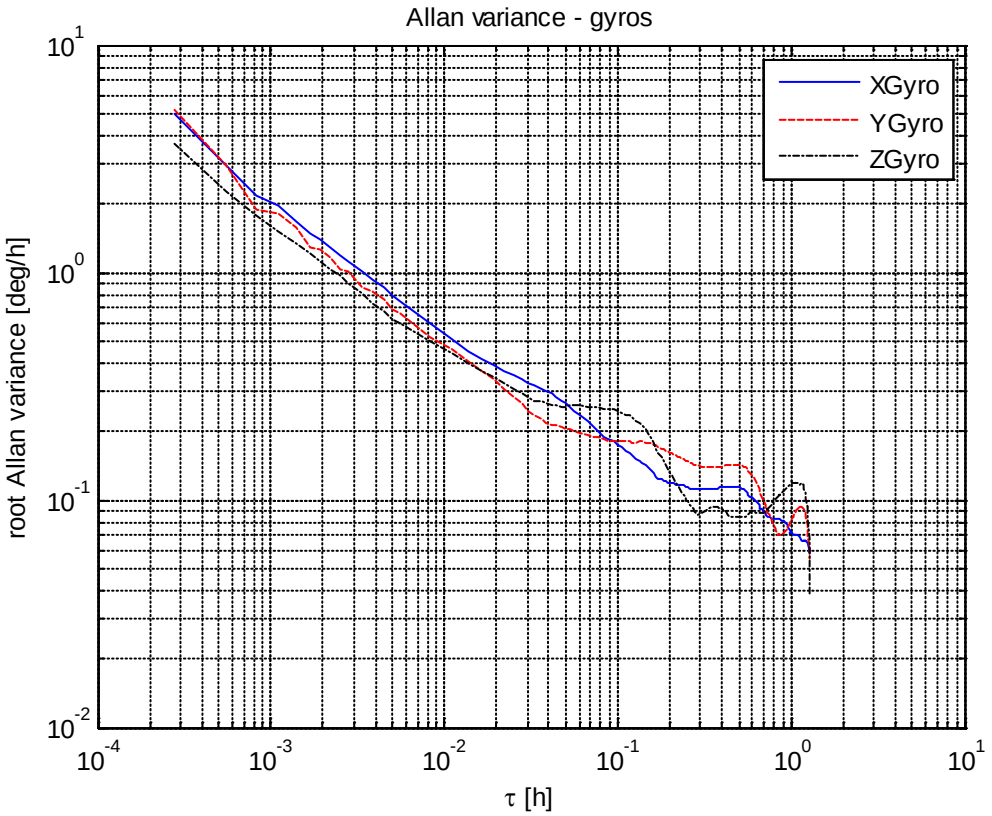

Figure 3.156 Computed Allan variance from HG1930 gyro data.

Figure 3.157 through Figure 3.159 show spectral density plots for the gyro measurements. The y gyro has a significant peak around 28 Hz. A similar but less significant peak can also be seen in the z gyro.

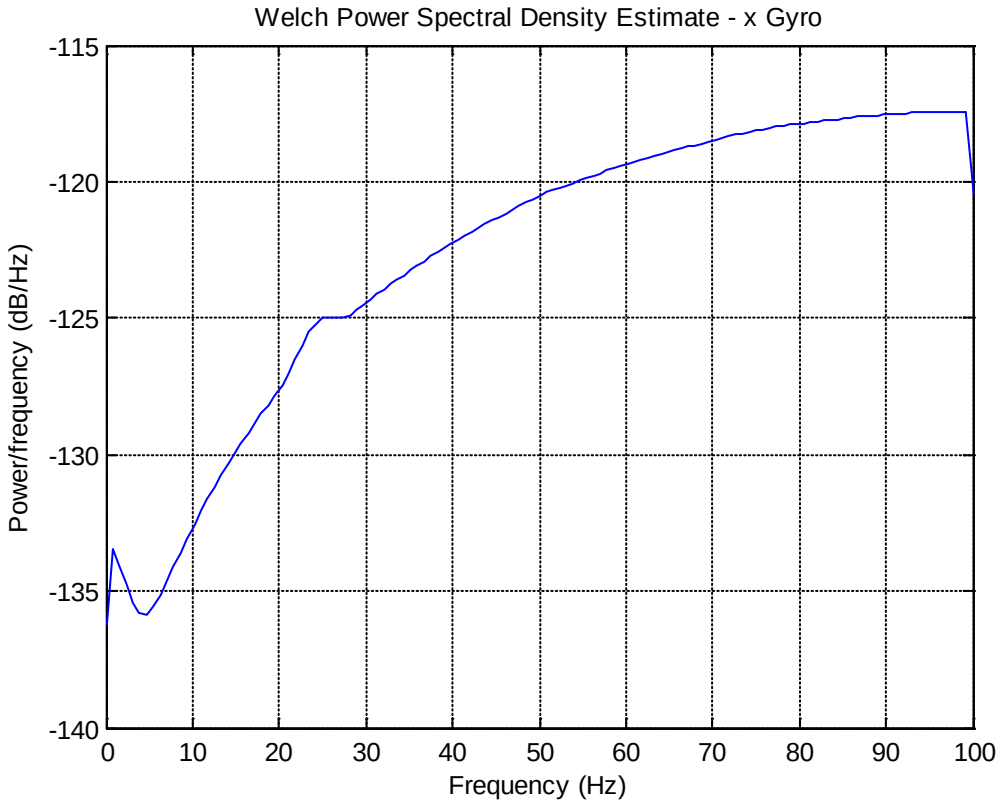

Figure 3.157 Spectral density plot – HG1930 x gyro.

Figure 3.158 Spectral density plot – HG1930 y gyro.

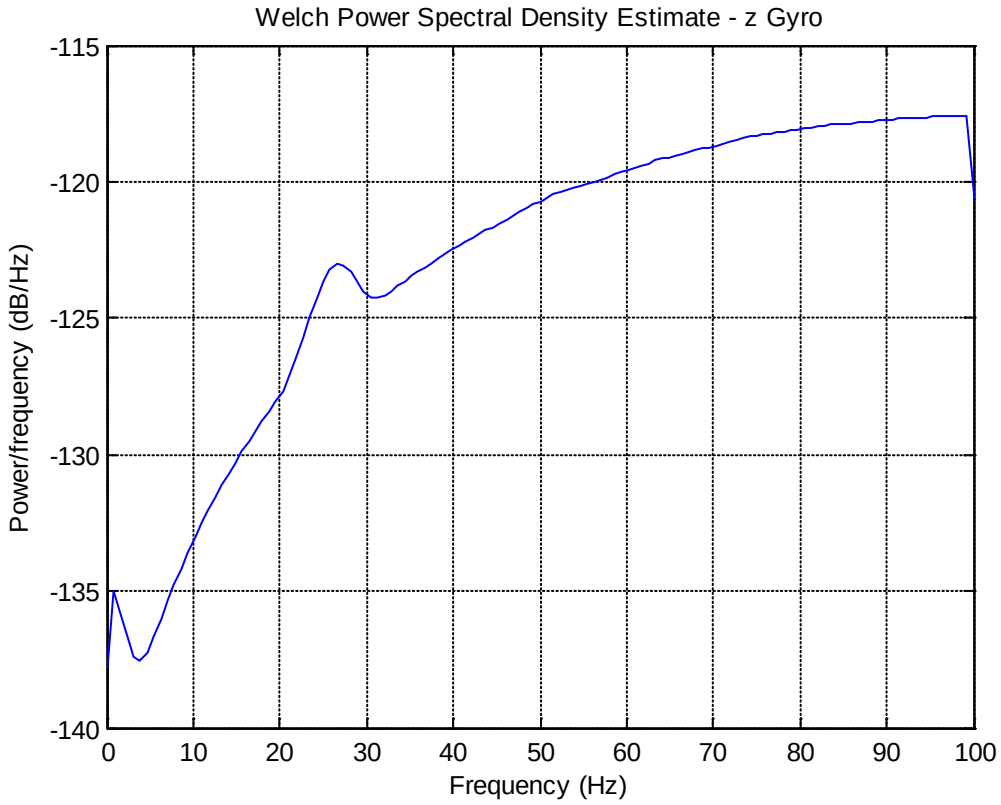

Figure 3.159 Spectral density plot – HG1930 z gyro.

Figure 3.160 through Figure 3.162 show histograms of the HG1930 gyro measurements. Again, the distributions are Gaussian-like. The standard deviations of the angular rates (delta theta divided by delta time) were (0.11, 0.13, 0.11) deg/s, for the x, y, and z gyro, respectively.

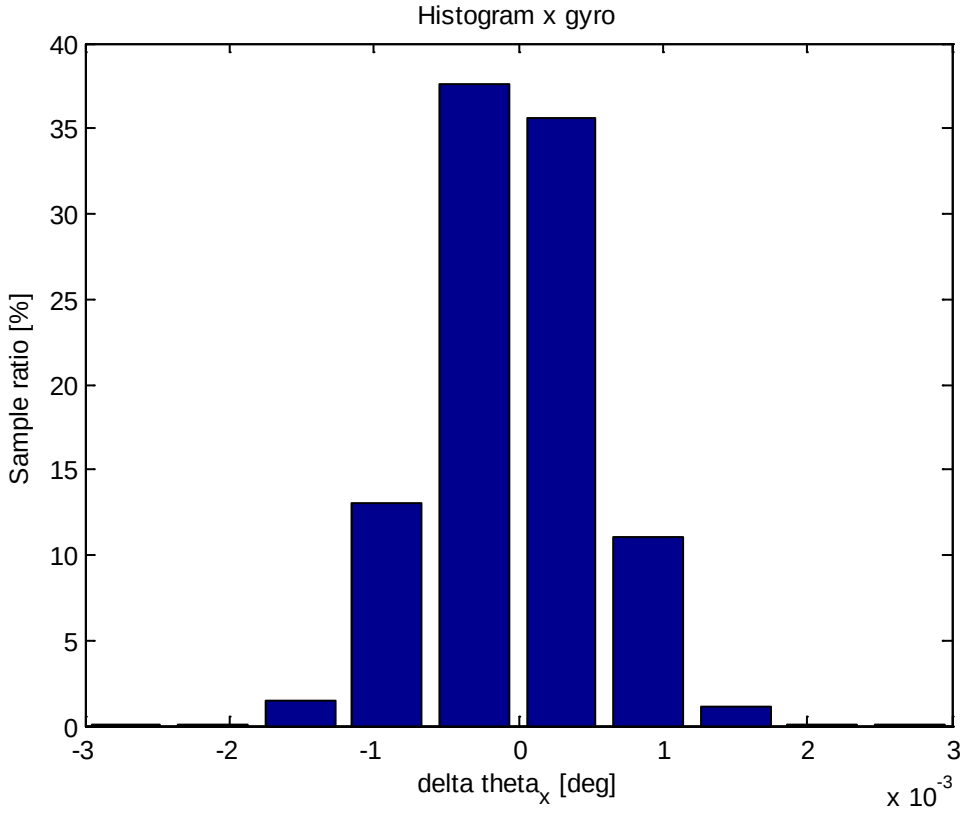

Figure 3.160 HG1930 x gyro histogram.

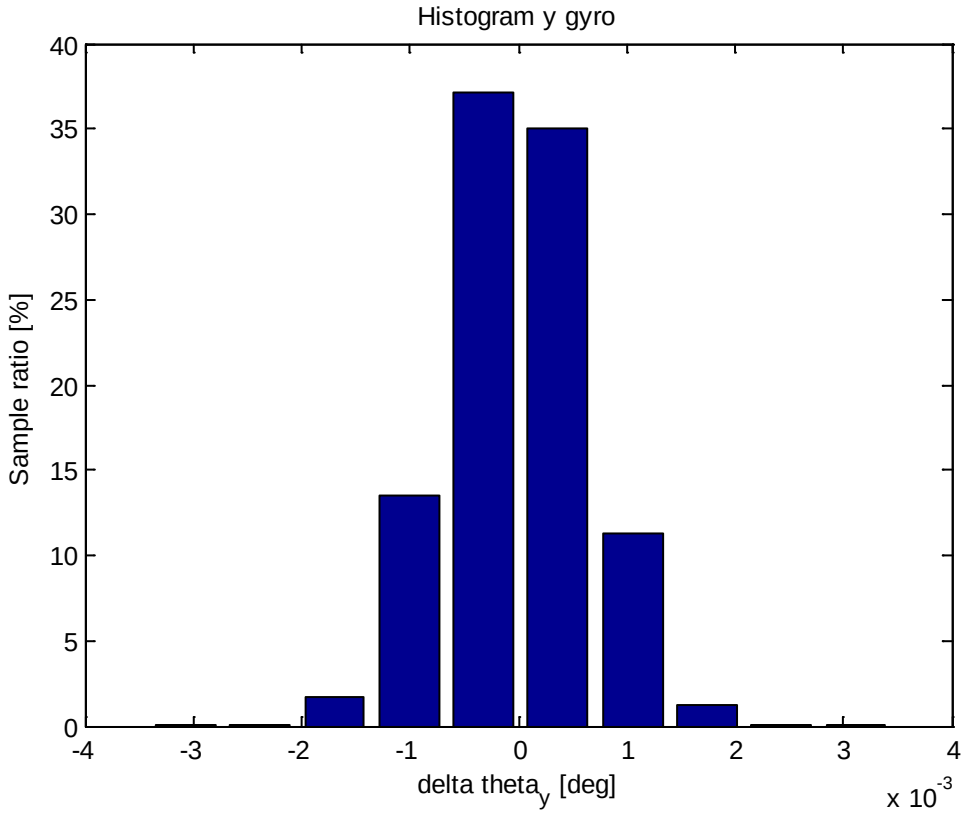

Figure 3.161 HG1930 y gyro histogram.

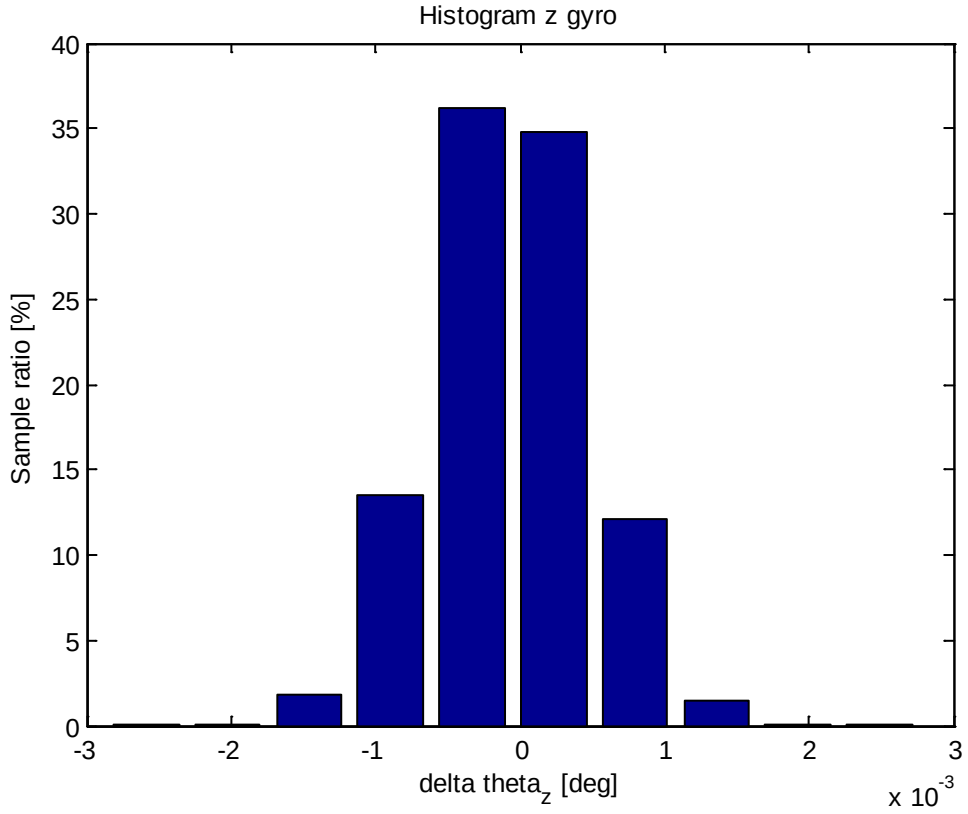

Figure 3.162 HG1930 z gyro histogram.

3.6.2 Repeatability tests

The results from the repeatability and temperature tests are shown in Table 3.27 and Table 3.28, for the accelerometers and gyroscopes, respectively. Temperature tests were not done for this unit. One of the tests, the one termed "Langtidstest" stands clearly out, both in the accelerometer and the gyro data. Since this was the first test done after the unit has been stored away for a long while, so this effect may be a result of this. Apart from this obvious effect, the means show fairly good repeatability, though the standard deviations vary slightly between power-ons.

Table 3.27 Mean HG1930 accelerometer measurements and standard deviations in repeatability and temperature tests.

Test name	norm(mean(f)) [m/s^2]	std f_x [m/s^2]	std f_y [m/s^2]	std f_z [m/s^2]
Langtidstest	9.9681	0.072	0.0489	0.0502
Langtidstest_2	10.3664	0.0025	0.0117	0.0145
Repeterbarhet	10.3675	0.0024	0.0067	0.0047
Repeterbarhet_2	10.3675	0.0024	0.0041	0.0042
Repeterbarhet_3	10.3676	0.0024	0.0039	0.004

Table 3.28 Mean HG1930 gyro measurements and standard deviations in repeatability and temperature tests.

Test name	norm(mean(ω)) [deg/s]	std ω_x [deg/s]	std ω_y [deg/s]	std ω_z [deg/s]
Langtidstest	0.0158	0.1086	0.1266	0.1067
Langtidstest_2	0.0065	0.0191	0.0043	0.0043
Repeterbarhet	0.0065	0.0152	0.0043	0.0043
Repeterbarhet_2	0.0065	0.0057	0.0043	0.0043
Repeterbarhet_3	0.0065	0.0058	0.0043	0.0043

4 Conclusions

This report contains the results of a series of tests of MEMS IMUs conducted at FFI during the fall of 2012. Table 4.1 gives a summary of the results for the different sensors. Only the parameters that did not meet the specifications are listed in the table.

Table 4.1 Summary of results from the different sensors.

Sensor name	Main results
SiIMU	• x and z accelerometer biases too high • y and z accelerometer scale factor too high • drift in accelerometer and gyro rate data
STIM300	• x, y and z accelerometer biases too high • random walk in x, y and z accelerometers too high • x, y and z gyro bias instability too high
MTI-300	• y accelerometer bias too high
MTI-30	• y accelerometer bias instability too high
MinIM	• y accelerometer scale factor too high • y gyro bias too high
HG1930	• random walk in x, y and z accelerometers too high • drift in y and z accelerometer rate data • drift in x, y and z gyro rate data

References

[1] Goodrich Atlantic Inertial Systems, "MEMS Inertial Measurement Unit SiIMU02," 2009.

[2] Gyro and Accelerometer Panel of the IEEE Aerospace and Electronic Systems Society, "Draft Recommended Practice for Inertial Sensor Test Equipment, Instrumentation, Data Acquisition, and Analysis," IEEE,2005.

[3] Sensonor, "STIM300 Inertia Measurement Unit Datasheet," 2013.

[4] XSens, "MTi 100-series," 2012.

[5] XSens, "MTi 10-series," 2013.

[6] Goodrich Atlantic Inertial Systems, "MinIM MEMS Inertial Measurement Unit," 2011.

[7] Honeywell, "User's manual, HG1930AA90," 2010.

Abbreviations

IMU – Inertial Measurement Unit

MEMS – Microelectromechanical System